DISCOVERY AND THERAPEUTIC PROMISE OF SELECTIVE ANDROGEN RECEPTOR MODULATORS FOR HORMONAL MALE CONTRACEPTION

DISSERTATION

Presented in Partial Fulfillment of the Requirements for the
Degree Doctor of Philosophy in the Graduate School of
The Ohio State University

By

Jiyun Chen, B.S.

*****

The Ohio State University
2005

Dissertation Committee:

Dr. James T. Dalton, Adviser

Dr. Randy J. Nelson

Dr. Thomas D. Schmittgen

Dr. Duxin Sun

Approved by

_____
Adviser
Graduate Program in Pharmacy

ABSTRACT

There is an urgent need to develop new forms of contraception that men are willing to use. Currently, testosterone-based hormonal contraceptives represent the most promising approach. However, testosterone demonstrates little activity after oral administration due to rapid hepatic elimination, precluding its use in oral contraceptives for men. The long-term safety of testosterone, as it relates to psychological function, cardiovascular disease, and prostate disease, is also of concern. Non-steroidal selective androgen receptor modulators (SARMs) may provide an alternative to the use of testosterone, with the advantages of oral bioavailability, tissue selectivity, lack of influence on lipoproteins, and androgen receptor (AR) specificity. We hypothesized that SARMs would mimic the pharmacologic activity of testosterone *in vivo* and can safely replace testosterone as a component of hormonal male contraceptives.

SARMs discovered previously demonstrated potential applications in the treatment of muscle wasting, osteoporosis, and benign prostate hyperplasia in animal models. However, low or no CNS effects were observed, which precluded their use for hormonal male contraception as a single regimen. Novel AR ligands were designed and synthesized using integrated knowledge of molecular modeling, structure-activity-relationships, and pharmacokinetics and metabolism of known SARMs. In the current

studies, the abilities of these compounds to bind AR and to stimulate (agonist) or inhibit (antagonist) AR-mediated transcriptional activation (Chapter 2) were determined. Compounds with high AR binding affinity and potent stimulatory activity in transcriptional assays were further investigated in castrated rats (Chapter 3) for their pharmacologic effects. Key *in vitro* and *in vivo* structure-activity-relationships of these ligands were identified. Differences in the pharmacokinetics and metabolism between SARMs resulted in a contradiction between the *in vitro* and *in vivo* pharmacologic activity, and also provided rationale for further structural modifications (Chapter 4). Through our iterative, step-wise experimental paradigm, more potent SARMs were discovered using structural modifications of our lead compound. The effects of the potent SARMs on spermatogenesis, reproductive and peripheral organs, body composition, hormonal biomarkers, sexual behavior, and fertility were further investigated (Chapters 5 through 7). As a whole, these studies provide valuable information regarding the physiologic and pharmacokinetic factors governing the pharmacology and feasibility of SARMs for hormonal male contraception.

DEDICATION

To Jim, Our Parents, and Justin

ACKNOWLEDGMENTS

I would like to thank Dr. James T. Dalton, my mentor, teacher, and friend. I have been very fortunate to have had a great teacher in the past four years who stimulated my interest in drug discovery and androgen receptor ligands, guided my efforts to learn and explore in pharmaceutical areas, and gave me constant encouragement with his enthusiasm.

I am indebted to my collaborators, Drs Duane D. Miller, Dong-Jin Hwang, and Kiwon Chang for synthesizing compounds and scientific discussion. Dr. Randy J. Nelson gave generously and amusingly of his time and expertise on behavior studies. Without his help, I could not have written Chapter 6 and Chapter 7. I also benefited from stimulating discussion and encouragement from my other committee members, Drs Thomas D. Schmittgen and Duxin Sun. My sincere thanks also go to all my lab mates for their timely assistance and friendship.

Financially, my studies were supported by grants from NIH, GTx Inc, and a Presidential Fellowship at the Ohio State University. I would like to thank them.

Through all these years, I have been so blessed to learn and grow up with love and support from my husband, Jim J. Xiao, who is also a great scientific partner of me. I would like to thank our parents for their unconditional love, support, and consideration.

Without their tremendous help, I could not have finished my studies. I also thank my baby, Justin, for bringing so much joy and wonderful memory to my life.

VITA

December 1, 1976……...Born in Wenling, P.R. China

1994 – 1998……B.S. Pharmacy, Beijing Medical University

1998 - 1999…….Research Associate
College of Pharmacy
Beijing Medical University

2000 - Present…….Graduate Research Associate,
The Ohio State University

PUBLICATIONS

Wang LD, Qiu DY, **Chen JY**, Han YF, Zheng JH, and Guo DA. Callus Cultures of Annona Squamosa for the Production of Annonaceous Acetogenins. *Journal of Asian Natural Product Research*. 2002 Sep; 4(3): 171-4.

Casey E. Bohl, Cheng Chang, Michael L. Mohler, **Jiyun Chen**, Duane D. Miller, and James T. Dalton. A Ligand-Based Approach to Identify Quantitative Structure-Activity Relationships for the Androgen Receptor. *Journal of Medicinal Chemistry* 2004 July; 47(15): 3765-76.

Jiyun Chen, Dong-Jin Hwang, Casey E. Bohl, Duane D. Miller, and James T. Dalton. A Selective Androgen Receptor Modulator (SARM) for Hormonal Male Contraception. *Journal of Pharmacology and Experimental Therapeutics* 2005, Jan; 312:546-53.

Jim J. Xiao, Amy B. Foraker, Peter W. Swaan, Shujun Liu, Ying Huang, Zunyan Dai, **Jiyun Chen**, Wolfgang Sadée, John Byrd, Guido Marcucci, and Kenneth K. Chan. Efflux of Depsipeptide FK228 (FR901228, NSC-630176) is mediated by both P-glycoprotein and MRP1. *Journal of Pharmacology and Experimental Therapeutics* 2005 Apr; 313(1): 268-76.

FIELDS OF STUDY

Major Field: Pharmacy

Studies in Pharmacokinetics, Pharmacodynamics, Drug Metabolism, and Pharmacology

TABLE OF CONTENTS

LIST OF TABLES

LIST OF FIGURES

LIST OF ABBREVIATIONS

SARM	Selective androgen receptor modulator
DHEA	Dehydroepiandrosterone
DHT	Dihydrotestosterone
AR	Androgen receptor
DBD	DNA binding domain
LBD	Ligand binding domain
TAU	Transcription activation unit
HSP	Heat shock protein
NLS	Nuclear localization signal
ARE	Androgen response element
RNA-pol II	RNA-polymerase II
GTFs	General transcription factors
TBP	TATA binding protein
TAFs	TBP associating factors
TP	Testosterone propionate
TE	Testosterone enanthate
TB	Testosterone buciclate
TU	Testosterone undecanoate
TD	Testosterone decanoate
MENT	7α-methyl-19-nortestosterone
BPH	Benign prostate hyperplasia
CNS	Central nervous system
GnRH	Gonadotropin-releasing hormone
LH	Luteinizing hormone
FSH	Follicle stimulating hormone
WHO	World Health Organization
CPA	Cyproterone acetate
DMPA	Depot medroxyprogesterone acetate
NETE	Norethisterone enanthate
LNG	Levonorgestrel
DSG	Desogestrel
ENG	Etonorgestrel
DNG	Dienogest
[^{3}H]-MIB	17α-methyl-^{3}H] Mibolerone

HAP	Hydroxyapatite
PMSF	Phenylmethylsulfonyl fluoride
PBS	Phosphate-buffered saline
SARs	Structure-activity relationships
DMSO	Dimethyl sulfoxide
PEG 300	Polyethylene glycol-300
ANOVA	Analysis of variance
$T_{1/2}$	Terminal half-life
$AUC_{0-\infty}$	Area under the plasma concentration-time curve
CL	Plasma clearance
Vd_{ss}	Apparent volume of distribution at equilibrium
MRT	Mean residual time
Cmax	Maximum plasma concentration
Tmax	Time to reach Cmax
$F_{p.o.}$	Oral bioavailability
ESI	Electrospray ionization
MS^n	Multiple stage mass spectrometry
CID	Collision-induced dissociation
HPLC	High performance liquid chromatograph
SIM	Selected ion monitoring
TIC	Total ion chromatogram
XICs	Extracted ion chromatogram
EB	Estrogen benzoate
MF	Mount frequency
IF	Intromission frequency
EF	Ejaculation frequency
ML	Mount latency
IL	Intromission latency
EL	Ejaculation latency
PEI	Post ejaculation interval
FM	Percent fat mass
LM	Percent lean mass
BMD	Bone mineral density
BMC	Bone mineral content
BMA	Bone mineral area
DEXA	Dual energy x-ray absorptiometry
SPT	Sperm counts per testis
SPG	Sperm Counts per gram of tissue
NIH	National Institute of Health

CHAPTER 1

INTRODUCTION

1.1 ANDROGEN BIOSYNTHESIS AND THE ANDROGEN RECEPTOR (AR)

Androgens are necessary and essential for supporting male development and maintaining spermatogenesis and male secondary characteristics (1). More than 95% of circulating testosterone is synthesized and secreted by the Leydig cells in the testes (2, 3). Peripheral tissues, mainly the adrenal cortex, produce about 5% of testosterone. Circulating testosterone plays an important role in the regulation of androgen production via the hypothalamus-pituitary-testis axis. Figure 1.1 shows the steroidogenic pathways in the human testis and peripheral tissues. Steroidogenic reactions start from the translocation of cholesterol (C_{27}) in the mitochondria and the production of pregnenolone (C_{21}) by the cleavage of the side chain of cholesterol. Pregnenolone is translocated from the mitochondria to the smooth endoplasmic reticulum, where testosterone is synthesized via a stepwise reaction catalyzed by oxidative enzymes belonging to the cytochrome P450 family (4, 5). Adrenal glands mainly synthesize two testosterone precursors, dehydroepiandrosterone (DHEA) and androstenedione, which also function as weak androgens with 5 and 10% of the activity of testosterone, respectively. In peripheral tissues, two important and active metabolites of testosterone are formed, namely dihydrotestosterone (DHT) and estradiol mediated by the 5α-reductase and aromatase (CYP19) enzymes, respectively (Figure 1.1).

The pharmacologic activity of testosterone and DHT is predominantly mediated by the androgen receptor (AR), a ligand-dependent transcription factor. The full length AR is translated as a protein of approximately 918 amino acids (6, 7) and molecular

weight of 110 kDa (8). The AR belongs to the nuclear receptor superfamily and contains four functional domains. As illustrated in Figure 1.2, AR is composed with following domains: the N-terminal transactivation domain, the DNA binding domain (DBD), the hinge region, and the ligand binding domain (LBD). Transcriptional activation of the AR is primarily mediated by sequences in the N-terminal domain and a short region in the LBD, referred to as AF-1 and AF-2, respectively (9). The AF-1 domain is functionally independent from ligand and can be further divided into a transcription activation unit (TAU)-1 (amino acids 100-370) and TAU-5 (amino acids 360-528) (10). However, the precise mechanism of AF-1 domain is not well defined. In contrast, the AF-2 domain is ligand-dependent and indispensable for AR-mediated transcriptional activation as proved by deletion and mutation studies (11-14). The crystal structure of the AR LBD reveals that it forms twelve α helixes (H1 – H12) and one β-turn, resulting in a three-layer α helical sandwich (15, 16). The core of AF-2 is formed by helix H12. Upon binding with an agonist, the AR LBD is thought to form a compact conformation, in which H12 fold back as a lid to cover the ligand binding pocket and stabilize the binding surface for coactivators (17). On the other hand, binding with AR agonists is thought to prevent the AR LBD from forming such a compact and stable conformation as needed for transactivation.

1.2 MOLECULAR MECHANISM OF AR ACTIONS

Prior to ligand binding, the AR (apoAR) forms a heterocomplex with chaperone proteins like Heat Shock Proteins 90 (HSP90) and other co-chaperones (18, 19). The HSP90-AR complex protects the apoAR in an inactive state and also maintains its high binding affinity conformation. Mutation of HSP90 to HSP82 diminishes the high binding affinity of AR with its ligand compared to its wild-type complex (20). Figure 1.3 is a schematic that shows the molecular mechanism of AR actions. Binding with ligand triggers the dissociation of the AR from the chaperone protein, conformational changes in the LBD, formation of AR dimmers, and translocation of the AR-ligand (holoAR) complex into the nucleus via an intrinsic nuclear localization signal (NLS) . The AR-

ligand complex then binds the enhancer region (androgen response element, ARE) located in the upstream promoter of target genes and interacts with several key components of the signaling cascade, including RNA-polymerase II (RNA-pol II), general transcription factors (GTFs), TATA binding protein (TBP), and TBP associating factors (TAFs) (21). The AR interacts with the transcriptional machinery by communication directly with GTFs or indirectly via coactivators (e.g., SRC-1) (22, 23), which in turn triggers production of the target mRNA and consequently protein synthesis (Figure 1.3).

In addition to the classical steroid receptor-mediated transcriptional activation, multiple lines of evidence support the existence of non-genomic effects of steroid receptors in the plasma membrane (24-27). Non-genomic effects of androgens were reported in osteoblasts (28), macrophage (29), adipose tissues (30), and Sertoli cells (31). However, the mechanisms of the non-genomic actions of steroid receptors are still poorly understood.

1.3 AR LIGANDS AND PHARMACOLOGY

Functionally, AR ligands can be divided into two categories-AR agonists (androgens) and AR antagonists (antiandrogens). Structurally, AR ligands can be further classified as steroidal and nonsteroidal compounds within each category. Testosterone and DHT are two naturally occurring androgens with a steroidal structure (Figure 1.4). Testosterone has been used for the treatment of hypogonadism for decades. However, testosterone undergoes rapid hepatic elimination (32) and is not oral bioavailable (33, 34) after oral administration. In order to prolong the action of testosterone, various testosterone derivatives were developed and clinically used, including 17α-methyltestosterone, testosterone propionate (TP), testosterone enanthate (TE), and testosterone buciclate (TB). Testosterone undecanoate (TU) was reported as an orally bioavailable androgen (35). However, its low efficacy in early clinical trials (36) of male contraception prevented its widespread use in this regard. To date, the main administration routes of steroidal androgens remain intramuscular injection, transdermal

patch, and pellet implantation. In addition to the treatment of hypogonadism, androgens have also been investigated intensively for hormonal male contraception (see Section 1.5) and androgen replacement for ageing men. Although testosterone demonstrated beneficial effects on the bone, cognitive function, body composition, muscle strength and function, mood, and sexual function in men, there are possible risks related to testosterone treatment including cardiovascular function, prostatic stimulation, changes in serum lipid and, erythropoiesis. The lack of large-scale trials of testosterone make it controversial and premature to make conclusions regarding the risk/benefit ratio of androgen replacement in aging men (37-40).

In men, the effects of testosterone on the growth of the reproductive tract (e.g., prostate) are amplified by conversion to DHT, which is a more potent androgen than testosterone. Co-administration of testosterone and a 5α-reductase inhibitor demonstrated that the androgenic activity of testosterone on the prostate and seminal vesicles is highly dependent on 5α-reductase activity, while the anabolic effect of testosterone in muscle occurs independently from conversion to DHT, indicating that the differential effect of testosterone action in androgenic and anabolic tissues is due to the high and low 5α-reductase activity in reproductive tissues and muscle, respectively (41-44). Recently, a tissue-selective steroidal androgen was discovered by the incorporation of a 7α-methyl group in a testosterone derivative. For instance, 7α-methyl-19-nortestosterone (MENT, Figure 1.4) demonstrates tissue selectivity with higher anabolic activity than androgenic activity both in rat (45) and in hypogonadal men (46). This tissue selectivity was mainly due to the inability of 5α-reductase to metabolize MENT.

Androgens are not only essential for the physiological development of the prostate, but also for the initiation and progression of prostate cancer. Antiandrogens are used as the first line treatment for prostate cancer by competitively binding with the AR in target tissues (47). Steroidal antiandrogens, such as cyproterone acetate and megestrol acetate (Figure 1.5), demonstrated mixed pharmacologic activity. Cyproterone acetate showed progestational activity and mixed AR agonist and antagonist activity (48). While megestrol acetate cross-reacts with the progesterone receptor, glucocordicoid receptor, and mineralocorticoid receptor (49-52). To date, these non-selective antiandrogens have

been largely replaced by nonsteroidal antiandrogens, including flutamide, nilutamide, and bicalutamide (Figure 1.5) due to their improved AR specificity, tissue selectivity, and pharmacokinetic properties. The use of nonsteroidal antiandrogens in prostate cancer treatment was recently reviewed (53-55).

1.4 NONSTEROIDAL SELECTIVE ANDROGEN RECEPTOR MODULATORS

In addition to the discovery of steroidal androgens using structural modifications of testosterone, another area in which progress has been made is the discovery of nonsteroidal androgens with multiple pharmacophores. Our laboratory was the first to report the discovery of nonsteroidal AR ligands structurally modified from known antiandrogens – flutamide and bicalutamide (56). The first generation of nonsteroidal androgens (e.g., acetothiolutamide) was the bicalutamide-derivatives, which displayed high binding affinity and potent activity *in vitro* (57) with poor pharmacologic activity *in vivo*. The contradictory *in vitro* and *in vivo* activity of acetothiolutamide was mainly due to its metabolic instability (58). Structural modification of the thio-ether linkage to an oxygen bridge (Figure 1.6) resulted in the identification, two potent and efficacious nonsteroidal AR ligands (**S-1** and **S-4**) (59, 60) as selective androgen receptor modulators (SARMs). Unique characteristics of the second generation of nonsteroidal androgens include: AR specificity, tissue-selectivity, oral bioavailability, and amenability for further structural modifications. Key structure-activity relationships were analyzed to facilitate the identification and discovery novel AR ligands (61-63). Recently, we reported the potential application of SARMs in the treatment of benign prostate hyperplasia (BPH) (64) and osteoporosis (Kearbey, OSU dissertation, 2005). These SARMs work as partial agonists in androgenic tissues (e.g., prostate) and full agonists in anabolic tissues (e.g., levator ani muscle and bone) without affecting the hypothalamus-pituitary-testis axis. More recently, we investigated the ability of a novel SARM to regulate gonadotropins, testosterone, and spermatogenesis (65). Results suggested that novel SARMs (e.g. **C-6**, Figure 1.6) with potent central nervous system (CNS) effects can be designed by incorporating multiple substituents in the aromatic B-ring for potential use in hormonal

male contraception. Meanwhile, crystallography studies conducted in our laboratory suggest that a unique B-ring subpocket exists in the AR for SARMs that can be used to provide fundamental rationale for B-ring structural modifications (Bohl, OSU dissertation, 2005).

The concept of nonsteroidal androgens has significantly progressed since it was first defined by Dalton et al. in 1999 (66). Several other groups later reported similar transformation from nonsteroidal antagonists to agonists of compounds structurally related to 2-quinoline and coumarin (67, 68). Markedly increased bone mineral density (BMD) was observed after treatment of orchiectomized male rat with quinoline-related SARMs prostate-sparing property (69, 70).

1.5 HORMONAL MALE CONTRACEPTION

Unlike women, effective male contraception is restricted to physical methods, namely condoms and vasectomy. A variety of attempts have been made to produce pharmacologic, effective, reversible and side effect-free contraceptive methods for the male. Among them, only hormonal contraception has reached the stage of clinical development (71). Figure 1.7 illustrates the hypothalamus-pituitary-testis axis of androgen regulation. In the brain, gonadotropin-releasing hormone (GnRH) is released from the hypothalamus and stimulates the secretion of pituitary luteinizing hormone (LH) and follicle-stimulating hormone (FSH) in a pulsatile fashion. In the testis, LH indirectly stimulates spermatogenesis through testosterone synthesized by Leydig cells, while FSH directly interacts with FSH receptors expressed in Sertoli cells and stimulates spermatogenesis (Figure 1.7). Both LH and FSH are required for quantitative and qualitative spermatogenesis (72). Testosterone and its aromatized metabolite (estradiol) negatively regulate circulating levels of testosterone and GnRH and LH production in the hypothalamus and pituitary, respectively. Activin and inhibin produced by Sertoli cells stimulate or inhibit, respectively, the secretion of FSH from the pituitary. (73). Theoretically, inhibition of one or more hormones involved in the hypothalamus-pituitary-testis axis will suppress spermatogenesis. GnRH secretion can be inhibited

either by exogenous androgens or by GnRH agonists. At the pituitary level, the stimulatoy effect of GnRH can be blocked either by competitive binding of a GnRH antagonist with GnRH receptors or by binding of GnRH by a GnRH antibody before it interacts with its receptor. Progestins and exogenous androgens inhibit secretion of LH and FSH, while inhibin selectively down regulates FSH levels. Additionally, the effects of FSH on Sertoli cells can be blocked using either FSH immunization or FSH antagonists. However, the only clinically proven effective methods are androgen alone or androgen combined with either progestins or GnRH antagonists. The use of FSH immunization, FSH antagonists, and inhibin for hormonal male contraception is still under early investigation.

1.5.1 Testosterone Single Regimen

Testosterone was one of the first choices for male contraception due to its natural role in spermatogenesis. However, testosterone demonstrates little pharmacologic activity after oral administration due to from its rapid hepatic elimination. To prolong effect, testosterone implants and longer acting esters, including testosterone enanthate (TE), testosterone propionate (TP), testosterone buciclate (TB), testosterone undecanoate (TU), and testosterone decanoate (TD), were developed (Figure 1.4). Except for TU, the administration methods of most testosterone esters are limited to intramuscular injection (i.m.) (74-80) or surgical implantation of implants and pellets (81-83). In the 1990's, two large international studies (n = 670) sponsored by the World Health Organization (WHO) (76, 77) tested TE (200 mg/week, i.m.) as a hormonal male contraceptive. In the first study (n = 271), azoospermia was achieved in 64% of men (76). In the second study (n = 357), 98% of men achieved as either azoospermia or severe oligozoospermia (< 3 million sperm/mL of ejaculation). The following efficacy studies demonstrated that the overall failure rate in preventing pregnancy by azoospermia and severe oligozoospermia was 1.4 per 100 person years (77), which was as the efficient as female pill and better than which can be afforded by condoms (12 to 15%). However, weekly injection and long-term side effects related to supraphysiologic levels of testosterone are not well tolerated. A single

intramuscular injection of TU provided normal serum testosterone levels for at least 6 weeks in hypogonadal men (35). Recently, the efficacy of male contraception using this longer-acting androgen was studied in China. Monthly injection of TU at a dose of 500 mg for 12 months demonstrated 97% success rate in achieving azoospermia and oligozoospermia and an overall failure rate in preventing pregnancy of 5.2 per 100 person years (78).

To prevent potential adverse effects of androgen treatment on the prostate, tissue selective steroidal androgens, such as 7α-methyl-19-nortestosterone (MENT), were also investigated for hormonal male contraception. MENT is a nonaromatizable steroidal androgen, which maintained libido in hypogonadal men (84) and demonstrated potent tissue-selective pharmacologic activity in animals (85) and men (46). The use of MENT for hormonal male contraception as a single regimen is being investigated in early-phase clinical trials (Table 1.1) (83).

1.5.2 Testosterone-Based Combination Regimens

In contrast to the high rate (91%) of azoospermia achieved in East Asian populations by testosterone alone, azoospermia was only observed in 50 to 70% of Caucasian men. To explain this heterogeneity in the spermatogenic response, multiple differences between responders and non-responders were studied and proposed, including the sensitivity of hypothalamus-pituitary-testis axis to the negative feedback signal from testosterone (86), intratesticular 5α-reductase activity (87), pretreatment hormonal status (88, 89), and the polymorphism of the common polyglutamine stretch (CAG repeats) length in exon 1 of the AR gene (90).

To increase the response rate of hormonal male contraception in Caucasians and to avoid those disadvantages caused by supraphysiologic doses of testosterone, other gonadotropin-suppressing substances (e.g., progestins and GnRH antagonists) were included and used as combination regimens. In principle, GnRH antagonists competitively bind to the GnRH receptor in the pituitary and consequently inhibit the secretion of gonadotropins. GnRH antagonist-testosterone regimens revealed more rapid

onset and complete suppression of spermatogenesis than testosterone alone (91). However, the widespread use of GnRH antagonists for hormonal male contraception is limited since these proteins are expensive to synthesize and difficult to deliver. On the contrary, progestins have been used as a key component of female contraception for decades. The administration of progestins alone in men resulted in faster and more potent gonadotropin suppression (92). However, nearly complete depletion of endogenous testosterone leads to loss of libido (93). Therefore, a physiological dose of testosterone was included during most clinical trials. Additionally, testosterone and progestins work synergistically in suppression of gonadotropins. The currently available progestins (Figure 1.8) include cyproterone acetate (CPA), depot medroxyprogesterone acetate (DMPA), norethisterone enanthate (NETE), levonorgestrel (LNG), desogestrel (DSG), etonorgestrel (ENG), and dienogest (DNG). Except for DMPA, all of the other progestins are orally active, making them good candidates for inclusion in a male contraceptive 'pill'. Clinical trials of hormonal male contraception are aimed at finding the best androgen-progestin combination and the minimum effective dose of these compounds.

1.5.3 Testosterone Plus DMPA or CPA

It has been three decades since the first attempts to use DMPA or CPA for hormonal male contraception. As shown in Table 1.2, DMPA in combination with TE, 19-nortestosteorne, or testosterone pellets achieved either azoospermia (50 to 100%) or oligozoospermia in all subjects (81, 94-98). In one major clinical study of 55 couples, no pregnancies occurred in a 426 person-months efficacy phase (98), suggesting testosterone-DMPA implantation is a promising approach for male contraception. However, disadvantages related to this method are a relatively high rate of extrusion and the requirement for a surgical procedure.

CPA is not only an oral bioavailable progestin, but also an antiandrogen, which provides dual effects in the suppression of spermatogenesis. A series of studies were performed to investigate oral CPA at doses ranging from 5 to 100 mg combined with a weekly injection (i.m.) of TE at 100 mg/week (99-101). Although small numbers of

subjects were enrolled in these studies, the combination regimen demonstrated high efficacy, which was superior to that observed with TE alone (Table 1.3 vs Table 1.1). Unfortunately, the antiandrogenic effect of CPA led to a dose-dependent fall in hemoglobin, hematocrit, and body weight. More recently, Meriggiola *et al*. observed that TU alone or combined with lower doses of CPA maintains sperm suppression for 32 weeks without significant side effects (102). However, the efficacy and safety of this prototype regimen need to be further investigated in larger populations.

1.5.4 Testosterone Plus LNG, DSG, ENG, NETE or DNG

LNG, DSG, ENG, NETE, and DNG are progestins that were structurally derived from 19-nortestosterone. Testosterone-LNG and testosterone-DSG combinations for male contraception have been extensively investigated. As shown in Table 1.4, weekly injection of TE combined with LNG tablets or implants suppressed spermatogenesis to azoospermia (61 to 93%) or severe oligozoospermia (89 to 100%) in men (74, 103, 104). Although it offers more efficient activity than TE alone in Caucasian men (Table 1.4 vs Table 1.1), again weekly injection is not applicable to routine or chronic clinical use. Monthly injection of 250 mg of TU combined with LNG (250 μg/day, p.o.) achieved either azoospermia (57%) or oligozoospermia (43%) in all subjects. However, no significant difference was observed between TU-LNG and TU alone groups in the suppression of spermatogenesis (79). Another study showed that preloading LNG for 4 weeks and then followed by 1000 mg of TU injection produces sustained suppression of spermatogenesis to azoospermia (90%) in Chinese men (80). Similarly, LNG did not offer significantly beneficial effects when TU-LNG was compared with TU alone regimen. When the same dose of LNG was combined with a testosterone transdermal patch, results were disappointing, indicating that the dose and administration route of testosterone is critical to success for androgen-progestin combination regimens (104).

Table 1.5 shows the suppression of spermatogenesis following treatment with testosterone esters combined with DSG (105-109). Among them, uniform azoospermia was achieved in multiple studies using this testosterone-DSG combination regimen (105-

108), which was more effective than the testosterone-LNG regimen in suppression of spermatogenesis in Caucasians with similar side effects (e.g., weight gain and decrease in HDL-cholesterol). Moreover, a self-applied regimen was also investigated using testosterone transdermal patch plus DSG at doses of 75, 150, and 300 μg/day (110). However, the azoospermia rate was significantly lower than that of TE or T-pellet combined with the same dose of DSG. Therefore, the combination of long acting testosterone pellets (3 months) plus DSG appears to be a promising regimen for male contraception based on the results of small studies. Larger clinical trials using this regimen are necessary for further development of this regimen for hormonal male contraception.

More recently, male contraception studies have focused on newer androgen-progestin combination regimens, such as TU + NETE (111-113) and TD + ENG (114) (Table 1.6). NETE is a progestin containing partial AR agonist activity, approximately 10% of the activity of testosterone. Since both TU and NETE are long-acting hormones, TU (1000 mg) and NETE (200 or 400 mg) were dissolved in castor oil and injected at 6, 8, or 12-week intervals (111-113). More than 90% of subjects in each treatment achieved azoospermia with injection interval of 6 and 8 weeks. In contrast, only 38% subjects developed azoospermia with an injection interval of 12 weeks. The contraceptive effect of TU (1000 mg) plus NETE (200 mg) in men is promising and needs to be further evaluated in larger clinical trials. ENG is a potent progestin and the active metabolite of DSG following by oral administration. For the first clinical trial with T plus ENG (115), depot-testosterone (400 mg) was implanted at a 12-week interval along with one-time ENG (68, 136, and 204 mg) implant(s) into subjects. Although spermatogenesis was suppressed to lower than 3 million sperm per mL of ejaculate in almost all subjects, T-ENG (204 mg) was the only regimen that induced uniform azoospermia in men (116). Most recently, a multicenter phase II study (n = 112) of TD + ENG for male hormonal contraception was reported (114). TD at a dose of 400 mg was injected every 4 or 6 weeks combined with ENG at an oral dose of 300 μg for 48 weeks. As shown in Table 1.6, more frequent injections (4 vs 6-week) induced a higher rate of azoospermia (96 vs

83%) and more rapid onset. Therefore, TD (400 mg/4 weeks) plus ENG (300 μg) represents a promising approach for male contraception.

1.5.5 Limitation of Testosterone-Based Hormonal Male Contraception

No major toxicological effects were reported in most clinical trials involving young, eugonadal subjects. The major limitations of using testosterone-based hormonal male contraception are inconvenient administration routes and steroidal related side effects, including decrease of HDL cholesterol, increase of hematologic parameters such as hemoglobin and hematocrit, increase of body weight, and acne. Although lower doses of testosterone were effectively used in testosterone-progestin combination regimens, similar but minor side effects were reported (see references in table 1.2 ~ 1.6). Additional concern of long-term treatment with testosterone is the potential risk of testosterone in the prostate and cardiovascular system (117), which needs to be evaluated in large prospective studies in the future.

1.6 SCOPE AND OBJECTIVES OF DISSERTATION

SARMs discovered in our laboratory offer potential use for androgen replacement with advantages such as high oral bioavailability, tissue selectivity (prostate-sparing effect), AR specificity, and absence of steroid-related side effects. We hypothesized that SARMs which mimic testosterone in regulating gonadotropin and testosterone levels could be used to achieve a male contraceptive 'pill', using SARM alone or in combination with progestins. This hypothesis was tested by an iterative and step-wise discovery paradigm.

The specific aims of this project were to: determine AR binding affinity and AR-mediated transcriptional activation *in vitro* of novel AR ligands with multiple substituents in the aromatic B-ring and analyze the *in vitro* structure-activity relationships (Chapter 2); examine the *in vivo* pharmacologic activity of AR ligands, analyze *in vivo* structure-

activity relationships, and select potent SARMs for male contraception studies (Chapter 3); illustrate the pharmacokinetics and metabolism of a SARM (**C-3**) in male rats (Chapter 4); characterize the pharmacologic activity of a SARM (**C-6**) in castrated and intact male rats and its effects on hormonal regulation and spermatogenesis (Chapter 5); examine the effects of **C-6** on masculine sexual behavior in castrated male rats (Chapter 6); determine the effects of a SARM (**C-31**) on spermatogenesis, hormonal regulation, endocrine physiology, and male fertility (Chapter 7). In Chapter 8, conclusions and major findings of the current studies are summarized.

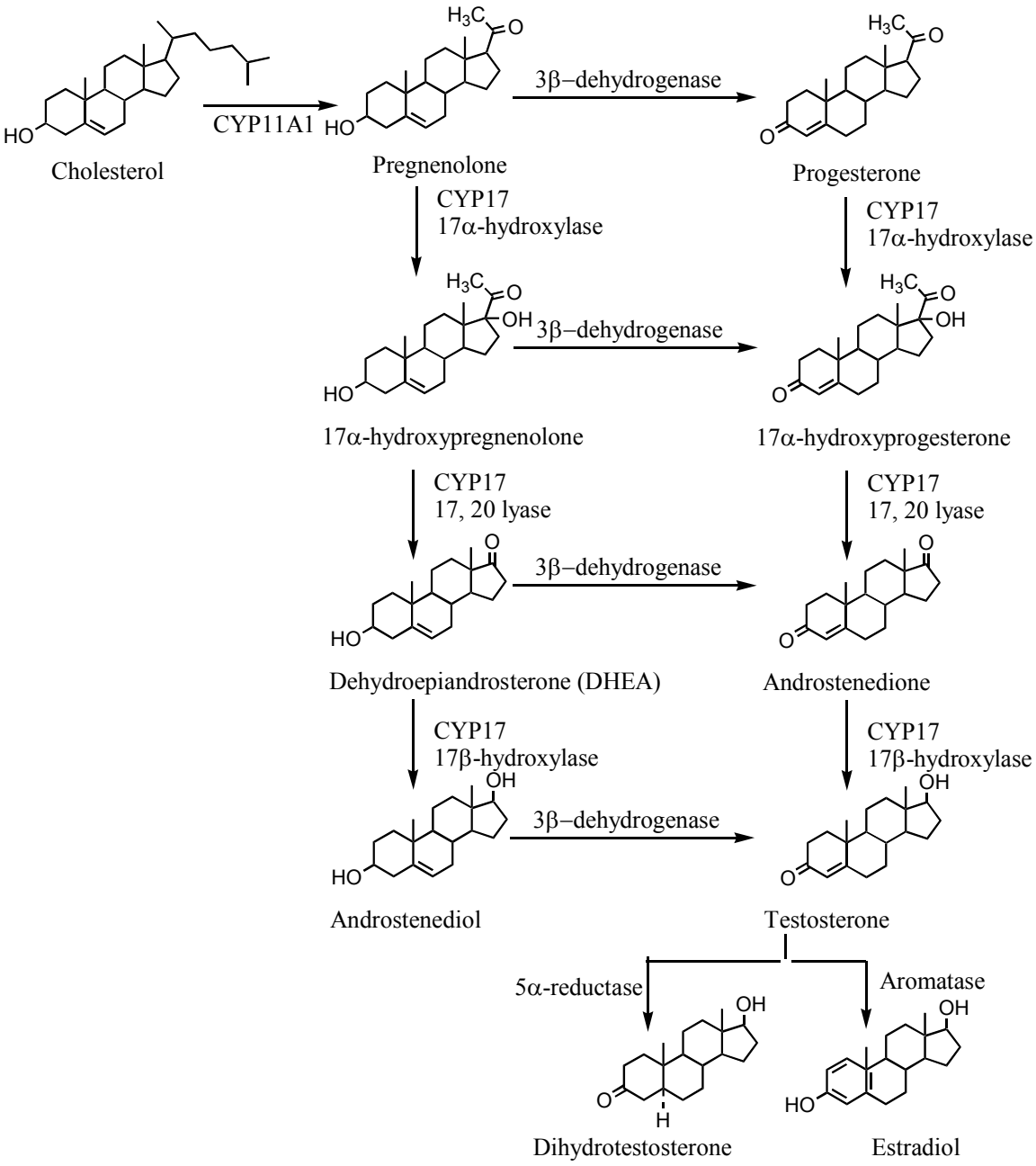

Figure 1. 1 Steroidogenic Pathways in the Human Testis and Peripheral Tissues.

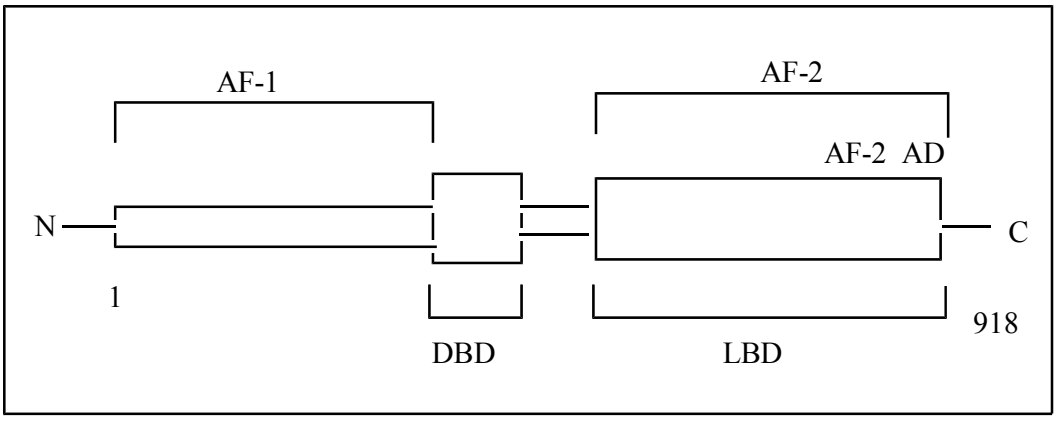

Figure 1. 2 Main Functional Domains of Androgen Receptor

AF: activation function; DBD: DNA binding domain; LBD: Ligand binding domain.

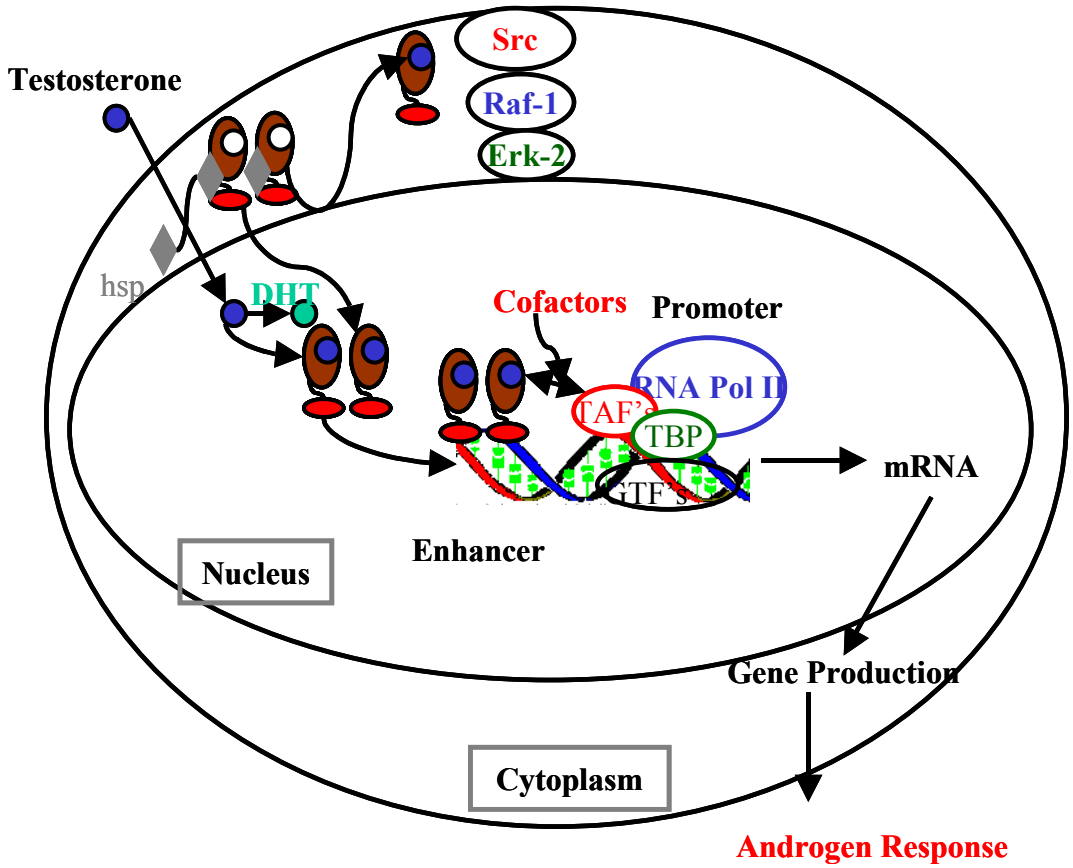

Figure 1. 3 Schematic of the Molecular Mechanism of AR Action.

After dissociation of heat shock proteins (hsp), the AR is translocated to the nucleus via an intrinsic nuclear localization signal, forms dimmers, and binds to specific DNA elements present as enhancers in upstream promoter sequences of androgen target genes. The AR complex directly or indirectly interacts with the transcription machinery, which triggers mRNA synthesis and consequently protein synthesis. A non-genomic pathway involving the classical AR via cross-talk with the Src/Raf-1/Erk-2 pathway is known.
Hsp: Heat shock protein; RNA-Pol II: RNA-polymerase II; GTFs: General transcription factors; TBP: TATA binding protein; TAF's: TBP associated factors; DHT: Dihydrotestosterone; Src: Oncogene Src; Raf-1: Oncogene Raf-1; Erk-2: Extracellular regulated kinase-2.

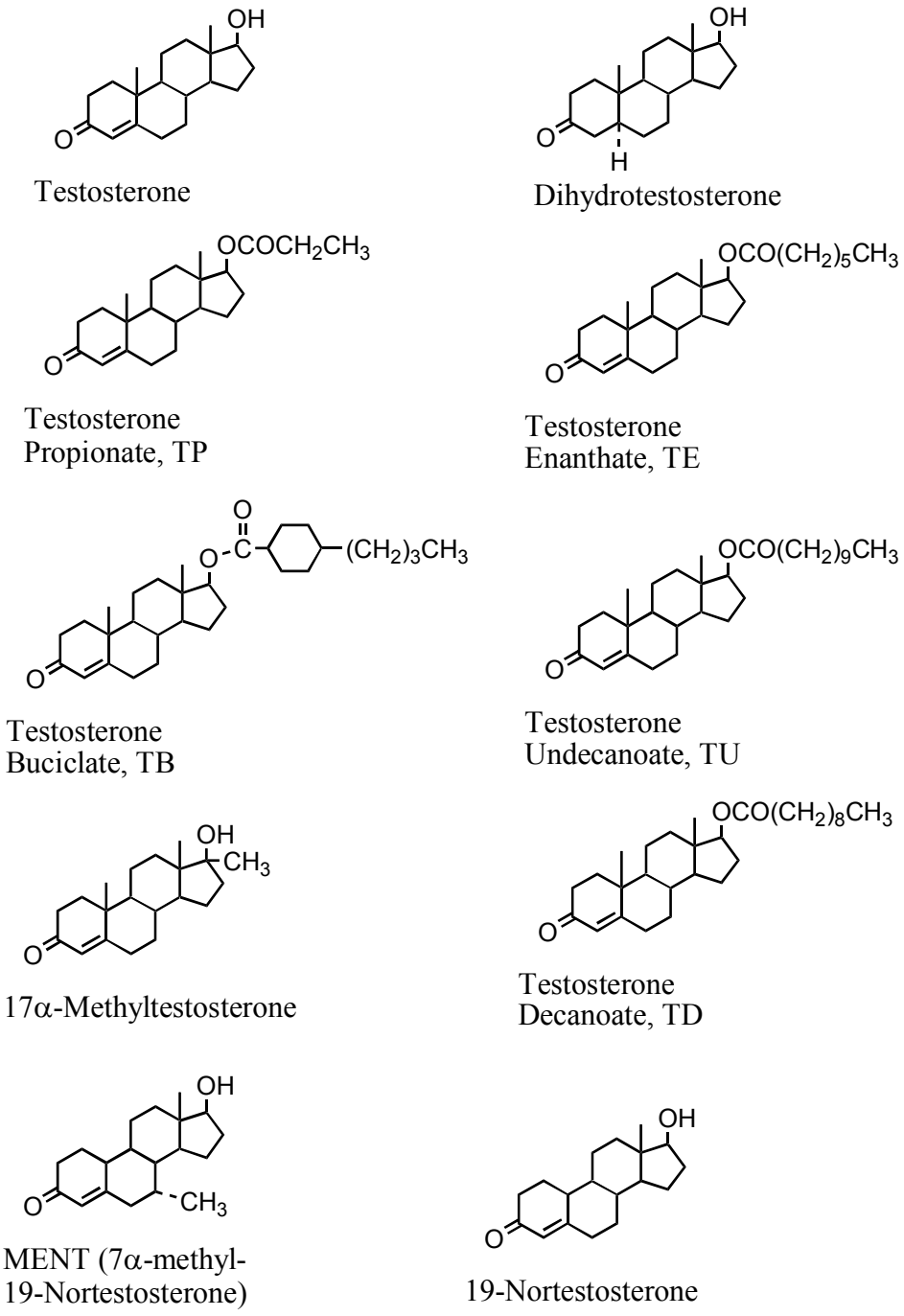

Figure 1. 4 The Chemical Structures of Steroidal Androgens.

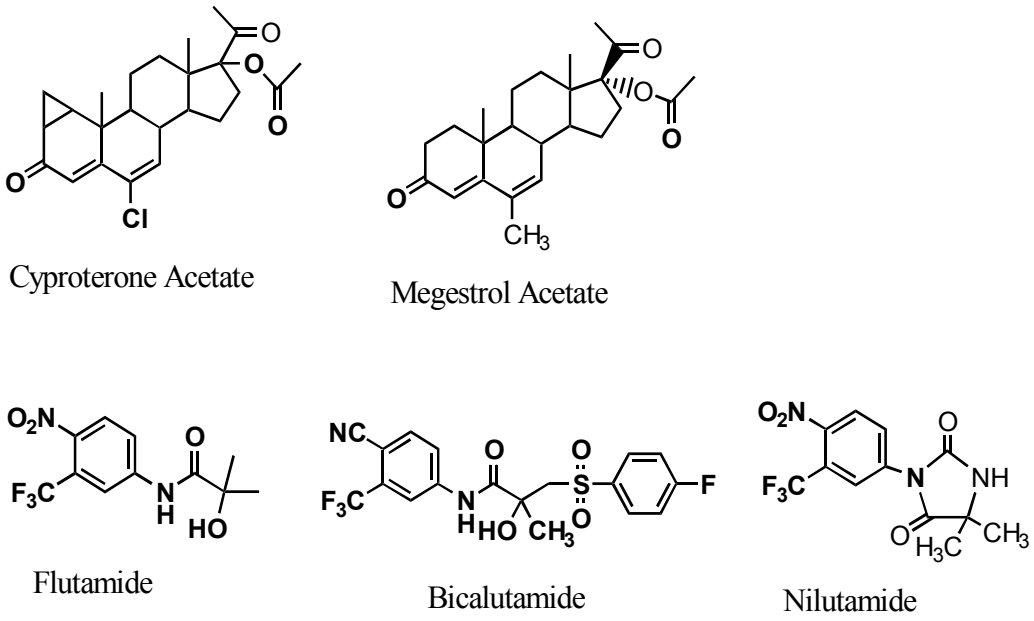

Figure 1. 5 The Chemical Structures of Steroidal and Nonsteroidal Antiandrogens.

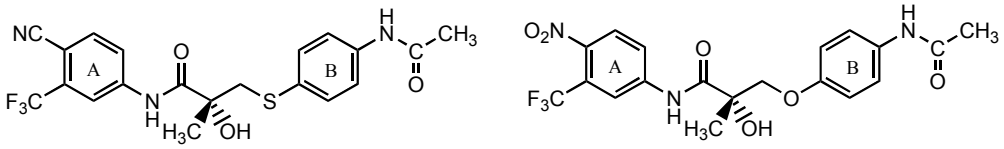

Acetothiolutamide

S-4

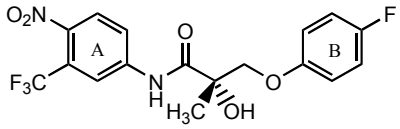

S-1

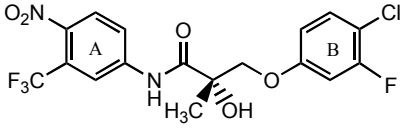

C-6

Figure 1. 6 The Chemical Structures of Recently Reported Nonsteroidal Androgens

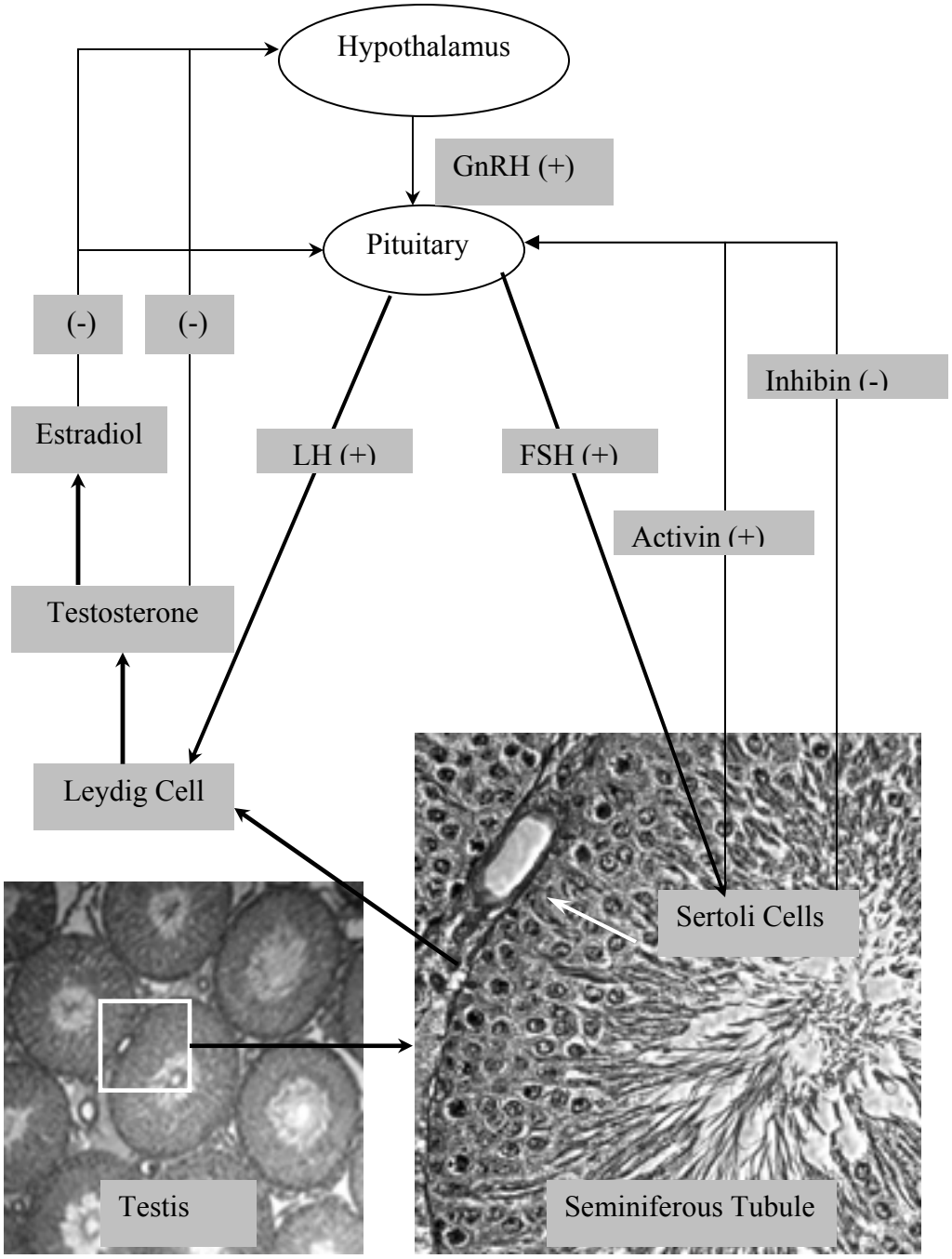

Figure 1. 7 Hypothalamus-Pituitary-Testis Axis of Androgen Regulation.

The production of testosterone is regulated by hormones produced in the hypothalamus and pituitary. (+) represents positive feedback and (-) represents negative feedback.

Androgen	Ethnicity	Androgen dose	Study size (n)	Azoospermia % (n)	Severe Oligozoospermia % (n)	Oligozoospermia % (n)	Reference
TE	Caucasion	100 mg/week i.m.	18	30 (6)	22 (4)	6 (1)	73
	Mixed	200 mg/week i.m.	225	65 (157)	13 (29)	3.5 (8)	75
	Mixed	200 mg/week i.m.	357	75 (267)	n/a	23 (83)	76
TU	Chinese	500 mg/4 week i.m.	12	92 (11)	8 (1)	0 (0)	74
	Chinese	1000 mg/4 week i.m.	12	100 (12)	0 (0)	0 (0)	74
	Chinese	1000 mg loading + 500 mg/4 week i.m.	305	93 (284)	2 (6)	2 (6)	77
	Caucasion	1000 mg/4 week i.m.	14	50 (7)	29 (4)	7 (1)	78
	Chinese	1000 mg/8 week i.m.	21	67 (14)	n/a	n/a	79
T Pellets	n/a	400 mg	10	0 (0)	0 (0)	0 (0)	80
	n/a	800 mg	10	40 (4)	0 (0)	0 (0)	80
	n/a	1200 mg	9	56 (5)	44 (4)	0 (0)	81
MENT Ac Implant 400 μg/day	n/a	1	12	0 (0)	0 (0)	0 (0)	82
	n/a	2	11	18 (2)	n/a	18 (2)	82
	n/a	4	12	58 (7)	n/a	8 (1)	82

Table 1. 1 Recent Studies Using Androgen Single Regimen for Hormonal Male Contraception (n > 9).

Severe oligozoospermia: <1 million sperm/mL; Oligozoospermia: 1 to 3 million sperm/mL.

Androgen + Progestin	Ethnicity	Androgen dose	Progestin dose	Study size (n)	Azoospermia % (n)	Severe Oligozoospermia % (n)	Oligozoospermia % (n)	Reference
TE + DMPA	Indonesian	100 mg/week i.m.	100 mg/4 week i.m.	10	100 (10)	0 (0)	0 (0)	94
	Indonesian	200 mg/week i.m.×7, then every 3 weeks	25 mg/6 week i.m.	45	96 (43)	4 (2)	0 (0)	95
	Indonesian	250 mg/week i.m.	200 mg/4 week i.m.	10	100 (10)	0 (0)	0 (0)	94
	Caucasian	250 mg/week i.m.	200 mg/4 week i.m.	10	60 (6)	0 (0)	40 (4)	96
19-Nortestosterone + DMPA	Indonesian	200 mg/week i.m.×7, then every 3 weeks	25 mg/6 week i.m.	45	98 (44)	2 (1)	0 (0)	95
	Caucasian	200 mg/3 week i.m.	250 mg/6 week i.m.	12	50 (6)	33 (4)	17 (2)	97
T + DMPA	n/a	800 mg Pellets	300 mg single dose i.m.	10	90 (9)	0 (0)	10 (1)	80
	n/a	800 mg/4 or 6 month Pellets	300 mg/3 month i.m.	55		94 (53)		98

Table 1. 2 Recent Studies Using Testosterone-DMPA for Hormonal Male Contraception (n >10).

Severe oligozoospermia: <1 million sperm/mL; Oligozoospermia: 1 to 3 million sperm/mL.

Androgen + Progestin	Ethnic origin	Androgen dose	Progestin dose	Study size (n)	Azoospermia % (n)	Severe Oligozoospermia % (n)	Oligozoospermia % (n)	Reference
TE + CPA	Caucasian	100 mg/week i.m.	5 mg/day p.o.	9	67 (6)	33 (3)	0 (0)	101
	Caucasian		12.5 mg/day p.o.	5	60 (3)	20 (2)	0 (0)	100
	Caucasian		25 mg/day p.o.	5	100 (5)	0 (0)	0 (0)	100
	Caucasian		50 mg/day p.o.	5	60 (3)	0 (0)	20 (1)	99
	Caucasian		100 mg/day p.o.	5	100 (5)	0 (0)	0 (0)	99
	Caucasian	200 mg/week i.m.	5 mg/day p.o.	7	0 (0)	57 (4)	29 (2)	101
TU + CPA	Caucasian	1000 mg/6 week i.m.	20 mg/day p.o.	24	54 (13)	46 (9)	0 (0)	102

Table 1. 3 Recent Studies Using Androgen Plus CPA for Hormonal Male Contraception (n > 5).

Severe oligozoospermia: <1 million sperm/mL; Oligozoospermia: 1 to 3 million sperm/mL.

Androgen + Progestin	Ethnicity	Androgen dose	Progestin dose	Study size (n)	Azoospermia % (n)	Severe Oligozoospermia % (n)	Oligozoospermia % (n)	Reference
TE + LNG	Caucasian	100 mg/week i.m.	125 µg/day p.o.	18	61 (11)	28 (5)	6 (1)	103
	Caucasian	100 mg/week i.m.	250 µg/day p.o.	18	78 (14)	11 (2)	0 (0)	103
	Caucasian	100 mg/week i.m.	500 µg/day p.o.	18	67 (12)	11 (2)	17 (3)	73
	Mixed	100 mg/week i.m.	4 rods Norplant II	14	93 (13)	7 (1)	0 (0)	104
TU + LNG	Caucasian	1000 mg/6 week i.m.	250 µg/day p.o.	14	57 (8)	29 (4)	14 (2)	78
	Chinese	250 mg/4 week i.m.	2 rods Sino-Implant	16	38 (6)	0 (0)	6 (1)	61
	Chinese	500 mg/8 week i.m. (4 weeks after LNG implantation)	4 rods, 75mg/each	21	62 (?)	n/a	24 (?)	79
	Chinese	1000 mg/8 week i.m. (4 weeks after LNG implantation)	4 rods, 75mg/each	20	90 (19)	n/a	5 % (1)	79
T+ LNG	Mixed	2 patches/day Testoderm TTS	4 rods Norplant II	20	35 (7)	25 (5)	10 (2)	104
	Mixed	2 patches/day Testoderm TTS	125 µg/day p.o.	15	30 (5)	7 (1)	7 (1)	104

Table 1. 4 Recent Studies Using Androgen Plus LNG for Hormonal Male Contraception (n > 13).

Severe oligozoospermia: <1 million sperm/mL; Oligozoospermia: 1 to 3 million sperm/mL.

Androgen + Progestin	Ethnic origin	Androgen dose	Progestin dose	Study size (n)	Azoospermia % (n)	Severe Oligozoospermia % (n)	Oligozoospermia % (n)	Reference
TE + DSG	Caucasian	50 mg/week i.m.	150 µg/day p.o.	7	57 (4)	14 (1)	0 (0)	105
	Caucasian		300 µg/day p.o.	8	100 (8)	0 (0)	0 (0)	106
	Caucasian	100 mg/week i.m.	150 µg/day p.o.	8	100 (8)	0 (0)	0 (0)	105
	Caucasian		150 µg/day p.o.	7	57 (4)	43 (3)	0 (0)	106
	Caucasian		300 µg/day p.o.	8	75 (6)	0 (0)	13 (1)	106
	Caucasian		300 µg/day p.o.	8	88 (7)	13 (1)	0 (0)	105
T Pellet	Asian	400 mg/12 week	150 µg/day p.o.	18	61 (11)	11 (2)	11 (2)	107
	Black			9	100 (9)	0 (0)	0 (0)	108
	Caucasian			13	85 (11)	15 (2)	0 (0)	107
	Caucasian			8	75 (6)	25 (2)	0 (0)	109
	Caucasian			7	71 (5)	14 (1)	0 (0)	109
	Mixed			11	82 (9)	0 (0)	1 (11)	108
	Asian	400 mg/12 week	300 µg/day p.o.	18	100 (18)	0 (0)	0 (0)	107
	Black			8	100 (18)	0 (0)	0 (0)	108
	Caucasian			15	100 (18)	0 (0)	0 (0)	107
	Mixed			12	67 (8)	0 (0)	0 (0)	108
T transdermal patch + DSG	Caucasian	patch, 5 mg/day	75 µg/day p.o.	4	0 (0)	25 (1)	0 (0)	110
	Caucasian	patch, 5 mg/day	150 µg/day p.o.	6	50 (3)	0 (0)	0 (0)	110
	Caucasian	patch, 5 mg/day	300 µg/day p.o.	7	71 (5)	0 (0)	0 (0)	110

Table 1. 5 Recent Studies Using Androgen Plus DSG for Hormonal Male Contraception.

Severe oligozoospermia: < 1 million sperm/mL; Oligozoospermia: 1 to 3 million sperm/mL.

Androgen + Progestin	Ethnicity	Androgen dose	Progestin dose	Study size (n)	Azoospermia % (n)	Severe Oligozoospermia % (n)	Oligozoospermia % (n)	Reference
TU + NETE	Caucasian	1000 mg/6 week i.m.	200 mg/6 week i.m.	14	93 (13)	0 (0)	0 (0)	111
	Caucasian		200 mg/6 week i.m.	14	93 (13)	7 (1)	0 (0)	112
	Caucasian		400 mg/6 week i.m.	14	93 (13)	7 (1)	0 (0)	112
	Caucasian	1000 mg/8 week i.m.	200 mg/8 week i.m.	10	90 (9)	n/a	n/a	113
	Caucasian	1000 mg/12 week i.m.	200 mg/12 week i.m.	8	38 (3)	13 (1)	13 (1)	113
T-Pellet + ENG	Caucasian	400 mg/12 week pellet	1 rod Implanon	14	64 (9)	7 (1)	21 (3)	115
	Caucasian		2 rods Implanon	14	64 (9)	29 (4)	0 (0)	115
	Caucasian		3 rods Implanon	14	100 (14)	0 (0)	0 (0)	116
TD + ENG	Mix	400 mg/4 week	300 μg/day p.o.	43	96 (41)	4 (2)	0 (0)	114
		400 mg/6 week	300 μg/day p.o.	40	83 (33)	15 (6)	2 (1)	114

Table 1. 6 Recent Studies Using Androgen Plus NETE or ENG for Hormonal Male Contraception.

Severe oligozoospermia: < 1 million sperm/mL; Oligozoospermia: 1 to 3 million sperm/mL.

CHAPTER 2

IN VITRO STRUCTURAL ACTIVITY RELATIONSHIPS (SARS) OF NONSTEROIDAL ANDROGEN RECEPTOR LIGANDS WITH MULTIPLE-SUBSTITUENTS IN THE AROMATIC B-RING

2.1 INTRODUCTION

The androgen receptor (AR) belongs to a superfamily of nuclear receptor proteins that are ligand-dependent transcriptional factors. Binding of androgens triggers the conformational change of the AR to its active DNA-binding state, which further interacts with target genes and regulates gene transcription in the presence of appropriate cofactors (118). Androgens act on a number of different target organs by interacting with the AR expressed in those tissues. As such, the AR is a key modulator of processes involved in differentiation, homeostasis, and development of male secondary character (119). Androgen-related diseases include hypogonadism, male infertility, prostate cancer, delay of puberty, hirsutism, and male pattern baldness, etc.

According to their functional activity or chemical structures, androgen receptor ligands generally are classified as androgens or antiandrogens and steroidal or nonsteroidal ligands, respectively. Androgens are widely used for androgen deficient diseases, androgen replacement in aging men, and the development of hormonal male contraception. Two naturally occurring steroidal androgens are testosterone and its metabolite, 5α-dihydrotestosterone (DHT). However, the unfavorable physiochemical properties and steroidal related side effects of these androgens prevent their widespread use in the clinic. Antiandrogens are clinically used to treat androgen-sensitive diseases, including prostate cancer, hirsutism, and androgenic alopecia in women. One class of presently available antiandrogens are steroidal derivatives, such as cyproterone acetate

(120) and megestrol acetate (121), which possess mixed agonist and antagonist androgenic activity and cross-react with progesterone receptor. The other class of antiandrogens is nonsteroidal derivatives, such as flutamide, bicalutamide, and nilutamide, which block the AR specifically by competitive binding with the receptor and are widely used for prostate cancer treatment. Considerable efforts are still being made to develop antiandrogens more potent than the first pure antiandrogen (i.e., flutamide), since it is superior to steroidal compounds in terms of AR specificity, selectivity, and pharmacokinetic properties (122).

As compared to nonsteroidal antiandrogens, the discovery and development of nonsteroidal androgens was delayed for decades. During attempts to affinity label the AR, our laboratory identified the first class of nonsteroidal androgens, which are structural derivatives of flutamide and bicalutamide (56, 63). More recently, new nonsteroidal selective androgen receptor modulators (SARMs) were developed in an attempt to obtain derivatives with higher *in vitro* activity (57, 62, 123), *in vivo* selective pharmacologic activity (59), and better pharmacokinetic properties (58, 60, 124). In previous studies, we outlined the key structure-activity relationships (SARs) of bicalutamide-related androgen agonists to improve AR binding affinity and AR-mediated transcriptional activation. These include the importance of an electron-withdrawing group at the *para*-position of the A-ring, a methyl group linked to the chiral carbon (***S***-isomer for ether linked compounds and ***R***-isomer for thio-ether linked compounds), an ether or thio-ether linkage, and an electronegative or acetamido group at the *para*-position of the B-ring. Although the size of the substituent on the B-ring was proved to be limited by both molecular modeling (61) and experiments (57), a novel SARM with a *para*-chloro group and a *meta*-fluoro group in the B-ring demonstrated more efficacious and potent pharmacologic activity than **S-1**, one of our known SARMs (65). Furthermore, the addition of electronegative and/or hydrophobic substituents in the B-ring may provide a feasible approach to modulate the hepatic metabolism or endocrine effects of SARMs , and identify new drug candidates for other therapeutic applications, including oral, male hormonal contraception. We therefore hypothesized that changing the type, position, and number of substituents in the B-ring would affect the binding affinity, functional activity, and tissue-selectivity of SARMs. The studies reported herein are the first to examine the

in vitro and *in vivo* pharmacologic effects of AR ligands with multiple substituents in the B-ring.

We investigated the effects and SARs of such structural modifications on AR binding affinity and AR-mediated transcriptional activation *in vitro*. This information reveals how important the B-ring structure is for AR binding and functional activity, information that is valuable for our understanding of the interaction between nonsteroidal androgen ligands and the subpocket within the AR binding site and that information provides candidates for *in vivo* pharmacologic studies.

2.2 MATERIALS AND METHODS

2.2.1 Chemicals and Animals

The *S*-isomer of synthetic AR ligands (Table 1) was synthesized in our laboratory with a purity greater than 99% using previously described methods (57, 60). [17α-methyl-^{3}H] Mibolerone ([^{3}H]-MIB, 84 Ci/mmol) and unlabeled MIB were purchased from PerkinElmer Life Sciences (Boston, MA). Hydroxyapatite (HAP) was purchased from Bio-Rad Laboratories (Hercules, CA). EcoLite (+) scintillation cocktail was purchased from ICN Research Products Division (Costa Mesa, CA). LipofectAMINE and Passive Lysis Buffer were purchased from Promega (Madison, WI). All other chemicals were purchased from Sigma-Aldrich (St. Louis, MO).

Male Sprague-Dawley rats were purchased from Harlan Bioproducts for Science (Indianapolis, IN). All animals were maintained on a 12h light/dark cycle with food and water available *ad libitum*. The animal protocol was reviewed and approved by the Institutional Laboratory Animal Care and Use Committee of The Ohio State University.

2.2.2 Buffers

Homogenization buffer contained 50 mM Tris, 1 mM potassium phosphate, and

0.1 mM phenylmethylsulfonyl fluoride (PMSF). Incubation buffer contained 10 mM Tris, 1.5 mM EDTA, 0.25 M sucrose, 10 mM sodium molybdate, and 1 mM PMSF. At 4 °C, The incubation buffer was adjusted to pH 7.4 using 1 M HCl. Washing buffer contained 50 mM Tris at pH 7.2. Beta-galactosidase buffer consisted of 200 mM sodium phosphate, 2 mM magnesium chloride, 100 mM B-mercaptoethanol, and 1.33 mg/ml ONGP. Luciferase assay buffer contained 25 mM glycylglycine, 15 mM magnesium chloride, and 5 mM ATP.

2.2.3 Preparation of Cytosolic ARs

Rat prostate cytosolic AR was prepared from ventral prostates of castrated male Sprague-Dawley rats using established methods (63). One day prior to the tissue preparation days, animals were castrated under anesthesia. The ventral prostate of each animal was dissected, removed from excess fat, and was minced with surgical blades. One ml of homogenization buffer was mixed with every 500 mg of prostate tissue. Prostate tissue was then homogenized in a mechanical homogenizer (Model PRO 200, Pro Scientific, Monroe, CT). The homogenate was centrifuged at 114000 g for 1 hour. The cytosolic supernatant, containing the AR, was decanted, aliquoted, and stored at -80°C. All process was carried out at 4°C.

2.2.4 *In Vitro* AR Binding Affinity

The AR binding affinity of synthetic AR ligands was determined using an *in vitro* radioligand competitive binding assay as previously described (62). An aliquot of AR cytosol was incubated with 1 nM of [^{3}H]MIB and 1 mM of triamcinolone acetonide at 4 °C for 18 h in the absence or presence of ten increasing concentrations of the compound of interest (10^{-1} nM to 10^4 nM). Triamcinolone was added into the incubation to block possible cross reaction between [^{3}H]MIB and the progesterone receptor (PR). Nonspecific binding of [^{3}H]MIB was determined by adding excess unlabeled MIB (1000 nM) to the incubate. After incubation, the AR-bound radioactivity was isolated using the HAP method (125). HAP pellets were centrifuged at 1000 g for 10 minutes and then

rinsed with washing buffer for three times. The bound radioactivity was extracted by an aliquot (1 mL) of ethanol at room temperature for 1 hour. The suspensions were centrifuged at 1000 g for 10 minutes and an aliquot (1 mL) of the supernatant was mixed well with 5 mL of scintillation cocktail. Radioactivity was counted in a Beckman LS6500 liquid scintillation counter (Beckman Instruments Inc., Irvine, CA).

2.2.5 *In Vitro* AR-Mediated Transcriptional Activation

The *in vitro* functional activities of nonsteroidal AR ligands were determined by the ability of each ligand to induce or suppress AR-mediated transcriptional activation, using a modification of the method of (62). On day one, CV-1 cells at 90% confluence were transiently transfected in T-175 flasks. The transfection was carried out in serum-free DMEM medium using LipofectAMINE according to the manufacturer's instruction. Cells in each flask were transfected with 0.8 μg of a human AR expression construct (pCMVhAR; generously provided by Dr. Donald Tindall, Mayo Clinic), 4 μg of an androgen-dependent luciferase reporter construct (pMMTV-Luc, generously provided by Dr. Ron Evans, Salk Institute), and 4 μg of a b-galactosidase expression construct (pSV-b-galactosidase; Promega Corporation) for 10 h. Cells were allowed to recover for 12 h and were then seeded into 24-well plates at a density of 8×10^4 cells/well and allowed to recover for an additional 10 h before drug treatment.

Cells were treated with the compound of interest (final concentrations ranging from 1 nM to 1,000 nM) in the presence or absence of 1 nM of DHT for 12 h. After drug treatment, cells were washed with ice-cold PBS twice and lysed with 110 μl/well of passive lysis buffer for 30 min at room temperature. An aliquot (50 μl) of cell lysate from each well was used for β-galactosidase assays and the other 50 μL of cell lysate was used for luciferase assays using the method previously described (62). An aliquot of (50 μL) of 1 mM beetle luciferin (Promega, Madison, WI) was added to 50 μL of cell lysate from each well and the luminescence was read by an AutoLumate LB953 luminometer (Wallace Inc., Gaithersberg, MD). Beta-galactosidase activity was determined by adding 50 μL of lysate to 50 μL of beta-galactosidase assay buffer. The optical density was

measured on a UV spectrophotometer (Cary Model 1E, Varian Associates, Sunnyvale CA) at a wavelength of 420 nm.

2.2.6 Data Analysis

2.2.6.1 AR Binding Affinity

The specific binding of [^{3}H]MIB at each concentration of the compound of interest was calculated by subtracting the nonspecific binding of [^{3}H]MIB, and expressed as the percentage of the specific binding in the absence of the compound of interest (B_0). The concentration of compound that reduced B_0 by 50% (i.e., IC_{50}) was determined using WinNonlin (Pharsight Corporation, Mountain View, CA). The equilibrium binding constant (Ki) of the compound of interest was calculated by $K_i = K_d \times IC_{50} /(K_d + L)$, where Kd was the dissociation constant of [^{3}H]MIB (0.19 ± 0.01 nM), and L was the concentration of [^{3}H]MIB used in the experiment (1 nM). The Ki value of each compound of interested was further compared.

2.2.6.2 AR-Mediated Transcriptional Activation

The transcriptional activity in each well was calculated as the ratio of luciferase activity to β-galactosidase activity to avoid variations caused by cell number and transfection efficiency. Transcriptional activity induced by compound of interest was expressed as the percentage of transcriptional activity induced by 1 nM of DHT.

2.3 RESULTS

2.3.1 *In Vitro* AR Binding Affinity

The structure-activity relationships (SARs) that define the interaction of nonsteroidal compounds with the AR have been studied intensively in our laboratories (56, 57, 60, 62, 63, 123) and by several other investigators (126-131). In our search for novel SARMs, a *para*-fluoro substituted analog known as **S-1** (59) was used as our

starting point. **S-1** was synthesized as a bicalutamide derivative and identified as a potent SARM with high *in vitro* and *in vivo* activities (64), and potential therapeutic application to benign prostatic hyperplasia. As shown in Figure 1, the key structural elements of **S-1** include an electron-deficient aromatic A-ring, a CH_3 linked to the chiral carbon (***S***-isomer), an ether linkage, and electronegative substituents on the aromatic B-ring. Recent crystallographic evidence suggests that the main difference between the AR binding pockets of steroidal androgens (e.g., DHT) and bicalutamide-related SARMs may be the unique interactions of the B-ring with additional amino acids near tryptophan 741 (132). A series of nonsteroidal compounds with multiple substitutions on the B-ring were designed and synthesized to study the effects of structural modification on AR-binding affinity and functional activity. The AR binding affinity of synthetic compounds was determined using an *in vitro* radioligand competitive binding assay and were reported here as the inhibition constant (Ki) in Tables 1 through 3. Synthetic compounds showed a wide range of binding affinity with Ki values ranging from 1.0 to 51 nM, which provide an index of the relative binding affinities of compounds of interest.

Table 1 shows the Ki values of compounds with a *para*- nitro group in the A-ring and two substituents in the B-ring. Previous studies from our laboratories confirmed that with a single substituent in the B-ring, *para*-substitution was superior to *meta*-substitution in terms of AR binding (62, 123). Compared with the lead compound **S-1**, the incorporation of an additional fluoro, chloro, or methyl group at the *ortho*-position (i.e., R1 of the general structure shown in Table 1) of the B-ring increased or maintained AR-binding affinity, suggesting that a electron-deficient B-ring is more favorable. We also examined the influence of an additional *meta*-fluoro substituent (i.e., R2) on AR binding affinity of a series of compounds with varying *para*-substituent. The order of AR binding affinity was NO_2 > F> Cl > $NHCOCH_3$ (**C-11** > **C-3** > **C-6** > **C-7**), corroborating crystallographic evidence with bicalutamide that hydrogen bonding with *para*-substituent of SARMs is likely important for high affinity binding. AR binding affinity was optimum when there were two electron-withdrawing groups present in the *meta* and *para* positions of the aromatic B-ring. This is exemplified by the low Ki values (~ 1.0 nM) of **C-10** and **C-11**. For these two compounds, moving the chloro group or fluoro group from the *meta*-position (**C-10** and **C-11**) to the *ortho*-position (**C-9** and **C-12**) resulted in a ten-

fold decrease in AR binding affinity. However, this regioselectivity was not true for other pairs of compounds **C-1**/**C-3**, **C-4**/**C-5**, and **C-6**/**C-8**, indicating that this selectivity may be substituent-dependent.

Having demonstrated that AR binding affinity improved by incorporation of additional electron-withdrawing groups in the aromatic B-ring, we applied more halogen groups to the B-ring to further explore the effects of substitution positions and types on AR binding affinity. Compounds with three or five substituents in the B-ring were designed and synthesized. As shown in Table 2, when three fluoro groups were incorporated in the different positions of the B-ring, high AR binding affinity was maintained in each case. In particular, **C-18**, which bears fluoro groups at the 2, 4 and 5-positions of the B-ring, had significantly improved AR binding affinity with a Ki value as low as 1.0 nM. These three positions of the B-ring were also the best combination for chloro-substituted compounds (**C-19** to **C-22**) in terms of binding affinity. However, in general, changing a fluoro group to a chloro group (**C-13**/**C-19**, **C-14**/**C-20**, **C-17**/**C-21**, and **C-18**/**C-22**) significantly decreased AR binding affinity, indicating that the size of substituents is critical when the B-ring has more than two substituents. To protect the aromatic B-ring from possible oxidation *in vivo*, all positions of the B-ring were occupied by introducing five halogen groups (**C-23** and **C-24**). The excellent AR binding affinity of **C-23** suggested that as many as five fluoro groups are well tolerated in the B-ring. Again, replacing the fluoro group of **C-23** with a chloro group increased the Ki value but still maintained a reasonable AR binding affinity *in vitro*.

In previous studies, AR binding affinity was significantly improved by replacing the *para*-cyano group with a nitro group in the aromatic A-ring of hydroxyflutamide analogs (56), but it was not true in bicalutamide derivatives (57). To investigate the effects of such a change on the AR binding affinity of compounds with multiple substituents in the B-ring, some compounds listed in Table 1 and Table 2 were structurally modified as shown in Table 3. For compounds with two fluoro groups in the B-ring (**C-25** and **C-16**), binding affinities were similar between analogs bearing a nitro group or a cyano group at the *para*-position of the A ring (compare **C-25** vs **C-1** and **C-26** vs **C-3**). In all other cases, the cyano-substituted compounds exhibited at least a 2-

fold lower AR binding affinity than their corresponding nitro-substituted counterparts (pair **C-27**/**C-9**, **C-28**/**C-10**, and **C-29**/**C-23**).

2.3.2 *In Vitro* AR-Mediated Transcriptional Activation

Transcriptional activation induced by DHT plateaued at a concentration of 1 nM, as reported previously (56) and was used as a positive control (i.e., 100%) in each experiment to facilitate comparison to previous studies (62). Agonist activity and antagonist activity were determined in the absence or presence of 1 nM DHT, respectively. Ligands were defined as full AR agonists if compounds induced a similar level of transcriptional activation as that of 1 nM DHT in the agonist assay; ligands were defined as partial agonists if compounds induced a certain level (≥ 10%) of transcriptional activation but still significantly lower than that of 1 nM DHT in the agonist assay; ligands were defined as antagonists if compounds induced a low level (< 10%) of transcriptional activation in the agonist assay and a significantly decreased level of transcriptional activation induced by 1 nM DHT in the antagonist assay (62).

Figure 2 shows the AR agonist activity of ligands with a *para*-nitro group in the A-ring and two substituents in the B-ring. All compounds examined in this series induced transcriptional activation in a concentration-dependent manner. In the presence of 1 nM DHT, no significant antagonist activity (data not shown) was observed for this series of compounds, suggesting that the introduction of two substituents does not interfere with the formation of the transcriptional active ligand binding domain (LBD) conformation. Except for **C-12**, the incorporation of two substituents in the aromatic B-ring maintained or improved the AR-mediated transcriptional activation as compared to previous studies (62). Compounds **C-1** through **C-11** therefore were identified as full agonists, while **C-12** was identified as a partial agonist. Among this series of compounds, **C-11** was one of the ligands with the highest AR binding affinity (Ki = 1.0 ± 0.02 nM) and exhibited the most potent agonist activity. It is noteworthy that at a concentration of 10 nM, compounds with high binding affinity (e.g., Ki < 5) are as efficient as 1 nM DHT. Additional consistency between AR binding affinity and transcriptional activation is that the *meta*- and *para*-

positions of the B-ring are the optimal substituent positions for both binding and functional activities as exemplified by **C-3**, **C-6**, and **C-11**. However, inconsistency was also observed. For instance, **C-10** (Ki ~ 1 nM) displayed less potent agonist activity than **C-3** and **C-6**, which demonstrated 4 to 5-fold lower binding affinity than **C-10**. Also interestingly, moving the fluoro-group of **C-11** from its *meta*-position to the *ortho*-position (**C-12**) of the B-ring caused a 10-fold increase of the Ki value but a more than 1000-fold decrease of the AR-mediated transcriptional activation. Although the presence of a fluoro group at the ortho-position of the B-ring was well tolerated in terms of binding with the AR, it appears to prevent the formation of transcriptionally active AR.

C-13 through **C-24** are AR ligands with a *para*-nitro group in the A-ring and three or five substituents in the B-ring. AR-mediated transcriptional activity induced by these compounds is shown in Figure 3. Five compounds were identified as full agonists (**C-13**, **C-14**, **C-18**, **C-22**, and **C-23**), while the other seven compounds were identified as partial agonists. In antagonist assays, full agonists exhibited no significant effect on transcriptional activation induced by 1 nM DHT, while partial agonists demonstrated a concentration-dependent inhibition with about a 60% decrease for the most potent ligand (i.e., **C-17**) (data not shown). Obviously, for these compounds with more than two substituents in the B-ring, the substituent type, number, and/or positions are critical in terms of both binding affinity and functional activity. **C-18** and **C-22**, two ligands that showed the optimal binding affinity, induced the most potent and efficacious transcriptional activation. It is important to note that the transcriptional activation induced by 1 nM **C-18** was as potent and efficacious as that of DHT, although **C-18** (Ki ~ 1 nM) demonstrated a 2~3-fold lower binding affinity than DHT (Ki ~ 0.4 nM). As the B-ring became bulkier due to incorporation of more substituents, we observed significant regioselectivity. Pairs of compounds (**C-14**/**C-15**, **C-18**/**C-17**, and **C-22**/**C-21**) were designed so that only a single substituent position was different in the B-ring between these two ligands. Moving the fluoro/chloro group from position 5 to position 6 (i.e., from R4 to R5 in the structure of Table 2) of the B-ring significantly decreased the transcriptional activation, indicating that the presence of two electron-withdrawing groups at both *ortho*-positions of the B-ring deteriorated the functional activity. For compounds **C-19** to **C-21**, the low transcriptional activation was most likely due to their

low binding affinity. However, despite the higher binding affinity of compounds **C-15** to **C-17**, functional activity induced by these compounds was lower than that of **C-13** and **C-14**. Again, both binding affinity and the potential to form a transcriptionally active AR of a ligand are important to determine its functional activity. The incorporation of five fluoro groups in the B-ring was well tolerated for both binding affinity and functional activity. Changing the *para*-fluoro group of **C-23** to a chloro group (**C-24**) significantly decreased its agonist activity.

In binding studies, all five ligands with a *para*-CN group in the A-ring demonstrated similar or lower binding affinity than their counterparts with a *para*-NO_2 group. In agonist assays, all five cyano-substituted compounds exhibited reasonably high agonist activity and were identified as full agonists, since no significant inhibition of activity induced by DHT was observed (data not shown). Comparing compounds with nitro-and cyano-substituents in the A-ring, it was obvious that the presence of the A-ring cyano group led to a slightly decreased functional activity in all cases, which correlated well with the binding affinity.

2.4 DISCUSSION

In the present study, we demonstrated that novel AR agonists with a wide range of *in vitro* and *in vivo* activities can be designed by structural modifications of the SARM pharmacophore. Early SAR work on hydroxyflutamide analogs (133) confirmed the importance of an electron-deficient aromatic A-ring and the substituents attached to the carbon atom bearing a tertiary hydroxyl group. Two years later, Tucker *et al*. (126) reported that the AR binding and antiandrogen activity of hydroxyflutamide and bicalutamide derivatives were optimum when the 4-substituent in the A-ring was either a cyano or nitro group and the 3-substituent was a chloro or trifluoromethyl group. Interestingly, partial androgen agonist activity was observed in some trifluoromethyl substituted compounds, indicating that AR agonists can be designed and developed by subtle structural modification (s) of known AR antagonists. When this concept was applied to discover novel bicalutamide-related AR agonists in our laboratories, important

in vitro SARs for the AR-binding affinity and agonist activity were further gained (62), including a *para*-nitro group in the A-ring, a trifluoromethyl group linked to the chiral carbon (R-isomer), a sulfide linkage, and a *para*-N-alkylamido group in the B-ring. However, when these compounds were tested *in vivo*, no pharmacologic activity was observed due to their unfavorable pharmacokinetic properties (58). Further structural modification was made to overcome this problem by changing the sulfide linkage to an ether bridge, which resulted in the successful discovery of SARMs (59). As shown in Figure 1, the lead compound of current studies (**S-1**) contains a *para*-nitro group and a *meta*-trifluoromethyl group in the A-ring, a methyl group linked to the chiral carbon (***S***-isomer), an ether linkage, and a *para*-fluoro substituent in the B-ring. Due to the difficult chemical synthesis and the small advantage of a trifluoromethyl group over a methyl group in terms of the AR binding affinity, a methyl group was linked to the chiral carbon. Results from our binding studies showed that the incorporation of multiple substituents in the B-ring was well tolerated. Four compounds with multiple electron-withdrawing substituents in the B-ring (**C-10**, **C-11**, **C-18**, and **C-23**) exhibited high AR binding affinity (Ki ~ 1.0 nM), which was even slightly higher than that of the endogenous androgen – testosterone. The significantly improved AR binding affinity was most likely either due to either increased hydrophobic interactions (**C-10**, **C-18**, and **C-23**) between halogen groups with the B-ring subpocket or the formation of hydrogen bonds formed between the *para*-nitro group (**C-11**) and the AR binding site. Crystallographic studies are underway in out laboratory to define the precise mechanism. Several structural modifications increased AR binding affinity, indicating that there is a free space surrounding the B-ring within the AR binding pocket, which is flexible to accommodate ligands with different B-ring. The interaction between the AR and bicalutamide-related compounds with multiple substituents in the B-ring is favorable if: 1) two electron-withdrawing groups are at the *para*- and *meta*-positions of the B-ring; 3) a H-bond acceptor is present at the *para*-position of the B-ring; 4) three substituents are at the 2-, 4-, and 5-positions of the B-ring; and 5) fluoro groups instead of chloro groups are incorporated in the B-ring for compounds with more than two substituents in that ring.

Structural studies on the ligand binding domain (LBD) of the AR revealed an α-helical sandwich fold consisting of 12 α-helices (H1-H12) and a short β-sheet (15, 16),

which was consistent with the canonical structure as those of the other nuclear hormone receptor LBDs (15, 16, 134-136). Comparison of the LBD structures of nuclear receptor in complex with an agonist and an antagonist suggested that receptor ligands trigger different conformation changes, especially the position of helix H12 and the unwinding of helix H11(134, 137). Upon binding with an agonist, helix H12 folds back, seals the ligand-binding pocket as a lid, and forms a surface to interact with coactivators. On the other hand, binding with an antagonist is thought to induce unwinding of helix H11 and allow helix H12 to disrupt the overall surface topography of AF-2 and/or the recruitment of coactivators (138). By incorporation of multiple substituents in the B-ring of our known SARM, novel AR agonists with higher binding affinity and pharmacologic activity were discovered, suggesting that the LBP around the B-ring area is flexible and that substituents with smaller atomic sizes can be well tolerated to stabilize a transcriptionally active LBP conformation via creation of new hydrophobic interactions or hydrogen bond. (56). It is noteworthy that significant regioselectivity was observed for compounds with three substituents in the B-ring. Functional activity changed between agonist and partial agonist by moving the fluoro/chloro groups along the aromatic ring and was optimized at the 2, 4, and 5-positions of the B-ring (**C-18** and **C-22**). Since high AR binding affinity was maintained by incorporation of three fluoro groups in the B-ring (**C-13** to **C-18**), functional results suggested that this regioselectivity may be related to the precise position of helix H12, strongly stabilized by pure agonist (**C-18**) or destabilized by partial agonist (**C-15** to **C-17**). It is possible that an intermediate position of helix H12 exists for these partial agonists. Additional site-directed mutagenesis data with the AR suggests that the interaction between Thr^{877} of the AR and nonsteroidal ligands is important to determine the functional activity of this series of AR ligands. For example, the partial agonist, **C-17**, behaved as a potent and pure agonist in CV-1 cells co-transfected with mutant AR (T877A) and reporter plasmids (forthcoming report). Up to date, crystal structures are only available for the wild type AR-LBD complex with steroidal AR ligands (15, 16) but not with any nonsteroidal AR ligands. Chemical structures reported herein make it possible to study the detailed interactions between the aromatic B-ring and AR-LBP, especially within the unique subpocket of nonsteroidal compounds. Ongoing studies focused on this subject include molecular modeling, site-

directed mutagenesis, and X-ray crystallography to define the precise molecular mechanisms underlying SARM interactions with the AR and functional activity.

In summary, current studies revealed the *in vitro* SARs of AR ligands; proved that structural modification in the B-ring of our known SARMs is a feasible method to discover and develop novel SARMs with higher AR binding affinity and *in vitro* functional activity.

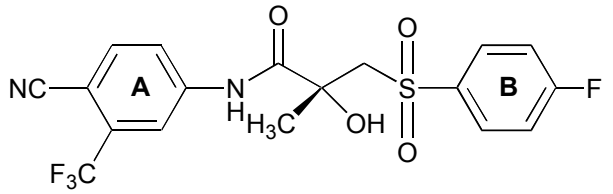

Bicalutamide (Casodex)

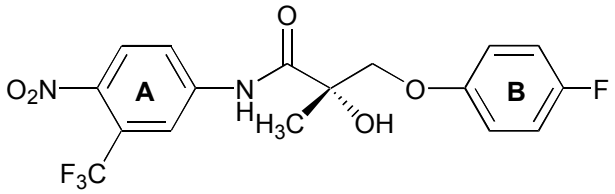

S-1

Figure 2. 1 Chemical Structures of Bicalutamide and **S-1**.

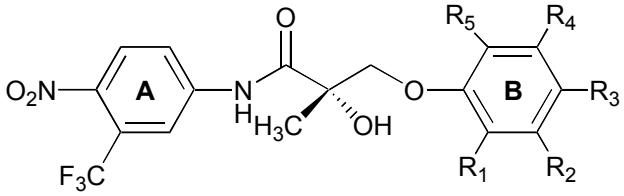

Compound	R1	R2	R3	R4	R5	Ki [a] (nM)
* S-1	H	H	F	H	H	6.1 ± 0.2
C-1	F	H	F	H	H	3.2 ± 0.3
C-2	CH_3	H	F	H	H	6.0 ± 0.7
C-3	H	F	F	H	H	3.4 ± 0.6
C-4	H	Cl	F	H	H	10.3 ± 2
C-5	Cl	H	F	H	H	5.2 ± 0.9
C-6	H	F	Cl	H	H	4.9 ± 0.3
C-7	H	F	$NHC(O)CH_3$	H	H	6.7 ± 0.9
C-8	F	H	Cl	H	H	2.6 ± 0.2
C-9	Cl	H	Cl	H	H	9.7 ± 2
C-10	H	Cl	Cl	H	H	1.0 ± 0.09
C-11	H	F	NO_2	H	H	1.0 ± 0.02
C-12	F	H	NO_2	H	H	11 ± 3

Table 2. 1 AR Binding Affinity of Nonsteroidal AR Ligands with a *para*-NO_2 in the A-ring and Two Substituents in the B-ring.

* The Ki value of **S-1** was previously reported in (59)

[a] The AR binding affinity (Ki) of each compound was determined using a competitive binding assay as described in the *Materials and Methods* section. Data represent the mean ± S.D. of three experiments.

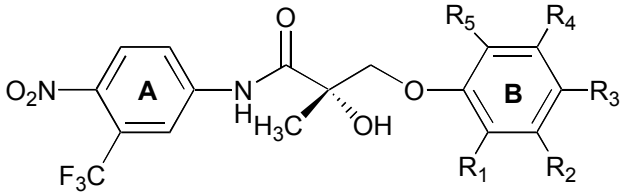

Compound	R1	R2	R3	R4	R5	Ki [a] (nM)
* S-1	H	H	F	H	H	6.1 ± 0.2
C-13	F	F	F	H	H	11 ± 1
C-14	F	F	H	F	H	9.1 ± 0.6
C-15	F	F	H	H	F	7.5 ± 1
C-16	H	F	F	F	H	4.0 ± 0.9
C-17	F	H	F	H	F	5.9 ± 0.6
C-18	F	H	F	F	H	0.97 ± 0.1
C-19	Cl	Cl	Cl	H	H	50 ± 5
C-20	Cl	Cl	H	Cl	H	27 ± 2
C-21	Cl	H	Cl	H	Cl	51 ± 5
C-22	Cl	H	Cl	Cl	H	10 ± 2
C-23	F	F	F	F	F	1.4 ± 0.3
C-24	F	F	Cl	F	F	11 ± 0.8

Table 2. 2 AR Binding Affinity of Nonsteroidal AR Ligands with a *para*-NO_2 in the A-ring and Three or Five Substituents in the B-ring.

* The Ki value of **S-1** was previously reported in (59)

[a] The AR binding affinity (Ki) of each compound was determined using a competitive binding assay as described in the *Materials and Methods* section. Data represent the mean ± S.D. of three experiments.

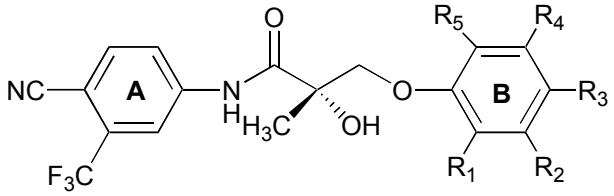

Compound	R1	R2	R3	R4	R5	Ki [a] (nM)
* S-1	H	H	F	H	H	6.1 ± 0.2
C-25	F	H	F	H	H	4.5 ± 0.4
C-26	H	F	F	H	H	4.1 ± 0.6
C-27	Cl	H	Cl	H	H	20 ± 0.2
C-28	H	Cl	Cl	H	H	5.0 ± 0.2
C-29	F	F	F	F	F	6.8 ± 0.4

Table 2. 3 AR Binding Affinity of Nonsteroidal AR Ligands with a *para*-CN in the A-ring and Multiple-Substituents in the B-ring.

* The Ki value of **S-1** was previously reported in (59)

[a] The AR binding affinity (Ki) of each compound of interested was determined using a competitive binding assay as described in the *Materials and Methods* section. Data represent the mean ± S.D. of three experiments.

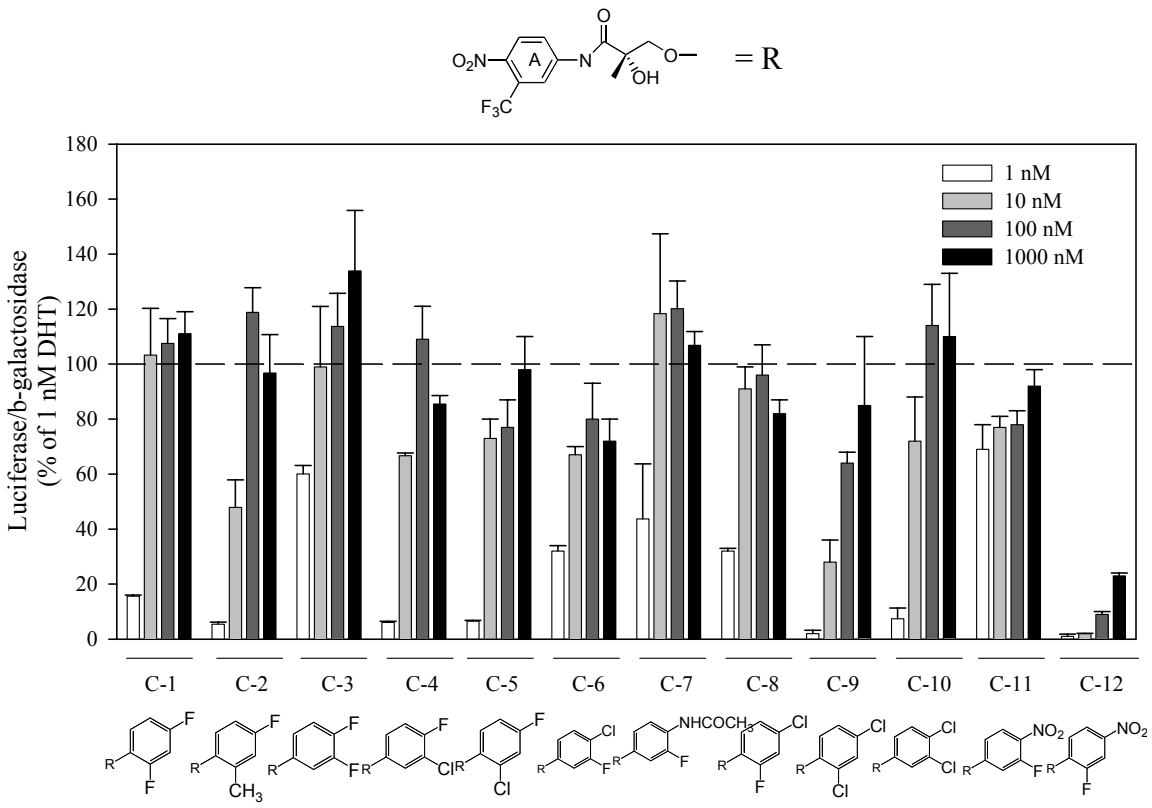

Figure 2. 2 AR-mediated Transcriptional Activation of Nonsteroidal AR Ligands with a *para*-NO_2 in the A-ring and Two Substituents in the B-ring.

CV-1 cells were transfected with a human AR plasmid, an androgen-responsive luciferase reporter plasmid, and a constitutively expressed β-galactosidase plasmid in a T-175 flask using LipofectAMINE. After transfection, cells were plated onto 24-well plates and allowed to recover for 12 h before drug treatment. Cells were then treated with vehicle or increasing concentrations of AR ligands alone or together with 1 nM of DHT for 24 h. Luciferase activity in each well was normalized with the β-galactosidase activity and then expressed as the percentage of that induced by 1 nM DHT. Each bar represents mean ± S.D. (n=3).

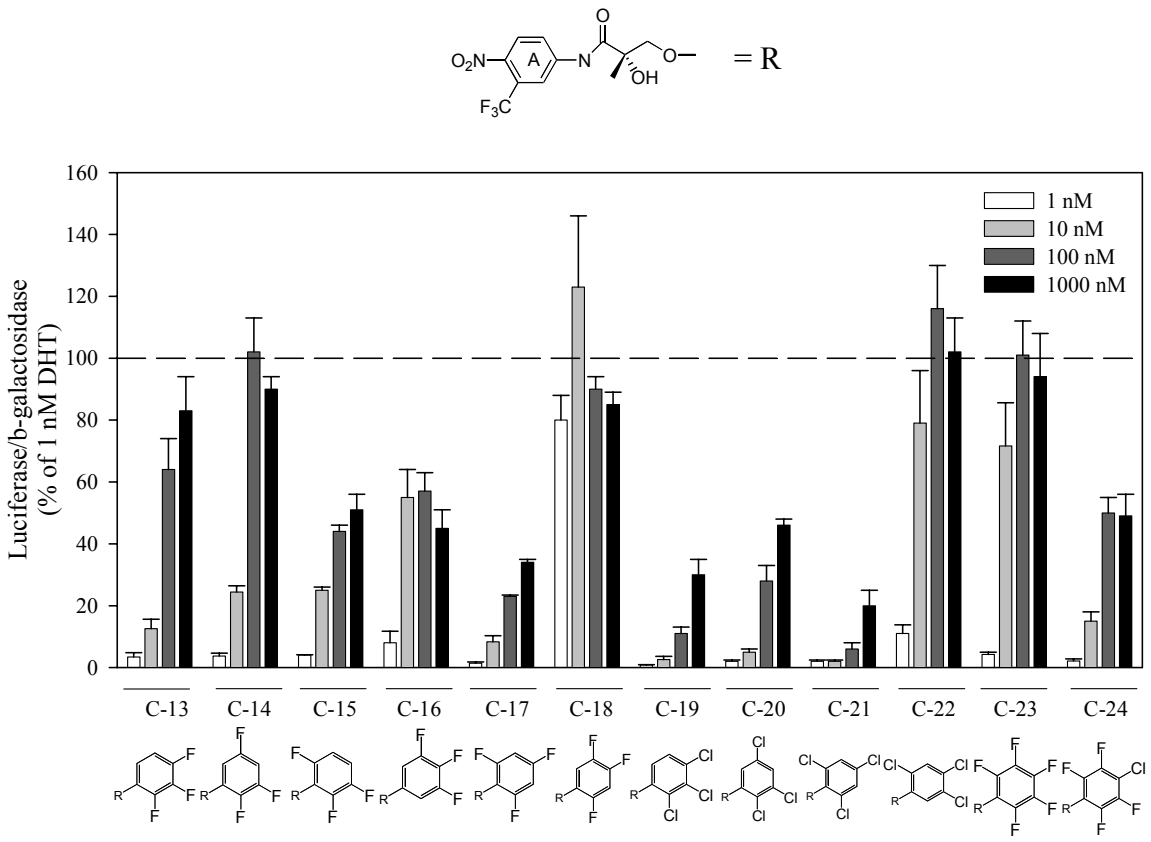

Figure 2. 3 AR-mediated Transcriptional Activation of Nonsteroidal AR Ligands with a *para*-NO_2 in the A-ring and Three or Five Substituents in the B-ring.

CV-1 cells were transfected with a human AR plasmid, an androgen-responsive luciferase reporter plasmid, and a constitutively expressed β-galactosidase plasmid in a T-175 flask using LipofectAMINE. After transfection, cells were plated onto 24-well plates and allowed to recover for 12 h before drug treatment. Cells were then treated with vehicle or increasing concentrations of AR ligands alone or together with 1 nM of DHT for 24 h. Luciferase activity in each well was normalized with the β-galactosidase activity and then expressed as the percentage of that induced by 1 nM DHT. Each bar represents mean ± S.D. (n=3).

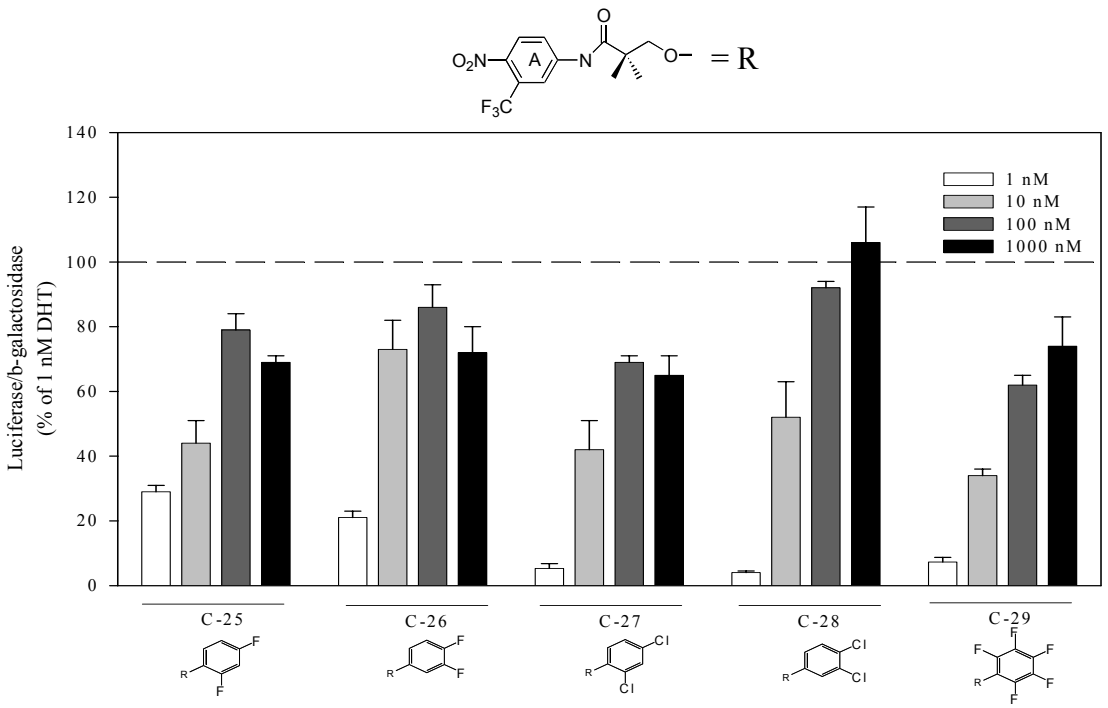

Figure 2. 4 AR-mediated Transcriptional Activation of Nonsteroidal AR Ligands with a *para*-CN in the A-ring and Multiple Substituents in the B-ring.

CV-1 cells were transfected with a human AR plasmid, an androgen-responsive luciferase reporter plasmid, and a constitutively expressed β-galactosidase plasmid in a T-175 flask using LipofectAMINE. After transfection, cells were plated onto 24-well plates and allowed to recover for 12 h before drug treatment. Cells were then treated with vehicle or increasing concentrations of AR ligands alone or together with 1 nM of DHT for 24 h. Luciferase activity in each well was normalized with the β-galactosidase activity and then expressed as the percentage of that induced by 1 nM DHT. Each bar represents mean ± S.D. (n=3).

CHAPTER 3

IN VIVO STRUCTURAL ACTIVITY RELATIONSHIPS (SARS) OF NONSTEROIDAL ANDROGEN RECEPTOR LIGANDS WITH MULTIPLE-SUBSTITUENTS IN THE AROMATIC B-RING

3.1 INTRODUCTION

Endogenous androgens, mainly testosterone and dihydrotestosterone (DHT), play important roles for male development and maintenance of male secondary characteristics. Pharmacologic effects of androgens include androgenic (masculinizing) effects and anabolic (tissue-building) effects. In men, androgenic effects are those that relate to the growth of male reproductive tract or to the development of secondary sexual characteristics, including increases in the length and diameter of the penis, development of the prostate and scrotum, and the appearance of the pubic, auxiliary, and facial hair (139). Anabolic effects of testosterone are the changes that occur in the nonreproductive tract tissue, such as bone, larynx, libido and sexual potential, muscle, and fat distribution. Immediately after the discovery of testosterone, its anabolic activity was recognized as a potential therapeutic application for patients with protein-deficient conditions (140). However, the androgenic activity of testosterone prevented its usage in women and children. The potential therapeutic value of the anabolic activity of testosterone and its commercial availability stimulated many investigators to discover anabolic reagents, using structural modifications of steroidal androgens.

Testosterone (Figure 3.1, a) undergoes multiple metabolism pathways *in vivo* and demonstrates differential effects on target tissues. Two active metabolites, 17β-estradiol (Figure 3.1, b) and 5α-dihydrotestosterone (DHT, Figure 3.1, c), are from aromatization or reduction of the Δ4 bond of testosterone, respectively. In many tissues, including

certain areas of the brain, liver, adipose tissue, and testis, the aromatase converts testosterone to estradiol (141, 142), which in turn exerts its effects via estrogen receptors. In male reproductive tracts and skin, testosterone undergoes 5α-reduction to DHT, which amplifies the apparent potency of its precursor(44, 143). Studies using specific 5α-reductase inhibitors revealed that the androgenic activity of testosterone on ventral prostate and seminal vesicles significantly decreased but no changes were observed on muscle, indicating that this differential effect of testosterone action is due to the high and low 5α-reductase activity in reproductive tissues and muscle, respectively (41-44). Recently, tissue-selective steroidal androgen was discovered by incorporation of 7α-methyl substituent in testosterone derivatives. For instance, 7α-methyl-19-nortestosterone (MENT) demonstrate tissue selectivity with higher anabolic activity than androgenic activity both in rat (45) and in hypogonadal men (46). This tissue selectivity was mainly due to the inability of 5α-reductase to metabolize MENT.

Although the discover of anabolic-androgenic steroids with tissue-selectivity provide potential alternative to testosterone for androgen replacement and male contraception (85), these compounds can only be administered via pellet implantation or transdermal patches due to their poor pharmacokinetic and physiochemical properties. On the other hand, potent and efficacious selective androgen receptor modulators (SARMs) reported by Yin et. al. are superior in terms of physicochemical, pharmacokinetic properties, and flexibility of structural modifications. Potential therapeutic applications include treatment for hypogonadism, delayed puberty, protein-deficiency induced by HIV/AIDS, male contraception, and aging males.

Our previous *in vitro* structure-activity relationship (SAR) studies of bicalutamide-related AR ligands revealed that compounds with higher AR binding affinity and *in vitro* functional activity can be successfully achieved by introduction of multiple electron-withdrawing substituents in the aromatic B-ring. We hypothesized that some AR ligands with improved AR binding affinity and/or *in vitro* functional activity will exhibit more potent and efficacious pharmacologic activity then the lead compound *in vivo*.

3.2 MATERIALS AND METHODS

3.2.1 Animals

Male Sprague-Dawley rats were purchased from Harlan Bioproducts for Science (Indianapolis, IN). All animals were maintained on a 12h light/dark cycle with food and water available *ad libitum*. The animal protocol was reviewed and approved by the Institutional Laboratory Animal Care and Use Committee of The Ohio State University.

3.2.2 *In Vivo* Pharmacologic Activity of Novel AR Ligands in Castrated Male Rats

The *in vivo* pharmacologic activity of each synthetic androgen receptor ligand was examined in five male Sprague-Dawley rats weighing approximately 200 g using Hershberger assay (144). Animals were castrated via a scrotal incision under anesthesia 24 h prior to drug treatments and received daily subcutaneous injections of compounds of interest at a dose rate of 1 mg/day for 14 days. All compounds of interest were freshly dissolved in vehicle containing DMSO (5%, v/v) in PEG 300 before dose administration. Additional two groups of animals with or without castration received vehicle only and served as castrated or intact control groups, respectively. Animals were sacrificed at the end of the treatment. Plasma samples were collected and stored at –80 °C for future use. The ventral prostate, seminal vesicles, and levator ani muscle were removed, cleared of extraneous tissue, and weighed. All organ weights were normalized to body weight and compared. The weights of prostate and seminal vesicles were used to evaluate androgenic activity, while the levator ani muscle weight was used as a measurement of anabolic activity. Compounds with higher anabolic activity than androgenic activity were identified as SARMs.

3.2.3 *In Vivo* Pharmacodynamics of SARMs in Castrated Male Rats

Some SARMs identified by method described in 3.2.2 were selected and further examined for pharmacodynamics of these compounds in castrated male rats. For each

compound of interest, 20 Sprague-Dawley rats weighing approximately 200 g were purchased and randomly divided into four groups with five rats per group. Group 1 through 4 received daily subcutaneous injection of SARM of interest at a dose rate of 0.1, 0.3, 0.5, and 0.75 mg/day, respectively. Combined the pharmacologic activity obtained at a dose rate of 1 mg/day (3.2.2), dose-response relationship of each SARM on androgenic tissues and anabolic tissue were simulated using a pharmacodynamic model - Sigmoidal Emax model with a baseline effect and WinNonlin software (Pharsight Corporation, Mountain View, CA). The maximal response (Emax) induced by each SARM and the dose rate of individual SARM that induced 50% of its maximal response (ED_{50}) were obtained and compared. The Emax value indicated the efficacy of each compound, whereas the ED_{50} indicated its potency. The relative efficacy of each compound to testosterone propionate (TP) was defined as the ratio of (Emax of the compound) to (Emax of TP). The relative potency was defined as the ratio of (ED_{50} of TP) to (ED_{50} of the compound). The Emax and ED_{50} values of TP in each organ were previously reported by Yin *et al*. (59).

3.2.4 Statistical Analyses

All statistical analyses were performed using single-factor ANOVA with the α value set a priori at $p < 0.05$.

3.3 RESULTS

3.3.1 *In Vivo* Pharmacologic Activity of Novel AR Ligands in Castrated Male Rats

As we have shown that certain structural modifications in the B-ring of nonsteroidal AR ligands improved the binding affinity and functional activity *in vitro*. However, high binding affinity and agonist activity not always predict high pharmacologic activity *in vivo* as showed by Yin et al. (58). Therefore, the pharmacologic effects of selected ligands on prostate, seminal vesicles, and levator ani muscle were further evaluated in castrated male rats at a dose rate of 1 mg/day. Since replacing a *para*-

nitro with a cyano group in the A-ring decreased the binding affinity and transcriptional activity of these compounds in most cases, compounds selected for *in vivo* studies all bear a *para*-nitro group in the A-ring. Figure 3.2 and figure 3.3 showed the effects of novel AR ligands in prostate and seminal vesicles, respectively, while figure 3.4 showed the anabolic activity (levator ani muscle) of AR ligands of interest. Due to the depletion of endogenous testosterone, castration lead to a rapid reduction of the weight in prostate, seminal vesicles, and levator ani muscle to 6.2, 8.1, and 41% of intact levels, respectively. According to the potency of AR agonists, the weights of androgen-dependent organs would remain low, partially, or fully maintained after drug treatment.

Figure 3.2 shows B-ring chemical structures of novel AR ligands selected for *in vivo* pharmacologic activity studies. For compounds with two substituents in the B-ring, the position and size of substituents clearly played an important role in the pharmacologic activity *in vivo*. Introduction of a fluoro group at the para-position (**C-1**) resulted an equipotent pharmacologic activity as that of **S-1**, suggesting that a small electron-withdrawing group at this position is well tolerated. However, changing this *ortho*-fluoro group to a methyl group (**C-2**) significantly decreased its anabolic activity, consisting with the SAR from the AR binding studies. Interestingly, when the *ortho*-fluoro group was moved to the *meta*-position of the B-ring (**C-3**), it demonstrated much higher pharmacologic activity than **C-1**, largely due to the improved transcriptional activation instead of the AR binding affinity. The *ortho*/*meta*-regioselectivity was further illustrated by the potencies of **C-6**, **C-10**, and **C-11** compared with those of **C-8**, **C-9**, and **C-12**. When the *meta*-fluoro group of **C-3** was replaced by a chloro group (**C-4**), significantly decreased pharmacologic activity was observed, indicating that the size of *meta*-substituent is critical. Besides **S-1**, Yin et al. (59) identified another more potent SARM (**S-4**), which bears a relatively larger substituent (acetamido group) at the *para*-position of the B-ring. Therefore, larger substituents were also incorporated into that position to discover new SARs in current studies. Replacing the *para*-fluoro group with a chloro group resulted in a 3-fold increase in androgenic activity (pairs **C-1**/**C-8** and **C-3**/**C-6**) and 30% increase in anabolic activity (pair **C-1**/**C-8**). As we previously reported (59, 65), the maximum effect of our SARMs in levator ani muscle plateaued about 120 ~ 140% of the intact control level, therefore, the great improved pharmacologic effects of **C-6** over

C-3 were only shown in the prostate and seminal vesicles but not in the muscle. Although at a dose rate of 1mg/day, **C-6** demonstrated both high androgenic and anabolic activity, a complete dose-response study has shown that **C-6** remain tissue-selectivity over the physiologic dose range (Chapter 5). Surprisingly, replacing the *para*-fluoro group of **C-3** with a nitro group (**C-11**) decreased the pharmacologic effect, in spite of the fact that the AR binding affinity of **C-11** was three-fold higher than that of **C-3** *in vitro*. This relatively low activity of **C-11** may be due to its rapid metabolic property *in vivo* since both nitro groups on the A-ring and B-ring are two mobile groups of *in vivo* metabolism (Chen et al, in preparation).

Partial agonists (**C-12**, **C-14**, **C-15**, and **C-18**) identified *in vitro* failed to show any activity *in vivo*. Besides the low functional activity identified *in vitro*, fast metabolism rate of these compounds could also cause its inactivity *in vivo*. Consistent with results of *in vitro* studies, 2, 4, and 5-position in the B-ring are the optimal locations to incorporate three electron-withdrawing substituents. Among compounds with three substituents in the B-ring, only **C-19** and **C-23** exhibited high activity *in vivo*. **C-19** demonstrated significantly higher androgenic and anabolic activity than **S-1**, which **C-23** selectively increased the androgenic activity and maintained the anabolic activity as compared with **S-1**. Obviously, changing the type and position of substituents in the B-ring altered the androgenic activity/anabolic activity ratio in rats. Although the incorporation of five fluoro groups in the B-ring significantly improved the AR binding affinity and transcriptional activation *in vitro*, the *in vivo* pharmacologic activity was similar as that of **S-1**.

3.3.2 *In Vivo* Pharmacodynamics of SARMs in Castrated Male Rats

Pharmacologic results from a single high dose (1 mg/day) treatment revealed that structural modifications in the B-ring not only changed the efficacy but also the tissue selectivity of SARMs. **C-6** demonstrated equal efficacy in reproductive tissues and muscle. Due to its unique 'non-tissue selectivity' at a dose rate of 1 mg/day, **C-6** was studied separately and discussed in Chapter 5. Dose-response relationships of **C-1**, **C-3**, **C-10**, and **C-23** were further studied for additional *in vivo* SARs.

The pharmacologic activity of **C-1**, **C-3**, **C-10**, and **C-23** was in a dose-dependent manner in three organs examined. Figure 3.6 shows the androgenic activity and anabolic activity of **C-1** in castrated male rats, which is in a dose-dependent manner. The weights of prostate, seminal vesicles, and levator ani muscle were maximally maintained by **C-1** to 21.9, 10.4, and 80.2% of those in intact control animals, respectively (Figure 3.6 B). Accordingly, the ED_{50} values of **C-1** in these three organs were 0.33 ± 0.1, 0.66 ± 0.03, and 0.42 ± 0.09 mg/day, respectively (Figure 3.6 B). The significantly higher activity of **C-1** in the muscle than that in the prostate and seminal vesicles indicate that **C-1** is an efficacious SARM in rats. The only structural difference between **C-1** and our lead compound – **S-1** was the presence of a fluoro group at the *ortho* position of the B-ring of **C-1**. As reported previously, the Emax values of **S-1** in the prostate, seminal vesicles, and levator ani muscle were 14.9, 13.4, and 74.3% of those in the intact animals, respectively; the ED_{50} values of **S-1** in the prostate, seminal vesicles, and levator an muscle were 0.42 ± 0.04, 0.38 ± 0.26, and 0.44 ± 0.01 mg/day, respectively (59). Such structural modification slightly increased activity in prostate, maintained high anabolic activity in muscle, and tissue-selectivity in rats.

Figure 3.7 shows the pharmacologic activity of **C-3** in castrated male rats at dose rates ranging from 0.1 to 1 mg/day. The maximal effects of this compound in the prostate, seminal vesicles, and levator ani muscle were 59%, 27%, and 132% of those observed in intact animals, respectively. ED_{50} values of **C-3**, using non-linear regression analysis, in the prostate, seminal vesicles, and levator ani muscle were 0.65 ± 0.4, 0.58 ± 0.04, and 0.33 ± 0.09 mg/day, respectively. Table 3.1 lists Emax values, ED_{50} values, and relative efficacy and potency of compound of interest. Structurally compare with **S-1**, **C-3** bears an additional fluoro group at the *meta* position of the B-ring. Such structural modification resulted in significantly improved relative efficacy (Emax) as indicated by a 4-fold and a 1.8-fold increase in the prostate and levator ani muscle, respectively (Table 3.1). As to the relative potency, changes in each organ were not that obvious. The significant increase of the relative efficacy in the prostate was also observed in animals treated with **C-10** (Figure 3.8 A), suggesting that di-halogen substituents in the *meta* and *para* position of the B-ring induced more profound increase in androgenic activity than anabolic activity. Although AR-binding affinity of **C-10** (Ki = 1.0 nM) is greater than

that of **C-3** (Ki = 3.4 nM), **C-10** revealed relatively lower pharmacologic activity than **C-3** *in vivo*. This discrepancy may due to the significantly lower intrinsic activity of **C-10** as illustrated in the transcriptional activation studies.

As shown in Figure 3.9 B and Table 3.1, the Emax values of this compound in the prostate, seminal vesicles, and levator ani muscle were 20.4, 12.7, and 70.8% of those observed in intact animals, respectively. While the ED_{50} values of **C-24** in the prostate, seminal vesicles, and levator ani muscle were 0.63 ± 0.04, 0.62 ± 0.07, and 0.70 ± 0.003 mg/day, respectively. Although the pharmacologic activity of **C-24** (Figure 3.9 A) was comparable with that of **S-1**, it was surprisingly lower than what we expected. **C-24** bears five fluoro groups in the B-ring, which was originally designed to prevent possible oxidation metabolism on the B-ring *in vivo*. In comparison with **S-1**, both AR-binding affinity and *in vitro* AR-mediated transcriptional activation were significantly improved. Especially, the Ki value of **C-5** was as low as 1 nM. This unpredicted low pharmacologic activity indicated that the pharmacokinetic properties of this compound may be significantly different from those of **S-1** in rats.

3.4 DISCUSSION

We have successfully discovered a series of novel AR ligands (Chapter 2) with high AR-binding affinity and AR-mediated transcriptional activation using structural modifications of our lead compound, **S-1**, which is a potent and efficacious SARM previously identified in our laboratory (59). However, the correlation between *in vitro* function and *in vivo* pharmacologic activity was poor as reported by Yin el. al. (58). The purposes of the structural modifications of our study was to improve *in vivo* activity of AR ligands by increasing AR binding affinity, intrinsic functional activity, and/or plasma exposure.

Compounds selected for *in vivo* pharmacologic activity studies all demonstrated high AR binding affinity *in vitro* with Ki values smaller than 15 nM. Since the AR-mediated transcriptional activation *in vitro* does not always a correct predictor of *in vivo* activity (58), compounds identified as partial agonists from *in vitro* studies were also included in the current study. Despite of the similarity in chemical structures and high

AR binding affinity *in vitro*, this series of compounds revealed a wide rang of pharmacologic activity in castrated rats. After castration, organ weights of prostate and levator ani muscle decreased to 6.2 and 40.9% of those in the intact animals, respectively. Partial agonists, **C-12**, **C-14**, **C-15**, and **C-18**, failed to demonstrate any pharmacologic activity *in vivo*, indicating that the AR-mediated transcriptional activation assay is an important screening step to select potential candidates for *in vivo* studies in the future.

Among active compounds, **C-2** maintained the weight of ventral prostate and levator ani muscle at 11.4% and 51.5% of those in intact animals, respectively and exhibited both the lowest androgenic activity and anabolic activity in male rats. The highest androgenic activity (83.4%) and anabolic activity (123%) were observed in animals treated with **C-6** and **C-18**, respectively. This observation indicates that the introduction of different size and type of electron-withdrawing substituents in the B-ring not only change the potency but also alter the tissue selectivity of compounds of interest. For decades, differential effects in tissues have been clearly illustrated between testosterone and dihydrotestosterone (DHT). DHT shows more profound androgenic activity in the prostate and seminal vesicles than testosterone. The underlying mechanisms of differential effects between these two androgens are still mysteries. To investigate possible mechanisms, several studies have been done both *in vivo* and *in vitro*. Using 5α-reductase inhibitor to block the conversion between testosterone to DHT significantly diminished the potent effects of DHT in ventral prostate (41, 145-149), suggesting that DHT bears higher androgenic activity than testosterone. *In vitro* assays reveals that DHT demonstrated higher AR-binding affinity (150) and AR-mediated transcriptional activation (151). Moreover, two kinds of androgen response elements (AREs) were identified to response differentially to testosterone and DHT (152), which provides a possible molecular mechanism for the difference between these two androgens. Mechanisms of the tissue-selectivity among nonsteroidal AR modulators are as interesting as those between nonsteroidal AR modulators and endogenous steroidal androgens. Since compounds of interest demonstrated high AR binding affinity and similar physiochemical properties, the high androgenic activity of **C-6** and **C-19** may due to their higher intrinsic activity, unique binding mode with AR, and recruitment of co-factors.

In conclusion, *in vivo* pharmacologic results demonstrated that pharmacologic activity of a SARM is determined by several ligand characteristics, including AR binding affinity, transcriptional activation, and metabolic stability. The Androgenic activity/anabolic activity ratio of this series of compounds can be altered by incorporation of halogen at the *para*-position of the B-ring. The effects of these compounds on hormonal regulation, including luteinizing hormone (LH), follicle stimulating hormone (FSH), and testosterone may also be changed by structural modifications.

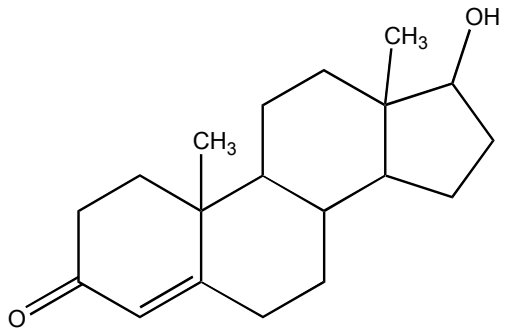

(a) Testosterone

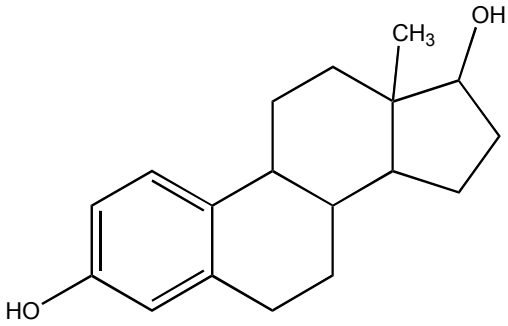

(b) Estradiol-17β

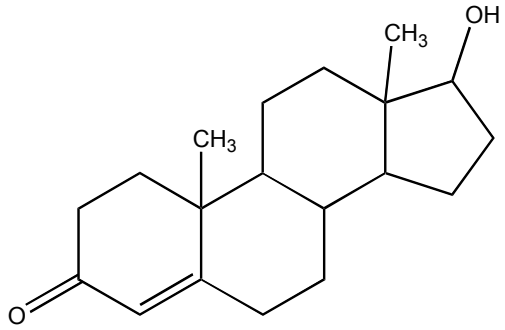

(c) Dihydrotestosterone (DHT)

Figure 3. 1 Chemical Structures of Testosterone, Estradiol-17β, and 5α-dihydrotestosterone (DHT).

Compound	Structure of the B-ring
S-1	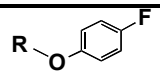
C-1	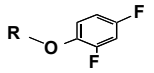
C-2	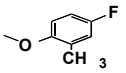
C-3	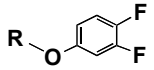
C-4	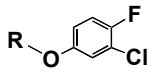
C-6	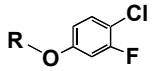
C-8	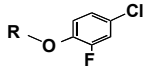
C-10	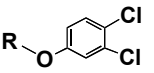
C-11	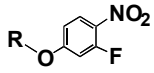
C-12	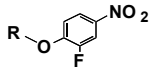
C-14	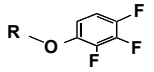
C-15	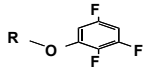
C-18	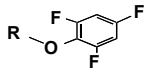
C-19	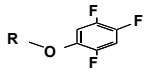
C-23	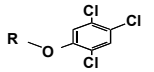
C-24	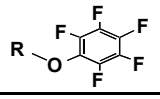

Figure 3. 2 The B-ring Chemical Structure of Novel AR Ligands Examined for *In vivo* Pharmacologic Activity.

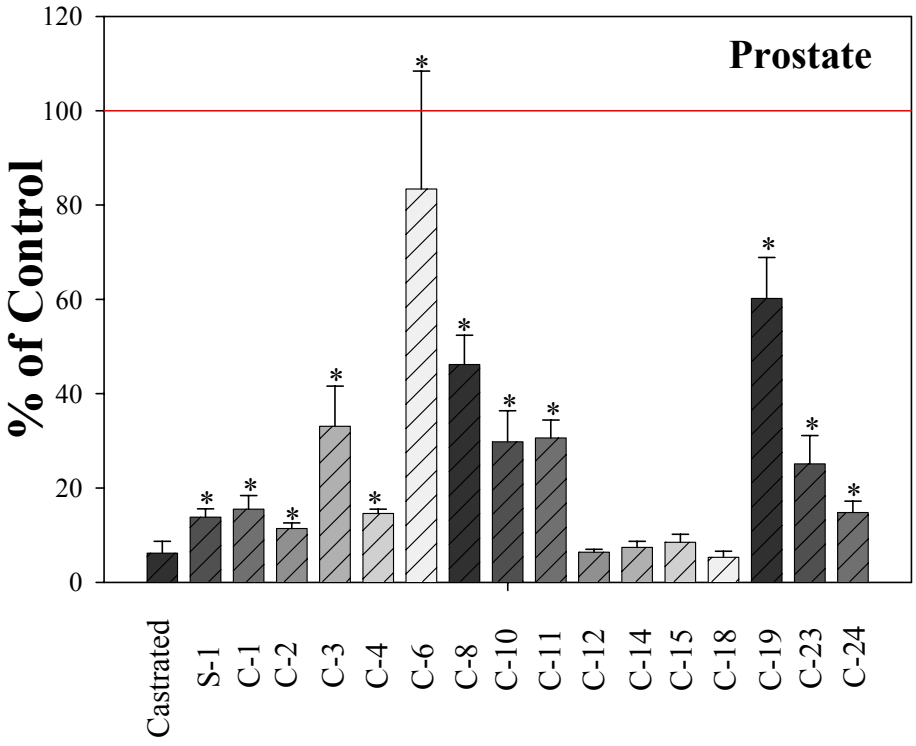

Figure 3. 3 The Effect of Novel AR Ligands on the Prostate in Castrated Male Rats.

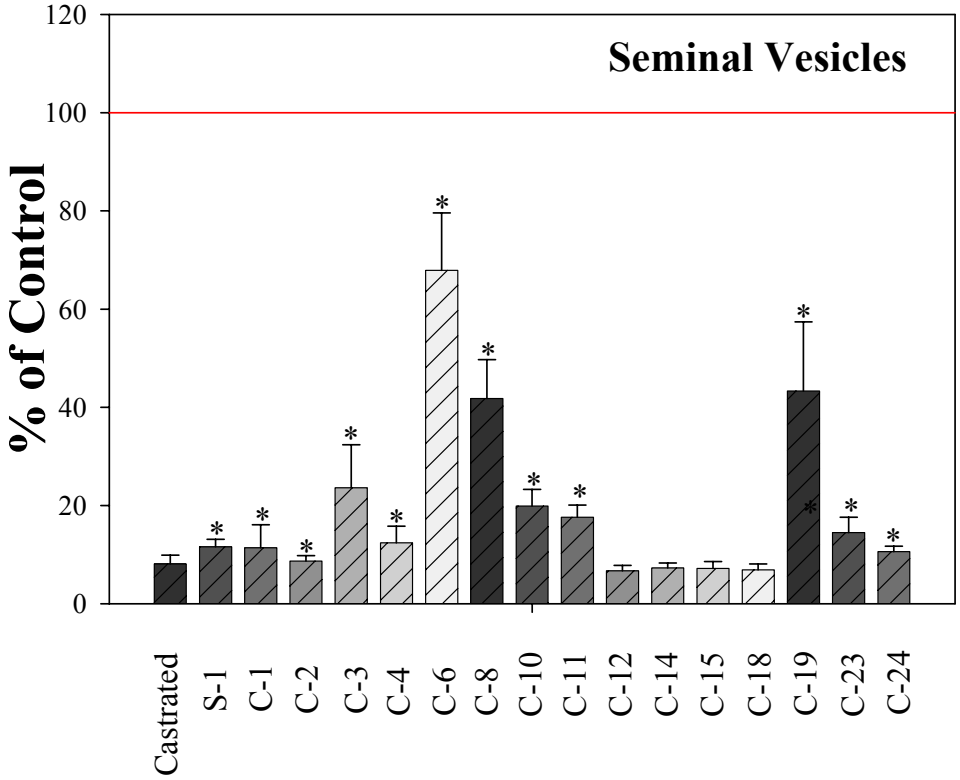

Figure 3. 4 The Effect of Novel AR Ligands on Seminal Vesicles in Castrated Male Rats.

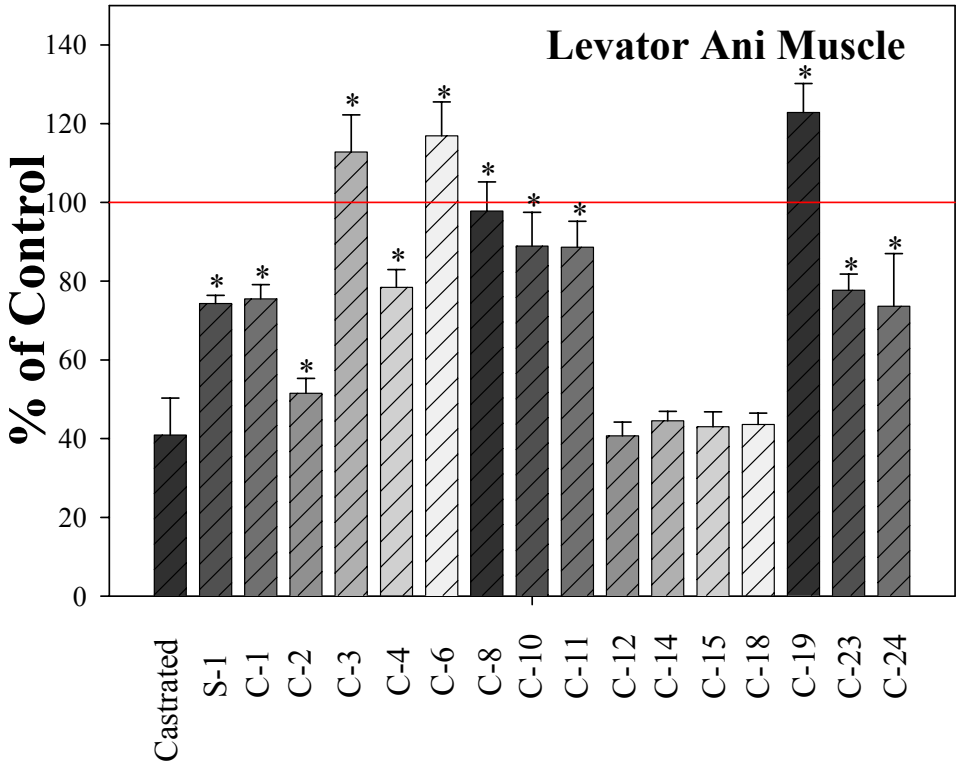

Figure 3. 5 The Effect of Novel AR Ligands on the Muscle in Castrated Male Rats.

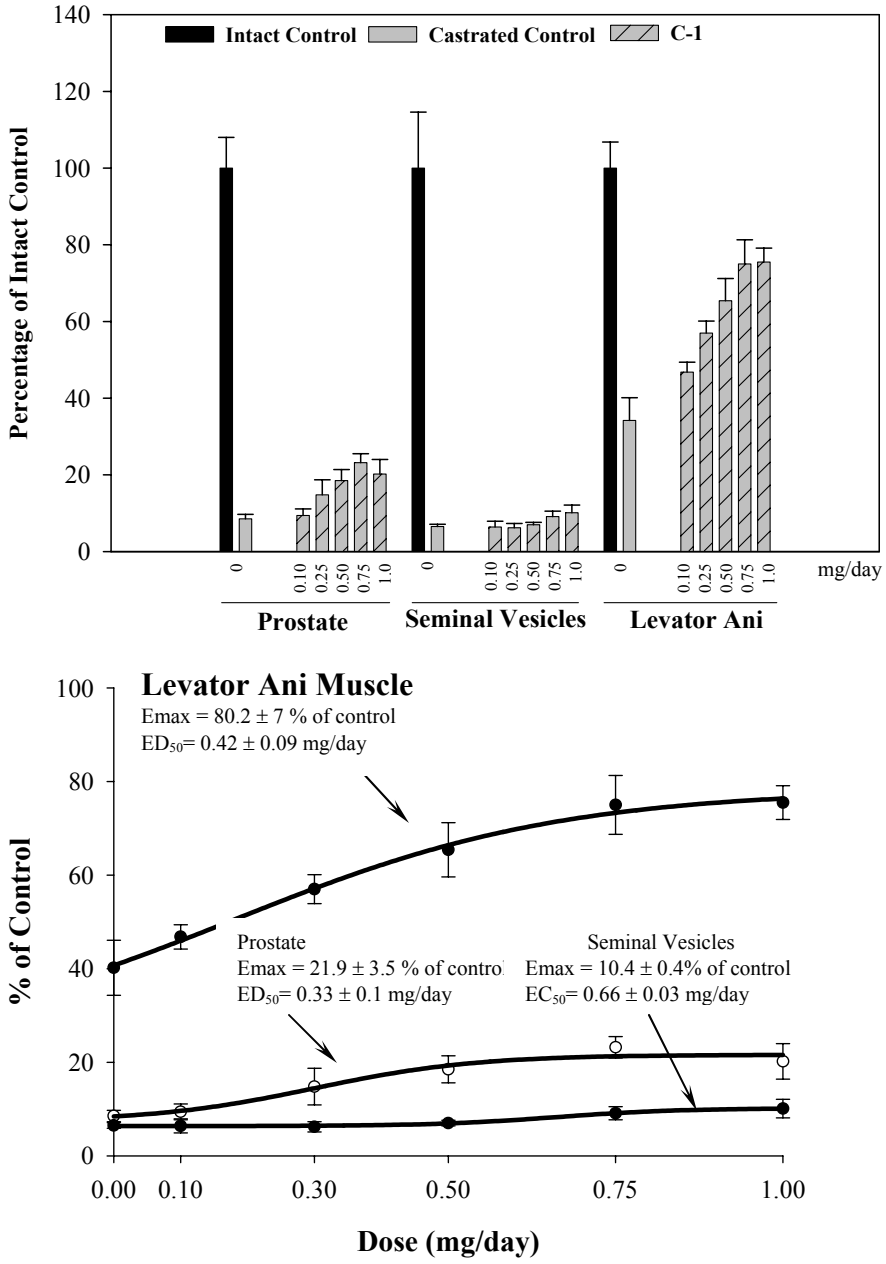

Figure 3. 6 Pharmacologic Effects of **C-1** in Castrated Male Rats (A) and Dose-Response Relationships (B).

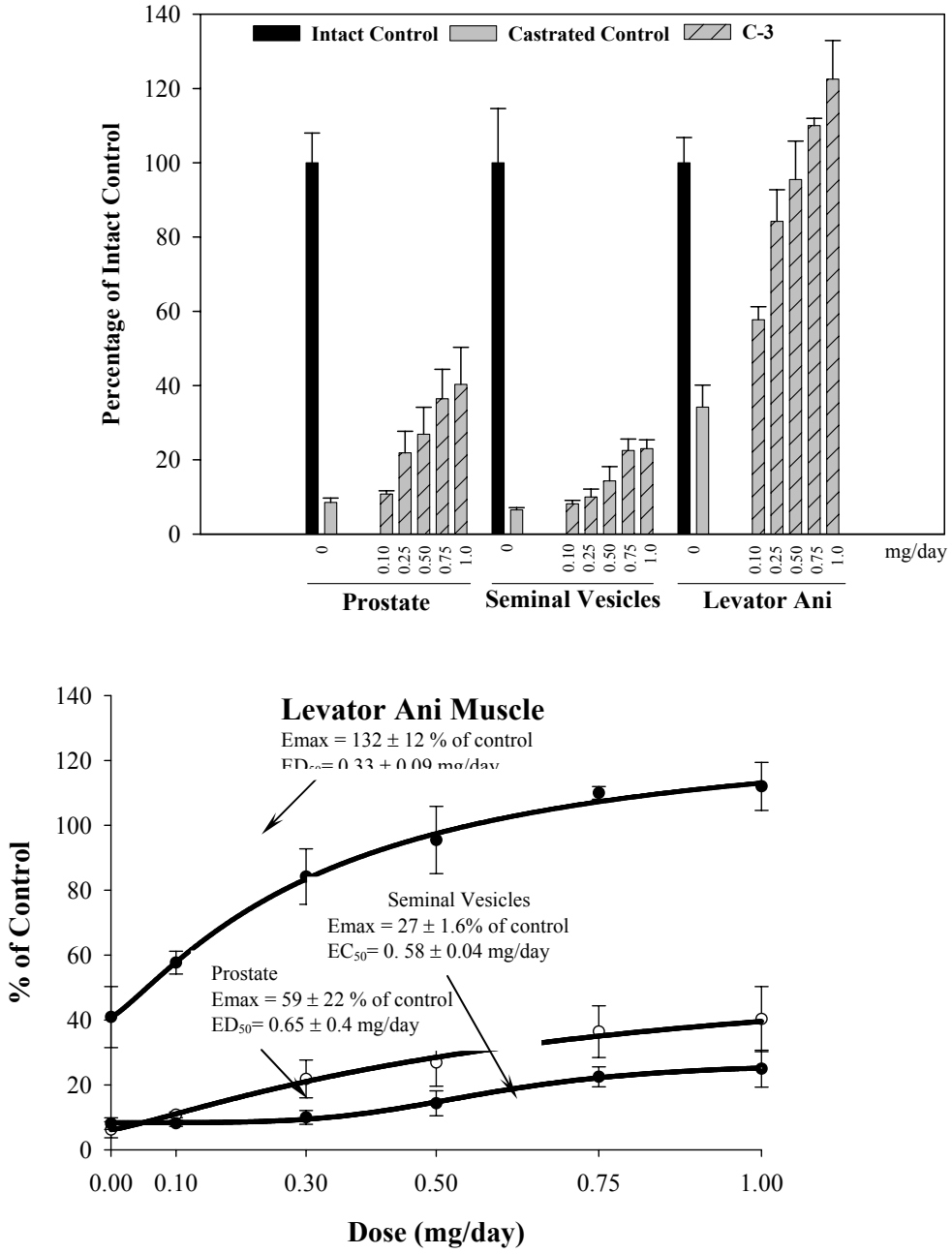

Figure 3. 7 Pharmacologic Effects of **C-3** in Castrated Male Rats (A) and Dose-Response Relationships (B).

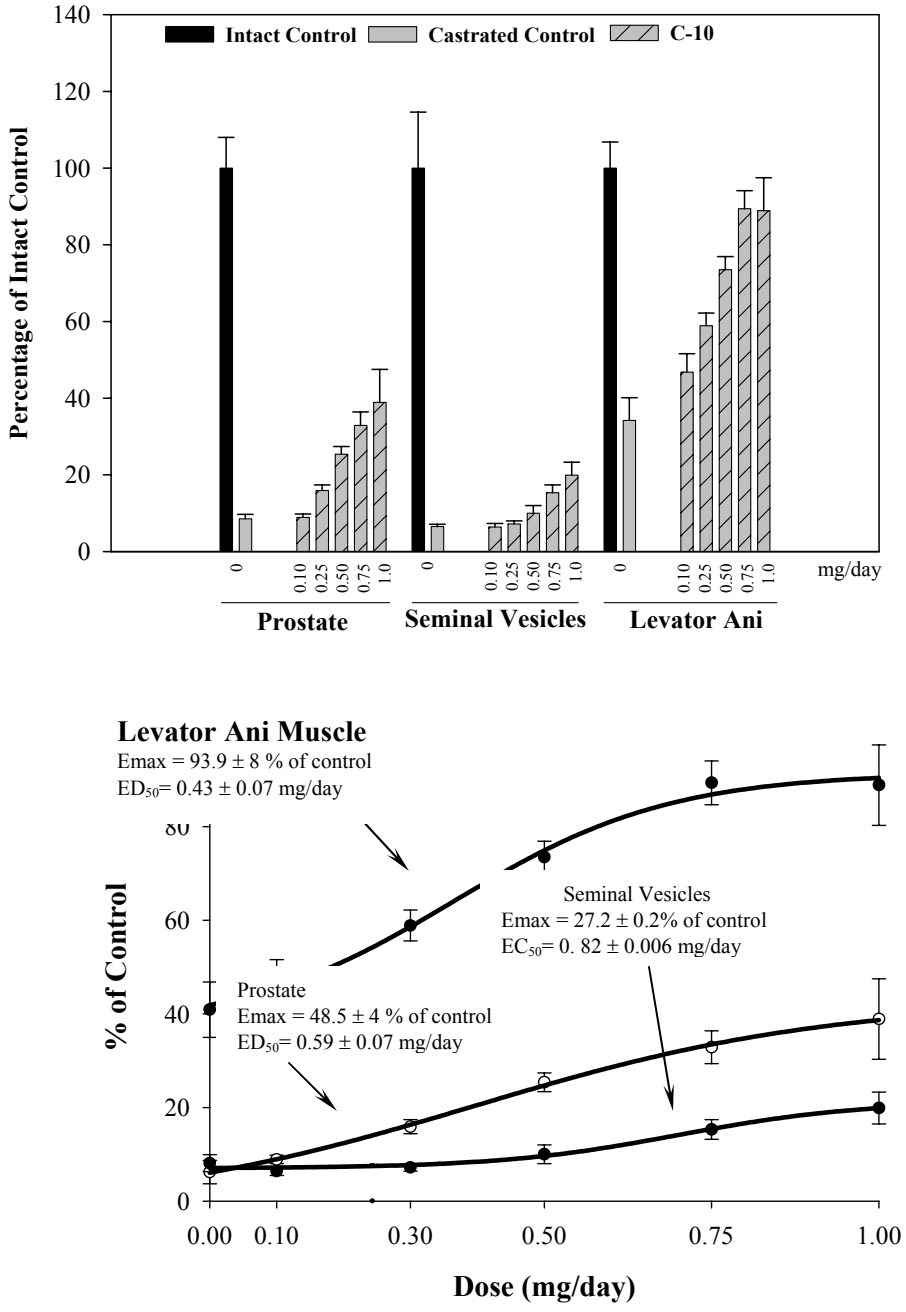

Figure 3. 8 Pharmacologic Effects of **C-10** in Castrated Male Rats (A) and Dose-Response Relationships (B).

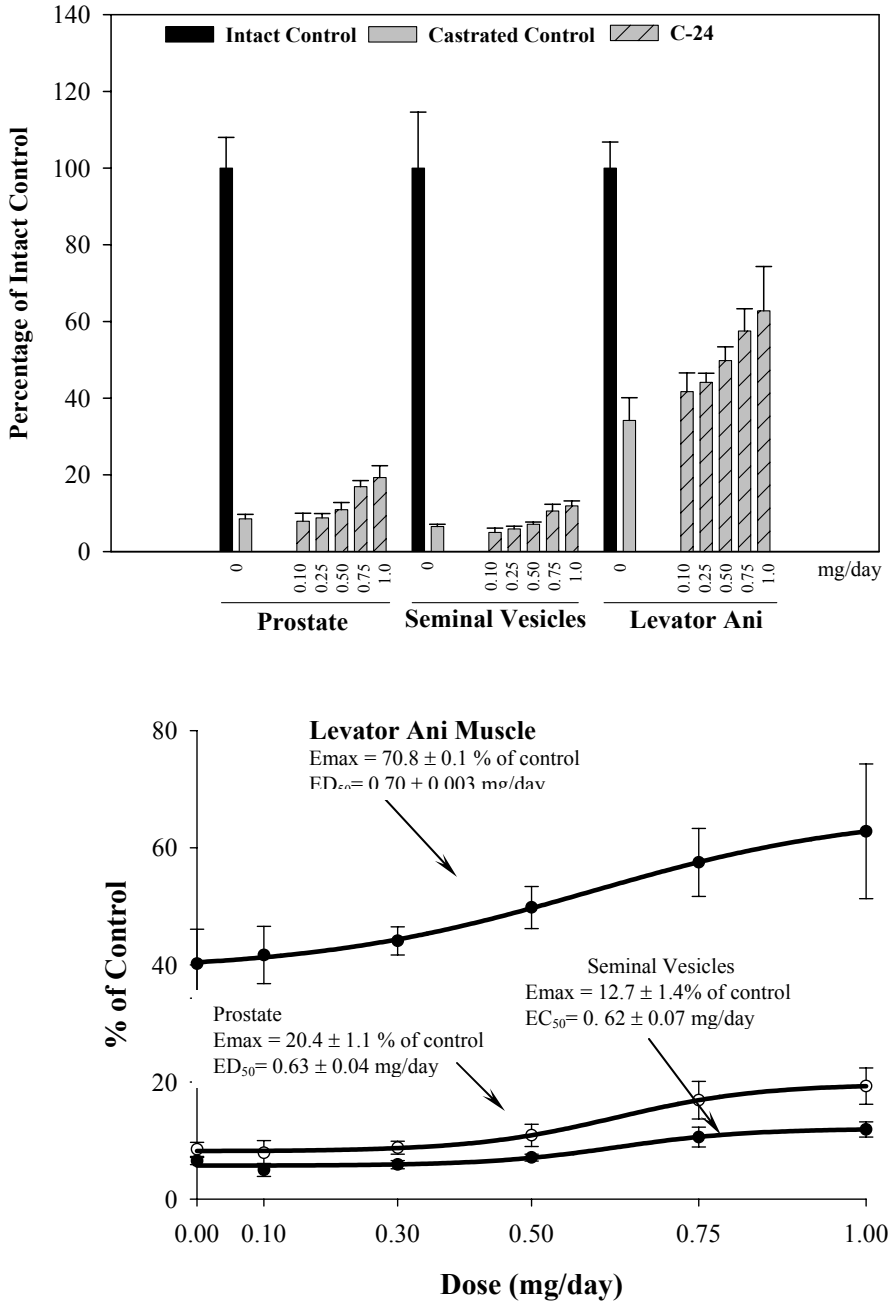

Figure 3. 9 Pharmacologic Effects of **C-24** in Castrated Male Rats (A) and Dose-Response Relationships (B).

Organs	Treatment	Emax (% of Intact Control)	Relative Efficacy	ED_{50} (mg/day)	Relative Potency
Androgenic					
Prostate	TP*	120.6 ± 13	1.0	0.13 ± 0.03	1.0
	C-1	21.9 ± 3.5	0.18	0.33 ± 0.1	0.39
	C-3	59 ± 22	0.49	0.65 ± 0.4	0.20
	C-10	48.5 ± 4	0.40	0.59 ± 0.07	0.22
	C-24	20.4 ± 1.1	0.17	0.63 ± 0.04	0.21
Seminal Vesicles	TP*	70.0 ± 19	1.0	0.12 ± 0.02	1.0
	C-1	10.4 ± 0.4	0.15	0.66 ± 0.03	0.18
	C-3	27 ± 1.6	0.39	0.58 ± 0.04	0.21
	C-10	27.2 ± 0.2	0.39	0.82 ± 0.006	0.15
	C-24	12.7 ± 1.4	0.18	0.62 ± 0.07	0.19
Anabolic	TP*	104.2 ± 10.1	1.0	0.15 ± 0.03	1.0
Levator Ani Muscle	C-1	80.2 ± 7.5	0.77	0.42 ± 0.09	0.36
	C-3	132 ± 12	1.27	0.33 ± 0.09	0.45
	C-10	93.9 ± 8	0.90	0.43 ± 0.07	0.35
	C-24	70.8 ± 0.1	0.68	0.70 ± 0.003	0.21

Table 3. 1 Comparison of Androgenic and Anabolic Activities of Novel SARMs to TP.

* The Emax and ED_{50} values of TP were previously reported by Yin et. al. (59)

CHAPTER 4

PRECLINICAL PHARMACOKINETICS AND METABOLISM OF C-3 IN THE RAT

4.1 INTRODUCTION

Clinically, the first choice for androgen replacement therapy is the endogenous androgen (testosterone). However, testosterone demonstrates negligible oral bioavailability and a very short half-life (153) due to rapid hepatic metabolism (32-34). To increase *in vivo* drug exposure, testosterone was structurally modified to testosterone esters, such as testosterone propionate, testosterone enanthate, and testosterone buciclat, etc. However, these esters also require intramuscular injection on a weekly basis (76, 77). Orally bioavailabe testosterone derivatives (e.g., testosterone undecanoate, TU) were developed and used for androgen replacement in hypogonadal men. However, TU requires multiple doses per day and produces widely variable serum testosterone levels (35, 154). As such, testosterone undecanoate is still administered intramuscularly for clinical use.

Besides the development of androgens using structural modifications of testosterone, nonsteroidal androgens were discovered based on several pharmacophores (60, 62, 67, 155-157). In our laboratories, the first series of androgen receptor ligands (e.g., acetothiolutamide) exhibited similar androgen receptor (AR) binding affinity as that of testosterone and high *in vitro* functional activity. Surprisingly, these compounds were inactive *in vivo*. The metabolism of acetothiolutamide was further studied and shown to be responsible for the contradiction between *in vitro* and *in vivo* activity (58). Three major metabolism pathways of acetothiolutamide were identified, including oxidation of

the thio-ether linkage, hydrolysis of the amide bond, and sulfate conjugation. A second generation of androgen receptor ligands were designed and synthesized with improved pharmacokinetic properties by structural optimization of acetothiolutamide. Replacing the thio-ether linkage of acetothiolutamide significantly decreased its hepatic metabolism. **S-1** and **S-4** (Figure 4.1.) were identified as potent and efficacious selective androgen receptor modulators (SARMs) (59). Therefore, the integration of knowledge related to *in vitro* and *in vivo* structure activity relationships, pharmacokinetics, and metabolism of known compounds is a useful tool to discover novel SARMs.

Previous pharmacologic studies illustrated that novel SARMs can be designed by introduction of multiple substituents in the aromatic B-ring of our lead compound, **S-1**. Comparing **C-3** with **S-1**, the only structural difference between these compounds is an additional fluoro group presented at the *meta* position of the B-ring of **C-3**. No significant difference was observed between these two compounds in terms of AR binding affinity. However, **S-1** and **C-3** exhibited significant different *in vitro* agonist activity, with a concentration of 10 nM inducing 99% and 43 % of the activation induced by 1 nM of DHT, respectively. Furthermore, **C-3** demonstrated much higher *in vivo* pharmacologic activity than **S-1**. For instance, the Emax values of **C-3** in the prostate, seminal vesicles, and levator ani muscle were 59%, 27%, and 132% of those observed in the control group, respectively, while the Emax values of **S-1** in the prostate, seminal vesicles, and levator ani muscle were 15%, 13%, and 75% of those in control animals, respectively. The significantly increased *in vivo* pharmacologic activity of **C-3** may due to multiple mechanisms, such as increased intrinsic functional activity and/or improved pharmacokinetic properties. In the present studies, we examined the pharmacokinetics and metabolism of **C-3** in male rats.

4.2 MATERIALS AND METHODS

4.2.1 Animals

Male Sprague-Dawley rats, weighing approximately 250 g, were purchased from Harlan Bioproducts for Science (Indianapolis, IN). All animals were maintained on a 12h light/dark cycle with food and water available *ad libitum*. The animal protocol was

reviewed and approved by the Institutional Laboratory Animal Care and Use Committee of The Ohio State University.

4.2.2 Chemicals

C-3 was synthesized using the methods described by Marhefka *et al.* (60). Chemical purity was confirmed using elemental analysis, mass spectrometry, and proton nuclear magnetic resonance. Dimethyl sulfoxide (DMSO), polyethylene glycol-300 (PEG 300), ketamine, xylazine, and acetonitrile were purchased from Sigma Chemical Co (St Louis, MO) and ethanol was purchased from Pharmco Products (Brookfield, CT).

4.2.3 Preclinical Pharmacokinetics of **C-3**

The pharmacokinetics of **C-3** were examined in five male SD rats weighing approximately 250 g after a dose of 10 mg/kg by intravenous injection. A catheter was implanted in the right external jugular vein of each animal 24 h prior to drug administration under anesthesia. **C-3** was dissolved in a vehicle containing DMSO (5%, v/v) in PEG 300 and administered to animals through the jugular vein catheter. Immediately after the drug administration, the catheter was flushed three times with saline (3× the volume of the dosing solution) before blood sampling. Blood samples (~ 200 μL) were then withdrawn through the jugular vein catheter at 5, 10, 30, 60, 90, 120, 240, 480, and 720 min after the i.v. dose. Blood samples were centrifuged at 1,000 g, 4°C for 10 min. Plasma samples were prepared and stored at -20°C until HPLC analysis.

4.2.4 HPLC Methods

An aliquot (100 μL) of each plasma sample from the pharmacokinetic studies was spiked with 10 μL of an internal standard (a structural analog of **C-3**) and mixed well with 1 mL of acetonitrile. After centrifugation at 16,000 g, 4°C for 10 min, the supernatant was collected and evaporated. The residues were reconstituted in 120 μL of

mobile phase. An aliquot of each sample was injected into a Nova-pak C_{18} column (3.9 × 150 mm, 4 μm particle size) purchased from Waters Corporation (Milford, MA). The HPLC system consisted of a model 515 HPLC pump (Waters), a model 717 plus autosampler (Waters), and a model 486 absorbance detector (Waters). HPLC separation was performed using an isocratic mobile phase (H_2O/Acetonitrile: 46/54, v/v) at a flow rate of 1 mL/min. The UV absorbance of eluents was monitored at 215 nm. Calibration standards were prepared in blank rat plasma with **C-3** concentrations ranging from 0.1 ~ 50 μg/mL. The recoveries of this compound over the calibration range were from 96.8% to 98.1%. The intra- and inter-day coefficients of variation of the assay were lower than 4.6% and 9.9%, respectively. The limit of quantitation of the HPLC assay was 0.1 μg/mL.

4.2.5 Pharmacokinetic Data Analysis

The plasma concentration-time data were analyzed using noncompartmental methods and WinNonlin software (Pharsight, Mountain View, CA). The terminal half-life ($T_{1/2}$) was calculated as $T_{1/2} = 0.693/\lambda$, where λ was the first-order rate constant describing the terminal decline in plasma drug concentration. The area under the plasma concentration-time curve ($AUC_{0-\infty}$) was calculated using the trapezoidal method with extrapolation to time infinity. The plasma clearance (CL) was calculated as $CL = Dose_{i.v.}/AUC_{0-\infty, i.v.}$, where the $Dose_{i.v.}$ and $AUC_{0-\infty, i.v.}$ were the intravascular dose and the corresponding area under the plasma concentration-time curve from time 0 to infinity, respectively. The apparent volume of distribution at equilibrium (Vd_{ss}) was calculated as $Vd_{ss} = CL \cdot MRT$, where the MRT was the mean residence time following the intravenous bolus dose.

4.2.6 Metabolism of **C-3** in the Male Rat

A catheter was implanted in the right external jugular vein of adult male Sprague-Dawley rats 24 h prior to drug administration. **C-3** was freshly dissolved in vehicle

containing DMSO (20%, v/v) in PEG 300 and administered to animals through the jugular vein catheter at a dose of 50 mg/kg. Each animal was individually housed in a Nalgene® metabolism cage. Urine and fecal samples were collected 24 h prior to the dose and for up to 24 h post after the dose. Samples were stored at –20°C until HPLC/MS^n analysis.

Urine samples were allowed to completely thaw at room temperature and centrifuged at 3,000 g, 4°C for 10 min before using the sample preparation method described by Yin *et al* (58). In brief, an aliquot (10 ml) of supernatant from each collection interval was extracted four times with the same volume of ethyl acetate. The combined organic and aqueous phase from these extractions were evaporated separately to dryness under reduced pressure. Before sample analysis, the residues were reconstituted with mobile phase consisting of H_2O/Acetonitrile (46/54, v/v). Each reconstituted sample was filtered through a membrane filter (0.45 μm, Millipore Corporation). An aliquot (20 μl) of the filtrate was injected in the HPLC/MS system and analyzed for metabolites of **C-3** using the method described below.

Similarly, fecal samples, approximately 8 g, were homogenized with a mechanical homogenizer after adding 10 ml of distilled water (58). The homogenates were further extracted three times with a mixture of methanol/ethyl acetate (2:1, v/v). After each extraction, samples were centrifuged at 3,000 g, 4°C for 10 min. The aqueous phase was collected, combined, and evaporated under reduced pressure. The resulting semi-solid residues were then mixed well with methanol, and an aliquot (200 μl) of each methanol extract was filtered through the same membrane mentioned above and used for LC/MS^n analysis.

4.2.7 LC-MS^n Analysis

The LC/MS system used consisted of a Surveyor Pump, Surveyor Autosampler, and a LCQ Deca ion-trap mass spectrometer (ThermoFinnigan Corp, San Jose, CA) coupled with an electrospray ionization (ESI) source. The negative ion mode was used, and the general system parameters were tuned with the parent compound **C-3** except for those used in collision-induced dissociation (CID), in which case the collision energy and

collision time for each ion were optimized. The temperature of the heated capillary was set at 300 °C, the spray voltage was 4.0 kv, and the sheath gas flow rate and auxiliary gas flow rate were 74 and 50 ml/min. Full MS scans in the range *m/z* 50-1000, selected ion monitoring (SIM) scans and MS^n scans of ions of interest were conducted as needed. Collision energy levels (He) and activation times for the MS^n analysis were adjusted for the target compounds individually.

For LC/MS, a reversed-phase column (5μm, 2mm × 250 mm, Ultrasphere ODS C18 column, (Deerfield, IL) was used with a gradient mobile phase consisting of acetonitrile and water at a flow rate of 100 μl/min. The gradient was initiated with 5% acetonitrile for 5 min, followed by a linear increase to 70% acetonitrile over 10 min, which was kept constant for 15 min. Then the mobile phase was linearly returned to the original condition over 3 min, and was maintained for 7 min. The cycle time for each analysis was 40 min.

Accurate mass determinations were performed using a Micromass Q-TOPTM II (Micromass, Wythenshawe, UK) equipped with an orthogonal electrospray source (Z-spray) operated in negative ion mode. Sodium iodide was used for mass calibration for the range m/z 50-1000. Data acquisition was controlled by Xcaliber software. Mass spectra data was analyzed by Metabolite ID software, version 1.0 and Mass Frontier software, version 3.0 (Thermo Electron Corp. San Jose, CA).

4.2.8 Statistical Analyses

All statistical analyses were performed using single-factor ANOVA with the α value set a *priori* at $p < 0.05$.

4.3 RESULTS

4.3.1 Preclinical Pharmacokinetics of **C-3**

The only structural difference between **C-3** and the lead compound **S-1** is an additional fluoro group at the *meta* position of the B-ring presented in **C-3**. However, the *in vivo* pharmacologic activity of **C-3** was much greater than that of **S-1**. The different

pharmacokinetic properties of these two compounds may contribute to the observed difference in their pharmacologic activity. As shown in Figure 4. 2, the mean plasma concentration-time profiles of **C-3** and **S-1** declined biexponentially in rats after a single i.v. bolus dose of 10 mg/kg. Pharmacokinetic parameters of these two compounds were analyzed using noncompartmental methods and WinNolin software (Version 4.0, Pharsight Corporation).

Table 4.1 lists the pharmacokinetic parameters of **C-3** and **S-1** in male rats. The terminal half-life ($T_{1/2}$) and total body clearance of **C-3** was 197 min and 5.37 ± 1.2 mL/min/kg. The average steady state volume of distribution for **C-3** (1.34 L/kg) was about twice that of the total body water (0.67 L/kg). The AUC of **C-3** (1.81 ± 0.28 mg · min/L) was significantly less than that of **S-1** (2.55 ± 0.27 mg · min/mL), suggesting that the increased pharmacologic activity of **C-3** was not due to increased *in vivo* drug exposure.

4.3.2 Profiling and Identification of Urinary Metabolites of **C-3** in the Rat

The purpose of this study was to qualitatively identify the metabolites of **C-3** in male rats. The metabolic profiles of **C-3** in urine and feces after high dose IV administration of a high (50 mg/kg) intravenous dose to rats were determined by ESI mass spectrometry after separation by reversed phase HPLC. The total ion spectra of post-dose urine samples were compared with blank urine samples taken prior to dosing to identify drug-related peaks. Molecular ions of interest were then subjected to LC/MS^n analysis for structural identification. Figure 4.3 shows the HPLC/ESI-MS chromatogram of the organic extracts of the blank and 24 h post-dose urine samples. Five major peaks observed in the 24 h post-dose urine samples were absent in the blank urine samples, indicating that these peaks were drug-related components (Figure 4.4).

Molecular ion at m/z 419 ($[M-H]^-$) of the parent compound. (Retention time 21.7 min) Initial scan of these peaks for molecular ions revealed a peak with $[M-H]^-$ of m/z 419. This peak was identified as the parent compound, which was based on its ESI/MS^2-MS^3 scans of the appropriate fragment ions. The mass spectra of this peak were identical in every respect to those of the synthetic standard. Collision-induced dissociation (CID)

of **C-3** generated three fragmentation ions at m/z 129, 261, and 289 as shown in Figure 4.5. The base peak ion at m/z 261 resulted from the cleavage of the chiral carbon-methylene carbon bond, with a loss of the methyl group. The cleavage at the bond between the ether linkage and the methylene carbon generated two fragmentation ions at m/z 129 and 289. The fragmentation ion at m/z 289 was generated by the cleavage mentioned above, followed by a loss of a hydrogen atom, and formed the epoxide product. Further CID of the fragment ion at m/z 289 (LC/MS^3) yielded an abundant granddaughter ion at m/z 205 and a less abundant ion at m/z 261. Since no peak ion at m/z 205 was detected during LC/MS scan, the contribution from the ion at m/z 289 to the formation of the ion at m/z 261 was minor. Figure 4.6 shows the proposed fragmentation pattern of **C-3**.

Molecular ion at m/z 403 ($[M-H]^-$) of M1. (Retention time 22.3 min) The $[M-H]^-$ ion at m/z 403 was 16 Da less than that of the parent compound, suggesting it to be a reduced product of **C-3** and was identified as the reduction product of **C-3** in which the nitro group was converted to a nitroso group (Table 4.2). The retention time of M1 was slightly longer than that of the parent compound, indicating that M1 is more hydrophobic than **C-3**. The $[M-H]^-$ at m/z 403 was 16 Da less than that of the parent compound, suggesting it to be a reduced product of **C-3**. Its MS^2 spectrum showed fragment peaks at m/z 129, 189, 245, and 273 with the fragment ion at m/z 245 as the base peak, consistent with the cleavage pattern of the parent compound. The simultaneous detection of peaks at m/z 129 for M1 and the parent compound suggested no metabolic changes in the B-ring. The existence of a fragment ion of 189 m/z in the MS^2 spectrum of M1 and MS^3 spectrum of the 273 m/a fragment ion further supports the assignment of M1 as the nitroso reduction product. Thus the only possible reduction, which would yield two fragment peaks containing an aromatic A-ring at m/z 245 and 273, was to reduce the nitro group to a nitroso group at the *para* position of the A-ring.

Molecular ion at m/z 485 ($[M-H]^-$) of M2. (Retention time 11.42 min) The $[M-H]^-$ ion at 485 m/z corresponded to a metabolite (M2) with two metabolic alterations; namely (1) hydroxylated B-ring and (2) an A-ring in which the nitro group was reduced and then conjugated with sulfate. Fragmentation of this molecular ion produced a base peak at m/z 405 and less abundant ions at m/z 145, 259, and 339 (Table 4.2). The proposed sulfate

conjugate was first confirmed by the loss of 80 Da., a mass that corresponds to SO_3, from the molecular ion at m/z 485 to an ion at m/z 405 and the fragment ion at m/z 339 to ion at m/z 259. The fragment ion at m/z 145, suggesting that oxidation occurred within the aromatic B-ring, was supported by the 16 m/z. increase in the corresponding fragment ion at m/z 129 produced by the parent compound. Further CID of the 405 m/z fragment ion yielded two ions of m/z 145 and 259 with the former being the base peak in the spectrum, which further supported the conclusion that the sulfate conjugate did not occur in the B-ring. The fragment ion at m/z 259 was 30 Da. less than the corresponding fragment ion at m/z 289 produced by the parent compound and suggested the reduction of the nitro group to an amine group in the A-ring. The overall fragmentation pattern of M3 proved that it was a B-ring hydroxylated, A-ring reduced sulfate conjugate. However, the site of oxidation in the B-ring could not be determined.

Molecular ion at m/z 485 ($[M-H]^-$) of M3. (Retention time 11.91 min) The $[M-H]^-$ ion showed the same m/z as that M2 but contained two metabolic alterations in the A-ring; namely (1) oxidation of the A-ring and (2) reduction and subsequent sulfate conjugation of the nitro group in the A-ring of **C-3**. Similar to M2, fragmentation of the molecular ion yielded a base peak at m/z 405 and less abundant peaks at m/z 275, 385, and 129 (Table 4.2). The loss of a SO_3 (80 Da.) from the molecular ion to the peak at m/z 405 confirmed that M3 was a sulfate conjugate. The presence of a fragment ion at m/z 129 suggested that the B-ring remained the same as that in the parent compound. Further CID of the ion at m/z 405 produced a base peak at m/z 275 and other fragment ions at m/z 129, 255, and 385. Consistent with parent compound, cleavage at the bond between the ether linkage and the methylene carbon generated ions at m/z 129 and 275. The latter ion was 14 Da. less than the fragment ion at m/z 289 observed upon fragmentation of the parent compound, which was proposed herein as the combination of the following changes: 1) B-ring nitro reduction to an amine group and 2) oxidation of the amine group or hydroxylation of the aromatic A-ring. The oxidation site in the A-ring was not certain. Interestingly, ions at m/z 385 and 255 derived from the fragment ion at m/z 405 were absent in the parent fragmentation pathways, indicating that the structural changes in the A-ring of M3 induced different dissociation pattern upon CID as proposed in Figure 4.6. The loss of a fluoro group from the trifluoromethyl carbon and a hydrogen from the

amine group of the ion at m/z 405 yielded the product ions at m/z 385 and 129. This proposed fragmentation pattern was further supported by the ion at m/z 255 (Figure 4.7).

Molecular ion at m/z 499 ($[M-H]^-$) of M4. (Retention time 13.22 min) The $[M-H]^-$ ion at m/z 499 was assigned as the sulfate conjugate of B-ring oxidized M1. The loss of 80 Da. from the molecular ion at m/z 499 to produce the fragment ion at m/z 419, which was identical in mass to the molecular ion of **C-3**, indicated that this molecular ion is a sulfate conjugate. However, the presence of a fragment ion at m/z 145 suggested that the B-ring has been oxidized. Further CID of the fragment ion at m/z 419 yielded product ions at m/z 145, 189, 245, and 273, consisting with the fragmentation pattern of M1. The sulfate conjugation occurred in the oxidized B-ring, as suggested by the presence of the 145 m/z ion upon fragmentation of the 499 and 419 m/z ions.

Molecular ion at m/z 515 ($[M-H]^-$) of M5. (Retention time 13.12 min) The $[M-H]^-$ ion at m/z 515 was assigned as the B-ring oxidated metabolite which had also undergone sulfate conjugation at the chiral hydroxyl group (C3). The loss of 80 Da. from the molecular ion at m/z 515 to produce the fragment ion at m/z 435 indicated that this molecular ion was a sulfate conjugate. In addition to this base peak ion, product ions at m/z 145, 289, and 370 were also observed. The fragment ions at m/z 145 and 370 were from the cleavage between the ether linkage and the methylene carbon, indicating that the molecular ion bears an oxidized B-ring and that the sulfate conjugation occurred at the tertiary hydroxyl group linked to the chiral carbon. Upon CID, the fragment ion at m/z 435 further yielded product ions at m/z 145, 205, 261, and 289, which matched well with the fragmentation pattern of **C-3** except for the oxidized B-ring product ion.

4.3.3 Profiling and Identification of 0- to 24-h Fecal Metabolites in Rat

The mass spectra of the organic extract of the blank and 24 hr rat fecal samples are shown in Figure 4.8. No molecular ions corresponding to the parent compound or other major metabolites observed in the 24 h urine sample were detected. Two molecular ions associated with the parent compound at m/z 389 (Figure 4.8; c) and 405 (Figure 4.8; d) were extracted and identified by LC/MS/MS.

Molecular ion at m/z 389 ($[M-H]^-$) of M6. (Retention time 19.18 min) The $[M-H]^-$ ion at m/z 389 was assigned as a nitro reduction product ion. Upon CID, this ion yielded a base peak at m/z 129 (Table 4.3), indicating that there was no metabolic alteration in the B-ring. The fragment ion at m/z 259 was 30 Da. less than the fragment ion at m/z 289 produced by the parent compound, suggesting that the nitro group in the A-ring was reduced to an amine group. The assignment of this structure for M6 corroborated by the presence of a fragment ion at m/z 175, a product ion resulted from the cleavage of the amide bond.

Molecular ion at m/z 405($[M-H]^-$) of M7. (Retention time 18.44 min) The $[M-H]^-$ ion at m/z 405 was assigned as the B-ring oxidized M6. Upon CID, this ion yielded a base peak at m/z 145 (Table 4.3), indicating a hydroxylated B-ring. The remaining fragment ions from M7 were very similar as those from M3.

4.4 DISCUSSION

Several generations of SARMs were developed by structural optimization of the first generation compounds. The first generation of AR ligands (e.g. acetothiolutamide, Figure 4.1) demonstrated high *in vitro* activity, but minor *in vivo* pharmacologic activity in animals (58). Metabolism studies identified three major metabolism pathways of acetothiolutamide in rats, including oxidation, hydrolysis, and sulfation (Figure 4.9.A). Oxidation of the thio-ether linkage happened rapidly and diminished its AR agonist activity *in vivo*. Hydrolysis of the amide bond of the *para*-acetamido group in the B-ring of acetothiolutamide produced an amine metabolite, which acted as an AR antagonist activity *in vitro*. Furthermore, multiple positions of the aromatic B-ring were susceptible to oxidation reactions *in vivo*. Previous *in vitro* structure-activity relationship of AR ligands showed that AR binding affinity and transcriptional activity were relatively lower for compounds with a *para*-cyano group than their nitro group containing counterparts. To improve the *in vivo* metabolic stability and pharmacologic activity, structural modification of acetothiolutamide included: 1) replacing the thio-ether linkage with an oxygen bridge; 2) changing the para-acetamido group to other electron-withdrawing groups according the structure-activity relationships of SARMs; 3) replacing the *para*-

cyano with a nitro group in the aromatic A-ring; and 4) incorporating multiple substituents in the B-ring.

The second generation of SARMs (e.g., **S-1** and **S-2**, Figure 4.2) demonstrated potent pharmacologic activity *in vivo* and much greater drug exposure than that of acetothiolutamide. Additional structural modification in the B-ring of **S-1** (e.g., **C-3**) further improved the pharmacologic activity of SARMs *in vivo* (Chapter 3), which was likely due to several factors, including AR binding affinity, intrinsic functional activity, and pharmacokinetic properties. The pharmacokinetics of **C-3** were then investigated. In contrast to what we expected, the plasma concentration – time curves of **C-3** and **S-1** were similar after an i.v. dose at 10 mg/day. The clearance of **C-3** was about 30% higher than that of **S-1** (5.37 vs 4.00 ml/min/kg) and consequently the total $AUC_{\mathbf{C\text{-}3}}$ was 70% of $AUC_{\mathbf{S\text{-}1}}$. Besides the difference in pharmacokinetics, the binding affinity of **S-1** and **C-3** were 6.1 ± 0.2 nM and 3.4 ± 0.6, respectively. Moreover, the *in vitro* functional activity of **C-3** (99%) was two-fold higher than that of **S-1** (43%). Therefore, the higher *in vivo* pharmacologic activity of **C-3** than **S-1** was likely due to improved binding affinity and intrinsic functional activity rather than the pharmacokinetic properties of this compound.

Previous pharmacokinetic studies with radioactive-labeled SARMs showed that this series of compounds undergoes extensive hepatic elimination in rats. Although the terminal half-life (3.3 h) of **C-3** in rats is moderate, it is likely too short for once per day treatment (e.g., hormonal male contraception). The metabolism of **C-3** was studied in rats for further structural optimization. Seven phase I or phase II metabolites were identified in urine and fecal samples 24 h after i.v. administration of **C-3** at a dose of 50 mg/kg. **C-3** was metabolized in rats through three major metabolism pathways: nitro-reduction in the A-ring, oxidation in the A or B-ring, and sulfate conjugation. A rational metabolic schematic of **C-3** in rats was proposed in Figure 4.10. The para-nitro group was first reduced to a nitroso group and produced a reduced metabolite, M1, of **C-3**. Moreover, the nitroso group was completely reduced to an amine group, resulting another reduced metabolite, M6. Oxidation reaction occurred in the aromatic rings of the parents and its reduced metabolites. Sulfate conjugate happened rapidly to those oxidation products and formed final metabolites, M2, M3, M4, M5, and M7. Similar to the metabolism pattern of acetothiolutamide (58), sulfate conjugates were the only phase II metabolites of **C-3**

detected by current study. In addition to the hydroxyl group introduced into the aromatic rings during oxidation, the hydroxyl group linked to the chiral carbon of **C-3** was also a possible site for sulfate conjugation If that was the case, a metabolite ion at m/z 499 would be detected and its mass spectra of LC/MS^n should match those of **C-3** after dissociating with the sulfate group. However, the only metabolite ion at m/z 499 showed a typical B-ring with a hydroxyl group and a reduced A-ring. Therefore, the sulfate conjugate site was uniformly assigned to the hydroxyl group in the A or B-ring.

In conclusion, the higher *in vivo* pharmacologic activity of **C-3** than **S-1** was likely due to its increased intrinsic functional activity, but not increased drug exposure than **S-1**. Nitro reduction and oxidation were the major phase I metabolism pathways of **C-3**, followed with rapid sulfate conjugation. Replacing the nitro group with a cyano group may increase the metabolic stability of **C-3** and maintain or increase its *in vivo* pharmacologic activity.

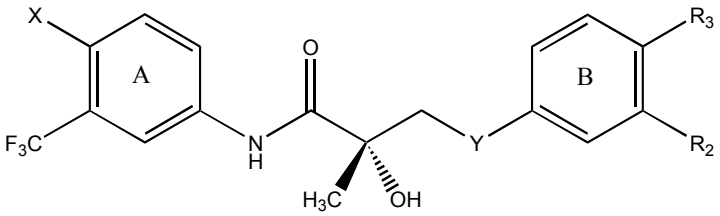

Compound Name	X	Y	R_2	R_3
R-Bicalutamide	CN	SO_2	H	F
Acetothiolutamide	CN	S	H	$NHC(O)CH_3$
S-1	NO_2	O	H	F
S-4	NO_2	O	H	$NHC(O)CH_3$
C-3	NO_2	O	F	F

Figure 4. 1 Chemical Structures of Bicalutamide, Acetothiolutamide, **S-1**, **S-4**, and **C-3**

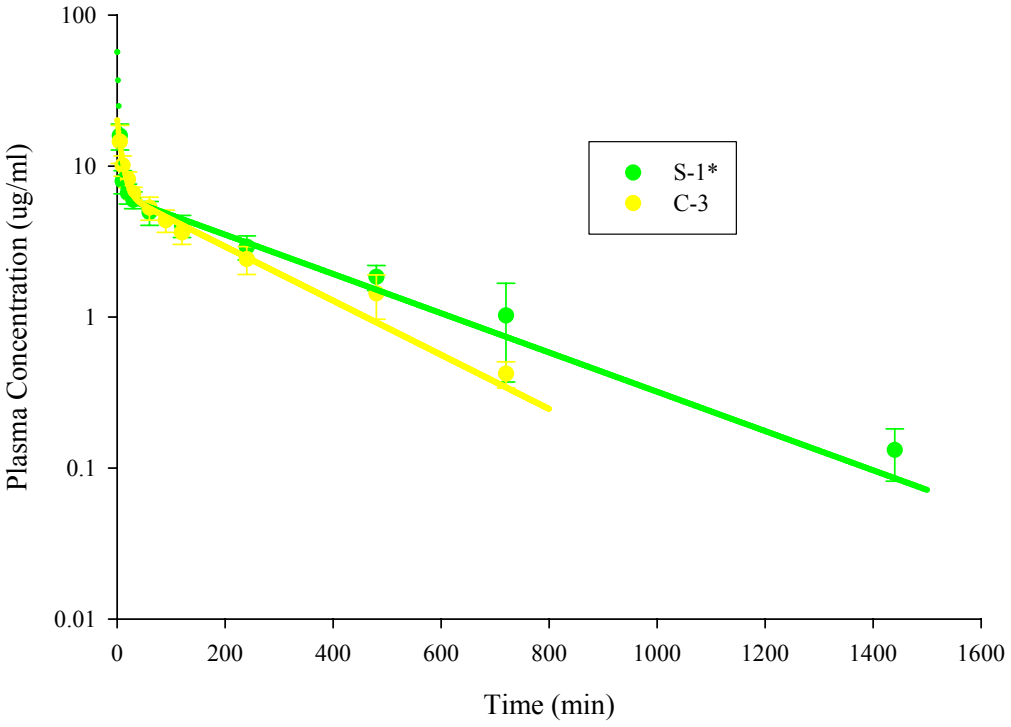

Figure 4. 2 Mean Plasma Concentration-Time Profiles of **C-3** and **S-1** in Male Rats.

Each data point represents the mean ± SD of five rats. (N = 5)
* Data was provided by Wu *et al*.

Parameter	S-1	C-3
$AUC_{0\rightarrow\infty}$ (min * mg/mL)	2.55 ± 0.27	1.81 ± 0.28
$T_{1/2}$ (min)	248	197
MRT (min)	363 ± 51	250 ± 37
CL (mL/min/kg)	4.00 ± 0.50	5.37 ± 1.2
V_{ss} (L/kg)	1.46 ± 0.35	1.34 ± 0.82

Table 4. 1 Mean Pharmacokinetic Parameters of **C-3** and **S-1** in Male Rats.

Dose: 10 mg/kg, i.v.
Data represent the mean ± SD of five rats. (N = 5)
* Data was provided by Di *et al*.

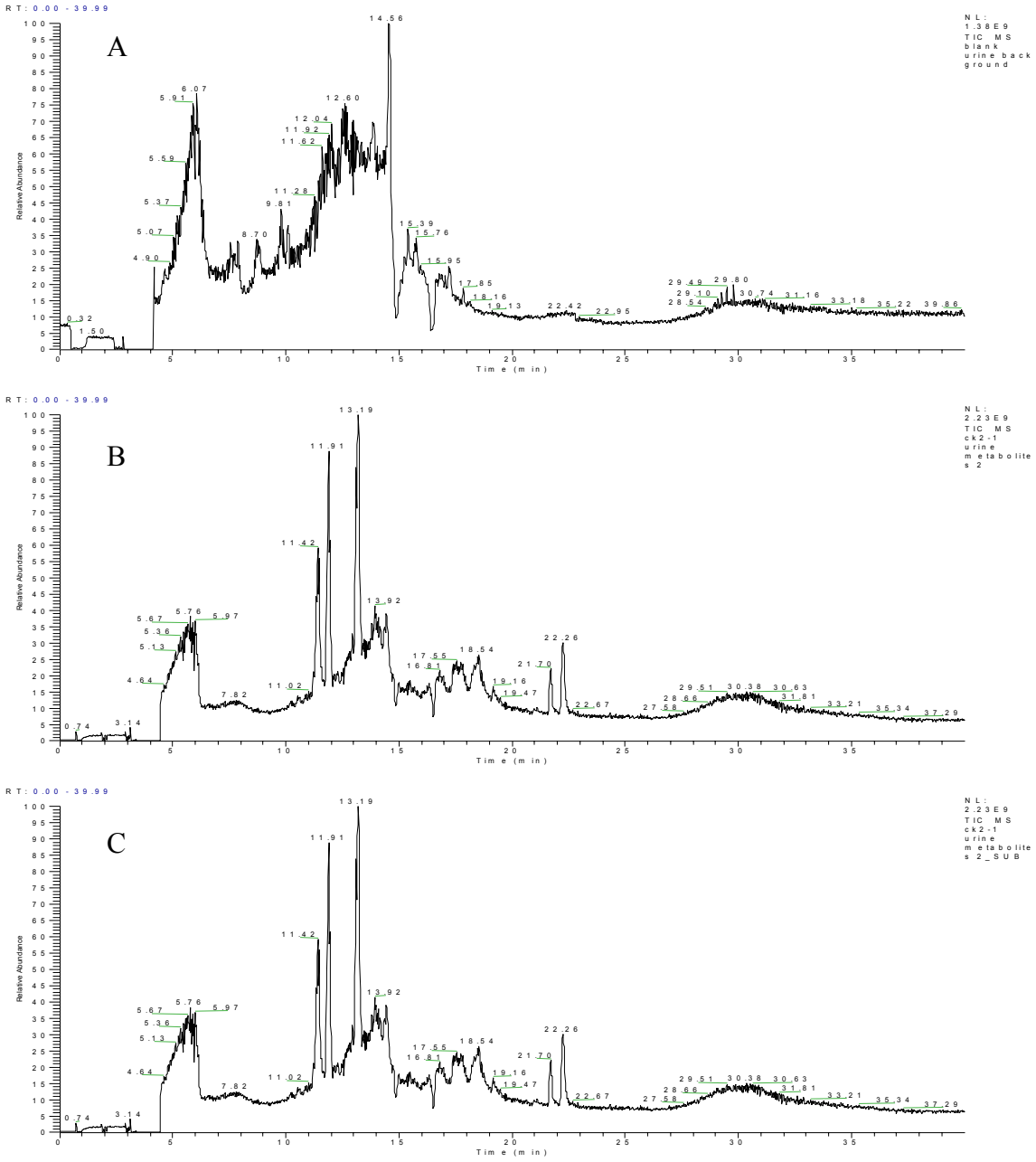

Figure 4. 3 HPLC/ESI-MS Chromatograms of Extracts from Rat Urine Samples

A: Blank urine samples; B: Urine samples taken 24 h after an i.v. dose of **C-3**; C: 24 h samples subtracted from the background of the blank urine samples.

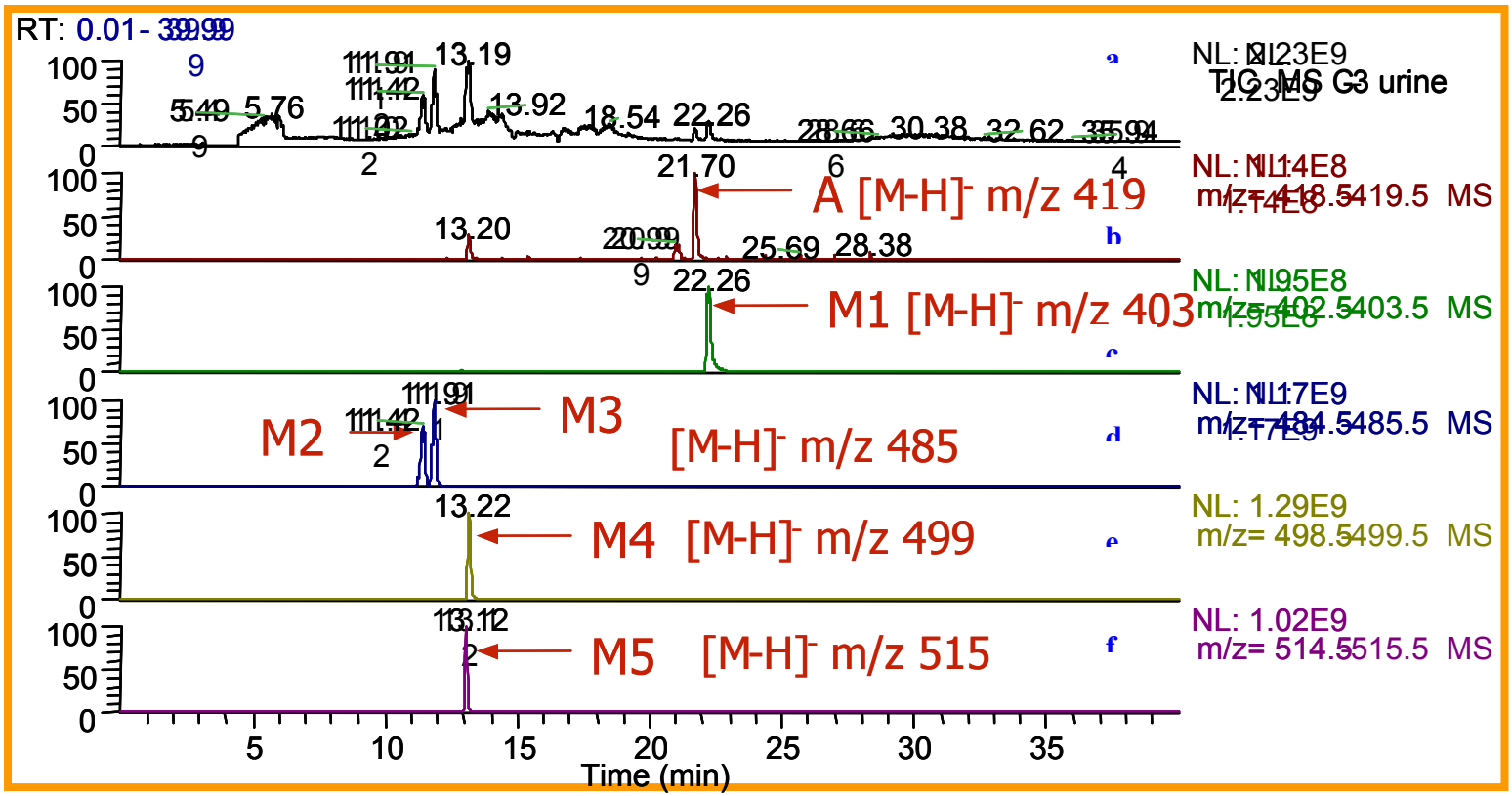

Figure 4. 4 HPLC/ESI-MS Chromatograms of Extracts from 24 h Rat Urine Samples.

(a) Total ion chromatogram (TIC); (b) Extracted ion chromatogram (XIC) of the parent drug **C-3** at *m/z* 419; (c) XIC of one reduction product M1 at *m/z* 403; (d) XIC of two reduction and sulfate conjugate M2 and M3 at *m/z* 485; (e) XIC of one sulfate conjugate M4 at *m/z* 499; (f) XIC of one oxidation and sulfate conjugate M5 at *m/z* 515.

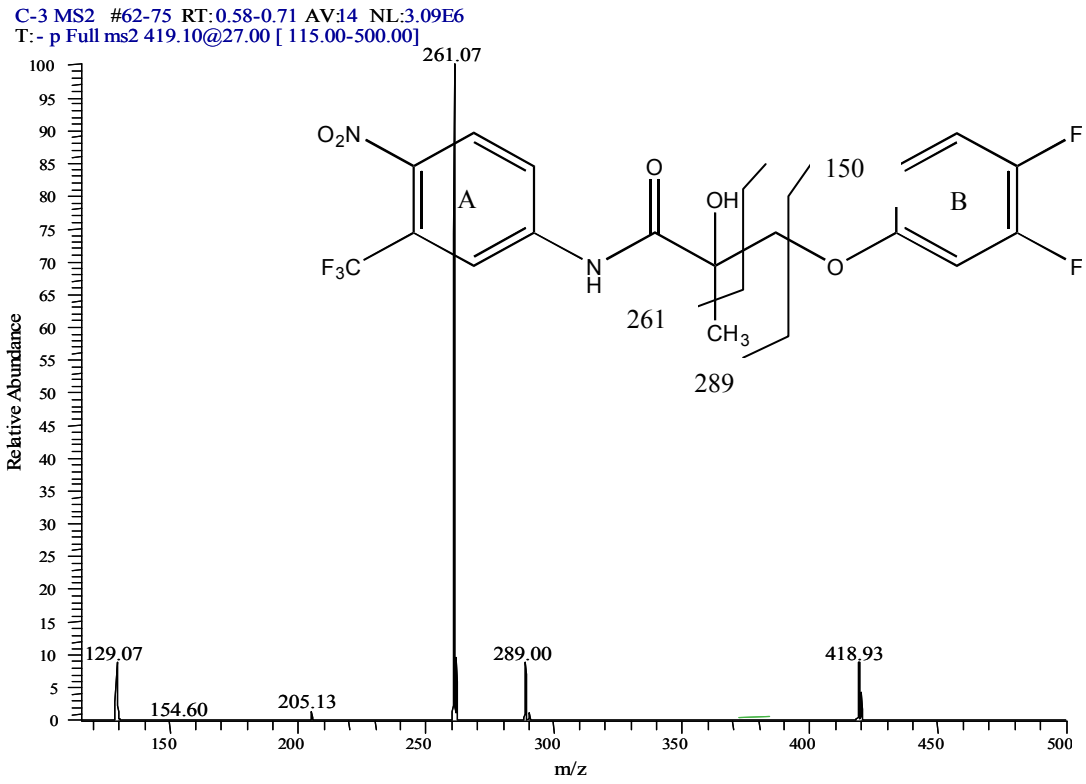

Figure 4. 5 Mass spectrum of **C-3** obtained from LC/MS/MS.

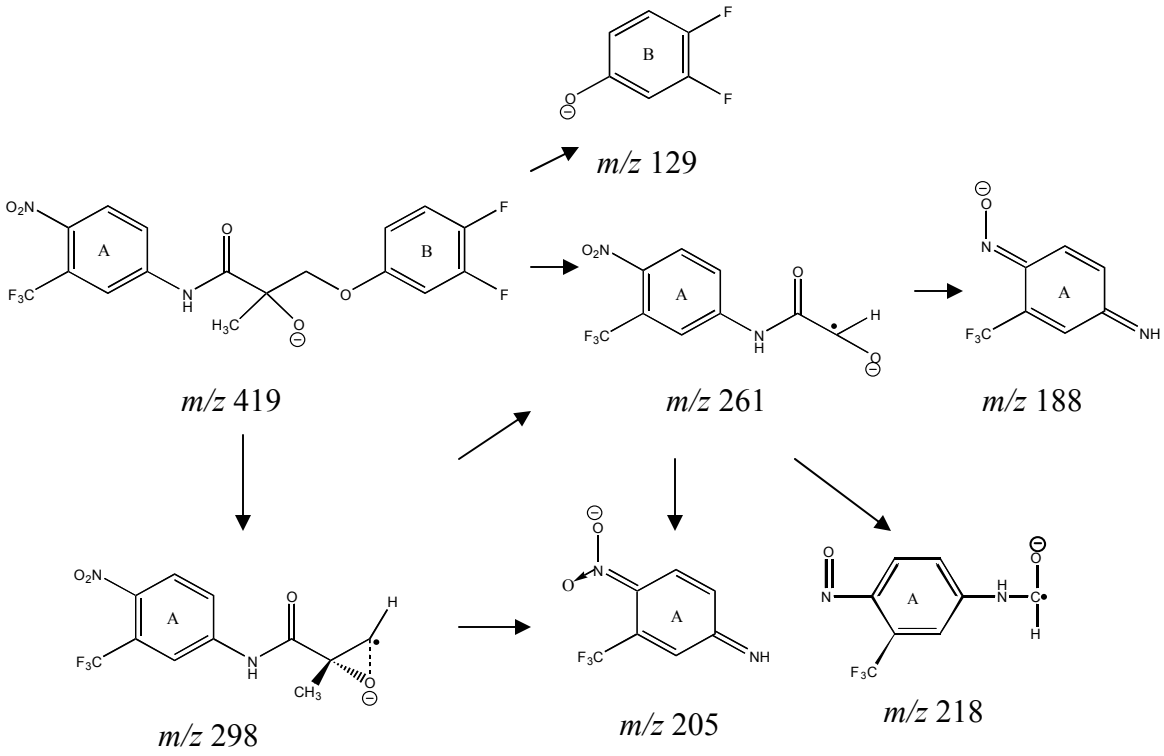

Figure 4. 6 Proposed Fragmentation Pattern of **C-3**

Structural information was determined by LC/MS^2 and LC/MS^3 fragmentation of the parent compound, **C-3**.

Molecular Ions $[M-H]^-$	Product Ions Observed (m/z Values)	Assigned Structure and Proposed Fragmentation Pattern
419 (C-3)	129, 261[a], 289	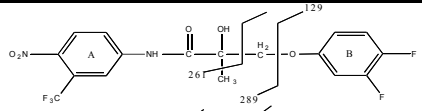
289	205[a], 261	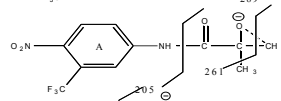
261	188, 218, 205[a]	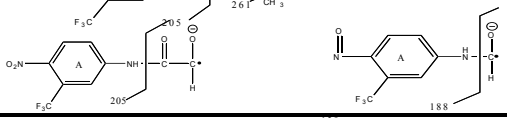
403 (M1)	129, 189, 245, 273[a]	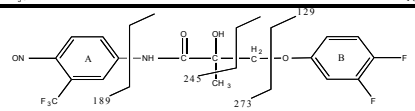
273	189[a], 245	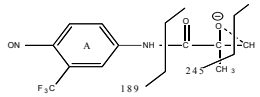
485 (M2)	145, 339, 259, 405[a]	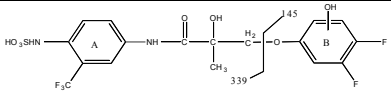
405	145[a], 259	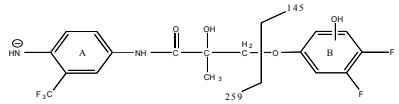
485 (M3)	129, 385, 405[a]	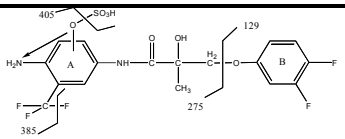
405	129, 255, 275[a], 385	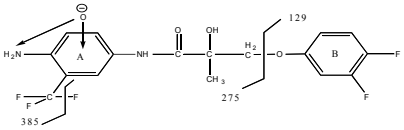
499 (M4)	145,189, 245, 419[a]	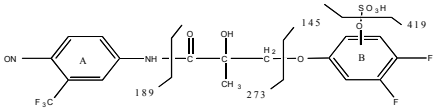
419	145[a], 189 245, 273	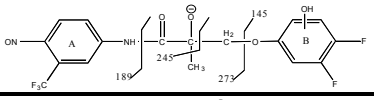
515 (M5)	145, 289, 370, 435[a]	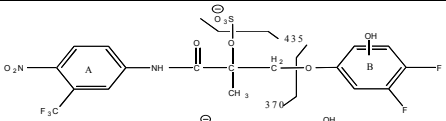
435	145[a], 205, 261, 289	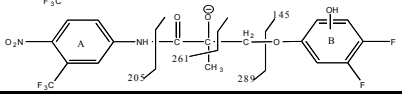

Table 4. 2 Product Ions of **C-3** and Its Metabolites from the 24 h Rat Urine Sample

[a] Denotes a base peak in the product ion mass spectra.

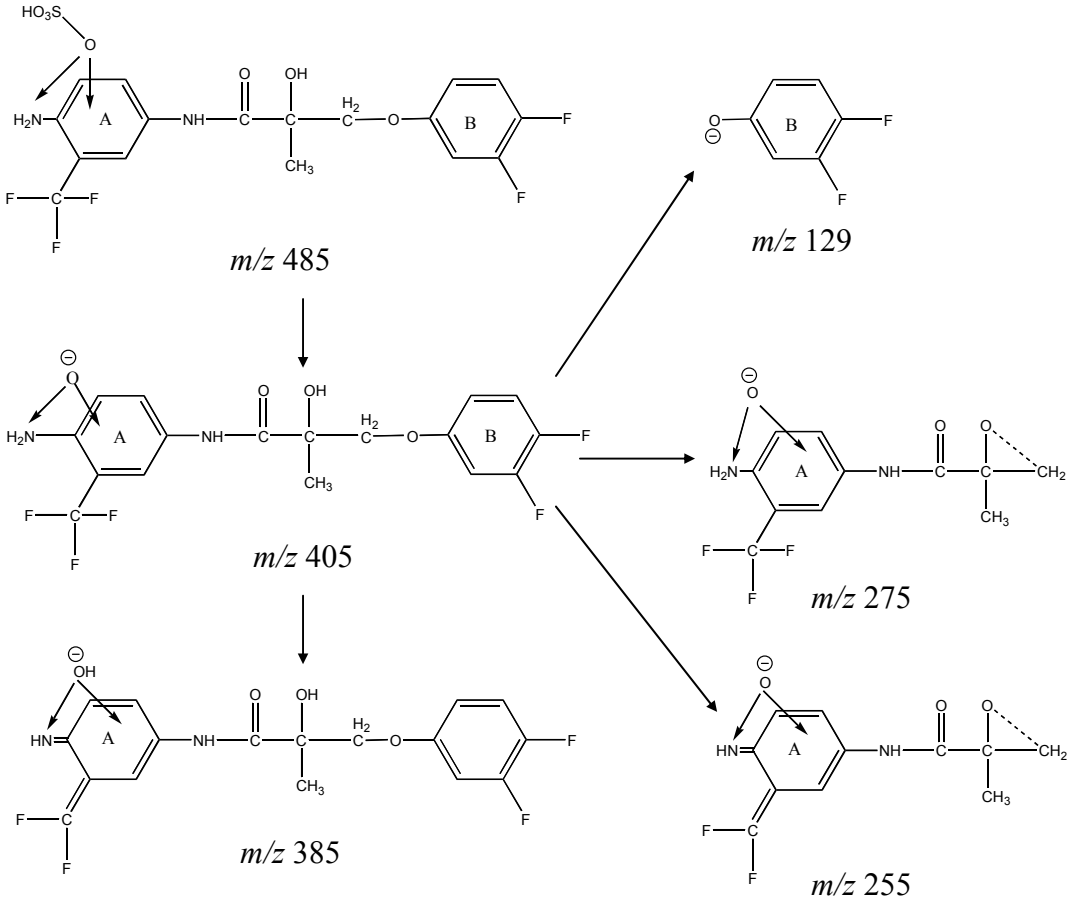

Figure 4. 7 Proposed Fragmentation Pattern of M**3**

Structural information was determined by LC/MS^2 and LC/MS^3 fragmentation of M3.

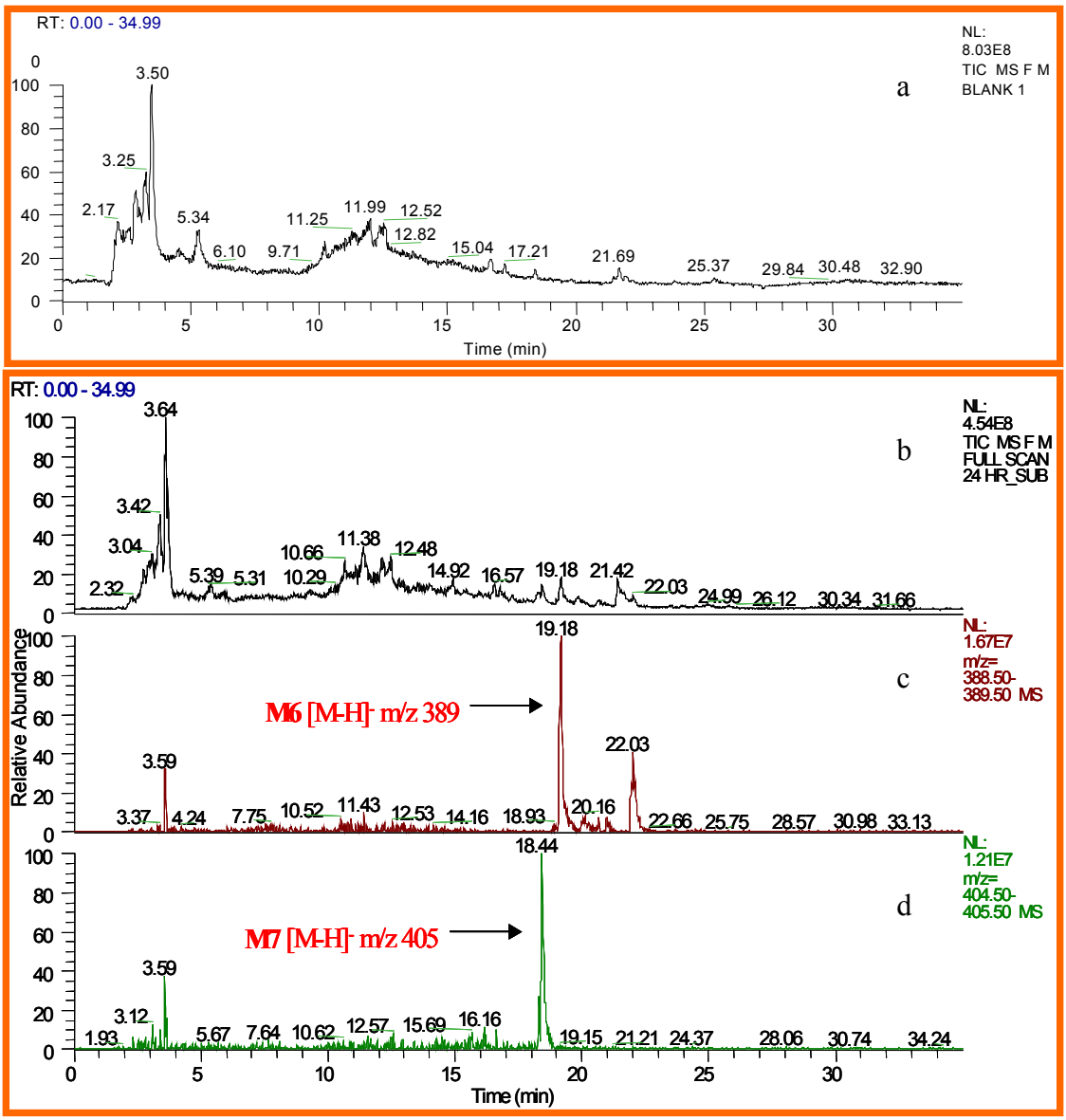

Figure 4. 8 HPLC/ESI-MS Chromatograms of Extracts from Rat Fecal Samples.

(a) Total ion chromatogram (TIC) of blank fecal sample; (b) TIC of 24 h fecal sample; (c) Extracted ion chromatogram (XIC) of one A-ring reduction product M6 at *m/z* 389; (d) XIC of one A-ring reduction B-ring hydroxylation product M7 at *m/z* 405.

Molecular Ions $[M-H]^-$	Product Ions Observed (m/z Values)	Assigned Structure and Proposed Fragmentation Pattern
419 (C-3)	129, 261[a], 289	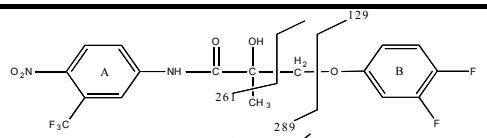
289	205[a], 261	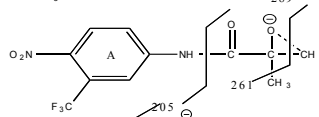
261	188, 218, 205[a]	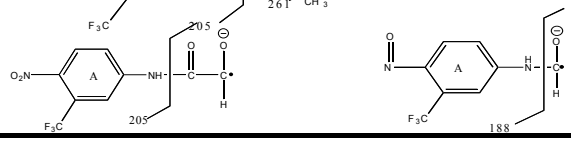
389 (M6)	129[a], 175, 259	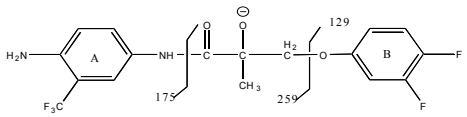
405 (M7)	145[a], 255, 275, 385	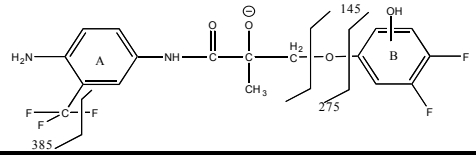

Table 4. 3 Product Ions of **C-3** and Its Metabolites from the 24 h Rat Fecal Sample.

[a] Denotes a base peak in the product ion mass spectra.

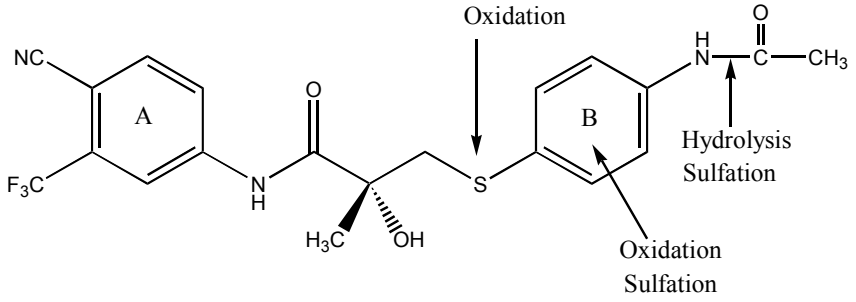

A: Acetothiolutamide

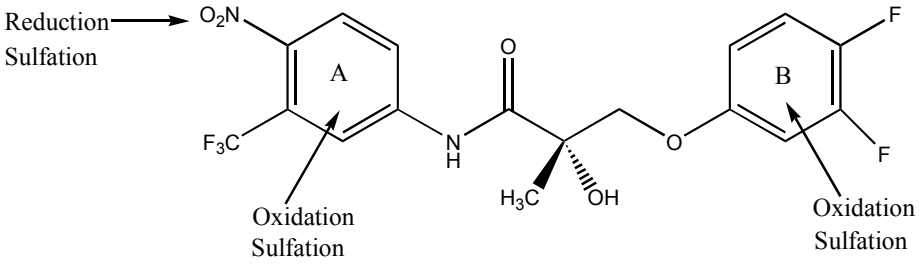

B: <u>C-3</u>

Figure 4. 9 Metabolism Sites of Acetothiolutamide and **<u>C-3</u>** in the Rat.

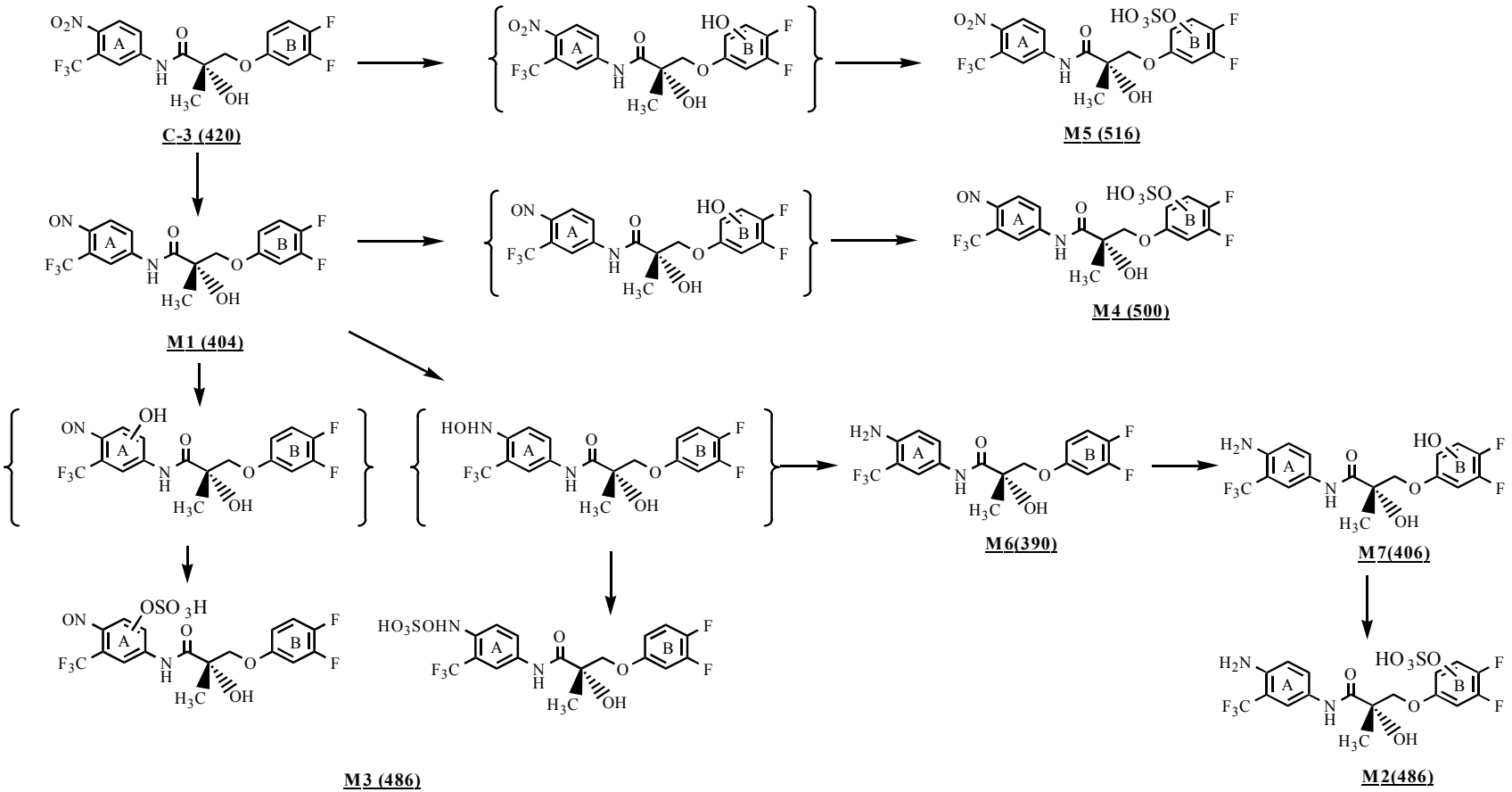

Figure 4. 10 Proposed Metabolism Pathways of **C-3** in Male Rats.

Structures in parenthesis are proposed intermediates.

CHAPTER 5

A SELECTIVE ANDROGEN RECEPTOR FOR HORMONAL MALE CONTRACEPTION

5.1 INTRODUCTION

Worldwide population growth and social awareness of reproductive health have stimulated a great deal of research in contraception. Although contraceptive pills have been available for women for decades, male contraception remains restricted to physical methods, such as condoms and vasectomy. However, many polls show that men would be more willing to be involved in family planning if appropriate contraceptive methods (e.g., a male contraceptive 'pill') were available (158, 159). Although the mechanism of spermatogenesis is not completely understood, inhibition of LH and FSH production is known to interrupt spermatogenesis. To date, the most practical method of male contraception is the hormonal approach. Potential regimens include androgen alone, androgen combined with progestins, and androgen combined with gonadotropin hormone releasing hormone (GnRH) analogs (160, 161). Among them, androgen-progestin combinations remain the most promising approach. Because androgens are essential for male development and the maintenance of male secondary characteristics, such as bone mass, muscle mass, fat tissue distribution, and spermatogenesis (119), an androgen supplement is a required component of hormonal male contraception. However, the lack of orally bioavailable and safe androgens has been a major limitation in the search for hormonal male contraceptives. The main disadvantages of steroidal androgens (e.g., testosterone and its esters) are their undesirable physicochemical and pharmacokinetic properties. Testosterone and the majority of its esters must be administered by intramuscular injection, implant, and/or transdermal patch. Besides their inconvenient

means of administration, steroidal androgens are associated with a variety of undesirable side effects. In fact, the major dose-limiting side effects observed in recent clinical trials of male contraception were androgen-related (161).

Several approaches to overcome the limitations of using testosterone preparations have been explored. One major approach focused on structural modifications of steroidal androgens to develop long-acting androgens. Another approach is nonsteroidal selective androgen receptor modulators (SARMs). In 1998, during our search for androgen receptor (AR) affinity labels, we discovered and reported a group of nonsteroidal androgens, which are derivatives of two known antiandrogens – bicalutamide (Fig. 1) and flutamide (56). In recent years, we determined important structure-activity relationships for AR binding affinity and transcriptional activation (57, 62), pharmacokinetics and key metabolism pathways of SARMs (58), and identified dozens of SARMs that demonstrate tissue-selective anabolic and androgenic *in vivo* pharmacologic effects, but are devoid of the side effects commonly associated with testosterone therapy (59, 60). The discovery of SARMs therefore provides a unique alternative for androgen replacement therapy with advantages including oral bioavailability, flexibility of structural modification, AR specificity, lower activity in the prostate, and the lack of steroid-related side effects.

Earlier studies demonstrated that minor structural modification of SARMs could result in dramatic changes in their *in vitro* and *in vivo* pharmacologic activity. To date, most of the SARMs reported in our laboratories are able to mimic various pharmacologic activities of testosterone in peripheral tissues, but are unable to do so in the central nervous system (Yin *et al*., 2003a). We hypothesized that novel SARMs can also be designed and synthesized to mimic the effects of testosterone on the hypothalamus-pituitary-testis axis. Such compounds would represent an important step toward the discovery and development of SARMs for hormonal male contraception. The present studies were designed to characterize the preclinical pharmacology of one such novel SARM.

5.2 MATERIALS AND METHODS

5.2.1 Chemicals and Animals

The *S*-isomer of **C-6** (Fig. 1) was synthesized in our laboratory with a purity greater than 99% using previously described methods (57, 60). [17α-methyl-^{3}H] Mibolerone ([^{3}H]-MIB, 84 Ci/mmol) and unlabeled MIB were purchased from PerkinElmer Life Sciences (Boston, MA). Phosphate-buffered saline (PBS, catalog# P5368, consisting of 0.01 M phosphate buffer, 0.0027 M potassium chloride, and 0.137 M sodium chloride) and all other chemicals were purchased from Sigma-Aldrich (St. Louis, MO).

Male Sprague-Dawley rats were purchased from Harlan Bioproducts for Science (Indianapolis, IN). All animals were maintained on a 12 h light/dark cycle with food and water available *ad libitum*. The animal protocol was reviewed and approved by the Institutional Laboratory Animal Care and Use Committee of The Ohio State University.

5.2.2 *In Vitro* Pharmacologic Activity

Rat prostate cytosolic AR was prepared from ventral prostates of castrated male SD rats using established methods (63). The AR binding affinity of **C-6** was determined using an *in vitro* radioligand competitive binding assay as previously described (62). In brief, an aliquot of AR cytosol was incubated with 1 nM [^{3}H]MIB and 1 mM triamcinolone acetonide at 4 °C for 18 h in the absence or presence of increasing concentrations of DHT or C –6 (10^{-1} nM to 10^4 nM). Nonspecific binding of [^{3}H]MIB was determined by adding excess unlabeled MIB (1000 nM) to the incubate. The separation of bound and free radioactivity at the end of incubation was achieved by the hydroxyapatite (HAP) method as previously described (Yin et al., 2003b), then the radioactivity was counted in a liquid scintillation counter (Model LS6500, Beckman Instruments Inc, Palo Alto, CA). The specific binding of [^{3}H]MIB at each concentration of DHT or **C-6** (B) was further calculated by subtracting the nonspecific binding of [^{3}H]MIB , and expressed as the percentage of the specific binding in the absence of DHT or **C-6** (B_0). Competitive displacement curves of DHT and **C-6** were constructed with B

on the vertical axis and ligand concentration (C) on the horizontal axis. The concentration of compound that reduced the B_0 by 50% (IC_{50}) was determined by computer-fitting the data to the following equation using WinNonlin (Pharsight Corporation, Mountain View, CA): $B = B_0 \times [1- C/(IC_{50} + C)]$. The equilibrium binding constant (Ki) of DHT or **C-6** was calculated by $K_i = K_d \times IC_{50} /(K_d + L)$, where Kd was the dissociation constant of [^{3}H]MIB (0.19 ± 0.01 nM, previously determined by Mukherjee et al., 1999), and L was the concentration of [^{3}H]MIB used in the experiment (1 nM).

The *in vitro* AR-mediated transcriptional activity of **C-6** was measured using a modification of the method of (62). Monkey kidney cells, CV-1, were maintained at 37°C in a humidified atmosphere of 5% CO_2/95% air in DMEM containing 10% fetal bovine serum (FBS). At ~90% confluence, cells were transfected in serum-free medium using Lipofect AMINE (Invitrogen, Carlsbad, CA) according to the manufacturer's instructions. Cells in each T-175 flask were transfected with 0.8 μg of a human AR expression construct (pCMVhAR; generously provided by Dr. Donald Tindall, Mayo Clinic), 8 μg of an androgen-dependent luciferase reporter construct (pMMTV-Luc, generously provided by Dr. Ron Evans, Salk Institute), and 8 μg of a β-galactosidase expression construct (pSV-β-galactosidase; Promega Corporation). After 3~5 h of transfection, cells were washed with serum-free medium and allowed to recover for 10 h in DMEM medium containing 0.2% FBS. Transfected cells were trypsinized, centrifuged, and counted. Cells were then plated into 24-well plates at a density of 8×10^4 cells/well. Before drug treatment, cells were allowed to attach to plates for 12 h. The agonist activity and antagonist activity of **C-6** were determined by incubating cells with **C-6** (1, 10, 100, 1000 nM) in the absence and presence of DHT (1 nM), respectively. In each experiment, vehicle control and positive control (activity induced by 1 nM of DHT) were included. For each treatment, compounds were dissolved in ethanol, and then diluted with medium to the desired concentrations. The final concentration of ethanol in each well was ≤ 0.05%.

After 24 h drug treatment, medium was removed by aspiration. Cells were washed twice with ice-cold PBS and lysed with 110 μL/well of Reporter Lysis Buffer (Promega Corporation) at room temperature for 30 min. An aliquot (50 μL) of cell lysate from each

well was used for β-galactosidase assays and the other 50 μL of cell lysate was used for luciferase assays using the method previously described (62). All results were expressed as the ratio of (luciferase activity/β galactosidase activity) to avoid variations caused by cell number and transfection efficiency.

5.2.3 *In vivo* Pharmacologic Activity

5.2.3.1 Androgenic and Anabolic Activity of **C-6** in Castrated and Intact Male Rats

Forty-five male SD rats weighing approximately 200 g were purchased and randomly divided into nine groups with five rats per group. One day before the start of treatment, groups 1 through 8 were castrated via a scrotal incision under anesthesia. Group 9 served as an intact vehicle control. **C-6** was dissolved in vehicle containing DMSO (5%, v/v) in PEG 300. Groups 1 through 7 received daily subcutaneous injections of **C-6** at a dose rate of 0.05, 0.1, 0.3, 0.5, 0.75, 1, and 3 mg/day, respectively. Groups 8 and 9 received vehicle. In another study, three groups of intact male rats were treated with vehicle, testosterone propionate (TP), or **C-6** at a dose rate of 0.5 mg/day. This dose rate was chosen based on the results from the aforementioned study in castrated rats. Rats were sacrificed after 14 days of treatment. Serum samples were collected and stored at –80 °C. The ventral prostate, seminal vesicles, and levator ani muscle were removed, cleared of extraneous tissue, and weighed. All organ weights were normalized to body weight and compared. The weights of prostate and seminal vesicles were used to evaluate androgenic activity, while the levator ani muscle weight was used as a measurement of anabolic activity. Non-linear regression analysis was performed to obtain the maximal response (Emax) induced by **C-6** and the dose rate of **C-6** that induced 50% of the maximal response (ED_{50}) using the sigmoid E_{max} model with a baseline effect parameter and WinNonlin software (Pharsight Corporation, Mountain View, CA). The value of Emax was constrained to an upper limit of 130%, slightly above the highest change in tissue weight observed in our study. Serum levels of LH and FSH were measured by the National Hormone & Peptide Program (Dr. A. Parlow, Torrance, CA) using RIA kits with rLH-NIDDK-RP-3 and r-FSH-NIDDK-RP-2 as reference standards, respectively.

Serum testosterone concentrations were measured using commercially available EIA kits (DSL, Webster, TX).

5.2.3.2 *In Vivo* Antireproductive Activity of **C-6** in Intact Male Rats

Fourteen mature, male Sprague Dawley rats (90 days old) were randomly assigned to two groups and received vehicle (5% DMSO + 95% PEG 300, n=6) or **C-6** dissolved in vehicle (n=8) at a dose rate of 1 mg/day. Compounds were freshly prepared immediately before dosing and delivered to animals via daily s.c. injections (100 μL/day) for 70 days. At the end of treatment, animals were sacrificed under anesthesia. Body weight was recorded at autopsy. Prostate, seminal vesicles, right testis, and right epididymis (divided in the middle of corpus epididymis to caput and cauda epididymis) were collected and weighed. All organ weights were normalized with body weights and compared. Blood was also collected. Serum samples were prepared and stored at -80°C until used. One testis from each rat was decapsulated and homogenized in PBS (pH 7.4). To obtain spermatozoa, the cauda epididymis was macerated in PBS (pH 7.4). Advanced spermatids (step 17-19) in the testis and the spermatozoa in cauda epididymis were counted with a hemacytometer. Results were expressed as number of spermatids per testis and spermatozoa per cauda epididymis, respectively. Testosterone concentrations in serum were measured with a commercially available EIA kit (DSL, Webster, TX).

5.2.4 Pharmacokinetics of **C-6** in the Rat

The pharmacokinetics of **C-6** was examined in male SD rats weighing approximately 250 g after a dose of 10 mg/kg by intravenous injection or oral gavage. A catheter was implanted in the right external jugular vein of each animal 24 h prior to drug administration. **C-6** was dissolved in a vehicle containing DMSO (10%, v/v) in PEG 300 and administered to animals through the jugular vein catheter (i.v. group) or oral gavage (p.o. group). For animals in the i.v. group, the catheter was flushed three times with saline (3× the volume of the dosing solution) before blood sampling. Blood samples (~ 200 μL) were then withdrawn through the jugular vein catheter at 5, 10, 30, 60, 90, 120,

180, 360, 720, 1440, and 1800 min after the i.v. dose and at 20, 30, 60, 90, 120, 240, 360, 480, 720, 1080, 1440, and 1800 min after the p.o. dose. Blood samples were immediately centrifuged at 1,000 g, 4°C for 10 min. Plasma samples were prepared and stored at -20°C until HPLC analysis.

5.2.5 HPLC Method

An aliquot (100 μL) of each plasma sample from the pharmacokinetic studies was spiked with 10 μL of an internal standard (a structural analog of **C-6**) and mixed well with 1 mL of acetonitrile. After centrifugation at 16,000 g, 4°C for 10 min, the supernatant was collected and evaporated. The residues were reconstituted in 120 μL of mobile phase. An aliquot of each sample was injected into a Nova-pak C_{18} column (3.9 × 150 mm, 4 μm particle size) purchased from Waters Corporation (Milford, MA). The HPLC system consisted of a model 515 HPLC pump (Waters), a model 717 plus autosampler (Waters), and a model 486 absorbance detector (Waters). HPLC separation was performed using an isocratic mobile phase (H_2O/Acetonitrile: 46/54, v/v) at a flow rate of 1 mL/min. The UV absorbance of eluents was monitored at 298nm. Calibration standards were prepared in blank rat plasma with **C-6** concentrations ranging from 0.1 ~ 50 μg/mL. The recoveries of this compound over the calibration range were from 93.4% to 100.4%. The intra- and inter-day coefficients of variation of the assay were lower than 2.9% and 8.9%, respectively. The limit of quantitation of the HPLC assay was 0.1 μg/mL.

5.2.6 Pharmacokinetic Data Analyses

The plasma concentration-time data were analyzed using noncompartmental methods and WinNonlin software (Pharsight, Mountain View, CA). The terminal half-life ($T_{1/2}$) was calculated as $T_{1/2} = 0.693/\lambda$, where λ was the terminal elimination constant. The area under the plasma concentration-time curve ($AUC_{0-\infty}$) was calculated using the

trapezoidal method with extrapolation to time infinity. The plasma clearance (CL) was calculated as $CL = Dose_{i.v.}/AUC_{0-\infty, i.v.}$, where the $Dose_{i.v.}$ and $AUC_{0-\infty, i.v.}$ were the intravascular dose and the corresponding area under the plasma concentration-time curve from time 0 to infinity, respectively. The apparent volume of distribution at equilibrium (Vd_{ss}) was calculated as $Vd_{ss} = CL \cdot MRT$, where the MRT was the mean residence time following the intravenous bolus dose. The peak plasma concentration (C_{max}) and time to reach the peak concentration (T_{max}) after a p.o. dose were obtained directly from the plasma concentration-time curves. Oral bioavailability ($F_{p.o.}$) was defined as $F_{p.o.} = (AUC_{0-\infty, p.o.} \cdot Dose_{i.v.})/(AUC_{0-\infty, i.v.} \cdot Dose_{p.o.})$, where the $Dose_{p.o.}$ and $AUC_{0-\infty, p.o.}$ were the oral dose and the corresponding area under the plasma concentration-time curve from time 0 to infinity after p.o. administration, respectively.

5.2.7 Statistical Analyses

All statistical analyses were performed using single-factor ANOVA with the α value set a *priori* at $p < 0.05$.

5.3 RESULTS

5.3.1 *In vitro* Pharmacologic Activity

Previous studies demonstrated that structural modification(s) of the A-ring, linkage, and/or the B-ring of nonsteroidal SARMs affect their *in vitro* and *in vivo* pharmacologic activity. Compared to bicalutamide, **C-6** has a NO_2 at the *para*-position of the A-ring, an ether linkage, and a chloro and a fluoro substituent at the *para*-position and *meta*-position of the B-ring, respectively (Fig. 1). The AR binding affinity of **C-6** was determined using a competitive binding assay. Dihydrotestosterone (DHT) and **C-6** displaced ^{3}H-MIB from AR binding sites (Fig. 2). The Ki values of DHT and **C-6** were 0.45 ± 0.2 nM and 4.9 ± 0.3 nM, respectively. Although the binding affinity of **C-6** was less than one-tenth that of DHT, it bound the AR with 2-fold higher affinity than R-bicalutamide (i.e., $Ki_{Bicalutamide}$ = 11.0 nM) (162) and 4~8-fold higher affinity than

hydroxyflutamide (128, 163), indicating that **C-6** interacted with the AR with high binding affinity.

Upon binding to the AR, **C-6** induced a concentration-dependent increase in AR-mediated transcriptional activation (Fig. 3, panel A). The transcriptional activity induced by **C-6** plateaued at concentrations equal to or greater than 10 nM (~100% of activity that was induced by 1 nM of DHT). The activity in the vehicle-treated wells was less than 3% of the transcriptional activation induced by 1 nM of DHT. **C-6** did not significantly inhibit transcriptional activity induced by DHT (Fig. 3, panel B) even at a concentration as high as 1,000 nM. These results clearly demonstrated that **C-6** binds to the AR with high affinity and potently stimulates AR-mediated transcriptional activity *in vitro*.

5.3.2 *In vivo* Pharmacologic Activity

5.3.2.1 Androgenic and Anabolic Activity of **C-6**

We then examined the *in vivo* androgenic and anabolic activities of **C-6**. In castrated male rats, the androgenic activity was evaluated by the ability of **C-6** to maintain the weights of ventral prostate and seminal vesicle, while levator ani muscle weight was used to assess anabolic activity. Castration resulted in a significant reduction in the weights of ventral prostate, seminal vesicle, and levator ani muscle to 8.5%, 6.5%, and 34% of that observed in intact animals, respectively. The administration of **C-6** increased the weights of these tissues in a dose-dependent manner (Fig. 4A). At the highest dose rate (3 mg/day), the weights of all three organs were increased to about 130% of those observed in intact controls. Nonlinear regression analysis of the dose-response relationships showed that the ED_{50} values of **C-6** were 0.77 ± 0.06, 0.88 ± 0.1, and 0.17 ± 0.04 mg/day in the ventral prostate, seminal vesicle, and levator ani muscle, respectively (Fig. 4B). These results clearly revealed the potent and efficacious androgenic and anabolic activity of **C-6** in male rats. The ED_{50} value of **C-6** in the levator ani muscle (0.17 ± 0.04 mg/day) was about 4 to 5-fold less than its ED_{50} values in prostate and seminal vesicle (0.77 ± 0.06 mg/day and 0.88 ± 0.14 mg/day, respectively). At a dose rate of 0.3 mg/day, **C-6** maintained the weight of levator ani muscle at a weight not different from that observed in intact controls. The effect of **C-6** in the ventral

prostate and seminal vesicle was about 30% of that observed in intact controls at this dose rate. Results suggested that **C-6** acts as a tissue-selective androgen with more potent anabolic activity than androgenic activity. The efficacy (maximum effect) of **C-6** in anabolic and androgenic tissues was about the same.

We also determined the serum levels of LH and FSH in animals treated with **C-6**, and compared them to the levels of those hormones observed in intact and castrated control animals. As shown in Table 1, castration led to a significant elevation in LH (8.4 ± 2.5 ng/mL) and FSH (63.4 ± 5.0 ng/mL) levels due to the lack of negative feedback inhibition by testosterone. **C-6** caused a dose-dependent decrease in LH and FSH levels and restored the levels of these hormones back to physiological levels at dose rates as low as 0.3 mg/day and 0.5 mg/day, respectively.

These data led us to immediately examine the pharmacologic activity of **C-6** in intact male rats to answer an important question: Would **C-6** mimic the ability of exogenous testosterone to inhibit the synthesis of endogenous testosterone? We chose a dose rate of 0.5 mg/day for this study. This dose was the minimum dose required to fully suppress LH and FSH, and yet maintain normal muscle mass in castrated rats. In a 14-day study (Fig. 5), testosterone propionate (TP) stimulated growth in all three organs, while **C-6** demonstrated tissue-selective pharmacologic effects in intact rats. The weights of the ventral prostate and seminal vesicles were significantly decreased to about 50% of those observed in intact controls, while the weights of levator ani muscle remained the same as those observed in intact controls. Surprisingly, the pharmacologic effects of **C-6** in intact rats were nearly identical to those found in castrated rats at this dose rate (0.5 mg/day) (Fig. 5). Based on this finding, we predicted that **C-6** reduced serum testosterone concentration to levels similar to those observed in castrated rats. Results showed that the average testosterone concentration in the intact control group was 4.47 ± 1.66 ng/mL. Testosterone concentrations in three animals of the **C-6**-treated group were below the detection limit (0.04 ng/mL) of the assay, while testosterone concentrations in the two remaining animals were 0.11 ng/mL and 0.46 ng/mL. Clearly, **C-6** potently and rapidly inhibited endogenous testosterone synthesis in male rats.

5.3.2.2 Antireproductive Activity of **C-6**

In this pilot study, we evaluated the effects of **C-6** on the reproductive system after long-term (1 mg/day, 10 weeks) treatment in adult male rats. Body and organ weights in control and **C-6**-treated rats are summarized in Table 2. No significant difference in the mean body weight was observed after **C-6** treatment. **C-6** caused a significant reduction in the size of the prostate, seminal vesicles, testis and epididymis to 68, 83, 60, and 64% of control values, respectively. Similar to our observations in castrated animals, **C-6** significantly increased the weight of levator ani muscle to 120% of that observed in controls. As shown in Figure 6, the mean sperm counts in both testis and cauda epididymis were significantly reduced to about 25% of those observed in the intact control group. Because of the marked decline in testicular and epididymal weight, the changes in serum testosterone level were further evaluated. The average testosterone concentration in intact control animals was 1.06 ± 0.78 ng/mL. These concentrations are within the normal range of testosterone concentration reported from male rats with a similar age (164, 165). Animals in **C-6**-treated group showed significantly suppressed testosterone levels that were lower than the quantitation limit (0.04 ng/mL) of the EIA kits. Clearly, the reduction of endogenous testosterone production was the main reason for the suppressed reproductive organ weights and sperm number in intact animals. Although a high dose rate (1 mg/day) of **C-6** was used in this study, low activity was observed in the prostate and seminal vesicles due to the tissue selectivity of **C-6**. In conclusion, **C-6** was able to mimic the effects of exogenous testosterone on spermatogenesis in male rat, while maintaining its tissue selectivity after chronic treatment. Additional studies over a wider dose range are warranted to more fully describe the effects of **C-6** on spermatogenesis and male reproductive activity.

5.3.3 Pharmacokinetics of **C-6** in the Rat

To develop a possible male contraceptive 'pill', high oral bioavailability and a suitable half-life of the compound are required. Therefore, the pharmacokinetics of **C-6**

were examined after i.v. and p.o. administration to male rats after a single dose of 10 mg/kg.

The time-courses of the changes in plasma concentrations of **C-6** following i.v. and p.o. administration are shown in Figure 7, and the pharmacokinetic parameters are listed in Table 3. Following intravenous administration, **C-6** concentrations declined and remained detectable until 30 h after the dose. The terminal $T_{1/2}$ of **C-6** in male rats was 6.3 h. The systemic clearance (CL) and steady state volume distribution (Vd_{ss}) were 0.72 mL/min · kg and 473 mL/kg, respectively. **C-6** appeared rapidly (within 5 minutes) in the systemic circulation after p.o. administration, suggesting gastric absorption of the drug. Oral absorption was prolonged with maximum plasma concentrations forming a plateau over 6 to 12 h post-dose. Plasma concentrations of **C-6** diminished with a mean terminal $T_{1/2}$ of 5.6 h. This terminal $T_{1/2}$ was smaller than that observed after i.v. administration, an observation which was likely due to individual variation of plasma drug concentration after p.o. administration. However, statistical analysis revealed no significant difference between these two values. The bioavailability of **C-6** following oral administration was 76%.

5.4 DISCUSSION

Earlier studies revealed that known nonsteroidal AR ligands (mainly bicalutamide derivatives) could be structurally modified to obtain a series of compounds with diverse *in vitro* (62) and *in vivo* pharmacologic activities (59). Subsequent research in our laboratories has focused on the discovery of novel SARMs as alternatives for testosterone replacement therapy and the treatment of muscle wasting diseases, osteoporosis, prostate hyperplasia (64), and hormonal male contraception. However, unlike testosterone, the SARMs that we have reported to date showed little to no effects on the hypothalamic-pituitary-testis axis, precluding their ability to regulate gonadotropins, serum testosterone levels, or serve as components of a male contraceptive regimen. Our previous studies showed that the aromatic B-ring is much more amenable to structural modification than other positions in the structure (60, 62). We used this and other structure-activity

relationships uncovered in our research to design and synthesize additional series of SARMs in the hopes of identifying compounds with enhanced central activity. Typically, these compounds were *S*-isomers with a structure that bears a NO_2 and a CF_3 at the *para*-position and *meta*-position of the A-ring, respectively, a CH_3 linked to the chiral carbon, an ether linkage, and an electronegative substituent(s) in the aromatic B-ring. **C-6** was one of these AR ligands.

When we compared the *in vitro* activity of **C-6** with one of our known SARMs (i.e., (*S*)-3-(3-fluorophenoxy)-2-hydroxy-2-methyl-*N*-(4-nitro-3-trifluoromethylphenyl) propionamide (**S-1**)) (59), we found that the *di*-halogen (*para*-Cl and *meta*-F) substituents in the aromatic B-ring retained high AR binding affinity (i.e., $K_{i,\ \mathbf{C\text{-}6}}$ = 4.9 nM vs $K_{i,\ \mathbf{S\text{-}1}}$ = 6.1 nM). Notably, at a concentration of 10 nM, **C-6** showed 2 to 3-fold higher transcriptional activation than **S-1** (i.e., 118% vs 43% of the activity induced by 1 nM of DHT). These findings were consistent with our prediction regarding the flexibility of structural modification in the B-ring. When **C-6** was tested in the castrated male rat model, it produced more potent and efficacious *in vivo* pharmacologic activity than **S-1**. Although **C-6** exhibited profound effects on all three androgen-dependent organs, it remained tissue selective. The potency (i.e., ED_{50}) and efficacy (i.e., E_{max}) of **C-6** and testosterone propionate (TP) (59) in levator ani muscle were comparable, while the potency of **C-6** in prostate and seminal vesicles was 6 to 7-fold less than that of TP. Further, the ED_{50} value for **C-6** in the levator ani muscle was 0.17 mg/day, or about 5-fold lower than that in the prostate and seminal vesicle. Thus, in castrated rats, a dose of **C-6** (i.e., 0.3 mg/day) that will fully maintain the weight of levator ani muscle will only partially maintain the weight of the prostate and seminal vesicles. The enhanced pharmacologic activity of **C-6** compared to our previously reported SARM (i.e., **S-1**) might have resulted from several factors, including: binding affinity, transcriptional activity, drug disposition, metabolism rate, and/or nuclear retention time. During *in vitro* studies, **C-6** showed higher transcriptional activity but similar binding affinity to **S-1**. The *in vivo* total body clearance of **C-6** was 0.72 mL/min/kg, which was significantly smaller than that of **S-1** (Data not published). Therefore, the increased efficacy and potency of **C-6** in rats may have been due to its higher intrinsic activity and greater *in vivo* exposure.

Due to the detection limit of the LH RIA assay and the limited sample volumes, LH concentrations in the high dose drug-treated group and intact group were undetectable. However, it was clear that the antigonadotropic activity of **C-6** was dose-dependent and more potent than TP (59). Others showed that testosterone and DHT inhibit LH secretion in response to LHRH stimulation in rats (166) in cultures of rat anterior pituitary fragments (167) and anterior pituitary cells (168). Studies using 5α-reductase inhibitors revealed that the conversion of testosterone to DHT is not critical to the antigonadotropic activity of testosterone. This conclusion is further supported by our current studies since **C-6** does not undergo 5α-reduction.

It is well known that exogenous testosterone interferes with spermatogenesis indirectly by decreasing pituitary gonadotropin secretion via negative feedback on the hypothalamus-pituitary-testis axis in different species (169-172). However, the effects of testosterone on spermatogenesis were biphasic depending on the dosage of androgen administered (173, 174). At low doses, androgen suppresses gonadotropin secretion, decreases testicular steroidogenesis, and then subsequently inhibits spermatogenesis. At higher androgen doses, endogenous testosterone levels remain suppressed but the exogenous androgen is sufficient to directly supports spermatogenesis. In our pilot antireproductive study, for the first time, we demonstrated that the administration of a nonsteroidal androgen receptor modulator (**C-6**) to adult male rats resulted in marked suppression of spermatogenesis. **C-6**-treatment reduced peripheral testosterone concentrations to undetectable levels, significantly suppressed spermatogenesis, reduced the size of testis and epididymis, and increased the weight of levator ani muscle. The magnitude of antireproductive effects of **C-6** could, like testosterone, be dose-dependent. Only one dose rate was examined in this pilot study. Although the androgenic activity of **C-6** was much lower than testosterone and its esters, this dose of **C-6** may still be sufficient to partially maintain spermatogenesis in rats. To date, our knowledge about the role of SARMs on the reproductive system is limited. Further dose-response relationships of SARMs on spermatogenesis, fertility, and libido are needed to understand and fully develop their potential for use in hormonal male contraception.

In conclusion, **C-6** is a novel SARM that was identified during studies to define structure-activity relationships for AR binding. **C-6** bound the AR with high affinity and

stimulated AR-mediated transcriptional activation to a similar extent as DHT. *In vivo* studies showed that **C-6** demonstrated tissue-selective pharmacologic activity, with more potent anabolic than androgenic activity. The high oral bioavailability and potent ability of **C-6** to suppress gonadotropins, testosterone, and spermatogenesis suggest that **C-6** is a promising candidate for hormonal male contraception either alone or in combination with a progestin.

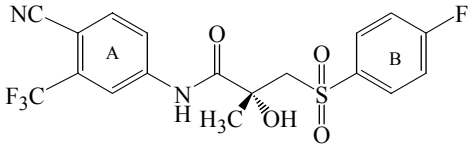

R-Bicalutamide

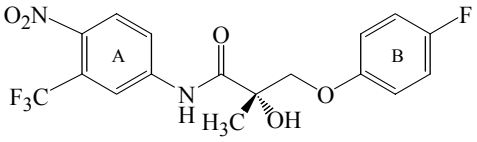

S-1

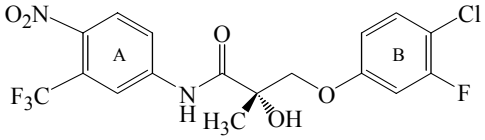

C-6

Figure 5. 1 Chemical Structures of Bicalutamide, **S-1,** and **C-6.**

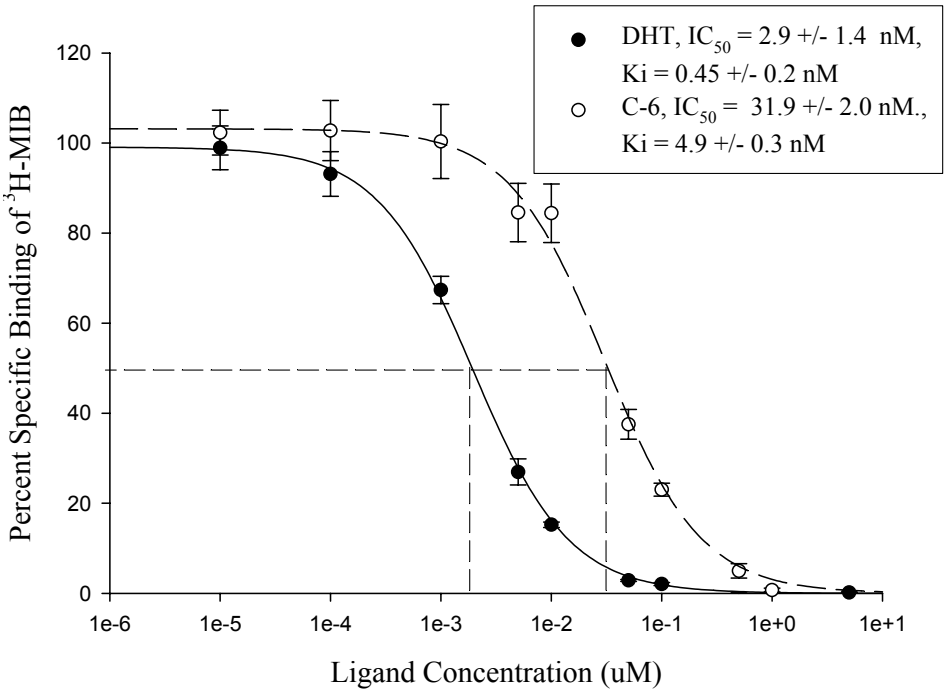

Figure 5. 2 Competitive Displacement Curves for DHT and **C-6.**

Various concentrations of DHT or **C-6** were incubated with ^{3}H-MIB (1 nM) for 18 hr as described in the *Material and Methods* section. Each data point represents the mean ± S.D. of triplicate measurements, expressed as a percentage of specific binding. The IC_{50} was estimated using nonlinear regression and the inhibitory effect sigmoid E_{max} model and defined as the ligand concentration that caused 50% reduction of the binding of ^{3}H-MIB.

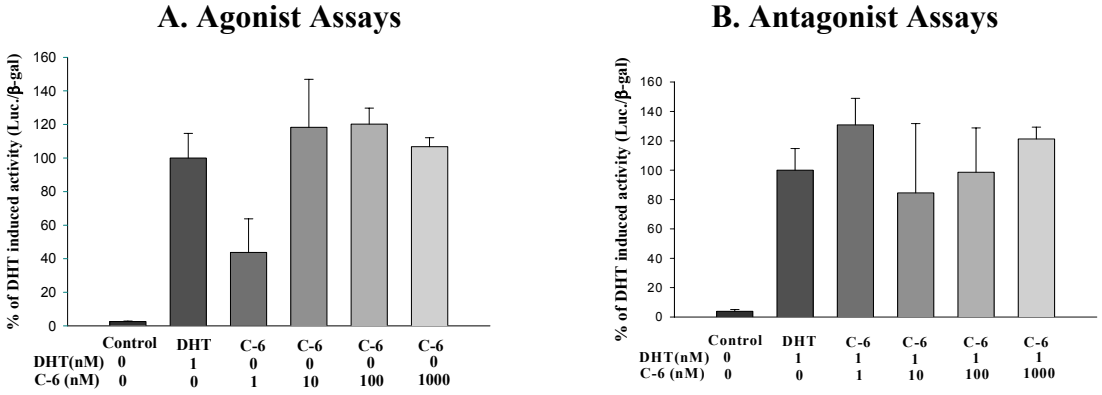

Figure 5. 3 AR-Mediated Transcriptional Activity Induced by DHT and **C-6.**

CV-1 cells were transfected with a human AR plasmid, an androgen-responsive luciferase reporter plasmid, and a constitutively expressed β-galactosidase plasmid in a T-125 flask using LipofectAMINE. After transfection, cells were plated onto 24-well plates and allowed to recover for 12 h before drug treatment. Cells were then treated with vehicle or increasing concentrations of **C-6** alone or together with 1 nM of DHT for 24 h. Luciferase activity in each well was normalized with the β-galactosidase activity and then expressed as the percentage of that induced by 1 nM DHT. Each bar represents mean ± S.D. (n=3).

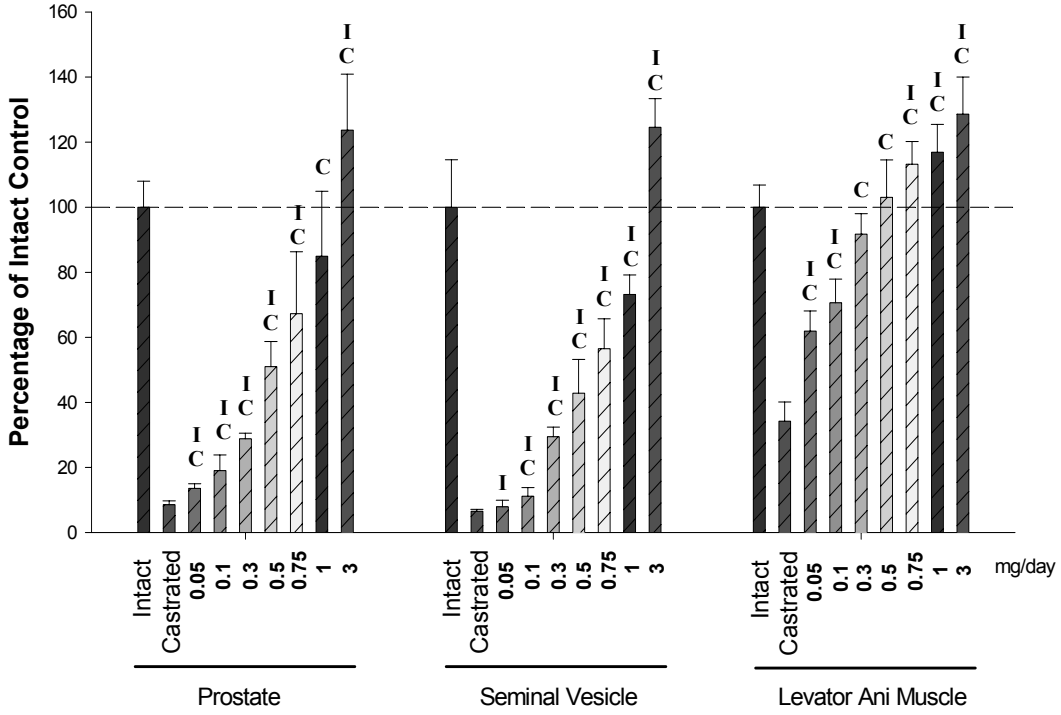

Figure 5. 4 Androgenic and Anabolic Activities of **C-6** in Castrated Male Rats.

Castrated male rats received **C-6** at a dose rate ranging from 0.05 to 3 mg/day by daily subcutaneous injection for 14 days. Organ weights were normalized with body weight and were expressed as the percentage of the weights in the intact control group. Each bar represents the mean ± S.D. (n=5/group). The letters "I" and "C" above each error bar represent a significant difference between the group and intact control group or castrated control group, respectively, as analyzed by single-factor ANOVA with $p < 0.05$.

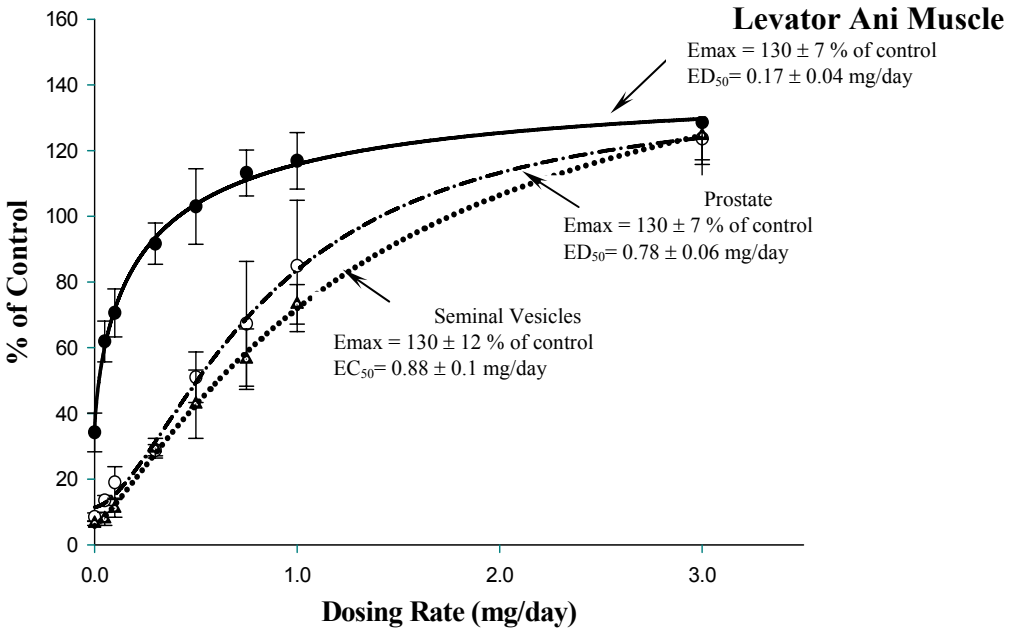

Figure 5. 5 Dose Response Relationship of **C-6** in Castrated Male Rats.

Dose-response curves, E_{max}, and ED_{50} in this figure were obtained by nonlinear least-square regression analysis.

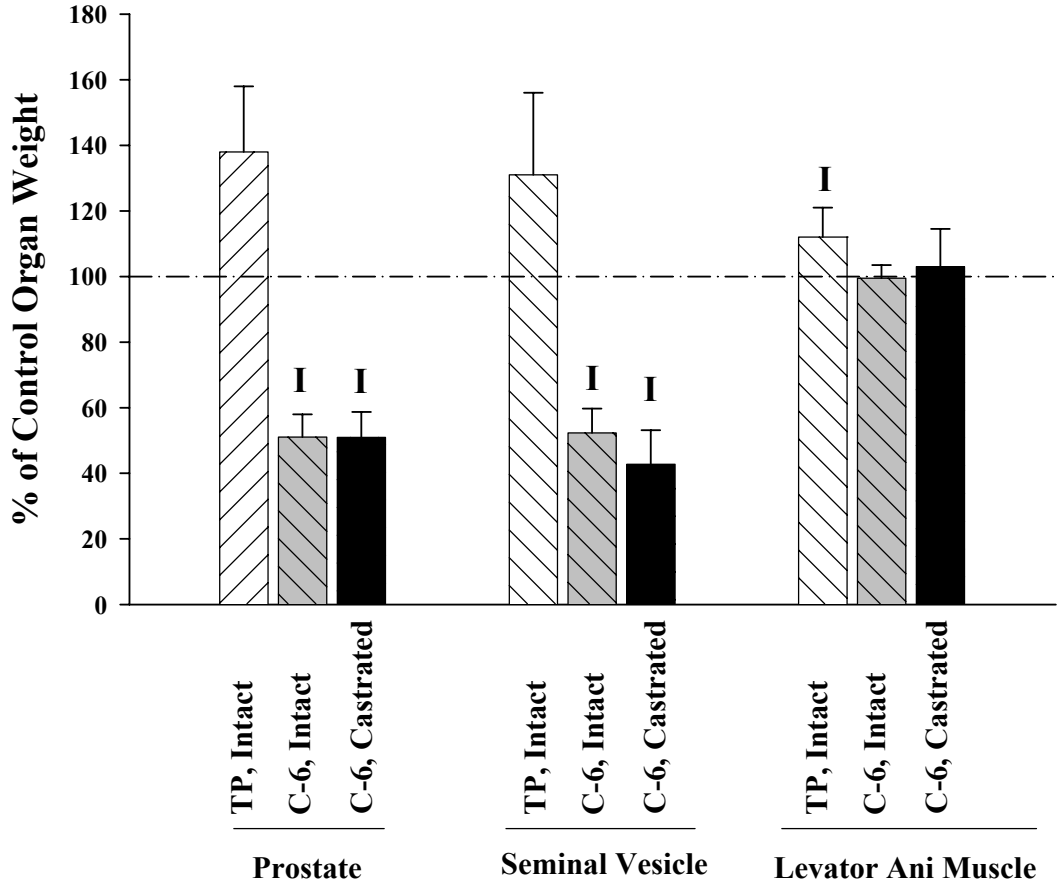

Figure 5. 6 Androgenic and Anabolic Activities of TP and **C-6** in Male Rats.

Intact male rats received vehicle, testosterone propionate (TP), or **C-6** at a dose rate of 0.5 mg/day by daily subcutaneous injection for 14 days. Additional five male rats were castrated 24 h prior to the treatment and received **C-6** at the same dose rate by daily subcutaneous injection for 14 days. Organ weights were normalized with body weight, expressed as the percentage of the weights in the intact control group (100%, the reference line), and compared. Each bar represents the mean ± S.D. (n=5/group). The letter "I" above each error bar represents a significant difference between the group and intact control group as analyzed by single-factor ANOVA with $p < 0.05$.

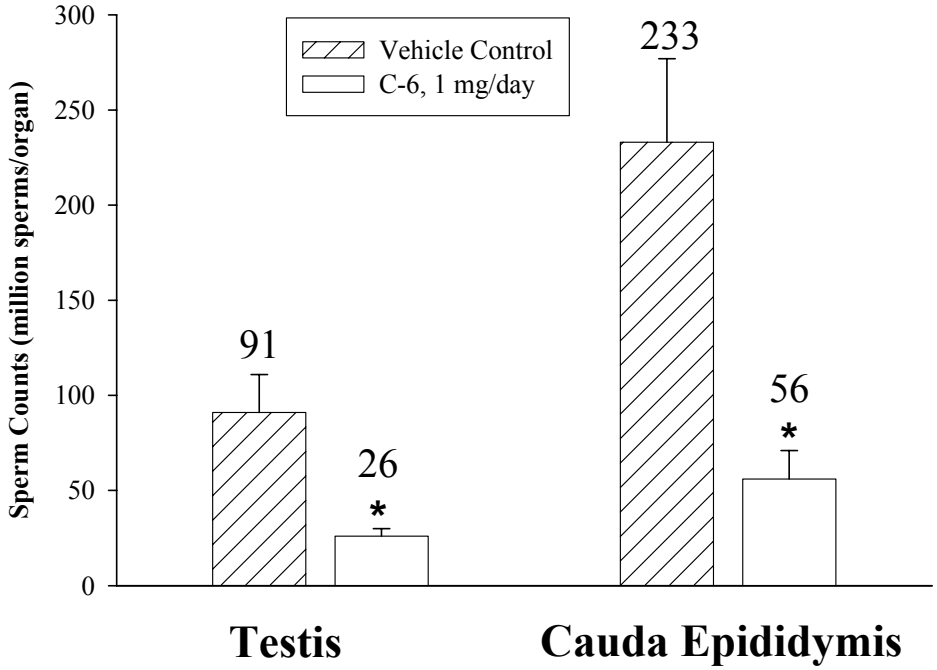

Figure 5. 7 Effects of **C-6** on Spermatogenesis in Intact Male Rats.

Adult male rats received **C-6** at a dose rate of 1 mg/day by daily subcutaneous injection for 10 weeks. One testis and one epididymis from each animal were collected and weighed. Sperm contents in the testis and cauda epididymis were examined as described in the *Material and Methods* section.
* Significant difference between groups, as analyzed by single-factor ANOVA with $p < 0.05$. Each bar represents the mean ± S.D. (n = 6 to 8/group).

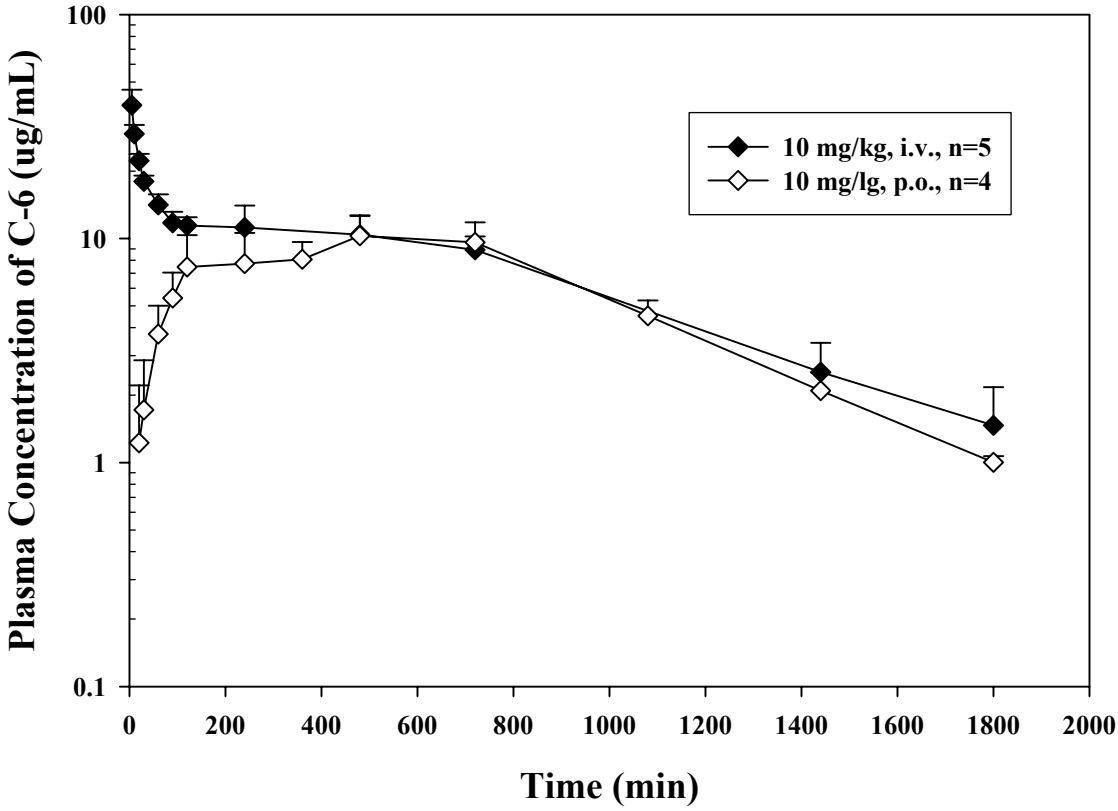

Figure 5. 8 Mean Plasma Concentration-Time Profile of **C-6** in Male Rats.

Plasma concentrations of **C-6** were measured using HPLC. Data were expressed as microgram per milliliter, and each point represents the mean ± S.D. (n = 5/group).

Group	LH (ng/ml)	FSH (ng/ml)
Intact Control	< 0.2	11.2 ± 2.0
Castrated Control	8.4 ± 2.5 [I]	63.4 ± 5.0 [I]
C-6, 0.1 mg/day	3.6 ± 0.8 [I C]	53.0 ± 5.1 [I C]
C-6, 0.3 mg/day	< 0.2 [C]	26.6 ± 8.9 [I C]
C-6, 0.5 mg/day	< 0.2 [C]	12.4 ± 1.1 [C]
C-6, 0.75 mg/day	< 0.2 [C]	12.8 ± 1.6 [C]

Table 5. 1 Effects of **C-6** on LH and FSH in Castrated Male Rats.

Letter I and C indicate a significant difference between the group and intact control group or castrated control group, respectively, as analyzed by single-factor ANOVA with $p < 0.05$. Values are mean ± SE (n = 5/group).

Group	Body Weight (g)	Normalized Organ Weight (% of Control)				
		Prostate	Seminal vesicles	Testis	Epididymis	Levator Ani Muscle
Intact (6)	422 ± 14	100 ± 18	100 ± 9.5	100 ± 9.6	100 ± 9.7	100 ± 6.1
C-6 (8)	414 ± 8	68 ± 5 *	83 ± 7 *	60 ± 4 *	63 ± 4 *	120 ± 10 *

Table 5. 2 Effects of **C-6** on Body Weight and Androgen-Dependent Organ Weights.

* Significant difference between groups, analyzed by single-factor ANOVA with $p < 0.05$. Values are mean ± SE. Figures in parentheses indicate number of animals

Parameter	i.v. 10 mg/kg (n=5)	p.o. 10 mg/kg (n=4)
$AUC_{0\rightarrow\infty}$ (min*mg/ml)	14003 ± 1784	10585 ± 478
λ_Z (min^{-1})	0.00182 ± 0.0004	0.002075 ± 0.00025
MRT (min)	662 ± 130	750 ± 51
CL (ml/min/kg)	0.72 ± 0.09	
V_{ss} (ml/kg)	473 ± 70	
F p.o. (%)		76
T_{max} (min)		540 ± 120
C_{max} (mg/ml)		11.6 ± 1.6

Table 5. 3 Average Pharmacokinetic Parameters of **C-6** in Male Rats.

Values are mean ± SE (n = 4 or 5/group).

CHAPTER 6

EFFECTS OF A SELECTIVE ANDROGEN RECEPTOR MODULATOR (C-6) ON MUSCLUINE SEXUAL BEHAVIOR IN MALE RATS

6.1 INTRODUCTION

Masculine sexual behavior in male rats is highly dependent on hormones. Testosterone is the primary steroid hormone secreted by the testes. Administration of synthetic testosterone to castrated male rats fully restored masculine sexual behavior (175). In the brain and peripheral tissues, testosterone is extensively metabolized to estradiol and 5α-dihydrotestosterone (DHT) by aromatase and 5α-reductase, respectively (176). The role of estrogen versus DHT in mediating the activation of mating behavior in male rats is controversial. In the hypothalamic and limbic structures of adult male rats, estrogen (177, 178), DHT (179), and their specific receptors (180-182) are present. Using castrated male rats, multiple lines of evidence indicated that estrogen stimulates masculine sexual behavior in a less quantitative and qualitative manner than testosterone (183-187). Furthermore, the aromatase inhibitor, androst-1,4,6,-triene-3,17-dione (ATD), inhibits the stimulation of ejaculation by testosterone in castrated male rats by blocking the conversion of testosterone to estradiol (188). On the other hand, administration of DHT, a nonaromatizable androgen, only activates minimal levels of masculine sexual behavior in castrated male rats (189, 190). While neither estradiol benzoate (EB) nor DHT fully restore mating behavior in castrated male rats when used a lone, combined administration of estrogen and DHT are as effective as testosterone in stimulating sexual behavior in rats (185, 191, 192). It has been suggested that the failure of DHT to

stimulate masculine sexual behavior in male rats is due to its unfavorable pharmacokinetic properties. To test this hypothesis, other synthetic androgens [e.g., methyltrienolone (R1881) and 7α-methyl-19-nortestosterone (MENT)] with better *in vivo* stability were also investigated for their effects on sexual behavior in male rats. Androgens with no estrogenic metabolites, such as R1881, fail to activate mating in castrated male rats as readily as testosterone or androgen plus estrogen (193). However, androgens with estrogenic metabolites, such as MENT, fully restore mating in castrated male rats (194). Taken together, these data suggest mating behavior in the castrated male rat requires the central effects of estrogen and peripheral effects of androgen.

Selective androgen receptor modulators (SARMs) discovered in our laboratories demonstrate no estrogenic activity with high androgen receptor specificity. An ideal SARM for androgen replacement therapy would mimic the pharmacologic activity of testosterone and be devoid of testosterone-related side effects. For the purpose of hormonal male contraception, SARMs should mimic the negative feedback actions of testosterone on the hypothalamic-pituitary-gonadal axis to suppress gonadotropins yet support peripheral organs like muscle and bone that require androgen. However, SARMs that can completely inhibit endogenous testosterone production and spermatogenesis must also support or maintain male sexual behavior. **C-6** demonstrated potent and rapid inhibition of gonadotropins and testosterone in castrated and intact male rats, respectively (65). To date, rats remain the best small animal model for hormonal male contraception. We examined the effects of **C-6** on masculine sexual behavior in rats as a first step toward designing studies to understand the therapeutic potential of SARMs in hormonal male contraception and the true role of androgens in masculine sexual behavior in rats. The results of these studies unequivocally establish the critical role of androgens and estrogens in sexual behavior in rats and are reported herein.

6.2 MATERIALS AND METHODS

6.2.1 Animals

Mature, male Sprague-Dawley rats (BW, ~ 300 g) and female SD rats (BW, ~200 g) were purchased from Harlan Bioproducts for Science (Indianapolis, IN). All animals were maintained on a 12h light/dark cycle with food and water available *ad libitum*. The

animal protocol was reviewed and approved by the Institutional Laboratory Animal Care and Use Committee of The Ohio State University.

6.2.2 Chemicals

C-6 was synthesized using the methods described by Marhefka *et al.* (60). Chemical purity was confirmed using elemental analysis, mass spectrometry, and proton nuclear magnetic resonance. Dimethyl sulfoxide (DMSO), polyethylene glycol-300 (PEG 300), ketamine, xylazine, estrogen benzoate (EB), progesterone and acetonitrile were purchased from Sigma Chemical Co (St. Louis, MO) and ethanol was purchased from Pharmco Products (Brookfield, CT).

6.2.3 Effects of **C-6** on Male Sexual Behavior in Castrated Rats

All sexual behavior tests were conducted in the early part of the dark portion of the light/dark cycle under dim red light for illumination. Each test began by placing a male into a glass observation box (25 × 47 × 29 cm). Five minutes later, a receptive female was introduced to the observation cage. During a 30 min observation period, the latency and frequency of all mounts (with palpation and pelvic thrusts), intromissions, and ejaculations were recorded. All female rats were ovariectomized under anesthesia with ketamine/xylazine (83/17 mg/kg, w/w). Sexual receptivity was induced by subcutaneous injections of EB (100 μg) at 24 h and 48 h prior to the test and progesterone 4 h prior to the test at a dose of 500 μg. The following behavioral indices were defined as: Mount Frequency (MF), number of mounts per 30-min test; Intromission Frequency (IF), number of intromissions per 30-min test; Ejaculation Frequency (EF), number of ejaculations per 30-min test; Mount Latency (ML), time from female's introduction to first mount or 1800 sec for nonresponders; Intromission Latency (IL), time from female's introduction to the first intromission or 1800 s for nonresponders; Ejaculation Latency (EL), time from the first intromission to the first ejaculation or 1800 s for nonresponders; Post-Ejaculation Interval (PEI), time from the first ejaculation to the first intromission of the next series or 1800 s for nonresponders.

On the day after the last behavioral test, male rats were anesthetized and sacrificed. Animals were weighted, and then osmotic pumps were removed and checked for proper delivery. Prostate, seminal vesicles, and levator ani muscle were collected, clear of extraneous fat tissues, weighed, and compared. All organ weights were expressed as a percentage of body weight for comparison between groups.

6.2.3.1 Behavior Studies in Sexually Naïve Male Rats

Sexually naïve male rats were castrated via a single scrotal incision while anesthetized with ketamine/xylazine (83/17 mg/kg, w/w). An additional five animals received a sham operation and served as intact controls. Four weeks after surgery, an osmotic pump containing vehicle (10% DMSO in PEG 300) was implanted subcutaneously at the lower back area of each animal in the intact control group. Osmotic pumps containing either **C-6** or **C-6** plus EB were implanted subcutaneously into animals in drug treatment groups (N = 5). The target delivery doses of **C-6** and EB were 1 mg/day and 5μg/day, respectively. This dose of EB was reported to be insufficient to fully restore masculine sexual behavior in male rats (191, 192, 195). However, it was an effective dose when combined with DHT at a dose of 1 mg/day. The sexual behavior of each animal was tested one day prior to and at 7-day intervals after implantation of the osmotic pumps. Results from five tests were reported.

6.2.3.2 Behavior Studies in Sexually Experienced Male Rats

The sexual behavior of sexually experienced male rats treated with **C-6** was also examined. Male animals included in these studies had ejaculated in three preliminary screening tests (1, 5, and 9 days prior to castration). An osmotic pump containing **C-6** at a target dose rate of 1 mg/day was implanted into five animals immediately after castration. An additional five animals served as an intact control group and received sham operation and osmotic pumps containing only vehicle (10% DMSO in PEG 300). The sexual behavior of each animal was tested seven days after implantation of the osmotic pump and at 4-day intervals thereafter for the next 27 days.

6.2.4 Statistical Analysis

All statistical analyses were performed using single-factor ANOVA with the α value set a *priori* at $p < 0.05$.

6.3 RESULTS

6.3.1 Effects of **C-6** in Sexually Naïve Rats

None of the animals showed any sexual activity during the pretreatment test (Figures 6.1 to 6.3). As expected on the basis of numerous previous studies (191), mating behavior of males was greatly reduced in castrated male rats four weeks castration. In the current study, sexually naive males from the intact control group also showed low mounts, intromissions, and ejaculations on the first two tests. Animals in the intact control group and the **C-6** + EB group demonstrated progressively increased measures of mating behavior over a five-week period: mounts Figure 6.1-A) increased first, then intromissions (Figure 6.2-A), and then ejaculations (Figure 6.3-A). Treatment with **C-6** alone had no effect on mounting, intromissions, or ejaculations as compared to castrated control group. By contrast, mounting and intromission rates of animals treated with **C-6** + EB were significantly higher than the castrated control group at all time points, beginning with the second week of treatment. Compared with the intact control group, **C-6** + EB-treated animals displayed lower mounting and intromission rates and longer ML (Figure 6.1-B) and IL (Figure 6.2-B) during the tests conducted before treatment and after one week of treatment. However, by the second week of treatment, animals in the **C-6** + EB group demonstrated significantly higher mounting and intromission rates and significantly shorter post-ejaculation interval (Figure 6.3-C) than those of intact control animals. There were no significant differences in sexual behavior between the intact control group and **C-6** + EB group during the last two weeks of the study (i.e., weeks 3 and 4). It is well known that mount and intromission rates and latencies are common measures of sexual motivation, whereas the ability to ejaculate is a common measure of

sexual performance in the male rats (196). These studies suggest that treatment with **C-6** + EB stimulates mating behavior in castrated male rats to a similar but slower extent as compared to intact controls. Since **C-6** alone failed to stimulate any mating behavior, the increased sexual motivation observed in animals treated with **C-6** + EB by the second week post-treatment was due to EB or the synergistic effects of androgen and estrogen.

At the conclusion of the behavioral studies with sexually naïve rats, we sacrificed the animals and determined their body weight and the weight of androgen-responsive tissues. As shown in Figure 6.4, animals treated with **C-6** + EB demonstrated significantly lower body weights than animals in the other treatment groups, suggesting that estrogen affected the growth of these animals. After long-term castration (60 days), the weights of the prostate, seminal vesicles, and levator ani muscle in castrated animals treated with vehicle alone decreased to 3.4%, 7.2%, and 42.7% of those observed in intact animals. Weights of the prostate, seminal vesicles, and levator ani muscle were increased to 24.6%, 57.1%, and 111% of the intact values after **C-6** treatment. Combination treatment with **C-6** + EB increased the weights of the prostate, seminal vesicles, and levator ani muscle to 39.5%, 69.8%, and 127% of those observed in intact animals. Although the increase of organ weights was slightly greater in **C-6** + EB-treated groups than **C-6** alone group, it was not statistically different. This difference was mainly due to the significant lower body weight of animals that received **C-6** + EB since all organ weights were normalized by the body weight. These results were consistent with the androgenic and anabolic activity of **C-6** that we observed during pharmacologic studies. The small (i.e., 5 μg/day) dose of EB significantly decreased the body weight without interfering with the pharmacologic activity and tissue selectivity of **C-6**.

6.3.2 Effects of **C-6** in Sexually Experienced Rats

The studies described above show that sexually naïve intact rats require several experiences with receptive females before demonstrating full mating behavior. Therefore, we later examined the effects of **C-6** on mating behavior in sexually experienced male rats after castration. All animals used in this study ejaculated in at least one of the mating tests conducted 1, 5, and 9 days prior to castration. After castration, all parameters of

mating behavior were progressively decreased in the vehicle control and **C-6**-treated groups, presumably due to the lack of endogenous testosterone. Figure 6.5 shows the percentage of castrated animals that displayed mounting, intromission, and ejaculation after treatment with vehicle or **C-6**. In both groups, ejaculations declined first, followed by intromissions, and then mounts. On the last two tests, animals in both groups demonstrated a high rate of mounts. Only one animal in the vehicle control group exhibited intromissions, while 3 to 4 animals in the **C-6**-treated group showed intromissions. Animals in the vehicle control group failed to ejaculate on the last two tests. Although the number of ejaculations also declined in animals that received **C-6**, at least two animals in the **C-6**-treated group (N = 5) ejaculated. These results clearly demonstrated that **C-6** can partially maintain mating behavior in sexually experienced animals when treatment was initiated immediately after castration.

No difference in body weight was observed between the two groups at the end of treatment. The pharmacologic activity of **C-6** in androgen-dependent organs was similar to that observed in previous studies (data not shown).

6.4 DISCUSSION

There has been a long debate over the ability of estrogen, either alone or in combination with DHT, to restore mating behavior in castrated male rats (183, 191, 192, 195, 197-199). The dose of EB used in these studies (5 μg/day) is insufficient to restore mating behavior alone but is known to be effective when given in combination with DHT (183, 191, 192). In sexually naïve rats, the only treatment to produce an equivalent mating behavior to that observed in the intact controls was **C-6** (1 mg/day) + EB (5 μg/day). Neither castrated controls nor **C-6**-treated animals displayed measurable mating behavior during one pretreatment test and four tests conducted during drug treatment. Thus, **C-6** failed to stimulate mating behavior in long-term castrated male rats, which is in agreement with reports using non-aromatizable androgens, such as DHT (189, 190) and R1881 (193). Due to its androgen receptor specificity, high dose rate (1 mg/day) used, and relatively low total body clearance of **C-6** in rats (65), it seems unlikely that the

inability of **C-6** to stimulate mating behavior was the result of insufficient levels of androgen acting on target androgen receptors. When **C-6** was administrated with 5 μg/day of EB, animals exhibited significantly greater sexual motivation by the second week of treatment and then reached a similar pattern of mating behavior as that observed in the intact control by the third week of treatment. Previous pharmacologic studies showed that it takes about two weeks for androgen-dependent organs to reach their minimal sizes after castration. In turn, it appears to take a similar amount of time to fully recover androgen activity in target organs, which may explain the observed transiently increase in sexual motivation (mounting and intromission) but delays in sexual performance (ejaculation) in sexually naïve animals treated with **C-6** + EB. We recorded the weights of the prostate, seminal vesicles, and levator ani muscle at the end of behavior studies. Both **C-6** alone and **C-6** + EB treatments significantly increased muscle weights to sizes greater than those of intact control, indicating that **C-6** exerted potent effects in the stimulation of the genitals. Clearly, combination treatment with estrogen and androgen restored sexual motivation and organ weights in peripheral organs.

To date, the mechanisms by which EB alone or EB in the combination with DHT stimulate mating behavior are not well understood. One possibility is that estrogen maintains the normal basal level of extracellular dopamine, an important neurotransmitter for sexual behavior, in the medial preoptic area (MPOA) of the brain at a level that sufficient for suboptimal copulation (200-202). In the presence of androgen and estrogen, castrated animals have normal basal dopamine levels and exhibit female-induced increases in dopamine to the same extent as testosterone-treated animals (200). Several characteristics of **C-6** make it more advantageous for behavioral studies, including its lack of cross-reactivity with other nuclear receptors, unique tissue selectivity, and high androgen receptor binding affinity. Studies using intracranial implantation of **C-6** might provide important insight to the mechanisms by which androgen and estrogen regulate sexual behavior, and should be seriously considerated as a component of future studies.

Butera and Czaja reported that DHT failed to maintain copulatory behavior in castrated male rats, in spite of the fact that it fully maintained peripheral structures (203). Consistently, our studies show that **C-6**, a potent SARM, failed to induce mating behavior in sexually naïve rats. However, it partially maintained mating behavior in

sexually experienced male rats. For example, **C-6** completely maintained mounting and partially maintained intromission and ejaculation in sexually experienced male rats. It remains unknown whether this partial maintenance was due to the delayed disappearance of mating behavior or a true suboptimal status. However, the inability of castrated males to ejaculate and suggests that the study was conducted for a sufficient duration. Studies of greater duration and that include intact and EB-treated groups will be necessary in the future to unequivocally answer this question.

It is well known that the relative contributions of androgen and estrogen to the activation of masculine sexual behavior differ among mammalian species. For instance, estrogen shows potent activation of mating behavior in multiple castrated animal species, including rats (184, 188, 197), hamsters (204), pigs (205), deer (206), sheep (207), and cows (208), but not in castrated guinea pigs (197) or rhesus monkeys (209). By contrast, DHT failed to stimulate any mating behavior in castrated male rats. However, it was quite effective in guinea-pigs (210), mice (211), rabbits (212), and rhesus monkeys (213, 214), but not in cynomolgus monkey (215) or stumptailed monkeys (216). Therefore, the effects of androgen and estrogen on sexual behavior in human can not be predicted by animal studies. Furthermore, sexual libido in humans is highly regulated by multiple social factors and much less dependent on hormones than other animal species.

The purpose of these studies was to define the appropriate treatment regimens prior to the design and conduct of a study to examine the feasibility of using a SARM for hormonal male contraception. Due to the fact that no male antifertility compounds have yet been developed, there is a lack of knowledge about which species or test systems best extrapolate to humans. Since all the compounds that have been reported to have male antifertility activity are active in the rat, it remains the primary small animal model for male contraception studies. Lack of sexual libido or appropriate mating behavior would confound the results of contraceptive efficacy studies (i.e., mating is a prerequisite for pregnancy). These studies with **C-6** alone and in combination with EB demonstrate: a) both androgen and estrogen are required to fully maintain masculine sexual behavior in castrated male rats; b) immediate SARM treatment can partilly maintain or support sexual behavior in castrated male rats; c) contraception studies of SARMs in rats should include EB to maintain sexual libido.

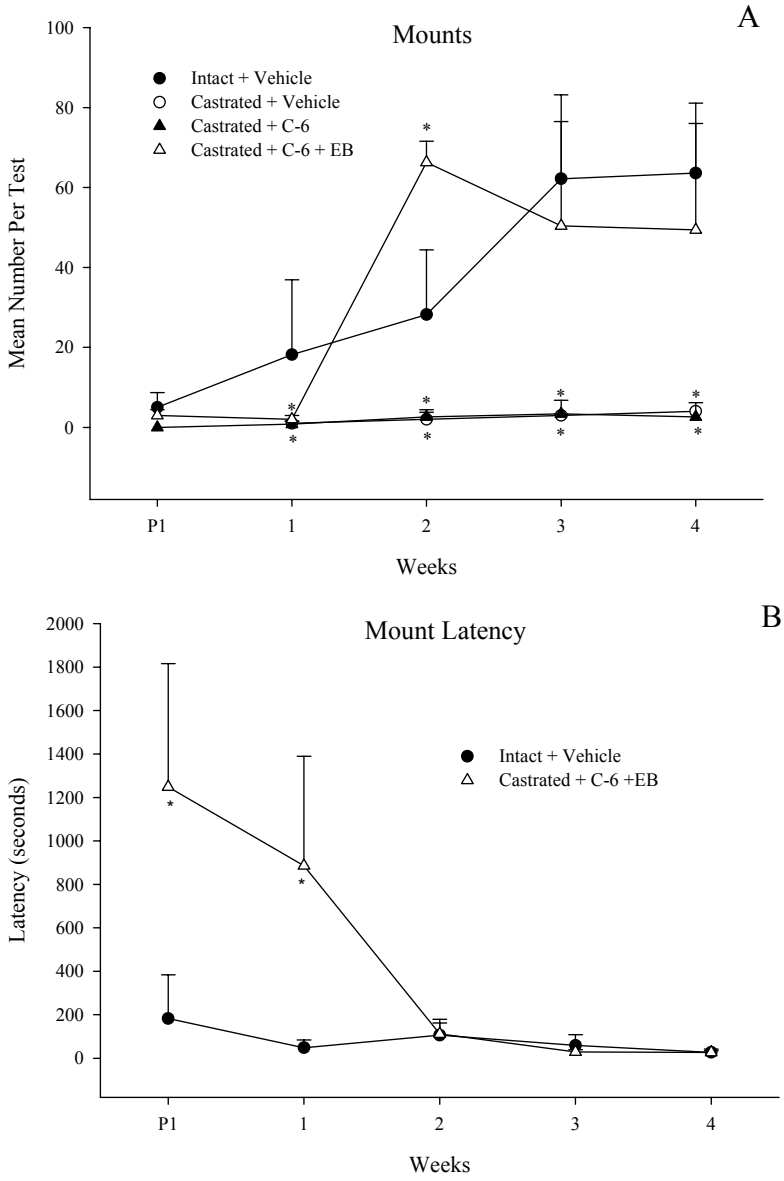

Figure 6. 1 Changes in Mounting Behavior as a Function of Time and Drug Treatment.

The number of mounts (Panel A) and mount latency (Panel B) were determined prior to treatment (P1) and at weekly intervals for up to four weeks after implantation of an osmotic pump containing vehicle (circles), **C-6** (closed triangles), or **C-6** + EB (open triangles). ML of animals in castrated and **C-6** alone groups was not analyzed because too few animals performed the behavior. Each value represents the mean ± s.d. of four or five rats. * indicates a significant difference from intact control group as tested by single-factor ANOVA ($p < 0.05$).

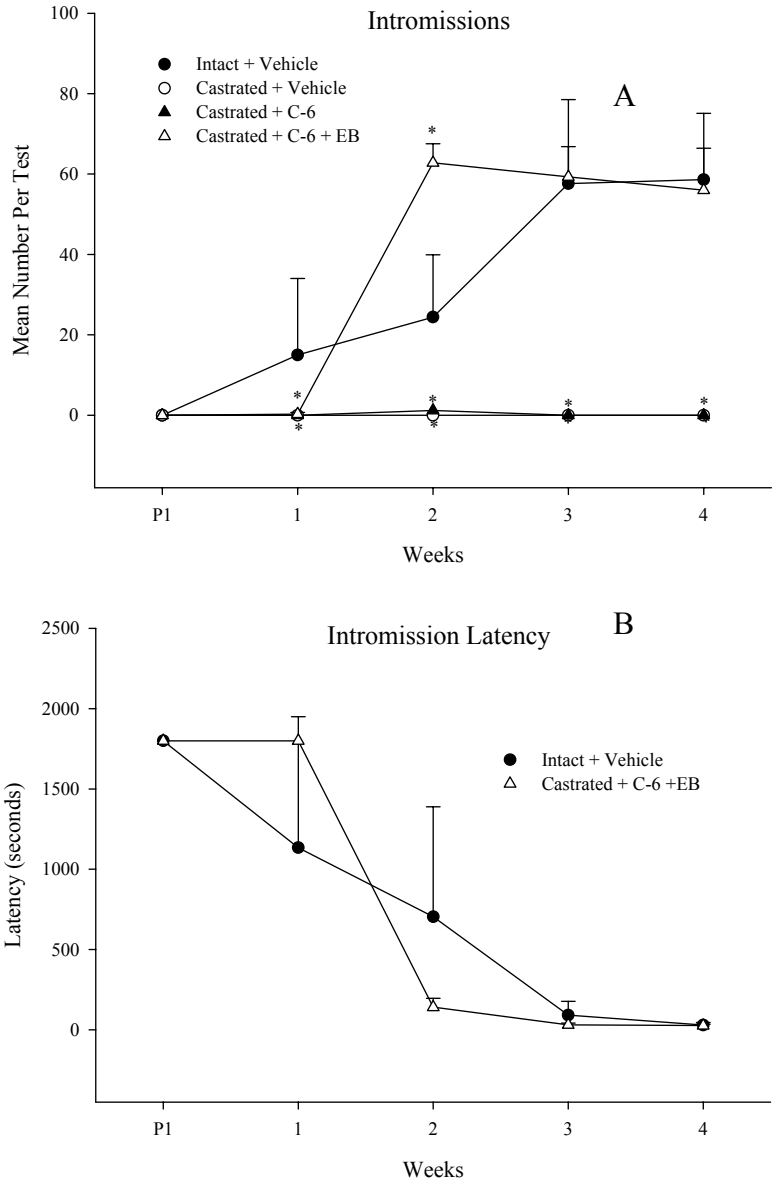

Figure 6. 2 Changes in Intromission Behavior as a Function of Time and Drug Treatment.

The number of intromissions (Panel A) and intromission latency (Panel B) were determined prior to treatment (P1) and at weekly intervals for up to four weeks after implantation of an osmotic pump containing vehicle (circles), **C-6** (closed triangles), or **C-6** + EB (open triangles). IL of animals in castrated and **C-6** alone groups was not analyzed because too few animals performed the behavior. Each value represents the mean ± s.d. of four or five rats. * indicates a significant difference from intact control group as tested by single-factor ANOVA ($p < 0.05$).

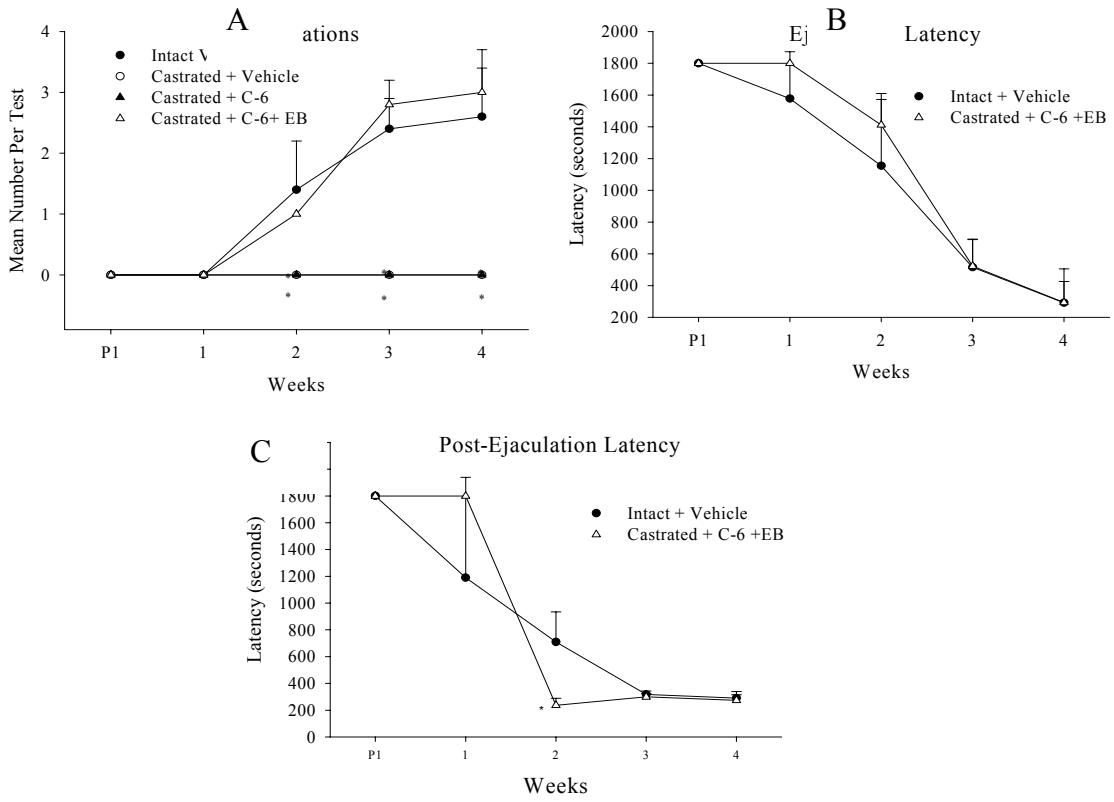

Figure 6. 3 Changes in Ejaculation Behavior as a Function of Time and Drug Treatment

The number of ejaculations (Panel A), ejaculation latency (Panel B), and post-ejaculation latency (Panel C) were determined prior to treatment (P1) and at weekly intervals for up to four weeks after implantation of an osmotic pump containing vehicle (circles), **C-6** (closed triangles), or **C-6** + EB (open triangles). EL of animals in castrated and **C-6** alone groups was not analyzed because too few animals performed the behavior. Each value represents the mean ± s.d. of five rats. * indicates a significant difference from intact control group as tested by single-factor ANOVA ($p < 0.05$).

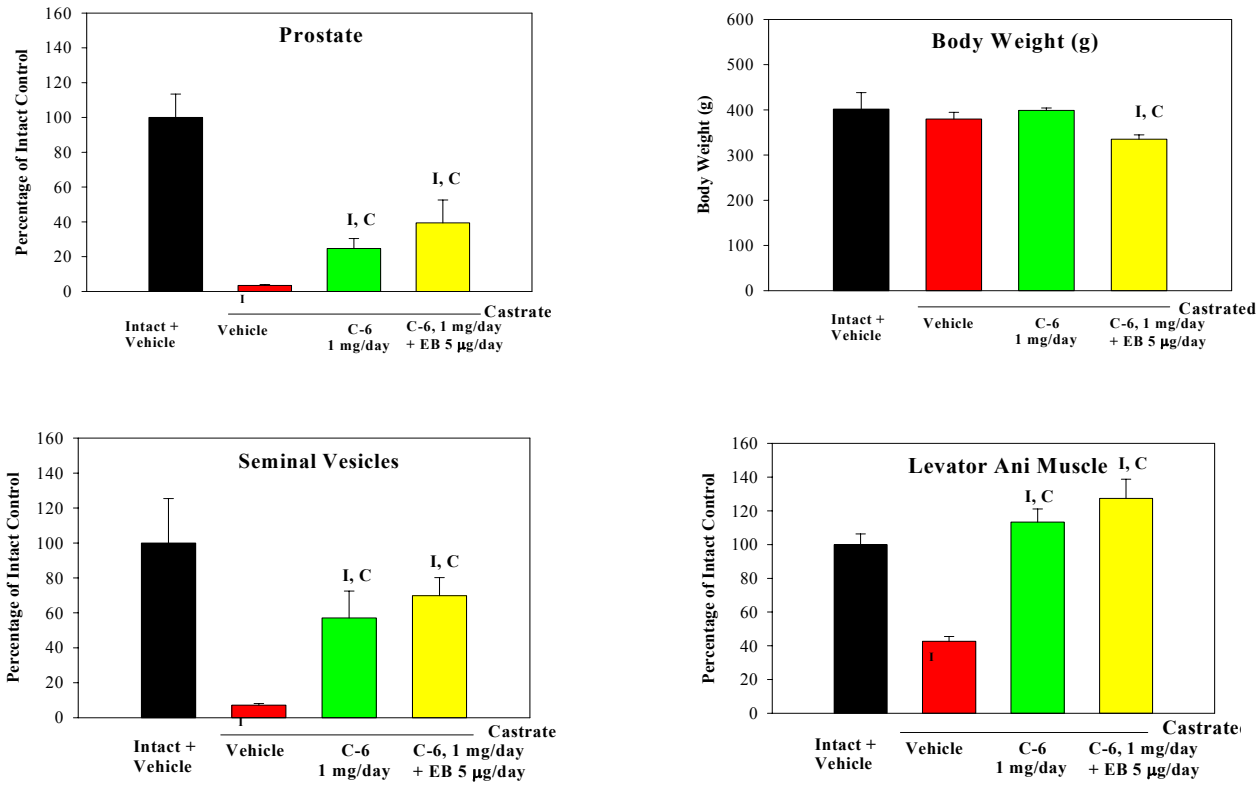

Figure 6. 4 Body Weights and Normalized Organs Weights of Animals in Sexually Naïve Male Rats.

The organ weights were normalized with body weight and were expressed as the percentage of the weights in the intact control group. Each bar represents the mean ± S.D. (n=5/group). The letters "I" and "C" above each error bar represent a significant difference between the group and intact control group or castrated control group, respectively, as analyzed by single-factor ANOVA with $p < 0.05$.

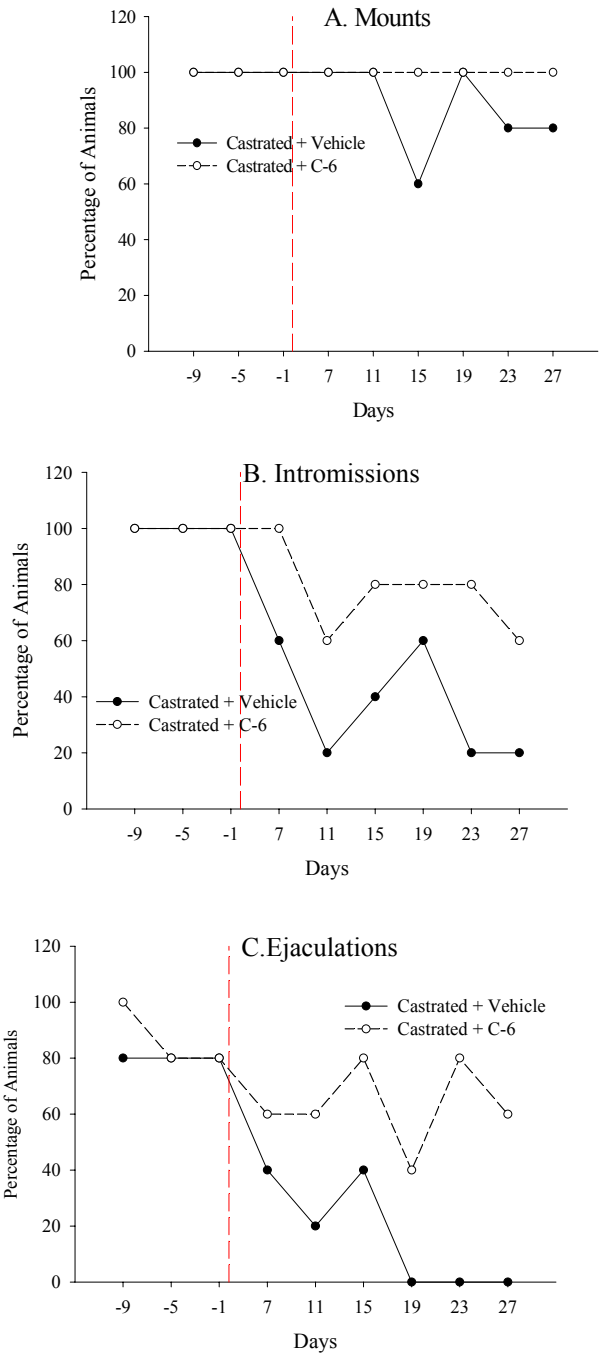

Figure 6. 5 The Percentage of Castrated Male Rats Displayed Mounting (Panel A), Intromission (Panel B), and Ejaculation (Panel C).

Three mating tests were performed at 9, 5, and 1 day prior to castration. The dotted vertical line indicates the day of castration. Six mating tests were performed at 7, 11, 15, 19, 23, and 27 days after osmotic pump implantation.

CHAPTER 7

IN VITRO AND *IN VIVO* CHARACTERIZATION OF A SELECTIVE ANDROGEN RECEPTOR MODULATOR (SARM), C-31, FOR HORMONAL MALE CONTRACEPTION

7.1 INTRODUCTION

The negative feedback loop between testosterone synthesized in the testis and gonadotropins released from the pituitary was first discovered in 1932 (217). In the following years, numerous studies proved the ability of androgens and anabolic steroids to inhibit endogenous testosterone synthesis (218-220). Although the detailed mechanism regarding hormonal regulation of spermatogenesis is still not fully understood, it is widely employed as the main principle of hormonal male contraception. Much higher testosterone concentrations are required to maintain normal spermatogenesis in the testis than are needed in the systemic circulation to maintain muscle mass, bone structure, and male secondary characteristics. The goal of hormonal male contraception is to suppress luteinizing hormone (LH) and follicle stimulating hormone (FSH), resulting in a depletion of intratesticular testosterone and suppression of spermatogenesis. However, depletion of endogenous androgen production results in a physiologic need for androgen replacement (221). The most clinically advanced approaches for male hormonal contraception use testosterone alone (76, 77) or in the combination of progesterone or gonadotropin-releasing hormone (GnRH) analogs.

In previous studies, we identified two potent selective androgen receptor modulators (SARMs), **S-1** and **S-4** (59), with potential use for androgen-related diseases, including muscle wasting, osteoporosis, and benign prostate hyperplasia (BPH) in animal models (64). However, these SARMs showed low or no effects in the central nervous

system (CNS), which precluded their usage as a single regimen for hormonal male contraception. More recently, we solved the x-ray crystal structure of the androgen receptor (AR) ligand-binding domain bound to bicalutamide and our nonsteroidal SARMs and proved that these nonsteroidal ligands bind in a unique subpocket within the AR that is not shared by steroidal AR ligands. The aromatic B-ring of **S-1** in the wide type AR is accommodated in close proximity to the indole ring of Trp-741 of the AR. Multiple electron-withdrawing groups were introduced to the B-ring of our lead compound-**S-1**. Such structural modifications not only maintained high AR binding affinity and *in vitro* functional activity, but also improved the *in vivo* pharmacologic activity of these compounds in castrated male rats. For example, when an additional fluoro group was introduced to the *meta* position in the B-ring of **S-1**, this structural modification led to a novel SARM (**C-3**), which was more efficacious (Emax) than **S-1** in maintaining the weights of prostate (59% vs 15%) and levator ani muscle (132% vs 75%) in castrated animals. This increased efficacy was not due to improved AR binding affinity or pharmacokinetics of **C-3**, but was through increased functional activity. *In vivo* metabolism studies revealed that the major metabolites of **C-3** arose from the step-wise reaction of the nitro group in the A-ring of **C-3**. Although structure-activity relationship studies showed that changing the nitro group to a cyano group slightly decreases AR binding affinity and *in vitro* functional activity, changing the nitro group of **C-3** to a cyano group should make the pharmacokinetic properties of this compound more desirable without compromising significant functional activity.

Another novel SARM (**C-6**), which bears a *para*-nitro group in the A-ring, a *para*-chloro group and a *meta*-fluoro group in the B-ring, was identified as the first SARM with the ability to regulate gonadotropin levels and testosterone concentrations in castrated and intact male rats, respectively (65). Pharmacokinetic studies showed that **C-6** is orally bioavailable (76%) with a fairly long terminal half-life (6.3 h) at a dose of 10 mg/kg in male rats. Additional pharmacologic studies of **C-6** demonstrated its profound suppressive effects on spermatogenesis in intact male rats after 70-days of treatment at 1 mg/day by s.c. daily injections. We hypothesized that a new molecule with the B-ring of **C-6** and a cyano-group in the A-ring (**C-31**) might be a more promising candidate for

hormonal male contraception, due to its structural properties that favor high intrinsic pharmacologic activity and improved pharmacokinetics.

In the current studies, the *in vitro* and *in vivo* characteristics of **C-31** were examined, including *in vitro* AR binding affinity, AR-mediated transcriptional activation, and pharmacologic activity in castrated male rats. The pharmacologic activity of **C-31** for hormonal male contraception was further investigated in male rats. To maintain libido, estrogen benzoate (EB) at a dose rate of 5μg/day was combined with **C-31** at doses ranging from 0.05 to 0.75 mg/day by s.c. daily injections for 70 days. The contraceptive properties of **C-31** were evaluated by examining the ability of this SARM to suppress spermatogenesis and reduce pregnancy rates during mating trials. The effects of **C-31** on body weight, androgen-dependent organ weights, body composition, and hormonal regulations were also reported. These studies are the first to fully demonstrate the ability of SARMs to completely suppress spermatogenesis, maintain peripheral androgenic tissues, and serve as a major step forward development of effective oral male contraception.

7.2 MATERIALS AND METHODS

7.2.1 Animals

Mature male Sprague-Dawley rats (BW, ~ 300 g) and female Sprague-Dawley rats (BW, ~200 g) were purchased from Harlan Bioproducts for Science (Indianapolis, IN). All animals were maintained on a 12h light/dark cycle with food and water available *ad libitum*. The animal protocol was reviewed and approved by the Institutional Laboratory Animal Care and Use Committee of The Ohio State University.

7.2.2 Chemicals

C-31 was synthesized using the methods described by Marhefka *et al.* (60). Chemical purity was confirmed using elemental analysis, mass spectrometry, and proton nuclear magnetic resonance. Unlabeled mibolerone (MIB) and 17α-methyl-[^{3}H] Mibolerone ([^{3}H]-MIB, 84 Ci/mmol) were purchased from PerkinElmer Life Sciences

(Boston, MA). Ethanol was purchased from Pharmco Products (Brookfield, CT). All other chemicals used in current studies were purchased from Sigma Chemical Co (St. Louis, MO).

7.2.3 *In Vitro* AR Binding Affinity and Transcriptional Activation of **C-31**

Cytosolic AR was prepared from the ventral prostates of male Sprague-Dawley rats 24 h after castration. The AR binding affinity of **C-31** was determined using the same radio-labeled competitive binding assay as described in the Method Section of Chapter 2. The *in vitro* functional activity of **C-31** was determined and characterized using a co-transfection assay previously described in the Method Section of Chapter 2.

7.2.4 *In Vivo* Pharmacologic Activity of **C-31** in Castrated Male Rats

The *in vivo* pharmacologic activity of **C-31** was examined in five male Sprague-Dawley rats weighing approximately 200 g. Animals were castrated via a scrotal incision under anesthesia 24 h prior to drug treatments and received daily subcutaneous injections of **C-31** at a dose rate of 0.01, 0.05, 0.1, 0.5, 1, and 3 mg/day for 14 days. **C-31** was freshly dissolved in vehicle containing DMSO (5%, v/v) in PEG 300 immediately before dose administration. An additional two groups of animals with or without castration received vehicle only and served as castrated or intact control groups, respectively. Animals were sacrificed at the end of the treatment. Plasma samples were collected and stored at –80 °C until use. The ventral prostate, seminal vesicles, and levator ani muscle were removed, cleared of extraneous tissue, and weighed. All organ weights were normalized to body weight and compared. The weights of prostate and seminal vesicles were used to evaluate androgenic activity, while the levator ani muscle weight was used as a measurement of anabolic activity. Non-linear regression analysis was performed to obtain the maximal response (Emax) induced by **C-31** and the dose rate of **C-31** that induced 50% of that maximal response (ED_{50}) using the sigmoid E_{max} model with a baseline effect parameter and WinNonlin software (Pharsight Corporation, Mountain View, CA). No upper or lower boundary was used for this modeling.

7.2.5 *In Vivo* Pharmacologic Activity of **C-31** in Castrated Male Rats

7.2.5.1 Animals and Treatment

Forty-two male Sprague Dawley rats (90 days old) were randomly assigned to seven groups (N = 6/group). Group 1 was the intact control group and received vehicle (5% DMSO + 95% PEG 300). Group 2 was the estradiol benzoate (EB) alone group and received EB at a dose of 5 μg/day. Animals in groups 3 to 7 were treated with **C-31** at dose rates of 0.05, 0.1, 0.3, 0.5, and 0.75 mg/day, respectively, in combination with EB (5 μg/day). Compounds were freshly prepared immediately before dosing and delivered to animals via daily s.c. injections (100 μL/day) for 70 days. Mating trials were conducted during the last week of treatment for animals in groups 1, 2, 4, and 5. On day 69, the total body composition of each animal was determined using dual energy x-ray absorptiometry (DEXA) (GE, Lunar Prodigy™).

7.2.5.2 Tissue and Blood Sample Collection and Preparation

At the end of treatment, animals were sacrificed under anesthesia. Body weight was recorded at autopsy. Prostate, seminal vesicles, right testis, and right epididymis (divided in the middle of corpus epididymis to caput and cauda epididymis) were collected and weighed. All organ weights were normalized with body weights and compared. Blood samples were collected in plastic tubes, stored at room temperature for 40 min, and centrifuged at 3,000 g for 10 min to prepare serum samples. Serum samples were aliquoted and stored at -80°C until hormonal assays. One testis from each rat was removed and weighed. After decapsulation, testicular parenchyma was homogenized in a volume of PBS (pH 7.4) that was equivalent to its weight. An aliquot of each testicular homogenate was used to count advanced spermatids (step 17-19) in the testis with a hemacytometer. Results were expressed as the number of spermatids per mL. The remaining testicular homogenates was centrifuged at 3,000 g for 10 min. The supernatant of each sample was collected and used to determine the intratesticular testosterone concentrations. The other testes were carefully dissected and fixed in Bouin's Solution for 24 h. Tissue samples were washed repeatedly with lithium-saturated 70% ethanol

until completely decolored. The testes were cut into small (~ 0.2-cm) transverse slices and preserved in 70% ethanol. One slice from the middle region of the testis was processed by routine paraffin embedding for histological analysis of spermatogenesis and morphology

7.2.5.3 Hormone Assays

Serum levels of LH and FSH and intratesticular testosterone concentrations were measured by the University of Virginia, Center for Research in Reproduction (Charlottesville, VA) using RIA kits. The sensitivity of LH, FSH, and intratesticular testosterone RIA kits were 0.040, 1.0, and 0.025 ng/mL, respectively. Testosterone concentrations in serum were measured with a commercially available EIA kit (DSL, Webster, TX). The detection limit of this EIA kit is 7.5 pg/mL.

7.2.5.4 Whole Body DEXA Analyses

One day prior to the end of treatment, body weight (BW), total body bone mineral density (BMD), percent fat mass (FM), bone mineral content (BMC), bone mineral area (BMA), and lean mass (LM) were determined by dual energy x-ray absorptiometry (DEXA) (GE, Lunar Prodigy™) using the small animal software (Lunar enCORE, version 6.60.041). For scanning, the animals were anesthetized with ketamine: xylazine (87:13 mg/kg) and positioned in a prone position as demonstrated in Figure 7.1. The total body data was obtained by selecting an area encompassing the entire animal as the region of interest during data processing.

7.2.5.5 Mating Trials

During the last week of treatment, each male rat from groups 1, 2, 4, and 5 was housed with two sexually active female rats. Female rats were individually housed after mating trials with free access to water and standard food chow. The female rats were allowed to bring the pregnancy to term. Upon delivery, numbers of the mother rats and litters were counted. A male rat was defined as fertile if it impregnated either one or two female partners.

7.2.6 Pharmacokinetics of **C-31** in Rats

7.2.6.1 Animals and Blood Sample Collection and Preparation

The pharmacokinetics of **C-31** were examined in male Sprague-Dawley rats weighing approximately 250 g after a dose of 10 mg/kg by intravenous injection or oral gavage. A catheter was implanted in the right external jugular vein of each animal 24 h prior to drug administration. **C-31** was dissolved in a vehicle containing DMSO (10%, v/v) in PEG 300 and administered to animals through the jugular vein catheter (i.v. group) or oral gavage (p.o. group). For animals in the i.v. group, the catheter was flushed three times with saline (3× the volume of the dosing solution) before blood sampling. Blood samples (~ 200 μL) were then withdrawn through the jugular vein catheter at 5, 10, 30, 60, 90, 120, 180, 360, 720, 1440, and 1800 min after the i.v. dose and at 20, 30, 60, 90, 120, 240, 360, 480, 720, 1080, 1440, and 1800 min after the p.o. dose. Blood samples were immediately centrifuged at 1,000 g, 4°C for 10 min. Plasma samples were prepared and stored at -20°C until HPLC analysis.

7.2.6.2 HPLC Method

An aliquot (100 μL) of each plasma sample from the pharmacokinetic studies was spiked with 10 μL of an internal standard (**C-3**) and mixed well with 1 mL of acetonitrile. After centrifugation at 16,000 g, 4°C for 10 min, the supernatant was collected and evaporated. The residues were reconstituted in 120 μL of mobile phase. An aliquot of each sample was injected into a Nova-pak C_{18} column (3.9 × 150 mm, 4 μm particle size) purchased from Waters Corporation (Milford, MA). The HPLC system consisted of a model 515 HPLC pump (Waters), a model 717 plus autosampler (Waters), and a model 486 absorbance detector (Waters). HPLC separation was performed using an isocratic mobile phase (H_2O/Acetonitrile: 46/54, v/v) at a flow rate of 1 mL/min. The UV absorbance of eluents was monitored at 298nm. Calibration standards were prepared in blank rat plasma with **C-31** concentrations ranging from 0.1 ~ 50 μg/mL. The recoveries of this compound over the calibration range were from 90.1% to 105.5%. The intra- and

inter-day coefficients of variation of the assay were lower than 3.6% and 7.0%, respectively. The limit of quantitation of the HPLC assay was 0.1 μg/mL.

7.2.6.3 Pharmacokinetic Data Analyses

The plasma concentration-time data were analyzed using noncompartmental methods and WinNonlin software (Pharsight, Mountain View, CA). The terminal half-life ($T_{1/2}$) was calculated as $T_{1/2} = 0.693/\lambda$, where λ was the rate constant describing the terminal phase decline in **C-31** plasma concentrations. The area under the plasma concentration-time curve ($AUC_{0-\infty}$) was calculated using the trapezoidal method with extrapolation to time infinity. The plasma clearance (CL) was calculated as $CL = Dose_{i.v.}/AUC_{0-\infty, i.v.}$, where the $Dose_{i.v.}$ and $AUC_{0-\infty, i.v.}$ were the intravascular dose and the corresponding area under the plasma concentration-time curve from time 0 to infinity, respectively. The apparent volume of distribution at equilibrium (Vd_{ss}) was calculated as $Vd_{ss} = CL \cdot MRT$, where the MRT was the mean residence time following the intravenous bolus dose. The peak plasma concentration (C_{max}) and time to reach the peak concentration (T_{max}) after a p.o. dose were obtained directly from the plasma concentration-time curves. Oral bioavailability ($F_{p.o.}$) was defined as $F_{p.o.} = (AUC_{0-\infty, p.o.} \cdot Dose_{i.v.})/(AUC_{0-\infty, i.v.} \cdot Dose_{p.o.})$, where the $Dose_{p.o.}$ and $AUC_{0-\infty, p.o.}$ were the oral dose and the corresponding area under the plasma concentration-time curve from time 0 to infinity after p.o. administration, respectively.

7.2.7 Statistical Analyses

All statistical analyses were performed using single-factor ANOVA with the α value set a *priori* at $p < 0.05$.

7.3 Results

7.3.1 *In Vitro* AR Binding Affinity and Transcriptional Activation of **C-31**

The AR binding affinity of AR ligands was determined using a competitive binding assay. DHT was used as the positive control in each assay and the Ki value of DHT was 0.45 ± 0.2 nM. Figure 7.2 shows the chemical structures and *in vitro* pharmacology of **S-1**, **C-6**, and **C-31**. The introduction of two halogen groups in the aromatic B-ring maintained or increased AR binding affinity. Both **C-6** and **C-31** showed higher binding affinity than **S-1**. **C-31** was structurally modified from **C-6** by changing the *para*-nitro group of **C-6** to a cyano group, which resulted about 2-fold higher binding affinity than that of **C-6**. However, previously discussed structure-activity relationships (SARs) based on five pairs of compounds suggested that cyano-substituted compounds exhibited lower AR binding affinity than their corresponding nitro-substituted counterparts. This inconsistency indicated that this known SAR might be substituent dependent.

The ability of **C-31** to induce AR-mediated transcriptional activation was determined using a co-transfection assay in CV-1 cells. Upon binding to the AR, **C-31** induced a concentration-dependent increase in AR-mediated transcriptional activation. Data listed in Figure 7.2 was the transcriptional activity induced by each compound at a final concentration of 10 nM and is reported as the percentage of activity observed for 1 nM of DHT. Compared with our lead compound (**S-1**), compounds with di-halogen substituents in the B-ring (**C-6** and **C-31**) exhibited significantly increased *in vitro* functional activity. Although the transcriptional activation induced by **C-6** was higher than that of **C-31**, the difference was not statistically significant.

7.3.2 *In Vivo* Pharmacologic Activity of **C-31** in Castrated Male Rats

The *in vivo* pharmacologic activity of **C-31** was further evaluated in castrated male rats after 14-day treatment. Previous pharmacologic studies of **C-6** revealed that the maximum effects of **C-6** in prostate and seminal vesicles were about 130% of those observed in intact controls at a dose of 3 mg/day. The highest dose rate of **C-31** used in

the current study was also 3 mg/day. The ED_{50} values of **C-6** in prostate, seminal vesicles, and levator ani muscle were 0.78 ± 0.06, 0.88 ± 0.1, and 0.17 ± 0.04 mg/day, respectively. According to the rationale of the structural modification, we expected to see higher potency in animals treated with **C-31** than **C-6**. Therefore, the lowest dose rate of **C-31** used in this study was 0.01 mg/day. Figure 7.3 shows the androgenic activity (prostate and seminal vesicles) and anabolic activity (levator ani muscle) of **C-31** in castrated male rats at doses ranging from 0.01 mg/day to 3 mg/day. After castration, the weight of prostate, seminal vesicles, and levator ani muscle dramatically decreased to 5.7%, 6.5%, and 34% of control values. Administration of **C-31** to castrated animals led to dose-dependent increases in androgen-dependent organ weights The maximum effect (Emax) of **C-31** in the prostate, seminal vesicles, and levator ani muscle was 138 ± 21%, 144 ± 1%, and 129 ± 4% of those observed in intact controls, respectively. Accordingly, the ED_{50} of **C-31**, calculated with non-linear regression analysis of dose-response relationship, in the prostate, seminal vesicles, and levator ani muscle was 0.43 ± 0.18, 0.41 ± 0.0070, and 0.079 ± 0.010 mg/day, respectively (Figure 7.4). As compared to **C-6**, **C-31** demonstrated 2-fold higher potency (ED_{50}) in all three organs without significantly increased efficacy (Emax) or change in androgenic/anabolic activity *in vivo*. Considering the *in vitro* characteristics of **C-31**, this increased *in vivo* potency was possibly due to its higher AR binding affinity than **C-6**. Another possibility was the improved *in vivo* drug exposure after administration, which would be verified by the results of pharmacokinetic studies.

7.3.3 *In Vivo* Antireproductive Activity of **C-31** in Male Rats

After identification of **C-31** as a more potent SARM than **C-6**, the *in vivo* antireproductive activity of this compound was immediately investigated in intact male rats. Previous studies of the effects of **C-6** on masculine mating behavior showed that **C-6** alone partially maintained mating behavior in sexually experienced rats, but failed to stimulate any mating behavior in sexually naïve male rats after long-term castration. A small amount of estrogen in combination with SARM is sufficient and effective to fully restore mating behavior in long-term castrated male rats. To examine the efficacy of male

contraception, mating trials were included at end of the treatment. Maintenance of libido plays a key role in mating and reproductive studies. Animals in group 1 served as vehicle controls. Animals in groups 2 through 7 were treated with EB at a dose of 5 μg/day in combination with **C-31** at a dose of 0, 0.05, 0.1, 0.3, 0.5, or 0.75 mg/day, respectively (Table 7.1). The doses of **C-31** were chosen based on the pharmacologic activity of this compound in castrated male rats, and covered the whole range of the observed therapeutic window. At the highest dose rate tested herein (0.75 mg/day), **C-31** maintained the weight of the prostate and seminal vesicles to values similar to those observed in intact animals. Notably, at the dose rate of 0.1 mg/day, **C-31** selectively maintained the weight of levator ani muscle at the intact control level, while its effects on the prostate and seminal vesicles were lower than 30% of those observed in intact controls.

7.3.3.1 Whole Body DEXA Analyses

Figure 7.5 shows the body weight of animals measured after 69 days of treatment. Body weight in the EB-treated group was significantly less as compared to the vehicle control, indicating the effects of estrogen in male body growth. In the presence of EB, **C-31** significantly increased body weight at the lowest doses (i.e., 0.05 mg/day), but further decreased body weight at intermediate doses (i.e., 0.5 and 0.75 mg/day). The 'bell-shaped' change in body weight most likely reflected the mixed effect of hormones on body composition, including estrogen, endogenous testosterone, and SARM. However, the mean body weight of all treatment groups was significantly less than that of intact controls. Subsequent comparisons of body composition and organ weights were therefore normalized with body weight. Besides the body weight, body composition was also analyzed using DEXA. As shown in Figure 7.6, the whole body bone mineral density (BMD) was increased in all drug treatment groups as compared to the intact vehicle-treated control group, which is in agreement with the known effects of estrogen on bone. Additionally, a further increase in BMD was observed in animals treated with EB + **C-31** (0.05 mg/day). The effects of treatment on the percentage of fat mass (FM) are shown in Figure 7.7. EB alone significantly increased FM compared to the intact control. Co-

administration of EB and **C-31** decreased FM in a dose-dependent manner. At doses equal or higher than 0.5 mg/day, FM was significantly less than that of intact controls. FM was linearly correlated to the dose of **C-31**, with $R^2 = 0.9825$. Correspondingly, the lean mass (LM) also exhibited a dose-dependent increase after EB + **C-31** treatment (Figure 7.8).

7.3.3.2 Effects of Treatment on Androgen-Dependent Organs

During screening studies, dozens of compounds demonstrated potent activity and tissue selectivity in castrated male rats after two weeks of treatment. However, the current studies ere the first time to investigate the androgenic and anabolic activity of **C-31** in intact animals with co-administration of estrogen. Significant inhibition of prostate and seminal vesicle growth was observed in the group treated with EB alone as shown in Figure 7.9, suggesting treatment with EB decreased systemic concentrations of testosterone. The effect of co-administered **C-31** was biphasic, meaning that **C-31** further decreased the weight of prostate and seminal vesicles at a dose of 0.05 and 0.1 mg/day, but stimulated re-growth of these organs at higher doses (e.g., ≥ 0.3 mg/day). At a dose of 0.75 mg/day, the prostate weight was fully maintained and the seminal vesicles weight was significantly higher as compared to the intact controls. In contrast to the effect of **C-31** on the peripheral sexual organs, EB caused a non-significant decrease in the weight of testis and epididymis (Figure 7.10), indicating that a high level of endogenous testosterone exists locally in these organs. Again, a biphasic effect of **C-31** on the testis and epididymis was observed. Since the levator ani muscle weight highly depends on the systemic concentrations of testosterone, EB alone reduced its weight to 62% of that observed in intact control (Figure 7.11). Co-administration of **C-31** increased levator ani muscle weight in a dose-dependent manner and fully maintained the muscle weight at a dose as low as 0.1 mg/day.

7.3.3.3 Effects of Treatment on Spermatogenesis and Hormonal Regulations

The effect of combined treatment with **C-31** and EB on spermatogenesis was evaluated by counting the number of homogenization-resistant, advanced (step 17-19) spermatids in the testis from control and drug-treated rats. As shown in Figure 7.12, mean sperm counts were expressed as number of spermatids per testis (SPT, upper panel) or as the number of spermatids per gram of tissue (SPG, lower panel) after normalization with testis weight. No differences in the mean sperm counts (SPT or SPG) were noticed between EB-treated and intact control animals. Co-administration of **C-31** with EB caused a biphasic effect on sperm counts in testis, which was consistent with the androgenic activity of **C-31** in the peripheral and sexual organs. The greatest inhibition of spermatogenesis was observed in animals treated with 5 μg/day of EB plus 0.1 mg/day of **C-31** (Group 4). Four out of six animals were azoospermic and sperm counts in the remaining two animals were lower than 1.5 million sperm per mL of testicular homogenate. Higher doses of **C-31** actually supported spermatogenesis in a dose-dependent manner, resulting a similar mean sperm count as observed in the group treated with EB alone at the highest dose of **C-31** used (Group 7, Figure 7.12, A). Notably, the mean sperm counts of animals in Group 7 were greater than those observed in intact and EB alone groups after normalization with testis weights, suggesting that SARMs might also be useful to restore fertility in androgen-deficient males.

Intratesticular testosterone levels and serum concentrations of LH, FSH, and testosterone were determined using RIA assays and summarized in Table 7.2. The average serum concentration of LH in the intact control group was 0.21 ± 0.050 ng/mL. Drug treatments caused a marked suppression of serum LH to levels that were lower than the assay detection limit (0.04 ng/mL). The average serum concentration of FSH in the intact control group was 5.6 ± 1.2 ng/mL. In contrast to LH, significantly lower levels of FSH were only apparent in animals treated with the highest doses of **C-31** (i.e., 0.5 and 0.75 mg/day). The average serum concentration of testosterone in the intact control group was 2.2 ± 1.1 ng/mL. EB alone caused a significant inhibition in the average concentration of serum testosterone to 0.35 ± 0.37 ng/mL. In the presence of **C-31**, serum testosterone level was further suppressed in a dose-dependent manner. Serum

testosterone concentrations were below the detection limit of this assay at **C-31** doses of 0.1 mg/day or higher, in combination with EB. Accordingly, **C-31** induced similar trends in the intratesticular testosterone levels (Table 7.2). The mean intratesticular testosterone concentration of animals in the intact group, EB group, and EB plus 0.05 mg of **C-31** group was 91.4 ± 50.3, 22.8 ± 29.9, and 11.7 ± 14.5 ng/mL, respectively. Although the minimum dose of **C-31** to completely suppress intratesticular testosterone production was 0.3 mg/day, the most remarkable decreases in spermatogenesis were observed in animals treated with EB plus 0.1 mg/day of **C-31**. Sixty-seven percent of the animals that received EB plus 0.1 mg/day of **C-31** achieved azoospermia (4/6) and the remaining animals achieved oligozoospermia (2/6) with an average intratesticular testosterone concentration at 4.36 ± 6.57 ng/mL. Although increased doses of **C-31** (0.3 to 0.75 mg/day) completely suppressed intratesticular testosterone production, spermatogenesis was either partially or completely maintained due to the androgenic activity of **C-31** in the testes

7.3.3.4 Mating Trials

Previous pharmacologic studies showed that the levator ani muscle of castrated rats was maintained at the intact control level in animals that received **C-31** at a dose of 0.1 or 0.3 mg/day for 14 days, identifying these doses as the "physiologic" doses of **C-31**. Mating trials were performed during the last week of treatment for animals in groups 1, 2, 4, and 5, receiving vehicle, EB alone, EB plus 0.1 mg of **C-31**, and EB plus 0.3 mg of **C-31**, respectively. The efficacy of hormonal male contraception was evaluated by the fertility rate of male rats in the mating trials. One hundred percent of the animals in the vehicle-treated intact control group were fertile. Four of five (80%) male rats were fertile after treatment with EB alone. The average numbers of littler in intact control and EB alone group were 14 ± 2 and 13 ± 2, respectively. All male rats, treated with EB plus 0.1 mg of **C-31**, were infertile, while only one out of six male rats treated with EB plus 0.3 mg of **C-31** was fertile and impregnated a female rat with five litters.

7.3.4 Pharmacokinetics of **C-31** in the Rat

The time-courses of the changes in plasma concentrations of **C-31** following i.v. and p.o. administration are shown in Figure 7.13, and the pharmacokinetic parameters are listed in Table 7.3. Following intravenous administration, **C-31** concentrations declined and remained detectable until 48 h after the dose. The terminal $T_{1/2}$ of **C-31** in male rats was 10.9 h. The systemic clearance (CL) and steady state volume distribution (Vd_{ss}) were 0.87 mL/min/kg and 655 mL/kg, respectively. **C-31** appeared rapidly in the systemic circulation after p.o. administration. Oral absorption was prolonged with maximum plasma concentrations forming a plateau from 6 to 10 h after dose administration. Plasma concentrations of **C-31** diminished with a mean terminal $T_{1/2}$ of 11.9 h. Statistical analysis revealed no significant difference between the values of λ after i.v. and p.o. doses. The bioavailability of **C-31** following oral administration was 95.9%, indicating the near complete absorption after oral administration.

7.4 DISCUSSION

Among the experimental methods for male contraception, the most promising approach is testosterone-based hormone therapy. Spermatogenesis is highly regulated by hormones through the hypothalamus-pituitary-testis axis. The goal of hormonal male contraception is to suppress spermatogenesis by interrupting the action of one or more hormones involved in the hypothalamus-pituitary-testis axis, including GnRH, LH, FSH, and testosterone. Testosterone is commonly chosen for hormonal contraception because of its ability to replace peripheral androgens while inhibiting LH, FSH, and intratesticular testosterone levels via endogenous negative feedback mechanisms. Although testosterone alone showed an overall safety rate higher than that afforded by condoms in an Asian population, the azoospermia rate in Caucasian population was only two thirds of that observed in Asians (76, 77). Other anti-gonadotropin substances, such as progesterone and GnRH analogs, were used in combination with testosterone to achieve more rapid and complete suppression of spermatogenesis (reviewed in Chapter 1). For hormonal

male contraception, the disadvantages of using testosterone include inconvenient dosing routes (e.g., i.m. injection or implantation) and unwanted effects on the prostate, coagulation system, and lipid metabolism (reviewed in Chapter 1).

In the current studies, multiple *in vitro* and *in vivo* assays were used to characterize the feasibility of **C-31** for hormonal male contraception. First, **C-31** was identified as a potent AR agonist with high AR binding affinity and specificity *in vitro*. In the following *in vivo* study using castrated male rats, **C-31** revealed the most potent and efficacious activity among SARMs with multiple substituents in the B-ring. The levator ani muscle weight was maintained at values similar to that observed in the intact control group using **C-31** at doses of 0.1 to 0.3 mg/day in castrated male rats. Previous masculine behavior studies (Chapter 6) showed that SARM alone can not fully maintain or induce mating behavior in castrated rats. However, SARM induced mating behavior in long-term castrated rats when co-administrated with a low dose (5 μg/day) of EB. To maintain the libido of animals during or after treatment, SARM and EB combination regimens were used for studies of hormonal contraception and mating in intact male rats. Efficacy endpoint for these studies included androgen-dependent organ weights, body composition, total body bone mineral density, spermatogenesis, serum levels of LH, FSH, and testosterone, and intratesticular testosterone concentrations. Consistent with prior literature reports (222, 223), EB alone significantly decreased LH concentration and testosterone levels due to its negative feedback signals. Consequently, EB alone caused a significant decrease in the body weight, peripheral and reproductive organ weights, and lean muscle mass, which was mainly due to the suppressed circulating levels of testosterone. In animals that received EB + SARM combination regimens, their physiologic needs of androgen were replace by **C-31**, as evidenced by the fully maintained levator ani muscle and partially maintained prostate and seminal vesicles. Furthermore, animals treated with EB + **C-31** were leaner than intact controls with lower average body weight and significantly lower percent fat mass. An inverse correlation existed between the dose rate of **C-31** and the percent of fat mass in rats. Both in man (224) and animals (225, 226), androgen levels were negatively associated with leptin concentrations. Our previous studies with **S-1** showed that administration of SARM significantly decreased leptin levels in castrated male rats (Chen et al. unpublished data).

Findings from the current studies further support our hypothesis that SARM may mimic the pharmacologic actions of testosterone on body weight and body composition.

In adult animals, testicular size is mainly determined by the intratesticular testosterone concentration and is the most common endpoint to assess quantitative maintenance of spermatogenesis with minor inter laboratory variations (223, 227). Testosterone concentrations in the testis are 40-fold and 250-fold higher than those in serum in the rat and men, respectively. The levels of intratesticular testosterone in normal, healthy male rats range from 60 to 400 ng/mL Considerable variations were observed between animals and studies. Nevertheless, studies have shown that much lower intratesticular levels of testosterone are sufficient to maintain various degrees of spermatogenesis (228). To date, it is still not clear why such high local concentrations of testosterone are physiologically needed or what is the minimum level of testosterone to maintain spermatogenesis. In the current studies, EB alone remarkably suppressed the intratesticular testosterone levels to 25% of those in intact animals. However, no significant inhibition in the weights of testis or epididymis was observed after EB treatment, presumably suggesting that the suppressed intratesticular concentration of testosterone was still sufficient to maintain normal spermatogenesis. Indeed, the sperm counts of animals treated with EB alone were similar to those of intact animals. Testosterone levels were suppressed to a further extent and in a dose-dependent manner when **C-31** was added to the treatment regimens. However, the overall effects of the combination regimens on spermatogenesis were biphasic. In the absence of testosterone, EB + **C-31** fully maintained spermatogenesis, indicating that **C-31** mimics the effects of testosterone on spermatogenesis. A similar biphasic phenomenon in spermatogenesis was reported by studies using testosterone-based hormonal male contraception (170). At the highest dose (0.75 mg/day) we studied herein, **C-31** maintained spermatogenesis with an average but subnormal testicular weight of 75 ± 7% of intact control values. This finding is consistent with a number of studies using testosterone to restore spermatogenesis in rats made azoospermic either by hypophysectomy or gonadotropin withdrawal (229-232). A possible explanation for this observation is that measurement of homogenization-resistant sperm number overestimates the true sperm counts caused by abnormal retention or failed release of step 19 spermatids beyond stage VIII, the most subtle abnormal

changes of spermatogenesis associated with various experimental conditions (233-235). Histological analysis of testis and epididymis from animals after drug treatment is ongoing in our laboratory. Furthermore, EB plus 0.75 mg of **C-31** (group 7) not only inhibited LH levels, but also significantly suppressed FSH concentrations. It is well known that FSH directly affects Sertoli cells, which in turn directly determine the size of the testis. The lack of a physiologic level of FSH may have partially contributed to the subnormal size of the testis. Additionally, synergistic effects of testosterone and estradiol on suppression of spermatogenesis were reported both in the rat (223) and in man (236). Although the current studies clearly demonstrated the promise of SARMs for hormonal male contraception, it remains unknown whether SARM and estradiol have a similar synergistic inhibition in spermatogenesis or not.

In summary, **C-31** was identified as a potent and efficacious SARM in castrated male rats with significantly higher anabolic activity than androgenic activity. In intact male rats, EB plus **C-31** demonstrated potential use for hormonal male contraception. Either azoospermia or oligozoospermia was successfully achieved in the EB plus 0.1 mg/day **C-31** combination regimen with a 100% infertile rate observed in the efficacy study. Unlike testosterone which showed biphasic effects in the testis and epididymis and nonselective increase in peripheral reproductive tracts (e.g., prostate and seminal vesicles), **C-31** displayed biphasic effects in all organs mentioned above. Additionally, **C-31** selectively increased levator ani muscle weight and improved body composition. In conclusion, this is the first study to show that azoospermia can be induced using EB plus SARM combination therapy, in which, EB was used to maintain libido without affecting quantitative spermatogenesis. This therapy selectively decreased weights of prostate, seminal vesicles, testis, and epididymis, retained muscle weight, decreased fat and increased lean mass, and increased BMD. Furthermore, **C-31** demonstrated high oral bioavailability (97%). The identification of EB plus **C-31** combination therapy represents an important step forward toward the “male pill”.

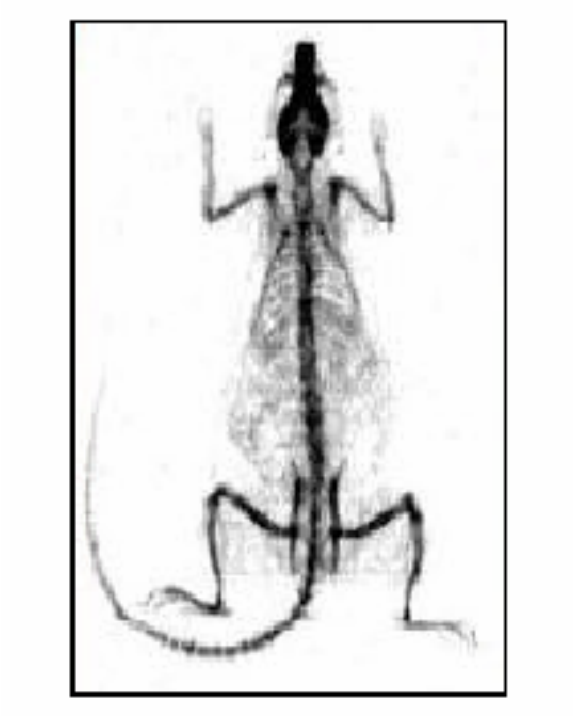

Figure 7. 1 Animal Positioning for DEXA Scan.

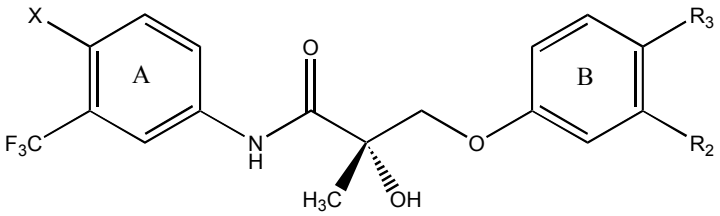

Compund Name	X	R_2	R_3	Ki (nM)	*In Vitro* Activity (% of DHT)
S-1	NO_2	H	F	6.1 ± 0.2 *	43 ± 2.6 *
C-3	NO_2	F	F	3.4 ± 0.6	99 ± 12
C-6	NO_2	F	Cl	4.9 ± 0.3	118 ± 19
C-31	CN	F	Cl	1.7 ± 0.2	96 ± 23

Figure 7. 2 Chemical Structures, AR Binding Affinity, and *In vitro* Transcriptional Activation of **S-1**, **C-3**, **C-6**, and **C-31**.

AR binding affinity of compound of interest was determined using a radioligand competitive assay. The ability of compound of interest to induce the AR-mediated transcriptional activation was determined using a co-transfection assay in CV-1 cells. Transcriptional activity induced by each compound at 10 nM was reported as the percentage of activity observed for 1 nM of DHT.
Each value represents the mean ± s.d. of three replicates.
* Data were reported previously by Yin et al. (59).

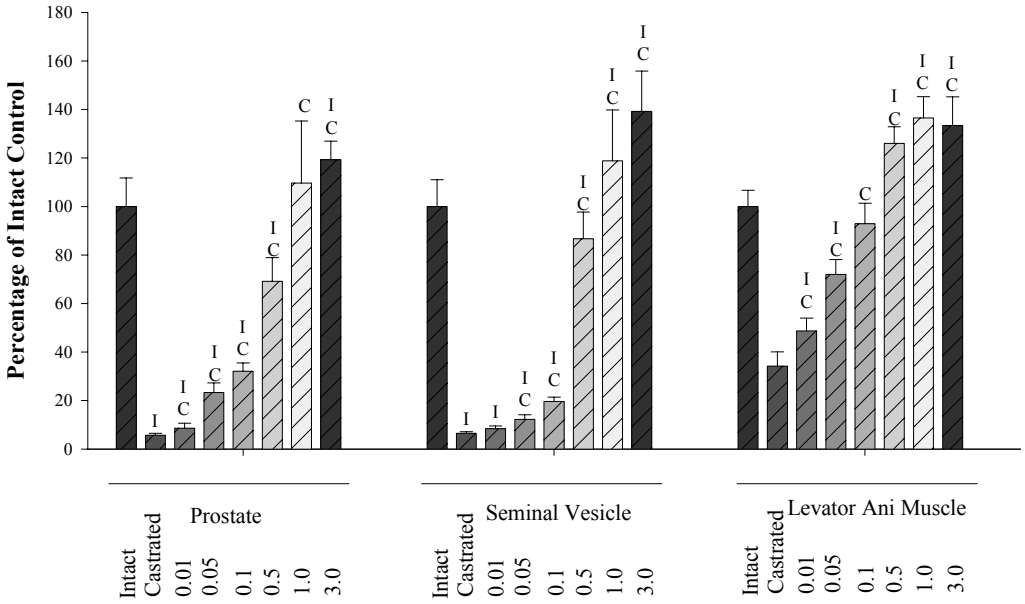

Figure 7. 3 The Androgenic Activity and Anabolic Activity of **C-31** in Castrated Male Rats.

C-31 was administrated to animals via daily s.c. injections for 14 days with doses ranging from 0.01 mg/day to 3 mg/day. All organ weights were normalized with body weight and presented as the percentage of intact control.
Each Bar represents the mean ± s.d. of five rats.
I and C indicate a significant difference from intact control and castrated control groups as tested by single-factor ANOVA ($p < 0.05$).

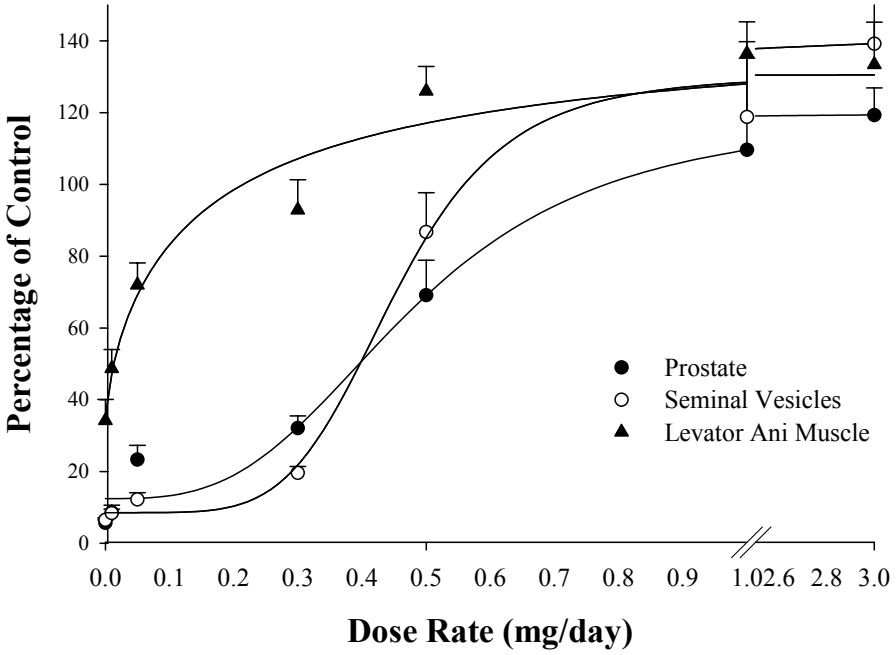

	Prostate	Seminal Vesicles	Levator Ani Muscle
Emax	138 ± 21%	144 ± 1%	139 ± 4%
ED_{50}	0.43 ± 0.18	0.41 ± 0.0070	0.079 ± 0.010

Figure 7. 4 Dose-Response Curves of **C-31** in Castrated Male Rats.

E_{max}, and ED_{50} in this figure were obtained by nonlinear least-square regression analysis. Each value represents the mean ± s.d. of five rats.

Group	EB (μg/day)	**C-31** (mg/day)	Animal Numbers
1	--	--	6
2	5	--	5
3	5	0.05	6
4	5	0.1	6
5	5	0.3	6
6	5	0.5	6
7	5	0.75	6

Table 7. 1 Summary of the Dosing Groups

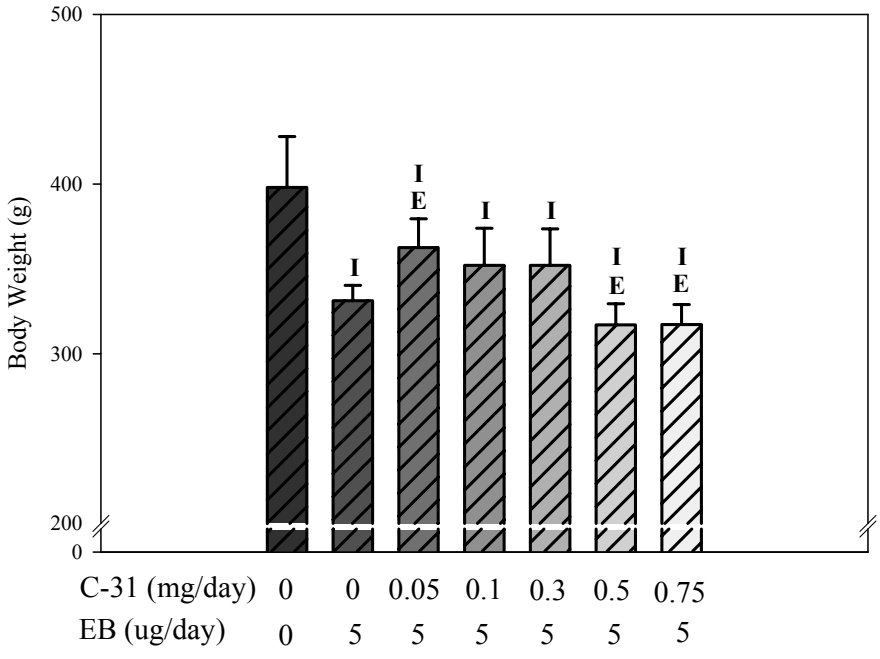

Figure 7. 5 Body Weights at Day 69 (DEXA).

Intact, male Sprague-Dawley rats received daily subcutaneous doses of the indicated drugs for 69 days. Each bar represents the mean ± S.D. (n=5 or 6/group). The letters "I" and "E" above each error bar represent a significant difference between the group and intact control group and EB group, respectively, as analyzed by single-factor ANOVA with $p < 0.05$.

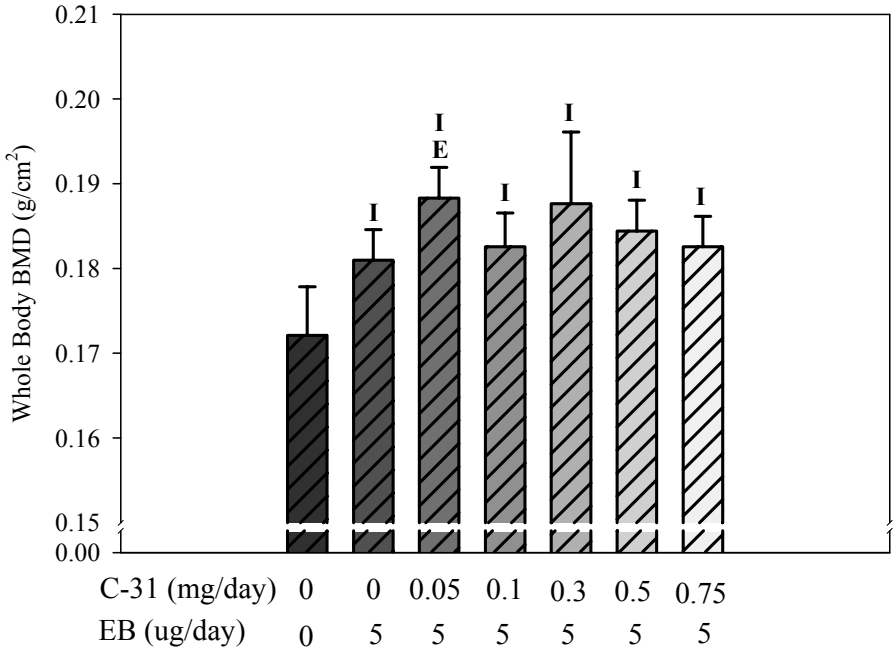

Figure 7. 6 Whole Body Bone Mineral Density (BMD) at Day 69 (DEXA).

Intact, male Sprague-Dawley rats received daily subcutaneous doses of the indicated drugs for 69 days. Each bar represents the mean ± S.D. (n=5 or 6/group). The letters "I" and "E" above each error bar represent a significant difference between the group and intact control group and estrogen-treated group, respectively, as analyzed by single-factor ANOVA with $p < 0.05$.

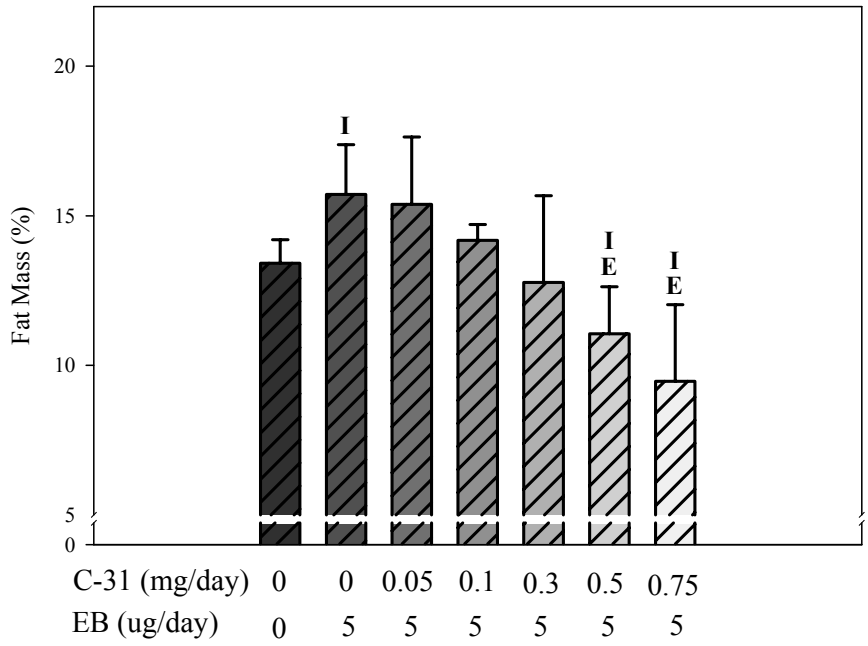

Figure 7. 7 Percentage of Fat Mass at Day 69 (DEXA).

Intact, male Sprague-Dawley rats received daily subcutaneous doses of the indicated drugs for 69 days. Each bar represents the mean ± S.D. (n=5 or 6/group). The letters "I" and "E" above each error bar represent a significant difference between the group and intact control group and estrogen-treated group, respectively, as analyzed by single-factor ANOVA with $p < 0.05$.

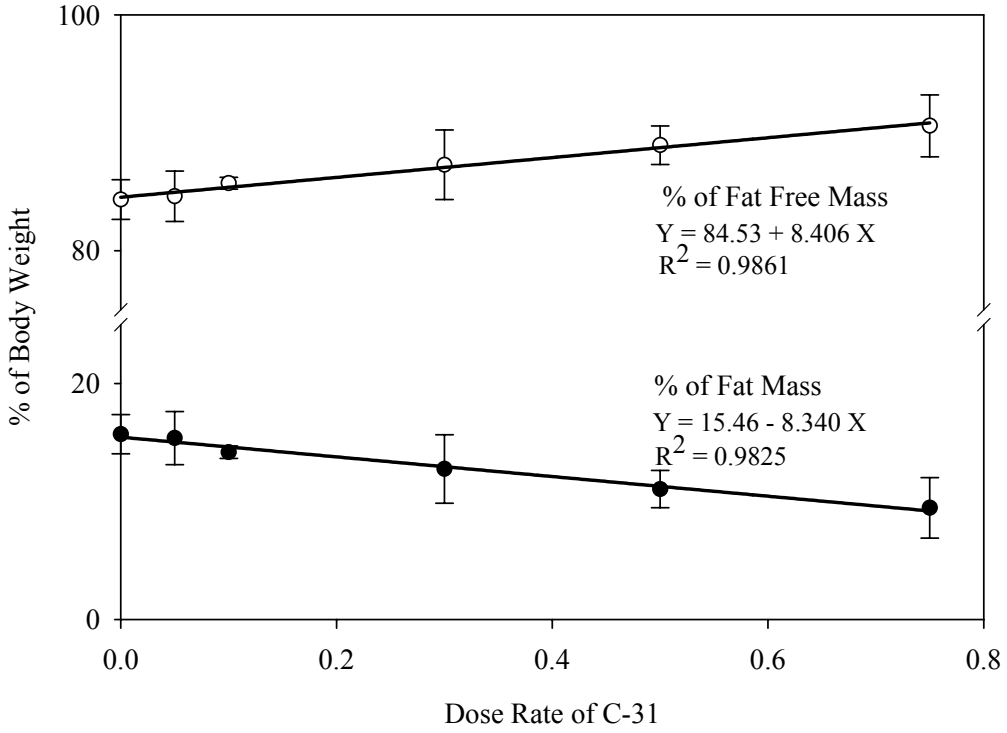

Figure 7. 8 The Linear Correlation Between the Dose Rate of **C-31** and Body Composition (% of Fat Mass and % of fat free Mass).

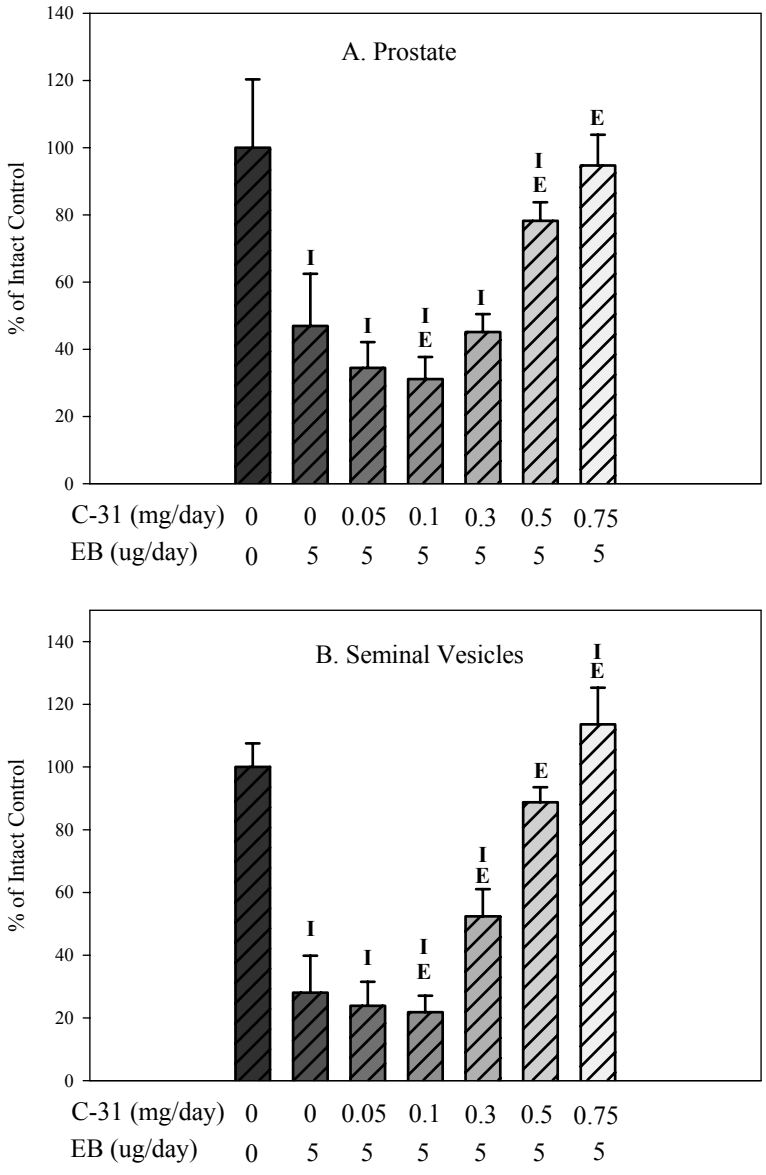

Figure 7. 9 The Weight of Prostate (A) and Seminal Vesicles (B).

Intact, male Sprague-Dawley rats received daily subcutaneous doses of the indicated drugs for 69 days. Each bar represents the mean ± S.D. (n = 5 or 6/group). The letters "I" and "E" above each error bar represent a significant difference between the group and intact control group and estrogen-treated group, respectively, as analyzed by single-factor ANOVA with $p < 0.05$.

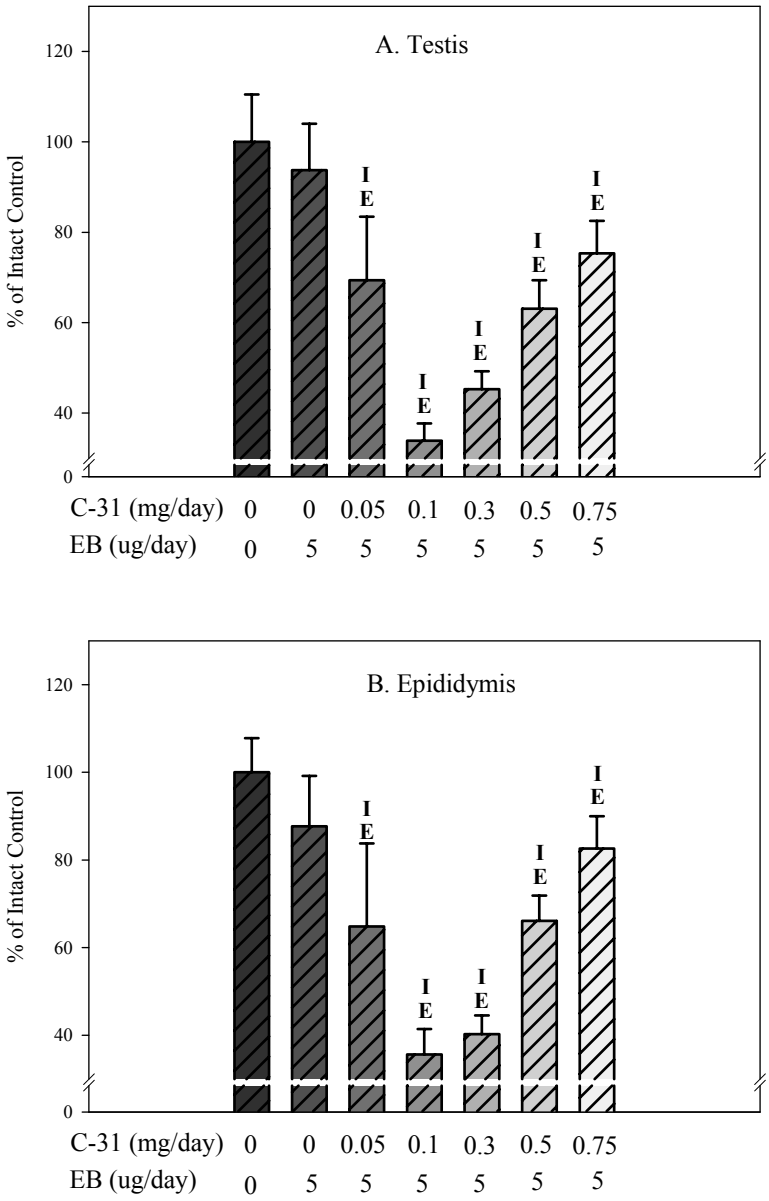

Figure 7. 10 The Weight of Testis (A) and Epididymis (B).

Intact, male Sprague-Dawley rats received daily subcutaneous doses of the indicated drugs for 69 days. Each bar represents the mean ± S.D. (n = 5 or 6/group). The letters "I" and "E" above each error bar represent a significant difference between the group and intact control group and estrogen-treated group, respectively, as analyzed by single-factor ANOVA with $p < 0.05$.

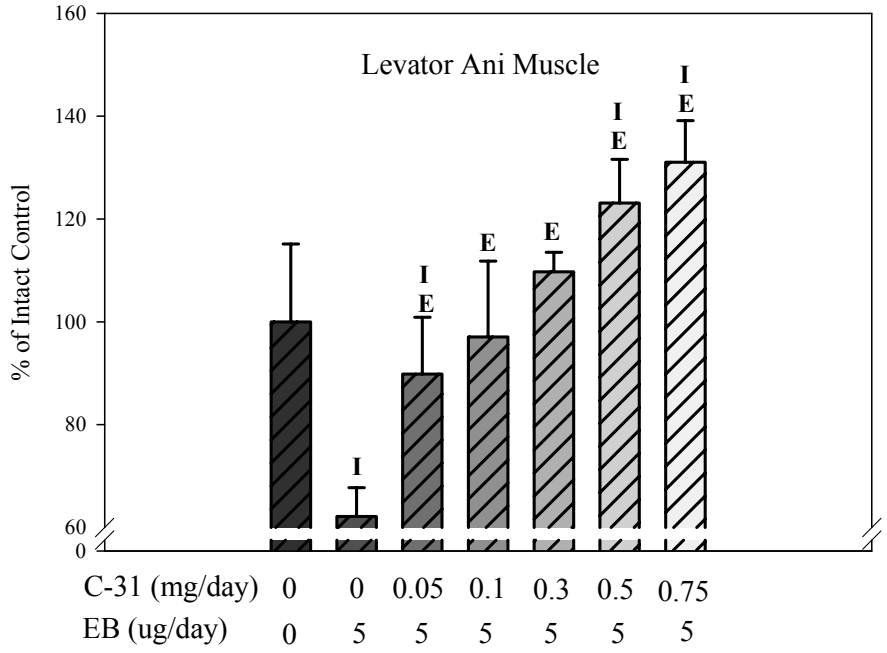

Figure 7. 11 The Weight of Levator Ani Muscle.

Intact, male Sprague-Dawley rats received daily subcutaneous doses of the indicated drugs for 69 days. Each bar represents the mean ± S.D. (n = 5 or 6/group). The letters "I" and "E" above each error bar represent a significant difference between the group and intact control group and estrogen-treated group, respectively, as analyzed by single-factor ANOVA with $p < 0.05$.

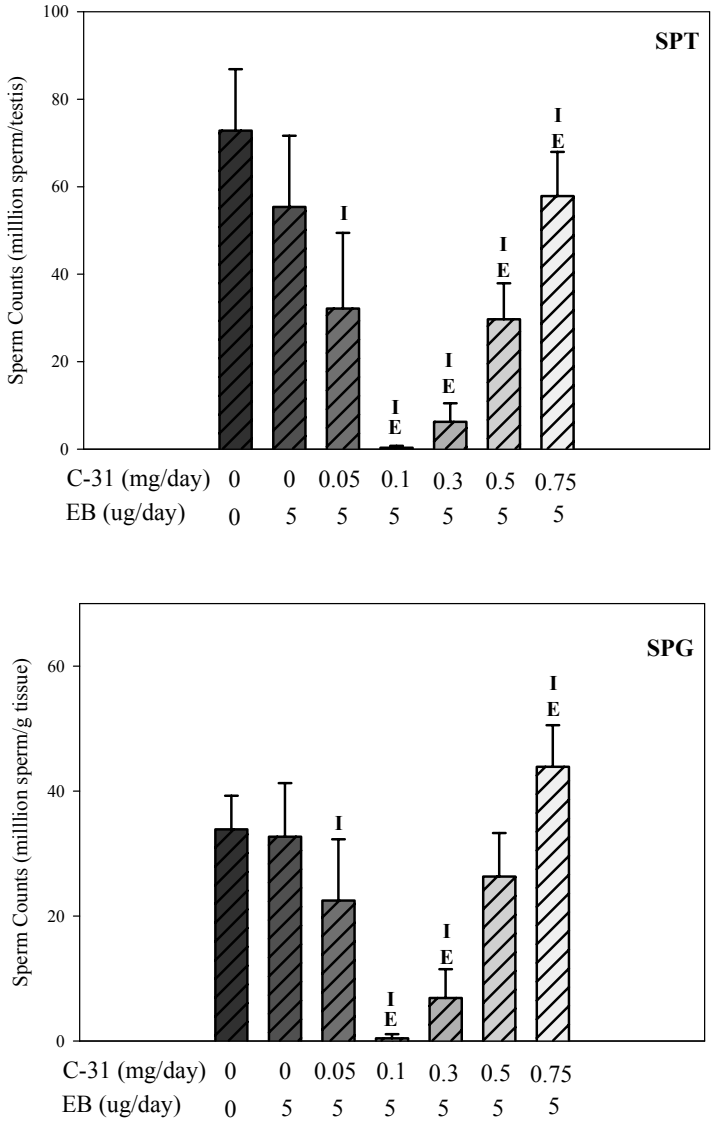

Figure 7. 12 Testicular Sperm Counts (Million Sperm/Testis) or (Million Sperm/g tissue).

Intact, male Sprague-Dawley rats received daily subcutaneous doses of the indicated drugs for 69 days. Each bar represents the mean ± S.D. (n = 5 or 6/group). The letters "I" and "E" above each error bar represent a significant difference between the group and intact control group and estrogen-treated group, respectively, as analyzed by single-factor ANOVA with $p < 0.05$.

Group	EB (μg/day)	C-31 (mg/day)	N	LH (ng/mL)	FSH (ng/mL)	Serum Testosterone (ng/mL)	Intratesticular Testosterone (ng/mL)
1	--	--	6	0.21 ± 0.050	5.6 ± 1.2	2.2 ± 1.1	91.4 ± 50.3
2	5	--	5	<0.04	5.2 ± 0.43	0.35 ± 0.37 [I]	22.8 ± 29.9[I]
3	5	0.05	6	<0.04	4.8 ± 1.4	0.092 ± 0.12 [I, E]	11.7 ± 14.5 [I, E]
4	5	0.1	6	<0.04	4.8 ± 0.90	<0.0075	4.36 ± 6.57 [I, E]
5	5	0.3	6	<0.04	4.3 ± 1.5	<0.0075	<0.025
6	5	0.5	6	<0.04	3.4 ± 0.30 [I, E]	<0.0075	<0.025
7	5	0.75	6	<0.04	3.6 ± 0.46 [I, E]	<0.0075	<0.025

Data presented as mean ± s.d.; I: $p < 0.05$ vs intact control; E: $p < 0.05$ vs EB group

Table 7. 2 Effects of Drug-Treatments on Pituitary and Testicular Hormones.

Intact, male Sprague-Dawley rats received daily subcutaneous doses of the indicated drugs for 69 days. The letters “I” and “E” above each error bar represent a significant difference between the group and intact control group and estrogen-treated group, respectively, as analyzed by single-factor ANOVA with $p < 0.05$.

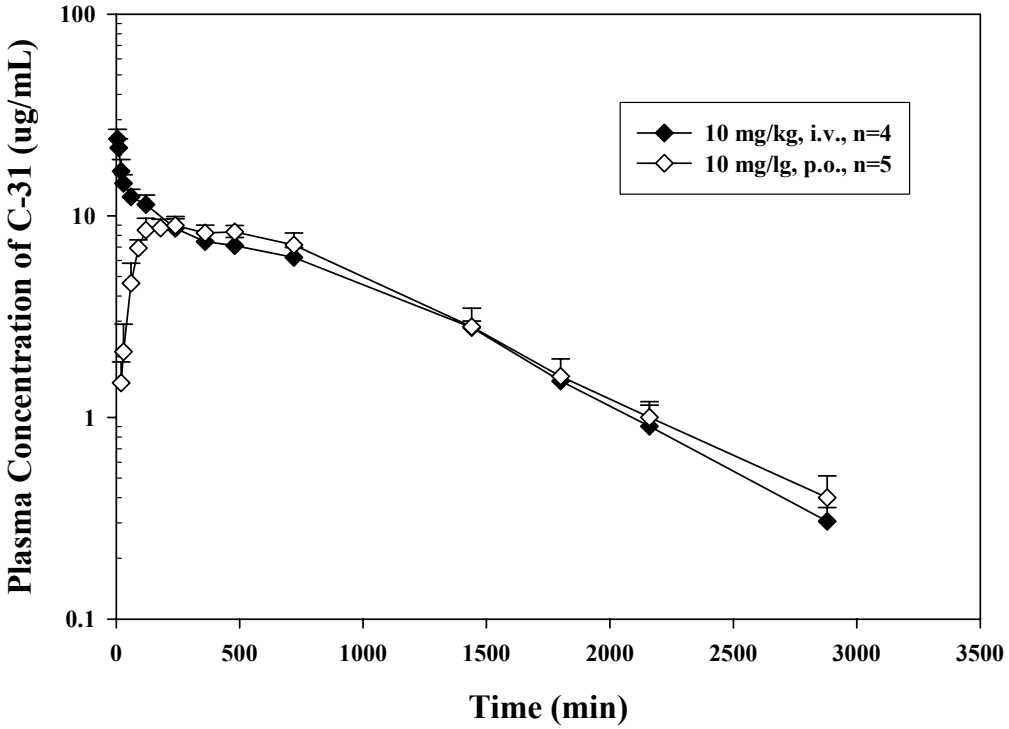

Figure 7. 13 Mean Plasma Concentration-Time Profile of **C-31** in Male Rats.

Plasma concentrations of **C-31** were measured using HPLC. Data were expressed as microgram per milliliter, and each point represents the mean ± S.D. (N = 4 or 5/group).

Parameter	i.v. 10 mg/kg (n = 4)	p.o. 10 mg/kg (n = 5)
$AUC_{0\rightarrow\infty}$ (min *μg/L)	11.3 ± 0.33	10.8 ± 0.66
λ_z (min^{-1})	0.00153 ± 0.00017	0.00140 ± 0.000156
MRT (min)	751 ± 67	879 ± 61
CL (mL/min/kg)	0.87 ± 0.02	
V_{ss} (mL/kg)	655 ± 78	
$F_{p.o.}$ (%)		95.9
T_{max} (min)		252 ± 137
C_{max} (mg/mL)		9.4 ± 0.7
CL/F (mL/min/kg)		0.90 ± 0.06
V_{ss}/F (mL/kg)		649 ± 68

Table 7. 3 Mean Pharmacokinetic Parameters of **C-31** in Male Rats.

CHAPTER 8

SUMMARY

Physical methods (e.g., condoms) remain the sole contraceptive choice for men. Clinical trials of testosterone-base hormonal male contraception represent the most advanced stage of research in male contraception. Nonsteroidal selective androgen receptor modulators (SARMs) discovered in our laboratory offer potential applications in androgen replacement, including hormonal male contraception. The advantages of SARMs over testosterone are: AR specificity, tissue selectivity, and better pharmacokinetic properties. The long-term goal of this research is to develop a safe, reversible, orally active, and affordable male contraceptive through an iterative and step-wise experimental paradigm. Studies completed during this dissertation project included:

1. Determination of the AR binding affinity of novel AR ligands with multiple substituents in the aromatic B-ring using a radiolabeled competitive binding assay *in vitro*.
2. Examination of the AR-mediated functional activity of novel AR ligands with multiple substituents in the B-ring using a cotransfection assay in CV-1 cells.
3. Testing the androgenic and anabolic activity of AR ligands, which demonstrated high AR binding affinity and/or *in vitro* functional activity, in castrated male rats as a means to identify AR ligands as SARMs.
4. Analysis of the *in vitro* and *in vivo* structure activity relationships of these AR ligands.
5. Elucidation of the pharmacokinetics and metabolism of a potent SARM (**C-3**) in the rat.
6. Characterization of the pharmacology of a potent SARM (**C-6**) in castrated and intact male rats for hormonal contraception.

7. Evaluation of the effects of **C-6** on masculine sexual behavior in male rats alone or in the combination with estradiol benzoate (EB).
8. Design of a novel SARM (**C-31**) with integrated knowledge of structure-activity relationships, pharmacokinetics, and metabolism of SARMs.
9. Examination of the effects of **C-31** plus EB regimens in male rats for hormonal male contraception.

Conclusions and major findings of the current studies are as following:

1. The inhibition constant (Ki) values of AR ligands varied from 1 to 51 nM. Compounds with significantly improved AR binding affinity were designed by incorporation of multiple substituents in the aromatic B-ring of a known SARM (e.g., **S-1**)
2. Most AR ligands examined in the current studies were identified as full agonists. Several compounds with high AR binding affinity were identified as partial agonists using an *in vitro* functional assay.
3. Compounds with halogen substituents at the *para* and *meta* positions of the B-ring demonstrated the highest *in vivo* pharmacologic activity, which was more potent and efficacious than that of a known SARM (e.g., **S-1**) in castrated male rats. Partial agonists were inactive *in vivo*, suggesting that both AR ligand binding assay and the in vitro functional assay are important screening assays to select candidates for *in vivo* tests. The pharmacokinetics, metabolism and pharmacology of two potent SARMs (i.e., **C-3** and **C-6**) were further studied in intact male rats as a prelude to male contraception studies.
4. When compared with **S-1**, no improvement was observed in terms of the pharmacokinetic properties of **C-3**. The major metabolism pathways of **C-3**, a potent SARM with di-fluoro groups in the B-ring, included nitro reduction in the A-ring, oxidation in the B-ring, and sulfate conjugation. Changing the cyano group in the A-ring to a nitro group may increase the *in vivo* stability of this series of compounds.
5. The introduction of a *para*-Cl group and a *meta*-F group to the B-ring resulted a unique SARM (**C-6**), which was as efficacious (Emax) in the prostate and levator ani muscle, but much more potent (ED_{50}) in terms of anabolic activity than

androgenic activity in castrated male rats. Additionally, **C-6** potently inhibited LH and FSH production in castrated male rats and suppressed testosterone biosynthesis and spermatogenesis in intact male rats.

6. **C-6** alone failed to induce masculine sexual behavior in sexually naïve, castrated male rats, which was in agreement with the concept that androgen alone is not sufficient to induce or maintain sexual behavior in castrated male rats. However, masculine sexual behavior was fully restored by **C-6** plus 5 μg/day of EB in sexually naïve rats. In sexually experienced male rats, **C-6** alone partially maintained sexual behavior.
7. **C-31** was identified as a potent and efficacious SARM, which was more potent than **C-6** in castrated male rats. Either azoospermia or oligozoospermia was successfully achieved in the EB plus 0.1 mg/day **C-31** combination regimen with a 100% infertility rate observed in the efficacy study. **C-31** and EB combination therapy selectively decreased weights of prostate, seminal vesicles, testis, and epdidymis, retained muscle weight, decreased fat and increased lean mass, and increased BMD. Furthermore, **C-31** demonstrated high oral bioavailability (97%).

In summary, introduction of multiple substituents in the aromatic B-ring of the SARM pharmacophore is a novel approach to discover new SARMs with high AR binding affinity, AR-mediated transcriptional activation, and *in vivo* pharmacologic activity. Additionally, such structural modifications provided candidates with profound CNS effects for hormonal male contraception. The identification of EB plus **C-31** combination therapy represents an important step forward toward the "male pill".

BIBLIOGRAPHY

1. 1. **Mooradian AD, Morley JE, Korenman SG** 1987 Biological actions of androgens. Endocr Rev 8:1-28

2. **Christensen AK, Mason NR** 1965 Comparative Ability of Seminiferous Tubules and Interstitial Tissue of Rat Testes to Synthesize Androgens from Progesterone-4-14c *in vitro*. Endocrinology 76:646-56

3. **Hall PF, Irby DC, De Kretser DM** 1969 Conversion of cholesterol to androgens by rat testes: comparison of interstitial cells and seminiferous tubules. Endocrinology 84:488-96

4. **Ewing LL, Zirkin B** 1983 Leydig cell structure and steroidogenic function. Recent Prog Horm Res 39:599-635

5. **Rommerts FF, Brinkman AO** 1981 Modulation of steroidogenic activities in testis Leydig cells. Mol Cell Endocrinol 21:15-28

6. **Chang CS, Kokontis J, Liao ST** 1988 Structural analysis of complementary DNA and amino acid sequences of human and rat androgen receptors. Proc Natl Acad Sci U S A 85:7211-5

7. **Lubahn DB, Joseph DR, Sullivan PM, Willard HF, French FS, Wilson EM** 1988 Cloning of human androgen receptor complementary DNA and localization to the X chromosome. Science 240:327-30

8. **Jenster G, de Ruiter PE, van der Korput HA, Kuiper GG, Trapman J, Brinkmann AO** 1994 Changes in the abundance of androgen receptor isotypes: effects of ligand treatment, glutamine-stretch variation, and mutation of putative phosphorylation sites. Biochemistry 33:14064-72

9. **Doesburg P, Kuil CW, Berrevoets CA, Steketee K, Faber PW, Mulder E, Brinkmann AO, Trapman J** 1997 Functional *in vivo* interaction between the

amino-terminal, transactivation domain and the ligand binding domain of the androgen receptor. Biochemistry 36:1052-64

10. **Jenster G, van der Korput HA, Trapman J, Brinkmann AO** 1995 Identification of two transcription activation units in the N-terminal domain of the human androgen receptor. J Biol Chem 270:7341-6

11. **Danielian PS, White R, Lees JA, Parker MG** 1992 Identification of a conserved region required for hormone dependent transcriptional activation by steroid hormone receptors. Embo J 11:1025-33

12. **Durand B, Saunders M, Gaudon C, Roy B, Losson R, Chambon P** 1994 Activation function 2 (AF-2) of retinoic acid receptor and 9-cis retinoic acid receptor: presence of a conserved autonomous constitutive activating domain and influence of the nature of the response element on AF-2 activity. Embo J 13:5370-82

13. **He B, Kemppainen JA, Wilson EM** 2000 FXXLF and WXXLF sequences mediate the NH2-terminal interaction with the ligand binding domain of the androgen receptor. J Biol Chem 275:22986-94

14. **Slagsvold T, Kraus I, Bentzen T, Palvimo J, Saatcioglu F** 2000 Mutational analysis of the androgen receptor AF-2 (activation function 2) core domain reveals functional and mechanistic differences of conserved residues compared with other nuclear receptors. Mol Endocrinol 14:1603-17

15. **Sack JS, Kish KF, Wang C, Attar RM, Kiefer SE, An Y, Wu GY, Scheffler JE, Salvati ME, Krystek SR, Jr., Weinmann R, Einspahr HM** 2001 Crystallographic structures of the ligand-binding domains of the androgen receptor and its T877A mutant complexed with the natural agonist dihydrotestosterone. Proc Natl Acad Sci U S A 98:4904-9

16. **Matias PM, Donner P, Coelho R, Thomaz M, Peixoto C, Macedo S, Otto N, Joschko S, Scholz P, Wegg A, Basler S, Schafer M, Egner U, Carrondo MA** 2000 Structural evidence for ligand specificity in the binding domain of the human androgen receptor. Implications for pathogenic gene mutations. J Biol Chem 275:26164-71

17. **Moras D, Gronemeyer H** 1998 The nuclear receptor ligand-binding domain: structure and function. Curr Opin Cell Biol 10:384-91

18. **Heinlein CA, Chang C** 2001 Role of chaperones in nuclear translocation and transactivation of steroid receptors. Endocrine 14:143-9

19. **Smith DF** 2000 Chaperones in progesterone receptor complexes. Semin Cell Dev Biol 11:45-52

20. **Fang Y, Fliss AE, Robins DM, Caplan AJ** 1996 Hsp90 regulates androgen receptor hormone binding affinity *in vivo*. J Biol Chem 271:28697-702

21. **Roeder RG** 1996 The role of general initiation factors in transcription by RNA polymerase II. Trends Biochem Sci 21:327-35

22. **Ma H, Hong H, Huang SM, Irvine RA, Webb P, Kushner PJ, Coetzee GA, Stallcup MR** 1999 Multiple signal input and output domains of the 160-kilodalton nuclear receptor coactivator proteins. Mol Cell Biol 19:6164-73

23. **Roeder RG** 2005 Transcriptional regulation and the role of diverse coactivators in animal cells. FEBS Lett 579:909-15

24. **Falkenstein E, Heck M, Gerdes D, Grube D, Christ M, Weigel M, Buddhikot M, Meizel S, Wehling M** 1999 Specific progesterone binding to a membrane protein and related nongenomic effects on Ca2+-fluxes in sperm. Endocrinology 140:5999-6002

25. **Falkenstein E, Christ M, Feuring M, Wehling M** 2000 Specific nongenomic actions of aldosterone. Kidney Int 57:1390-4

26. **Falkenstein E, Wehling M** 2000 Nongenomically initiated steroid actions. Eur J Clin Invest 30 Suppl 3:51-4

27. **Wehling M** 1997 Specific, nongenomic actions of steroid hormones. Annu Rev Physiol 59:365-93

28. **Kang HY, Cho CL, Huang KL, Wang JC, Hu YC, Lin HK, Chang C, Huang KE** 2004 Nongenomic androgen activation of phosphatidylinositol 3-kinase/Akt signaling pathway in MC3T3-E1 osteoblasts. J Bone Miner Res 19:1181-90

29. **Benten WP, Guo Z, Krucken J, Wunderlich F** 2004 Rapid effects of androgens in macrophages. Steroids 69:585-90

30. **Mayes JS, Watson GH** 2004 Direct effects of sex steroid hormones on adipose tissues and obesity. Obes Rev 5:197-216

31. **Walker WH** 2003 Nongenomic actions of androgen in Sertoli cells. Curr Top Dev Biol 56:25-53

32. **Nieschlag E, Cuppers JH, Wickings EJ, Kruskemper HL** 1975 [Plasma-androgens following oral administration of testosterone. Influence of sex, age, and liver function (author's transl)]. Dtsch Med Wochenschr 100:1773-4, 1779-80

33. **Frey H, Aakvaag A, Saanum D, Falch J** 1979 Bioavailability of oral testosterone in males. Eur J Clin Pharmacol 16:345-9

34. **Nieschlag E, Cuppers HJ, Wickings EJ** 1977 Influence of sex, testicular development and liver function on the bioavailability of oral testosterone. Eur J Clin Invest 7:145-7

35. **Zhang GY, Gu YQ, Wang XH, Cui YG, Bremner WJ** 1998 A pharmacokinetic study of injectable testosterone undecanoate in hypogonadal men. J Androl 19:761-8

36. **Nieschlag E, Hoogen H, Bolk M, Schuster H, Wickings EJ** 1978 Clinical trial with testosterone undecanoate for male fertility control. Contraception 18:607-14

37. **Morales A** 2004 Testosterone treatment for the aging man: the controversy. Curr Urol Rep 5:472-7

38. **Liu PY, Swerdloff RS, Veldhuis JD** 2004 Clinical review 171: The rationale, efficacy and safety of androgen therapy in older men: future research and current practice recommendations. J Clin Endocrinol Metab 89:4789-96

39. **Krause W** 2004 [Testosterone substitution in aging males. Which questions are answered?]. Urologe A 43:1097-100

40. **Gooren LJ, Bunck MC** 2004 Androgen replacement therapy: present and future. Drugs 64:1861-91

41. **Blohm TR, Laughlin ME, Benson HD, Johnston JO, Wright CL, Schatzman GL, Weintraub PM** 1986 Pharmacological induction of 5 alpha-reductase deficiency in the rat: separation of testosterone-mediated and 5 alpha-dihydrotestosterone-mediated effects. Endocrinology 119:959-66

42. **Krieg M, Voigt KD** 1976 *In vitro* binding and metabolism of androgens in various organs: a comparative study. J Steroid Biochem 7:1005-12

43. **Stenstad P, Eik-Nes KB** 1981 Androgen metabolism in rat skeletal muscle *in vitro*. Biochim Biophys Acta 663:169-76

44. **Wilson JD, Gloyna RE** 1970 The intranuclear metabolism of testosterone in the accessory organs of reproduction. Recent Prog Horm Res 26:309-36

45. **Kumar N, Didolkar AK, Monder C, Bardin CW, Sundaram K** 1992 The biological activity of 7 alpha-methyl-19-nortestosterone is not amplified in male reproductive tract as is that of testosterone. Endocrinology 130:3677-83

46. **Anderson RA, Wallace AM, Sattar N, Kumar N, Sundaram K** 2003 Evidence for tissue selectivity of the synthetic androgen 7 alpha-methyl-19-nortestosterone in hypogonadal men. J Clin Endocrinol Metab 88:2784-93

47. **Hirawat S, Budman DR, Kreis W** 2003 The androgen receptor: structure, mutations, and antiandrogens. Cancer Invest 21:400-17

48. **Goldenberg SL, Bruchovsky N** 1991 Use of cyproterone acetate in prostate cancer. Urol Clin North Am 18:111-22

49. **Geller J, Albert J, Yen SS** 1978 Treatment of advanced cancer of prostate with megestrol acetate. Urology 12:537-41

50. **Dawson NA, McLeod DG** 1995 Dramatic prostate specific antigen decrease in response to discontinuation of megestrol acetate in advanced prostate cancer: expansion of the antiandrogen withdrawal syndrome. J Urol 153:1946-7

51. **Osborn JL, Smith DC, Trump DL** 1997 Megestrol acetate in the treatment of hormone refractory prostate cancer. Am J Clin Oncol 20:308-10

52. **Sartor O, Eastham JA** 1999 Progressive prostate cancer associated with use of megestrol acetate administered for control of hot flashes. South Med J 92:415-6

53. **Culig Z, Bartsch G, Hobisch A** 2004 Antiandrogens in prostate cancer endocrine therapy. Curr Cancer Drug Targets 4:455-61

54. **Schmitt B, Wilt TJ, Schellhammer PF, DeMasi V, Sartor O, Crawford ED, Bennett CL** 2001 Combined androgen blockade with nonsteroidal antiandrogens for advanced prostate cancer: a systematic review. Urology 57:727-32

55. **Migliari R, Muscas G, Murru M, Verdacchi T, De Benedetto G, De Angelis M** 1999 Antiandrogens: a summary review of pharmacodynamic properties and tolerability in prostate cancer therapy. Arch Ital Urol Androl 71:293-302

56. **Dalton JT, Mukherjee A, Zhu Z, Kirkovsky L, Miller DD** 1998 Discovery of nonsteroidal androgens. Biochem Biophys Res Commun 244:1-4

57. **He Y, Yin D, Perera M, Kirkovsky L, Stourman N, Li W, Dalton JT, Miller DD** 2002 Novel nonsteroidal ligands with high binding affinity and potent functional activity for the androgen receptor. Eur J Med Chem 37:619-34

58. **Yin D, Xu H, He Y, Kirkovsky LI, Miller DD, Dalton JT** 2003 Pharmacology, pharmacokinetics, and metabolism of acetothiolutamide, a novel nonsteroidal agonist for the androgen receptor. J Pharmacol Exp Ther 304:1323-33

59. **Yin D, Gao W, Kearbey JD, Xu H, Chung K, He Y, Marhefka CA, Veverka KA, Miller DD, Dalton JT** 2003 Pharmacodynamics of selective androgen receptor modulators. J Pharmacol Exp Ther 304:1334-40

60. **Marhefka CA, Gao W, Chung K, Kim J, He Y, Yin D, Bohl C, Dalton JT, Miller DD** 2004 Design, synthesis, and biological characterization of metabolically stable selective androgen receptor modulators. J Med Chem 47:993-8

61. **Bohl CE, Chang C, Mohler ML, Chen J, Miller DD, Swaan PW, Dalton JT** 2004 A ligand-based approach to identify quantitative structure-activity relationships for the androgen receptor. J Med Chem 47:3765-76

62. **Yin D, He Y, Perera MA, Hong SS, Marhefka C, Stourman N, Kirkovsky L, Miller DD, Dalton JT** 2003 Key structural features of nonsteroidal ligands for binding and activation of the androgen receptor. Mol Pharmacol 63:211-23

63. **Mukherjee A, Kirkovsky LI, Kimura Y, Marvel MM, Miller DD, Dalton JT** 1999 Affinity labeling of the androgen receptor with nonsteroidal chemoaffinity ligands. Biochem Pharmacol 58:1259-67

64. **Gao W, Kearbey JD, Nair VA, Chung K, Parlow AF, Miller DD, Dalton JT** 2004 Comparison of the pharmacological effects of a novel selective androgen receptor modulator, the 5alpha-reductase inhibitor finasteride, and the antiandrogen hydroxyflutamide in intact rats: new approach for benign prostate hyperplasia. Endocrinology 145:5420-8

65. **Chen J, Hwang DJ, Bohl CE, Miller DD, Dalton JT** 2005 A selective androgen receptor modulator for hormonal male contraception. J Pharmacol Exp Ther 312:546-53

66. **Negro-Vilar A** 1999 Selective androgen receptor modulators (SARMs): a novel approach to androgen therapy for the new millennium. J Clin Endocrinol Metab 84:3459-62

67. **Zhi L, Tegley CM, Marschke KB, Jones TK** 1999 Switching androgen receptor antagonists to agonists by modifying C-ring substituents on piperidino[3,2-g]quinolinone. Bioorg Med Chem Lett 9:1009-12

68. **Higuchi RI, Edwards JP, Caferro TR, Ringgenberg JD, Kong JW, Hamann LG, Arienti KL, Marschke KB, Davis RL, Farmer LJ, Jones TK** 1999 4-Alkyl- and 3,4-dialkyl-1,2,3,4-tetrahydro-8-pyridono[5,6-g]quinolines: potent, nonsteroidal androgen receptor agonists. Bioorg Med Chem Lett 9:1335-40

69. **Hanada K, Furuya K, Yamamoto N, Nejishima H, Ichikawa K, Nakamura T, Miyakawa M, Amano S, Sumita Y, Oguro N** 2003 Bone anabolic effects of **S-4**0503, a novel nonsteroidal selective androgen receptor modulator (SARM), in rat models of osteoporosis. Biol Pharm Bull 26:1563-9

70. **Rosen J, Negro-Vilar A** 2002 Novel, non-steroidal, selective androgen receptor modulators (SARMs) with anabolic activity in bone and muscle and improved safety profile. J Musculoskelet Neuronal Interact 2:222-4

71. **Anderson RA, Baird DT** 2002 Male contraception. Endocr Rev 23:735-62

72. **Sairam MR, Krishnamurthy H** 2001 The role of follicle-stimulating hormone in spermatogenesis: lessons from knockout animal models. Arch Med Res 32:601-8

73. **Vale W, Wiater E, Gray P, Harrison C, Bilezikjian L, Choe S** 2004 Activins and inhibins and their signaling. Ann N Y Acad Sci 1038:142-7

74. **Bebb RA, Anawalt BD, Christensen RB, Paulsen CA, Bremner WJ, Matsumoto AM** 1996 Combined administration of levonorgestrel and testosterone induces more rapid and effective suppression of spermatogenesis than testosterone alone: a promising male contraceptive approach. J Clin Endocrinol Metab 81:757-62

75. **Zhang GY, Gu YQ, Wang XH, Cui YG, Bremner WJ** 1999 A clinical trial of injectable testosterone undecanoate as a potential male contraceptive in normal Chinese men. J Clin Endocrinol Metab 84:3642-7

76. 1990 Contraceptive efficacy of testosterone-induced azoospermia in normal men. World Health Organization Task Force on methods for the regulation of male fertility. Lancet 336:955-9

77. 1996 Contraceptive efficacy of testosterone-induced azoospermia and oligozoospermia in normal men. Fertil Steril 65:821-9

78. **Gu YQ, Wang XH, Xu D, Peng L, Cheng LF, Huang MK, Huang ZJ, Zhang GY** 2003 A multicenter contraceptive efficacy study of injectable testosterone undecanoate in healthy Chinese men. J Clin Endocrinol Metab 88:562-8

79. **Kamischke A, Ploger D, Venherm S, von Eckardstein S, von Eckardstein A, Nieschlag E** 2000 Intramuscular testosterone undecanoate with or without oral levonorgestrel: a randomized placebo-controlled feasibility study for male contraception. Clin Endocrinol (Oxf) 53:43-52

80. **Gui YL, He CH, Amory JK, Bremner WJ, Zheng EX, Yang J, Yang PJ, Gao ES** 2004 Male hormonal contraception: suppression of spermatogenesis by injectable testosterone undecanoate alone or with levonorgestrel implants in chinese men. J Androl 25:720-7

81. **Handelsman DJ, Conway AJ, Howe CJ, Turner L, Mackey MA** 1996 Establishing the minimum effective dose and additive effects of depot progestin in suppression of human spermatogenesis by a testosterone depot. J Clin Endocrinol Metab 81:4113-21

82. **Handelsman DJ, Conway AJ, Boylan LM** 1992 Suppression of human spermatogenesis by testosterone implants. J Clin Endocrinol Metab 75:1326-32

83. **von Eckardstein S, Noe G, Brache V, Nieschlag E, Croxatto H, Alvarez F, Moo-Young A, Sivin I, Kumar N, Small M, Sundaram K** 2003 A clinical trial of 7 alpha-methyl-19-nortestosterone implants for possible use as a long-acting contraceptive for men. J Clin Endocrinol Metab 88:5232-9

84. **Anderson RA, Martin CW, Kung AW, Everington D, Pun TC, Tan KC, Bancroft J, Sundaram K, Moo-Young AJ, Baird DT** 1999 7Alpha-methyl-19-nortestosterone maintains sexual behavior and mood in hypogonadal men. J Clin Endocrinol Metab 84:3556-62

85. **Cummings DE, Kumar N, Bardin CW, Sundaram K, Bremner WJ** 1998 Prostate-sparing effects in primates of the potent androgen 7alpha-methyl-19-nortestosterone: a potential alternative to testosterone for androgen replacement and male contraception. J Clin Endocrinol Metab 83:4212-9

86. **Wallace EM, Gow SM, Wu FC** 1993 Comparison between testosterone enanthate-induced azoospermia and oligozoospermia in a male contraceptive study. I: Plasma luteinizing hormone, follicle stimulating hormone, testosterone, estradiol, and inhibin concentrations. J Clin Endocrinol Metab 77:290-3

87. **Anderson RA, Wallace AM, Wu FC** 1996 Comparison between testosterone enanthate-induced azoospermia and oligozoospermia in a male contraceptive study. III. Higher 5 alpha-reductase activity in oligozoospermic men administered supraphysiological doses of testosterone. J Clin Endocrinol Metab 81:902-8

88. **Behre HM, Baus S, Kliesch S, Keck C, Simoni M, Nieschlag E** 1995 Potential of testosterone buciclate for male contraception: endocrine differences between responders and nonresponders. J Clin Endocrinol Metab 80:2394-403

89. **Handelsman DJ, Farley TM, Peregoudov A, Waites GM** 1995 Factors in nonuniform induction of azoospermia by testosterone enanthate in normal men. World Health Organization Task Force on Methods for the Regulation of Male Fertility. Fertil Steril 63:125-33

90. **Eckardstein SV, Schmidt A, Kamischke A, Simoni M, Gromoll J, Nieschlag E** 2002 CAG repeat length in the androgen receptor gene and gonadotrophin suppression influence the effectiveness of hormonal male contraception. Clin Endocrinol (Oxf) 57:647-55

91. **Swerdloff RS, Bagatell CJ, Wang C, Anawalt BD, Berman N, Steiner B, Bremner WJ** 1998 Suppression of spermatogenesis in man induced by Nal-Glu gonadotropin releasing hormone antagonist and testosterone enanthate (TE) is maintained by TE alone. J Clin Endocrinol Metab 83:3527-33

92. **Prasad MR, Rajalakshmi M** 1976 Target sites for suppressing fertility in the male. Adv Sex Horm Res 2:263-87

93. **Sarkar NN** 2000 Steroidal contraception for men. Int J Clin Pract 54:594-603

94. **Pangkahila W** 1991 Reversible azoospermia induced by an androgen-progestin combination regimen in Indonesian men. Int J Androl 14:248-56

95. 1993 Comparison of two androgens plus depot-medroxyprogesterone acetate for suppression to azoospermia in indonesian men. World Health Organization. Task Force on Methods for the Regulation of Male Fertility. Fertil Steril 60:1062-8

96. **Wu FC, Aitken RJ** 1989 Suppression of sperm function by depot medroxyprogesterone acetate and testosterone enanthate in steroid male contraception. Fertil Steril 51:691-8

97. **Knuth UA, Yeung CH, Nieschlag E** 1989 Combination of 19-nortestosterone-hexyloxyphenylpropionate (Anadur) and depot-medroxyprogesterone-acetate (Clinovir) for male contraception. Fertil Steril 51:1011-8

98. **Turner L, Conway AJ, Jimenez M, Liu PY, Forbes E, McLachlan RI, Handelsman DJ** 2003 Contraceptive efficacy of a depot progestin and androgen combination in men. J Clin Endocrinol Metab 88:4659-67

99. **Meriggiola MC, Bremner WJ, Paulsen CA, Valdiserri A, Incorvaia L, Motta R, Pavani A, Capelli M, Flamigni C** 1996 A combined regimen of cyproterone acetate and testosterone enanthate as a potentially highly effective male contraceptive. J Clin Endocrinol Metab 81:3018-23

100. **Meriggiola MC, Bremner WJ, Costantino A, Di Cintio G, Flamigni C** 1998 Low dose of cyproterone acetate and testosterone enanthate for contraception in men. Hum Reprod 13:1225-9

101. **Meriggiola MC, Costantino A, Bremner WJ, Morselli-Labate AM** 2002 Higher testosterone dose impairs sperm suppression induced by a combined androgen-progestin regimen. J Androl 23:684-90

102. **Meriggiola MC, Costantino A, Cerpolini S, Bremner WJ, Huebler D, Morselli-Labate AM, Kirsch B, Bertaccini A, Pelusi C, Pelusi G** 2003 Testosterone undecanoate maintains spermatogenic suppression induced by cyproterone acetate plus testosterone undecanoate in normal men. J Clin Endocrinol Metab 88:5818-26

103. **Anawalt BD, Bebb RA, Bremner WJ, Matsumoto AM** 1999 A lower dosage levonorgestrel and testosterone combination effectively suppresses spermatogenesis and circulating gonadotropin levels with fewer metabolic effects than higher dosage combinations. J Androl 20:407-14

104. **Gonzalo IT, Swerdloff RS, Nelson AL, Clevenger B, Garcia R, Berman N, Wang C** 2002 Levonorgestrel implants (Norplant II) for male contraception clinical trials: combination with transdermal and injectable testosterone. J Clin Endocrinol Metab 87:3562-72

105. **Anawalt BD, Herbst KL, Matsumoto AM, Mulders TM, Coelingh-Bennink HJ, Bremner WJ** 2000 Desogestrel plus testosterone effectively suppresses spermatogenesis but also causes modest weight gain and high-density lipoprotein suppression. Fertil Steril 74:707-14

106. **Wu FC, Balasubramanian R, Mulders TM, Coelingh-Bennink HJ** 1999 Oral progestogen combined with testosterone as a potential male contraceptive: additive effects between desogestrel and testosterone enanthate in suppression of spermatogenesis, pituitary-testicular axis, and lipid metabolism. J Clin Endocrinol Metab 84:112-22

107. **Kinniburgh D, Zhu H, Cheng L, Kicman AT, Baird DT, Anderson RA** 2002 Oral desogestrel with testosterone pellets induces consistent suppression of spermatogenesis to azoospermia in both Caucasian and Chinese men. Hum Reprod 17:1490-501

108. **Anderson RA, Van Der Spuy ZM, Dada OA, Tregoning SK, Zinn PM, Adeniji OA, Fakoya TA, Smith KB, Baird DT** 2002 Investigation of hormonal male contraception in African men: suppression of spermatogenesis by oral desogestrel with depot testosterone. Hum Reprod 17:2869-77

109. **Kinniburgh D, Anderson RA, Baird DT** 2001 Suppression of spermatogenesis with desogestrel and testosterone pellets is not enhanced by addition of finasteride. J Androl 22:88-95

110. **Hair WM, Kitteridge K, O'Connor DB, Wu FC** 2001 A novel male contraceptive pill-patch combination: oral desogestrel and transdermal testosterone in the suppression of spermatogenesis in normal men. J Clin Endocrinol Metab 86:5201-9

111. **Kamischke A, Venherm S, Ploger D, von Eckardstein S, Nieschlag E** 2001 Intramuscular testosterone undecanoate and norethisterone enanthate in a clinical trial for male contraception. J Clin Endocrinol Metab 86:303-9

112. **Kamischke A, Heuermann T, Kruger K, von Eckardstein S, Schellschmidt I, Rubig A, Nieschlag E** 2002 An effective hormonal male contraceptive using testosterone undecanoate with oral or injectable norethisterone preparations. J Clin Endocrinol Metab 87:530-9

113. **Meriggiola MC, Costantino A, Saad F, D'Emidio L, Morselli Labate AM, Bertaccini A, Bremner WJ, Rudolph I, Ernst M, Kirsch B, Martorana G, Pelusi G** 2005 Norethisterone enanthate plus testosterone undecanoate for male contraception: effects of various injection intervals on spermatogenesis, reproductive hormones, testis, and prostate. J Clin Endocrinol Metab 90:2005-14

114. **Hay CJ, Brady BM, Zitzmann M, Osmanagaoglu K, Pollanen P, Apter D, Wu FC, Anderson RA, Nieschlag E, Devroey P, Huhtaniemi I, Kersemaekers WM** 2005 A multicenter phase IIb study of a novel combination of intramuscular androgen (testosterone decanoate) and oral progestogen (etonogestrel) for male hormonal contraception. J Clin Endocrinol Metab 90:2042-9

115. **Anderson RA, Kinniburgh D, Baird DT** 2002 Suppression of spermatogenesis by etonogestrel implants with depot testosterone: potential for long-acting male contraception. J Clin Endocrinol Metab 87:3640-9

116. **Brady BM, Walton M, Hollow N, Kicman AT, Baird DT, Anderson RA** 2004 Depot testosterone with etonogestrel implants result in induction of azoospermia in all men for long-term contraception. Hum Reprod 19:2658-67

117. **Wang C, Cunningham G, Dobs A, Iranmanesh A, Matsumoto AM, Snyder PJ, Weber T, Berman N, Hull L, Swerdloff RS** 2004 Long-term testosterone gel (AndroGel) treatment maintains beneficial effects on sexual function and mood, lean and fat mass, and bone mineral density in hypogonadal men. J Clin Endocrinol Metab 89:2085-98

118. **Zhou ZX, Wong CI, Sar M, Wilson EM** 1994 The androgen receptor: an overview. Recent Prog Horm Res 49:249-74

119. **Matsumoto AM** 1994 Hormonal therapy of male hypogonadism. Endocrinol Metab Clin North Am 23:857-75

120. **Mowszowicz I** 1989 [Antiandrogens. Mechanisms and paradoxical effects]. Ann Endocrinol (Paris) 50:189-99

121. **McLeod DG** 1993 Antiandrogenic drugs. Cancer 71:1046-9

122. **Gaillard-Moguilewsky M** 1991 Pharmacology of antiandrogens and value of combining androgen suppression with antiandrogen therapy. Urology 37:5-12

123. **Kirkovsky L, Mukherjee A, Yin D, Dalton JT, Miller DD** 2000 Chiral nonsteroidal affinity ligands for the androgen receptor. 1. Bicalutamide analogues bearing electrophilic groups in the B aromatic ring. J Med Chem 43:581-90

124. **Kearbey JD, Wu D, Gao W, Miller DD, Dalton JT** 2004 Pharmacokinetics of S-3-(4-acetylamino-phenoxy)-2-hydroxy-2-methyl-N-(4-nitro- 3-trifluoromethyl-phenyl)-propionamide in rats, a non-steroidal selective androgen receptor modulator. Xenobiotica 34:273-80

125. **Hechter O, Mechaber D, Zwick A, Campfield LA, Eychenne B, Baulieu EE, Robel P** 1983 Optimal radioligand exchange conditions for measurement of

occupied androgen receptor sites in rat ventral prostate. Arch Biochem Biophys 224:49-68

126. **Tucker H, Crook JW, Chesterson GJ** 1988 Nonsteroidal antiandrogens. Synthesis and structure-activity relationships of 3-substituted derivatives of 2-hydroxypropionanilides. J Med Chem 31:954-9

127. **Morris JJ, Hughes LR, Glen AT, Taylor PJ** 1991 Non-steroidal antiandrogens. Design of novel compounds based on an infrared study of the dominant conformation and hydrogen-bonding properties of a series of anilide antiandrogens. J Med Chem 34:447-55

128. **Teutsch G, Goubet F, Battmann T, Bonfils A, Bouchoux F, Cerede E, Gofflo D, Gaillard-Kelly M, Philibert D** 1994 Non-steroidal antiandrogens: synthesis and biological profile of high-affinity ligands for the androgen receptor. J Steroid Biochem Mol Biol 48:111-9

129. **Wakeling AE, Furr BJ, Glen AT, Hughes LR** 1981 Receptor binding and biological activity of steroidal and nonsteroidal antiandrogens. J Steroid Biochem 15:355-9

130. **Ishioka T, Kubo A, Koiso Y, Nagasawa K, Itai A, Hashimoto Y** 2002 Novel non-steroidal/non-anilide type androgen antagonists with an isoxazolone moiety. Bioorg Med Chem 10:1555-66

131. **Hamann LG, Higuchi RI, Zhi L, Edwards JP, Wang XN, Marschke KB, Kong JW, Farmer LJ, Jones TK** 1998 Synthesis and biological activity of a novel series of nonsteroidal, peripherally selective androgen receptor antagonists derived from 1,2-dihydropyridono[5,6-g]quinolines. J Med Chem 41:623-39

132. **Bohl CE, Gao W, Miller DD, Bell CE, Dalton JT** 2005 Structural basis for antagonism and resistance of bicalutamide in prostate cancer. Proc Natl Acad Sci U S A

133. **Lambert RW, Royal Society of Chemistry (Great Britain). Fine Chemicals and Medicinals Group., Society of Chemical Industry (Great Britain). Fine Chemicals Group.** 1986 Third SCI-RSC Medicinal Chemistry Symposium : the proceedings of a symposium organised by the Fine Chemicals and Medicinals Group of the Industrial Division of the Royal Society of Chemistry and the Fine Chemicals Group of the Society of Chemical Industry, Cambridge, England, 15-18 September 1985. Royal Society of Chemistry, London

134. **Bourguet W, Ruff M, Chambon P, Gronemeyer H, Moras D** 1995 Crystal structure of the ligand-binding domain of the human nuclear receptor RXR-alpha. Nature 375:377-82

135. **Renaud JP, Rochel N, Ruff M, Vivat V, Chambon P, Gronemeyer H, Moras D** 1995 Crystal structure of the RAR-gamma ligand-binding domain bound to all-trans retinoic acid. Nature 378:681-9

136. **Wagner RL, Apriletti JW, McGrath ME, West BL, Baxter JD, Fletterick RJ** 1995 A structural role for hormone in the thyroid hormone receptor. Nature 378:690-7

137. **Brzozowski AM, Pike AC, Dauter Z, Hubbard RE, Bonn T, Engstrom O, Ohman L, Greene GL, Gustafsson JA, Carlquist M** 1997 Molecular basis of agonism and antagonism in the oestrogen receptor. Nature 389:753-8

138. **Greschik H, Moras D** 2003 Structure-activity relationship of nuclear receptor-ligand interactions. Curr Top Med Chem 3:1573-99

139. **Yesalis C** 2000 Anabolic steroids in sport and exercise, 2nd ed. Human Kinetics, Champaign, IL

140. **Arimasa N, Kochakian CD** 1976 Anabolic-androgenic steroids. Springer-Verlag, Berlin ; New York

141. **Naftolin F, Ryan KJ, Petro Z** 1972 Aromatization of androstenedione by the anterior hypothalamus of adult male and female rats. Endocrinology 90:295-8

142. **Nimrod A, Ryan KJ** 1975 Aromatization of androgens by human abdominal and breast fat tissue. J Clin Endocrinol Metab 40:367-72

143. **Bardin CW, Catterall JF** 1981 Testosterone: a major determinant of extragenital sexual dimorphism. Science 211:1285-94

144. **Hershberger LG, Thompson CR, Clegg MT** 1966 Myotrophic effects of estrogen in mice and lack of effect in rats. Proc Soc Exp Biol Med 121:785-8

145. **Ghusn HF, Shao TC, Klima M, Cunningham GR** 1991 4-MAPC, a 5 alpha-reductase inhibitor, reduces rat ventral prostate weight, DNA, and prostatein concentrations. J Androl 12:315-22

146. **Shao TC, Kong A, Cunningham GR** 1994 Effects of 4-MAPC, a 5 alpha-reductase inhibitor, and cyproterone acetate on regrowth of the rat ventral prostate. Prostate 24:212-20

147. **Lamb JC, English H, Levandoski PL, Rhodes GR, Johnson RK, Isaacs JT** 1992 Prostatic involution in rats induced by a novel 5 alpha-reductase inhibitor, SK&F 105657: role for testosterone in the androgenic response. Endocrinology 130:685-94

148. **Rittmaster RS, Manning AP, Wright AS, Thomas LN, Whitefield S, Norman RW, Lazier CB, Rowden G** 1995 Evidence for atrophy and apoptosis in the ventral prostate of rats given the 5 alpha-reductase inhibitor finasteride. Endocrinology 136:741-8

149. **Wright AS, Douglas RC, Thomas LN, Lazier CB, Rittmaster RS** 1999 Androgen-induced regrowth in the castrated rat ventral prostate: role of 5alpha-reductase. Endocrinology 140:4509-15

150. **Saartok T, Dahlberg E, Gustafsson JA** 1984 Relative binding affinity of anabolic-androgenic steroids: comparison of the binding to the androgen receptors in skeletal muscle and in prostate, as well as to sex hormone-binding globulin. Endocrinology 114:2100-6

151. **Deslypere JP, Young M, Wilson JD, McPhaul MJ** 1992 Testosterone and 5 alpha-dihydrotestosterone interact differently with the androgen receptor to enhance transcription of the MMTV-CAT reporter gene. Mol Cell Endocrinol 88:15-22

152. **Hsiao PW, Thin TH, Lin DL, Chang C** 2000 Differential regulation of testosterone vs. 5alpha-dihydrotestosterone by selective androgen response elements. Mol Cell Biochem 206:169-75

153. **Parkes AS** 1938 Effective absorption of hormones. Br. J. Med:371-373

154. **Maisey NM, Bingham J, Marks V, English J, Chakraborty J** 1981 Clinical efficacy of testosterone undecanoate in male hypogonadism. Clin Endocrinol (Oxf) 14:625-9

155. **Van Dort ME, Robins DM, Wayburn B** 2000 Design, synthesis, and pharmacological characterization of 4-[4, 4-dimethyl-3-(4-hydroxybutyl)-5-oxo-2-thioxo-1-imidazolidinyl]- 2-iodobenzonitrile as a high-affinity nonsteroidal androgen receptor ligand. J Med Chem 43:3344-7

156. **Hamann LG, Mani NS, Davis RL, Wang XN, Marschke KB, Jones TK** 1999 Discovery of a potent, orally active, nonsteroidal androgen receptor agonist: 4-ethyl-1,2,3,4-tetrahydro-6- (trifluoromethyl)-8-pyridono[5,6-g]- quinoline (LG121071). J Med Chem 42:210-2

157. **Burden PM, Ai TH, Lin HQ, Akinci M, Costandi M, Hambley TM, Johnston GA** 2000 Chiral derivatives of 2-cyclohexylideneperhydro-4,7-methanoindenes, a novel class of nonsteroidal androgen receptor ligand: synthesis, X-ray analysis, and biological activity. J Med Chem 43:4629-35

158. **Anderson RA, Baird DT** 1997 Progress towards a male pill. IPPF Med Bull 31:1-5

159. **Martin CW, Anderson RA, Cheng L, Ho PC, van der Spuy Z, Smith KB, Glasier AF, Everington D, Baird DT** 2000 Potential impact of hormonal male contraception: cross-cultural implications for development of novel preparations. Hum Reprod 15:637-45

160. **Amory JK, Bremner W** 2001 Endocrine regulation of testicular function in men: implications for contraceptive development. Mol Cell Endocrinol 182:175-9

161. **Kamischke A, Nieschlag E** 2004 Progress towards hormonal male contraception. Trends Pharmacol Sci 25:49-57

162. **Mukherjee A, Kirkovsky L, Yao XT, Yates RC, Miller DD, Dalton JT** 1996 Enantioselective binding of Casodex to the androgen receptor. Xenobiotica 26:117-22

163. **Furr BJ, Valcaccia B, Curry B, Woodburn JR, Chesterson G, Tucker H** 1987 ICI 176,334: a novel non-steroidal, peripherally selective antiandrogen. J Endocrinol 113:R7-9

164. **Sun YT, Irby DC, Robertson DM, de Kretser DM** 1989 The effects of exogenously administered testosterone on spermatogenesis in intact and hypophysectomized rats. Endocrinology 125:1000-10

165. **Lue Y, Hikim AP, Wang C, Im M, Leung A, Swerdloff RS** 2000 Testicular heat exposure enhances the suppression of spermatogenesis by testosterone in rats: the "two-hit" approach to male contraceptive development. Endocrinology 141:1414-24

166. **Debeljuk L, Vilchez-Martinez JA, Arimura A, Schally AV** 1974 Effect of gonadal steroids on the response to LH-RH in intact and castrated male rats. Endocrinology 94:1519-24

167. **Schally AV, Redding TW, Arimura A** 1973 Effect of sex steroids on pituitary responses to LH-and FSH-releasing hormone *in vitro*. Endocrinology 93:893-902

168. **Liang T, Brady EJ, Cheung A, Saperstein R** 1984 Inhibition of luteinizing hormone (LH)-releasing hormone-induced secretion of LH in rat anterior pituitary cell culture by testosterone without conversion to 5 alpha-dihydrotestosterone. Endocrinology 115:2311-7

169. **Matsumoto AM** 1990 Effects of chronic testosterone administration in normal men: safety and efficacy of high dosage testosterone and parallel dose-dependent suppression of luteinizing hormone, follicle-stimulating hormone, and sperm production. J Clin Endocrinol Metab 70:282-7

170. **Berndtson WE, Desjardins C, Ewing LL** 1974 Inhibition and maintenance of spermatogenesis in rats implanted with polydimethylsiloxane capsules containing various androgens. J Endocrinol 62:125-35

171. **Moger WH** 1976 Effect of testosterone implants on serum gonadotropin concentrations in the male rat. Biol Reprod 14:665-9

172. **Bansal MR, Davies AG** 1986 Effect of testosterone oenanthate on spermatogenesis and serum testosterone concentrations in adult mice. J Reprod Fertil 78:219-24

173. **Walsh PC, Swerdloff RS** 1973 Biphasic effect of testosterone on spermatogenesis in the rat. Invest Urol 11:190-3

174. **Ewing LL, Robaire B** 1978 Endogenous antispermatogenic agents: prospects for male contraception. Annu Rev Pharmacol Toxicol 18:167-87

175. **Beach FAH, A.M.** 1946 Mating behavior in male rats castrated a various ages and injected with androgen. Experimental Zoology 101:91-142

176. **Balthazart J** 1989 Molecular and cellular basis of social behavior in vertebrates. Springer-Verlag, Berlin

177. **Ryan KJ, Naftolin F, Reddy V, Flores F, Petro Z** 1972 Estrogen formation in the brain. Am J Obstet Gynecol 114:454-60

178. **Naftolin F, Brown-Grant K, Corker CS** 1972 Plasma and pituitary luteinizing hormone and peripheral plasma oestradiol concentrations in the normal oestrous cycle of the rat and after experimental manipulation of the cycle. J Endocrinol 53:17-30

179. **Denef C, Magnus C, McEwen BS** 1973 Sex differences and hormonal control of testosterone metabolism in rat pituitary and brain. J Endocrinol 59:605-21

180. **Naess O, Hansson V, Djoeseland O, Attramadal A** 1975 Characterization of the androgen receptor in the anterior pituitary of the rat. Endocrinology 97:1355-63

181. **Vreeburg JT, Schretlen PJ, Baum MJ** 1975 Specific, high-affinity binding of 17beta-estradiol in cytosols from several brain regions and pituitary of intact and castrated adult male rats. Endocrinology 97:969-77

182. **Cooke BM, Breedlove SM, Jordan CL** 2003 Both estrogen receptors and androgen receptors contribute to testosterone-induced changes in the morphology of the medial amygdala and sexual arousal in male rats. Horm Behav 43:336-46

183. **Lodder J, Baum MJ** 1977 Facilitation of mounting behavior by dihydrotestosterone propionate in castrated estradiol benzoate-treated male rats following pudendectomy. Behav Biol 20:141-8

184. **Sodersten P** 1973 Estrogen-activated sexual behavior in male rats. Horm Behav 4:247-56

185. **Sodersten P, Eneroth P, Hansson T** 1988 Oestradiol synergizes with 5 alpha-dihydrotestosterone or 3 alpha- but not 3 beta-androstanediol in inducing sexual behaviour in castrated rats. J Endocrinol 119:461-5

186. **Parrott RF** 1975 Aromatizable and 5alpha-reduced androgens: differentiation between central and peripheral effects on male rat sexual behavior. Horm Behav 6:99-108

187. **Agmo A, Sodersten P** 1975 Sexual behaviour in castrated rabbits treated with testosterone, oestradiol, dihydrotestosterone or oestradiol in combination with dihydrotestosterone. J Endocrinol 67:327-32

188. **Sodersten P, Eneroth P, Hansson T, Mode A, Johansson D, Naslund B, Liang T, Gustafsson JA** 1986 Activation of sexual behaviour in castrated rats: the role of oestradiol. J Endocrinol 111:455-62

189. **McDonald P, Beyer C, Newton F, Brien B, Baker R, Tan HS, Sampson C, Kitching P, Greenhill R, Pritchard D** 1970 Failure of 5alpha-dihydrotestosterone to initiate sexual behaviour in the castrated male rat. Nature 227:964-5

190. **Feder HH** 1971 The comparative actions of testosterone propionate and 5 -androstan-17 -ol-3-one propionate on the reproductive behaviour, physiology and morphology of male rats. J Endocrinol 51:241-52

191. **Baum MJ, Vreeburg JT** 1973 Copulation in castrated male rats following combined treatment with estradiol and dihydrotestosterone. Science 182:283-5

192. **Larsson K, Sodersten P, Beyer C** 1973 Induction of male sexual behaviour by oestradiol benzoate in combination with dihydrotestosterone. J Endocrinol 57:563-4

193. **Baum MJ, Kingsbury PA, Erskine MS** 1987 Failure of the synthetic androgen 17 beta-hydroxy-17 alpha-methyl-estra-4,9,11-triene-3-one (methyltrienolone, R1881) to duplicate the activational effect of testosterone on mating in castrated male rats. J Endocrinol 113:15-20

194. **Morali G, Lemus AE, Munguia R, Arteaga M, Perez-Palacios G, Sundaram K, Kumar N, Bardin CW** 1993 Induction of male sexual behavior in the rat by 7

alpha-methyl-19-nortestosterone, an androgen that does not undergo 5 alpha-reduction. Biol Reprod 49:577-81

195. **Feder HH, Naftolin F, Ryan KJ** 1974 Male and female sexual responses in male rats given estradiol benzoate and 5 alpha-androstan-17 beta-ol-3-one propionate. Endocrinology 94:136-41

196. **Knobil E, Neill JD** 1994 The Physiology of reproduction, 2nd ed. Raven Press, New York

197. **Davidson JM** 1969 Effects of estrogen on the sexual behavior of male rats. Endocrinology 84:1365-72

198. **Hawkins CA, Everitt BJ, Herbert J** 1988 The influence of steroid hormones on competing sexual and ingestive behavior in the male rat. Physiol Behav 44:291-300

199. **Vagell ME, McGinnis MY** 1998 The role of gonadal steroid receptor activation in the restoration of sociosexual behavior in adult male rats. Horm Behav 33:163-79

200. **Putnam SK, Sato S, Hull EM** 2003 Effects of testosterone metabolites on copulation and medial preoptic dopamine release in castrated male rats. Horm Behav 44:419-26

201. **Putnam SK, Du J, Sato S, Hull EM** 2001 Testosterone restoration of copulatory behavior correlates with medial preoptic dopamine release in castrated male rats. Horm Behav 39:216-24

202. **Hull EM, Lorrain DS, Du J, Matuszewich L, Lumley LA, Putnam SK, Moses J** 1999 Hormone-neurotransmitter interactions in the control of sexual behavior. Behav Brain Res 105:105-16

203. **Butera PC, Czaja JA** 1985 Maintenance of target tissue and sexual behavior with dihydrotestosterone in male rats and guinea pigs. Physiol Behav 34:319-21

204. **Noble RG, Alsum PB** 1975 Hormone dependent sex dimorphisms in the golden hamster (Mesocricetus auratus). Physiol Behav 14:567-74

205. **Joshi HS, Raeside JI** 1973 Synergistic effects of testosterone and oestrogens on accessory sex glands and sexual behaviour of the boar. J Reprod Fertil 33:411-23

206. **Fletcher TJ, Short RV** 1974 Restoration of libido in castrated red deer stag (Cervus elaphus) with oestradiol-17beta. Nature 248:616-8

207. **D'Occhio MJ, Brooks DE** 1980 Effects of androgenic and oestrogenic hormones on mating behaviour in rams castrated before and after puberty. J Endocrinol 86:403-11

208. **Dykeman DA, Katz LS, Foote RH** 1982 Behavioral characteristics of beef steers administered estradiol, testosterone and dihydrotestosterone. J Anim Sci 55:1303-9

209. **Phoenix CH** 1978 Sexual behavior of laboratory- and wild-born male Rhesus monkeys. Horm Behav 10:178-92

210. **Alsum P, Goy RW** 1974 Actions of esters of testosterone, dihydrotestosterone, or estradiol on sexual behavior in castrated male guinea pigs. Horm Behav 5:207-17

211. **Luttge WG, Hall NR** 1973 Androgen-induced agonistic behavior in castrate male Swiss-Webster mice: comparison of four naturally occurring androgens. Behav Biol 8:725-32

212. **Beyer C, Rivaud N** 1973 Differential effect of testosterone and dihydrotestosterone on the sexual behavior of prepuberally castrated male rabbits. Horm Behav 4:175-80

213. **Phoenix CH** 1974 Effects of dihydrotestosterone on sexual behavior of castrated male rhesus monkeys. Physiol Behav 12:1045-55

214. **Phoenix CH** 1974 The role of androgens in the sexual behavior of adult male rhesus monkeys. Adv Behav Biol 11:249-58

215. **Michael RP, Zumpe D, Bonsall RW** 1986 Comparison of the effects of testosterone and dihydrotestosterone on the behavior of male cynomolgus monkeys (Macaca fascicularis). Physiol Behav 36:349-55

216. **Schenck PE, Slob AK** 1986 Castration, sex steroids, and heterosexual behavior in adult male laboratory-housed stumptailed macaques (Macaca arctoides). Horm Behav 20:336-53

217. **Hohlweg WaJ, K.** 1932 Die Hormonal-Nervose Regulierung der Funktion des Hypophysenvorderlappens. Klin. Wochenschr. 11:321

218. **Dischreit J** 1939 Wirkung des Testikelhormonpraparates Erugon auf den juvenilen Rat-tenhoden. Klin. Wochenschr. 18:1493

219. **Gaarenstroom JH** 1939 Inhibition of the 'antimasculine effect' of oestrone by testosterone propionate. Acta Brev. Neerl. Physiol. 9:134

220. **Ludwig DJ** 1950 The effect of androgen on spermatogenesis. Endocrinology 46:453

221. **Nieschlag E, Nieschlag S, Behre HM** 1998 Testosterone : action, deficiency, substitution, 2nd ed. Springer, Berlin ; New York

222. **Hunt DM, Lau IF, Saksena SK, Chang MC** 1978 Endocrinological and physiological features after steroid treatment of male rats. Arch Androl 1:311-20

223. **Ewing LL, Desjardins C, Irby DC, Robaire B** 1977 Synergistic interaction of testosterone and oestradiol inhibits spermatogenesis in rats. Nature 269:409-11

224. **Hislop MS, Ratanjee BD, Soule SG, Marais AD** 1999 Effects of anabolic-androgenic steroid use or gonadal testosterone suppression on serum leptin concentration in men. Eur J Endocrinol 141:40-6.

225. **Watanobe H, Suda T** 1999 A detailed study on the role of sex steroid milieu in determining plasma leptin concentrations in adult male and female rats. Biochem Biophys Res Commun 259:56-9.

226. **Pinilla L, Seoane LM, Gonzalez L, Carro E, Aguilar E, Casanueva FF, Dieguez C** 1999 Regulation of serum leptin levels by gonadal function in rats. Eur J Endocrinol 140:468-73.

227. **Dewan ZF, Morris ID, Lendon RG** 2000 Administration of exogenous testosterone in the adult rat and its effects on reproductive organs, sex hormones and body-weight. Bangladesh Med Res Counc Bull 26:48-55

228. **Sharpe R** 1987 Testosterone and spermatogenesis. J Endocrinol 113:1-2

229. **Awoniyi C, Santulli, R, Chandrashekar, V, Schanbacher, BD, Zirkin, BR.** 1989 Quantitative resoration of advanced spermatogenic cells in adult male rats made azoospermic by active immunization against LH or GnRH. Endocrinology 125:1303-1309

230. **Awoniyi C, Zirkin, BR, Chandrashekar, V, Schlaff, WD.** 1992 Exogenously administered testosterone maintains spermatogenesis quantitatively in adult rats actively immunized against GnRH. Endocrinology 130:3283-3288

231. **Zirkin B, Santulli, R, Awoniyi CA, Ewing, LL.** 1989 Maitenance of advanced spermatogenic cells in the adult rat testis: quantitative relationship to testosterone concentration within the testis. Endocrinology 124:3043-3049

232. **Awoniyi C, Sprando, RL, Santulli, RL, Chandrashekar, V, Ewing, LL, Zirkin, BR.** 1990 Restoration of spermatogenesis by exogenously administered testosterone in rats made azoospermic by hypophysectomy or withdrawal of luteinizing hormone alone. Endocrinology 127:177-184

233. **Russell L** 1991 The perils of sperm release - "let my children go". Int J Androl 14:307-311

234. **Russell LD, Griswold MD** 1993 The Sertoli cell, 1st ed. Cache River Press, Clearwater, FL

235. **Russell L, Ettlin, RA, Sinha Hikim, AP, Clegg, ED.** 1990 Histological and histopathological evaluation of the testis. Clearwater, Florida: Cache River Press

236. **Handelsman DJ, Wishart S, Conway AJ** 2000 Oestradiol enhances testosterone-induced suppression of human spermatogenesis. Hum Reprod 15:672-9